Vol. 15. No 1, 2013

ISSN 1507-2711
Cena: 25 zł (w tym 5% VAT)

# EKSPLOATACJA I NIEZAWODNOŚĆ
# MAINTENANCE AND RELIABILITY

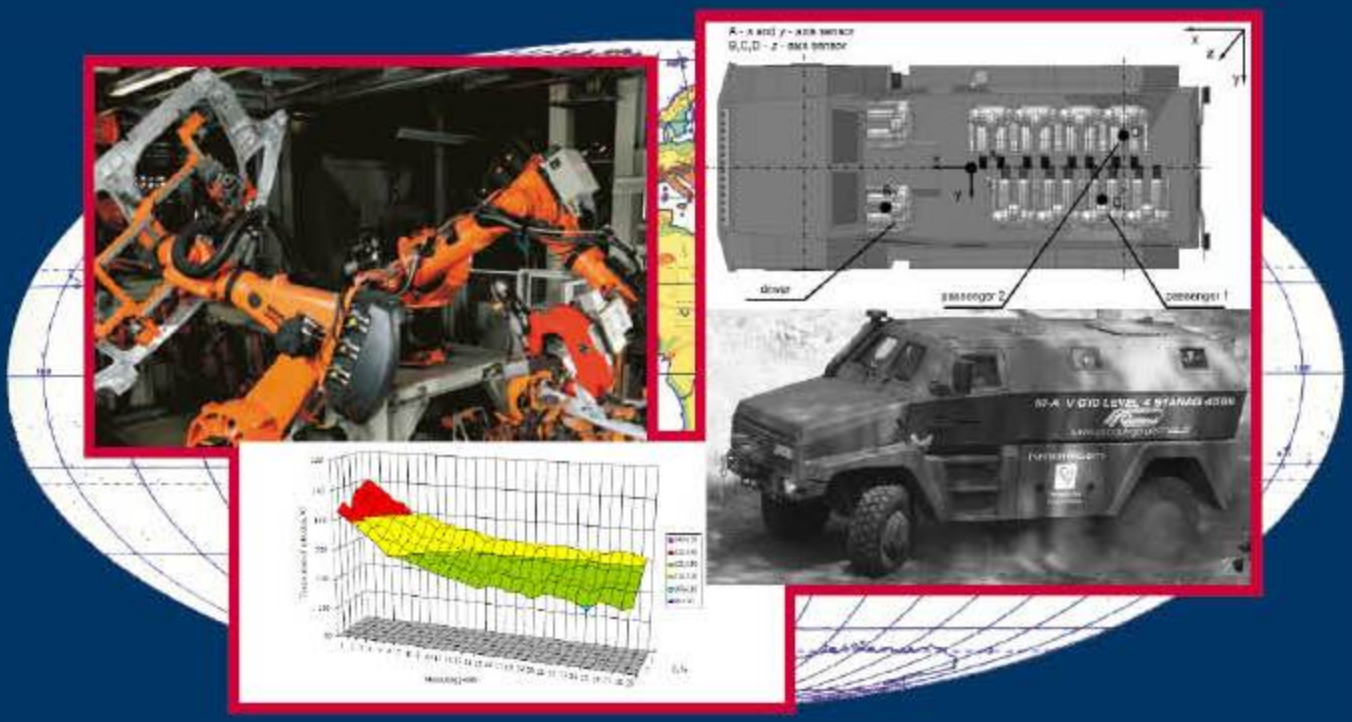

Polskie Naukowo Techniczne Towarzystwo Eksploatacyjne
Warszawa

Polish Maintenance Society
Warsaw

**Co-financed by the Minister of Science and Higher Education**

The Journal is indexed and abstracted in the Journal Citation Reports (JCR Science Edition), Scopus, Science Citation Index Expanded (SciSearch®) and Index Copernicus International.

The Quarterly appears on the list of journals credited with a high impact factor by the Polish Ministry of Science and Higher Education and is indexed in the Polish Technical Journal Contents database – BAZTECH and the database of the Digital Library Federation.

**All the scientific articles have received two positive reviews from independent reviewers.**

**Our IF is 0.333**

| | |
|---|---|
| **Editorial staff:** | Dariusz Mazurkiewicz, PhD, DSc (Eng), Associate Professor (Editor-in-Chief, Secretary of the Scientific Board)<br>Tomasz Klepka, PhD, DSc (Eng) (Deputy Editor-in-Chief)<br>Teresa Błachnio-Krolopp, MSc (Eng) (Editorial secretary)<br>Andrzej Koma (Typesetting and text makeup)<br>Krzysztof Olszewski, PhD (Eng) (Webmaster) |
| **Publisher:** | Polish Maintenance Society, Warsaw |
| **Scientific patronage:** | Polish Academy of Sciences Branch in Lublin |
| **Address for correspondence:** | "Eksploatacja i Niezawodność" - Editorial Office<br>20-618 Lublin, ul. Nadbystrzycka 36, Poland<br>e-mail: office@ein.org.pl<br>http://www.ein.org.pl/ |
| **Circulation:** | 550 copies |

## Science and Technology

**Abstracts** ..... II

Andrzej LOSKA

**Exploitation assessment of selected technical objects using taxonomic methods**
**Eksploatacyjna ocena wybranych obiektów technicznych z zastosowaniem metod taksonomicznych** ..... 1

Chiming GUO, Wenbin WANG, Bo GUO, Rui PENG

**Maintenance optimization for systemswith dependent competing risks using a copula function**
**Optymalizacja eksploatacji dla systemów z zależnymi zagrożeniami konkurującymi przy wykorzystaniu funkcji kopuły** ..... 9

Daniel PIENIAK, Paweł OGRODNIK, Marcin OSZUST, Andrzej NIEWCZAS

**Reliability of the thermal treated timber and wood-based materials in high temperatures**
**Niezawodność konstrukcyjna drewna modyfikowanego termicznie i materiałów drewnopochodnych w podwyższonych temperaturach** ..... 18

Krzysztof JAMROZIAK, Mariusz KOSOBUDZKI, Jerzy PTAK

**Assessment of the comfort of passenger transport in special purpose vehicles**
**Ocena warunków komfortu transportu osób w pojazdach specjalnego przeznaczenia** ..... 25

Mariusz KRAWCZYK

**Conditions for unmanned aircraft reliability determination**
**Przesłanki determinujące niezawodność samolotów bezpilotowych** ..... 31

Andrzej BAIER, Sławomir ZOLKIEWSKI

**Initial research of epoxy and polyester warp laminates testing on abrasive wear used in car sheathing**
**Badania wstępne ścieralności laminatów o osnowie epoksydowej i poliestrowej do zastosowania w budowie poszycia wagonu towarowego** ..... 37

Zdzisław CHŁOPEK, Jakub LASOCKI

**Comprehensive environmental impact assessment of the process of preparation of bioethanol fuels of the first and second generation**
**Kompleksowa ocena oddziaływania na środowisko procesu przygotowania paliw bioetanolowych pierwszej i drugiej generacji** ..... 44

Tadeusz MARKOWSKI, Jacek MUCHA, Waldemar WITKOWSKI

**FEM analysis of clinching joint machine's C-frame rigidity**
**Analiza MES sztywności C-ramy urządzenia do wytwarzania połączeń przetłoczeniowych** ..... 51

Aneta TOR-ŚWIĄTEK, Bronisław SAMUJŁO

**Use of thermo vision research to analyze the thermal stability of microcellular extrusion process of poly(vinyl chloride)**
**Wykorzystanie badań termowizyjnych do analizy stabilności procesu wytłaczania mikroporującego poli(chlorku winylu)** ..... 58

Grzegorz KRÓLCZYK, Maksymilian GAJEK, Stanisław LEGUTKO

**Predicting the tool life in the dry machining of duplex stainless steel**
**Prognozowanie okresu trwałości ostrza w obróbce na sucho stali nierdzewnej duplex** ..... 62

Miloš TANASIJEVIĆ, Dejan IVEZIĆ, Predrag JOVANČIĆ, Dragan IGNJATOVIĆ, Uglješa BUGARIĆ

**Dependability assesment of open-pit mines equpment – study on the bases of fuzzy algebra rules**
**Ocena niezawodności sprzętu wykorzystywanego w kopalniach odkrywkowych – badania oparte na regułach rozmytej algebry** ..... 66

Zdzisław CHŁOPEK

**Research on energy consumption by an electrically driven automotive vehicle in simulated urban conditions**
**Badania zużycia energii przez samochód elektryczny w warunkach symulujących jazdę w mieście** ..... 75

Piotr KULINOWSKI

**Simulation studies as the part of an integrated design process dealing with belt conveyor operation**
**Badania symulacyjne jako element zintegrowanego procesu projektowania w aspekcie eksploatacji przenośników taśmowych** ..... 83

LOSKA A. **Exploitation assessment of selected technical objects using taxonomic methods**. Eksploatacja i Niezawodnosc – Maintenance and Reliability 2013; 15 (1): 1–8.

The article is an attempt to answer the formulated problems in industrial enterprises problems on practical aspects of use of specific measures to assess exploit of technical facilities. In this regard, bibliography study has been conducted, including an overview of opportunities to develop the values of selected exploitation characteristics, as well as industrial research as a need analysis of technical departments in the assessment of their performance. As a result of these studies and their conclusions method of preliminary mutual exploitation evaluation has been developed, based on the values of standardized and aggregated ranks of technical objects, in the context of exploitation measurements calculated. This method, as well as an example of its use, relating to a selected network technical system, are the subject of further sections of this article.

LOSKA A. **Eksploatacyjna ocena wybranych obiektów technicznych z zastosowaniem metod taksonomicznych**. Eksploatacja i Niezawodnosc – Maintenance and Reliability 2013; 15 (1): 1–8.

Artykuł jest próbą odpowiedzi na formułowane w przedsiębiorstwach przemysłowych problemy dotyczące praktycznych aspektów wykorzystania określonych miar do oceny eksploatowania obiektów technicznych. W tym zakresie, przeprowadzono badania literaturowe obejmujące przegląd możliwości kształtowania wartości wybranych cech eksploatacyjnych, a także badania przemysłowe dotyczące analizy potrzeb służb technicznych przedsiębiorstw w zakresie oceny ich funkcjonowania. Wynikiem przeprowadzonych badań i sformułowanych w tym zakresie wniosków, została opracowana metoda wstępnej wzajemnej oceny eksploatacyjnej w oparciu o wartości normowanych i zagregowanych rang obiektów technicznych w świetle wyznaczanych miar eksploatacyjnych. Metoda ta, jak również przykład jej zastosowania, odnoszący się do wybranego sieciowego systemu technicznego są przedmiotem dalszej treści tego artykułu.

GUO C, WANG W, GUO B, PENG R. **Maintenance optimization for systems with dependent competing risks using a copula function**. Eksploatacja i Niezawodnosc – Maintenance and Reliability 2013; 15 (1): 9–17.

This paper develops a joint copula reliability model for systems subjected to dependent competing risks caused by two degradation processes and random shocks. The two degradation processes follow gamma processes and the random shocks follow a non-homogeneous Poisson process (NHPP). Their interdependence relationship is modeled by a copula function, which is determined by a two-stage method based on simulated data. It is shown that the proposed model can provide more precise results than the model without considering the dependent relationship. Through the proposed reliability model, two maintenance models are studied and compared. It is found that the inspection cost has significant effects on the choosing of maintenance policy.

GUO C, WANG W, GUO B, PENG R. **Maintenance optimization for systems with dependent competing risks using a copula function**. Eksploatacja i Niezawodnosc – Maintenance and Reliability 2013; 15 (1): 9–17.

W niniejszej pracy opracowano wspólny model niezawodności z użyciem kopuły dla systemów poddawanych zależnym zagrożeniom konkurującym powodowanym przez dwa procesy degradacji i zaburzenia losowe. Owe dwa procesy degradacji reprezentują typ procesu gamma, podczas gdy zaburzenia losowe są typem niejednorodnego procesu Poissona (non-homogeneous Poisson process - NHPP). Ich związek wzajemnej zależności modelowany jest przy użyciu funkcji kopuły, która jest wyznaczana na podstawie dwuetapowej metody opartej o dane symulowane. Wykazano, iż proponowany model może zapewnić bardziej precyzyjne wyniki niż model, w którym nie ujęto związku zależności. W oparciu o proponowany model niezawodności, badane i porównywane są dwa modele eksploatacji. Stwierdzono, iż koszt przeglądu ma duży wpływ na wybór polityki eksploatacyjnej.

PIENIAK D, OGRODNIK P, OSZUST M, NIEWCZAS A. **Reliability of the thermal treated timber and wood-based materials in high temperatures**. Eksploatacja i Niezawodnosc – Maintenance and Reliability 2013; 15 (1): 18–24.

Existing wood and wood-based materials have had several drawbacks limiting their use, which in consequence resulted in replacing them by other materials. The most significant problems were limitations regarding maximum dimensions of the components cross – section and capabilities of manufacturing of the large-scale components. Durability and flammability of surfaces were the limiting factors as well. Nowadays, thermally treated wood and wood composites are more and more commonly used in the engineering constructions, such as: glued laminated timber (GL), laminated veneer lumber (LVL) and thermally treated timber (TT). The timber undergoes a process of thermal degradation. In high temperatures timber structure is subject to simultaneous influence in the form of forces and thermal impacts. These factors influence stress distribution in the wood structure and limit its load capacity, reflecting structure decohesion. The aim of the presented studies was to determine impact of increased temperatures on strength of the wood materials and wood-based composites. Additionally, based on the results of the strength studies, analysis of the probability of survival in high temperatures was performed. Samples used in the static bending strength studies were made of the laminated veneer lumber – LVL, glued laminated pine timber – GL, and thermally treated – TT and non-treated spruce timber - NTT. The samples were in a cuboidal shape with dimensions of 20x20x300 mm. The evaluation of bending strength was performed by means of the universal strength device - FPZ 100/1 (VEB Thuringer Industriewerk Rauenstein, Germany). Fire temperatures conditions were simulated by blowing hot air (GHG 650 LCE). The studies were conducted in the following temperature ranges: 20, 50, 100, 150, 200 and 230ºC. Based on the obtained results a reliability analysis was performed. For the analysis a two-parameter Weibull distribution was applied. In case of materials with laminated structure – LVL and GL, an increase in standard deviation of the results of bending strength in the successive temperature ranges has been observed. Higher values of shape parameter c of Weibull distribution have been demonstrated for TT spruce timber (the highest c = 5.58) and NTT (the highest c = 3.31).

PIENIAK D, OGRODNIK P, OSZUST M, NIEWCZAS A. **Niezawodność konstrukcyjna drewna modyfikowanego termiczniei materiałów drewnopochodnych w podwyższonych temperaturach**. Eksploatacja i Niezawodnosc – Maintenance and Reliability 2013; 15 (1): 18–24.

Dotychczasowe materiały drewniane i drewnopochodne miały wiele wad ograniczających ich zastosowanie, co prowadziło do zastępowania ich innymi. Największy problem stanowiły ograniczenia, co do maksymalnych wymiarów przekroju elementów oraz możliwości wykonywania elementów o znacznych rozpiętościach, również trwałość powierzchni a także łatwopalność ograniczały zastosowanie. Obecnie w konstrukcjach inżynierskich coraz częściej wykorzystuje się drewno modyfikowane termicznie oraz materiały drewnopochodne m.in. drewno klejone warstwowo (GL), drewno fornirowane warstwowe (LVL) oraz drewno modyfikowana termicznie (TT). Drewno jest materiałem ulegającym termicznej degradacji. W warunkach oddziaływania wysokich temperatur konstrukcja drewniana jest poddana jednoczesnym wymuszeniom w formie sił oraz oddziaływaniom termicznym. Oddziaływanie tych dwóch czynników wpływa na rozkład naprężeń w strukturze drewna oraz ogranicza nośność konstrukcji, powodując de kohezję struktury. Celem prezentowanych badań było określenie wpływu podwyższonych temperatur na wytrzymałość materiałów drewnianych i drewnopochodnych. Ponadto, na podstawie wyników badań wytrzymałości przeprowadzono analizę prawdopodobieństwa przetrwania w podwyższonych temperaturach. Próbki do badań wytrzymałości na zginanie statyczne zostały wykonane z drewna fornirowego warstwowego – LVL, drewna sosny pospolitej klejonego warstwowo – GL oraz drewna świerkowego poddanego – TT i niepoddanego modyfikacji termicznej – NTT, w formie prostopadłościanów o wymiarach 20x20x300mm. Oceny wytrzymałości na zginanie dokonano na uniwersalnej maszynie wytrzymałościowej FPZ 100/1 (VEB Thuringer Industriewerk Rauenstein, Germany). Temperatury środowiska pożaru symulowano za pomocą nawiewu gorącego powietrza (GHG 650 LCE). Oceny dokonywano w zakresach temperatur: 20, 50, 100, 150, 200, 230ºC. Uzyskane wyniki posłużyły ocenie niezawodności. W analizie wykorzystano dwuparametrowy rozkład Weibulla. W przypadku materiałów o strukturze laminowanej – LVL i GL zaobserwowano wzrost odchylenia standardowego wytrzymałości na zginanie w kolejnych zakresach temperatur. Wyższe wartości parametru kształtu c Rozkładu Weibulla zostały wykazane dla świerku TT (najwyższe c = 5.58) i NTT(najwyższe c = 3.31).

JAMROZIAK K, KOSOBUDZKI M, PTAK J. **Assessment of the comfort of passenger transport in special purpose vehicles**. Eksploatacja i Niezawodnosc – Maintenance and Reliability 2013; 15 (1): 25–30

The article discusses the issue of comfort, that should characterize a vehicle which has been designed to work under special conditions. If the criteria of ensuring the proper comfort of the passengers of special purpose vehicles are not met, it might lead to a serious disturbances in perception and in other factors that affect the logical behavior. Performance characteristics generated by the body of the vehicle during tests on the range can be assessed only through research and then related to the characteristics of the human body-vehicle system. The presented results concern the assessment of the ride comfort in the selected vehicles under special conditions and capacity of the crew to effectively perform tasks after long-lasting ride.

JAMROZIAK K, KOSOBUDZKI M, PTAK J. **Ocena warunków komfortu transportu osób w pojazdach specjalnego przeznaczenia**. Eksploatacja i Niezawodnosc – Maintenance and Reliability 2013; 15 (1): 25–30

W artykule omówiono zagadnienia dotyczące komfortu, jakim powinien charakteryzować się pojazd do pracy w warunkach szczególnych. Nie spełnienie kryteriów właściwego komfortu u przewożonych osób pojazdami specjalnego przeznaczenia prowadzi do powstawania poważnych zaburzeń na tle percepcji i innych czynników niezbędnych w logicznym postępowaniu. Jedynie na drodze badań możemy ocenić charakterystyki generowane przez nadwozie w testach poligonowych i odnieść to do charakterystyk organizm ludzki-pojazd. Prezentowane wyniki dotyczą oceny charakterystyk komfortu poruszania się wybranymi pojazdami w warunkach szczególnych i możliwości wykonania zadań przez przewożony personel po długotrwałej jeździe.

KRAWCZYK M. **Conditions for unmanned aircraft reliability determination**. Eksploatacja i Niezawodnosc – Maintenance and Reliability 2013; 15 (1): 31–36

In the paper the required level of reliability is determined for several Unmanned Aerial Vehicles developed in Poland in order to get an achievement enabling these vehicles to operate within the Single European Sky. Calculations were made on the basis of an air crash model as well as the model capable to estimate the number of casualties resulting from an aircraft catastrophe. The provided examples allow us to specify Tactical and Technical Conditions pertaining in particular to the area of the operation of the aforementioned aircraft.

KRAWCZYK M. **Przesłanki determinujące niezawodność samolotów bezpilotowych**. Eksploatacja i Niezawodnosc – Maintenance and Reliability 2013; 15 (1): 31–36

W pracy wyznaczono niezbędną niezawodności kilku opracowanych w Polsce samolotów bezpilotowych, której osiągnięcie umożliwia ich eksploatację w połączonej przestrzeni powietrznej. Obliczenia prowadzone były wg modelu katastrofy powietrznej oraz modelu pozwalającego na oszacowanie liczby ofiar na skutek rozbicia się samolotu. Podane przykłady pozwalają na sprecyzowanie Warunków Taktyczno – Technicznych, w szczególności dotyczących obszaru eksploatacji tychże samolotów.

BAIER A, ZOLKIEWSKI S. **Initial research of epoxy and polyester warp laminates testing on abrasive wear used in car sheathing**. Eksploatacja i Niezawodnosc – Maintenance and Reliability 2013; 15 (1): 37–43

The subject of the work is to present the preliminary investigations over epoxy and polyester warp laminates and its abrasion. The exploitation of various types of containers used in industry is often connected with its usage of composite materials. The composite materials are exposed to tribological wear. Basing on reality and the common tribology wear hazard testing on abrasive wear of composite materials is well-founded and significant in technical and technological point of view. The results of the experimental part of the work are only the substitute of the widely presented researches over composite materials used in the structure of the side of the freight wagons. There are presented the results of the laminates, performed in the laboratory conditions depicting the real work conditions of freight wagons. There were compared the exemplified parameters of the geometrical profile of the structure mass losses of the investigated samples, both the epoxy and polyester and other used hardeners.

BAIER A, ZOLKIEWSKI S. **Badania wstępne ścieralności laminatów o osnowie epoksydowej i poliestrowej do zastosowania w budowie poszycia wagonu towarowego**. Eksploatacja i Niezawodnosc – Maintenance and Reliability 2013; 15 (1): 37–43

Praca dotyczy badań wstępnych ścieralności laminatów o osnowie epoksydowej i poliestrowej. Eksploatacja różnego rodzaju zbiorników do zastosowań przemysłowych często wiąże się z użyciem materiałów kompozytowych narażonych na zużycie tribologiczne. Zasadne jest więc podjęcie istotnych z technicznego i technologicznego punktu widzenia badań ścieralności tych materiałów. Prezentowane w pracy wyniki badań eksperymentalnych są jedynie częścią szeroko zakrojonych badań materiałów kompozytowych mających zastosowanie w budowie burt wagonów towarowych. Przedstawiono wyniki badań laminatów, przeprowadzonych na autorskim stanowisku laboratoryjnym do porównawczego badania zużycia ściernego odzwierciedlającego warunki pracy wagonu towarowego. Zestawiono przykładowe parametry struktury geometrycznej profilu oraz ubytki masowe badanych próbek zarówno w przypadku próbek epoksydowych jak i poliestrowych oraz różnych, zastosowanych utwardzaczy.

CHŁOPEK Z, LASOCKI J. **Comprehensive environmental impact assessment of the process of preparation of bioethanol fuels of the first and second generation**. Eksploatacja i Niezawodnosc – Maintenance and Reliability 2013; 15 (1): 44–50.

The paper provides some information regarding comprehensive evaluation of the environmental hazard caused by the operation of automotive vehicles with internal combustion (IC) engines powered by bioethanol fuel. It presents the assumptions made for the life cycle assessment (LCA) of the environmental impact of fuel, carried out according to the Well-to-Wheel (WtW) method, where the fuel preparation stage, including the acquisition of raw materials as well as the production, transport, and distribution processes, and the vehicle operation stage are taken into account. The technologies and raw materials used to make bioethanol of the first and second generation have been presented and compared with each other. Results of research on greenhouse gas (GHG) emissions and non-renewable energy input in the process of preparation of bioethanol fuels of the first and second generation have been analysed. Nine versions of the production process, differing from each other in the process methods used and the types of the biomass processed, have been examined.

CHŁOPEK Z, LASOCKI J. **Kompleksowa ocena oddziaływania na środowisko procesu przygotowania paliw bioetanolowych pierwszej i drugiej generacji**. Eksploatacja i Niezawodnosc – Maintenance and Reliability 2013; 15 (1): 44–50.

W pracy przedstawiono informacje na temat kompleksowej oceny zagrożenia środowiska przez eksploatację pojazdów samochodowych z silnikami spalinowymi zasilanymi paliwem bioetanolowym. Przedstawiono założenia analizy ekologicznej cyklu istnienia paliwa według metody Well–to–Wheel, uwzględniającej etap przygotowania paliwa, składający się z pozyskiwania surowców, wytwarzania, transportu i dystrybucji, oraz etap użytkowania pojazdów. Zaprezentowano i porównano technologie oraz surowce stosowane w wytwarzaniu bioetanolu pierwszej i drugiej generacji. Przeanalizowano wyniki badań emisji gazów cieplarnianych oraz zużycia energii ze źródeł nieodnawialnych w procesie przygotowania paliw bioetanolowych pierwszej i drugiej generacji. Rozważono dziewięć wariantów przebiegu procesu wytwarzania, różniących się zastosowaną technologią i rodzajem przetwarzanej biomasy.

MARKOWSKI T, MUCHA J, WITKOWSKI W. **FEM analysis of clinching joint machine's C-frame rigidity**. Eksploatacja i Niezawodnosc – Maintenance and Reliability 2013; 15 (1): 51–57.

This paper presents the results of FEM analysis for clinching joint machine's C-frame. Several versions of frame geometry were accounted for when analyzing the straining of material, including the mass reduction. The purpose of this FEM simulation was to determine the effect of mass reducing material recess on the structure rigidity. ABAQUS software was used to analyze the frame material straining from both the qualitative and quantitative point of view.

MARKOWSKI T, MUCHA J, WITKOWSKI W. **Analiza MES sztywności C- ramy urządzenia do wytwarzania połączeń przetłoczeniowych**. Eksploatacja i Niezawodnosc – Maintenance and Reliability 2013; 15 (1): 51–57.

W artykule przedstawiono wyniki symulacji MES C-kształtnej ramy urządzenia do montażu połączeń konstrukcji blaszanych. Podczas analizy wytężenia materiału ramy wzięto pod uwagę kilka wariantów wykonania jej geometrii, uwzględniając zmniejszenie masy. Celem symulacji MES było wykazanie wpływu postaci wybrań materiału zmniejszających jej masę na sztywność takiej konstrukcji. Do tak postawionego zadania użyto programu ABAQUS umożliwiającego ilościową i jakościową ocenę wytężenia materiału ramy.

TOR-ŚWIĄTEK A, SAMUJŁO B. **Use of thermo vision research to analyze the thermal stability of microcellular extrusion process of poly(vinyl chloride)**. Eksploatacja i Niezawodnosc – Maintenance and Reliability 2013; 15 (1): 58–61.

Essential role in polymer processing takes processing conditions i.e. temperature, pressure, screw rotational speed and time. During the polymer modification in cellular and microcellular extrusion process significant changes in the process ensue. Influence of this two factors caused also another changes in properties and physical structure of obtained extruded products. Because of that, proper selection of processing conditions, specially temperature, machines and equipment parameters is necessary. Is such a case, process will be effective and stable.

TOR-ŚWIĄTEK A, SAMUJŁO B. **Wykorzystanie badań termowizyjnych do analizy stabilności procesu wytłaczania mikroporującego poli(chlorku winylu)**. Eksploatacja i Niezawodnosc – Maintenance and Reliability 2013; 15 (1): 58–61.

Znaczącą rolę w procesach przetwórstwa tworzyw odgrywają warunki procesu takie jak temperatura, ciśnienie, szybkość obrotowa ślimaka, czas. Podczas modyfikacji tworzywa polimerowego w procesie wytłaczania porującego oraz mikroporującego na skutek działania podwyższonej temperatury oraz jednocześnie działania poroforu następują istotne zmiany w przebiegu procesu wytłaczania. Kolejną zmianą, jaką niesie za sobą wpływ obu czynników jest zmiana właściwości oraz struktury fizycznej otrzymanych wytworów. Z tego względu konieczny staje się taki dobór poszczególnych warunków przetwórstwa, w tym szczególnie temperatury oraz parametrów maszyn i urządzeń przetwórczych, aby proces mógł być prowadzony efektywnie i stabilnie.

KRÓLCZYK G, GAJEK M, LEGUTKO S. **Predicting the tool life in the dry machining of duplex stainless steel**. Eksploatacja i Niezawodnosc – Maintenance and Reliability 2013; 15 (1): 62–65.

This paper examines the influence of cutting parameters, namely cutting speed, feed and depth of cut onto tool life in DSS turning process. The study included developing a mathematical model to determine the tool life. Verification research has been carried out on CNC lathe, hence the test plan has been adjusted to the possibility of programmable machines controlling GE Fanuc series 0 - T. The comparison of results obtained by given experimental plan was performed in industrial company.

KRÓLCZYK G, GAJEK M, LEGUTKO S. **Prognozowanie okresu trwałości ostrza w obróbce na sucho stali nierdzewnej duplex**. Eksploatacja i Niezawodnosc – Maintenance and Reliability 2013; 15 (1): 62–65.

W artykule przedstawiono wpływ parametrów obróbki, a mianowicie prędkości skrawania, posuwu i głębokości skrawania na okres trwałości ostrza w procesie toczenia stali duplex. Badania obejmowały opracowanie modelu matematycznego dla określenia okresu trwałości ostrza skrawającego. Badania weryfikacyjne wykonywano na tokarce sterowanej numerycznie, stąd plan badań dostosowany został do możliwości programowych maszyny ze sterowaniem GE Fanuc seria 0 – T. Porównanie wyników przeprowadzono w warunkach produkcyjnych.

TANASIJEVIĆ M, IVEZIĆ D, JOVANČIĆ P, IGNJATOVIĆ D, BUGARIĆ U. **Dependability assesment of open-pit mines equpment – study on the bases of fuzzy algebra rules**. Eksploatacja i Niezawodnosc – Maintenance and Reliability 2013; 15 (1): 66–74.

This article aims to present a new approach for assessing of maintenance support and model for its introduction into dependability concept. Process of expertise judgment is used directly for assessing the organization of maintenance support and it is shown in the form of linguistic variables as appropriate fuzzy sets. For the introduction of maintenance support into dependability, fuzzy composition is used. Since reliability and maintainability are also influential indicators of dependability, it was necessary to develop a methodology for fuzzification of corresponding reliability and maintainability probability functions. This methodology is developed by using empirical scaling. The proposed approach has been applied to different types of bulldozers, as a usual technical system that operates at open pit mine.

TANASIJEVIĆ M, IVEZIĆ D, JOVANČIĆ P, IGNJATOVIĆ D, BUGARIĆ U. **Ocena niezawodności sprzętu wykorzystywanego w kopalniach odkrywkowych – badania oparte na regułach rozmytej algebry**. Eksploatacja i Niezawodnosc – Maintenance and Reliability 2013; 15 (1): 66–74.

Niniejszy artykuł ma na celu przedstawienie nowej metody oceny wspomagania obsługi oraz modelu opisującego jej zastosowanie w odniesieniu do pojęcia niezawodności. Proces wydawania opinii eksperckiej wykorzystano bezpośrednio do oceny organizacji wspomagania obsługi i przedstawiono go w postaci zmiennych lingwistycznych jako odpowiednie zbiory rozmyte. W celu odniesienia wspomagania obsługi do niezawodności, posłużono się kompozycją zbiorów rozmytych. Ponieważ nieuszkadzalność i obsługiwalność są również ważnymi wskaźnikami niezawodności, konieczne było opracowanie metodologii rozmywania odpowiednich funkcji prawdopodobieństwa działania i obsługi. Niniejsza metodologia została opracowana przy użyciu skalowania empirycznego. Proponowane podejście zastosowano w odniesieniu do różnych typów spychaczy, składających się na przeciętny układ techniczny funkcjonujący w obrębie kopalni odkrywkowej.

CHŁOPEK Z. **Research on energy consumption by an electrically driven automotive vehicle in simulated urban conditions**. Eksploatacja i Niezawodnosc – Maintenance and Reliability 2013; 15 (1): 75–82.

In recent years, dynamic development of electric drives in automotive applications has been taking place. Electrically driven vehicles are considered to offer a possibility of solving the most important ecological problems posed by motorisation. The paper presents results of testing the energy consumption by an electric car in conditions corresponding to actual operation of such vehicles, i.e. at drive tests where urban, extra –urban, and traffic jam conditions were simulated. The disitance energy consumption and total vehicle efficiency were determined at drive tests. An energy consumption characteristic was determined in pseudorandom conditions of urban operation of the car, with employing the Monte Carlo method for this purpose.

CHŁOPEK Z. **Badania zużycia energii przez samochód elektryczny w warunkach symulujących jazdę w mieście**. Eksploatacja i Niezawodnosc – Maintenance and Reliability 2013; 15 (1): 75–82.

W ostatnich latach następuje dynamiczny rozwój napędów elektrycznych w motoryzacji. W samochodach elektrycznych upatruje się możliwości rozwiązania najważniejszych problemów ekologicznych motoryzacji. W pracy przedstawiono wyniki badań zużycia energii przez samochód elektryczny w warunkach odpowiadających rzeczywistej eksploatacji takich pojazdów, mianowicie w testach jezdnych symulujących ruch w miastach, poza miastami, a także w zatorach drogowych. Wyznaczono drogowe zużycie energii i sprawność ogólną pojazdu w testach jezdnych. Wyznaczono charakterystykę zużycia energii w warunkach pseudoprzypadkowych użytkowania samochodu w mieście. Wykorzystano do tego celu metodę Monte Carlo.

KULINOWSKI P. **Simulation studies as the part of an integrated design process dealing with belt conveyor operation**. Eksploatacja i Niezawodnosc – Maintenance and Reliability 2013; 15 (1): 83–88.

This article presents simulation studies of transient working states of a conveyor as an indispensable, important part of the integrated process of its design. Simplified block diagrams and equations describe the structure of a dynamic model of a belt conveyor and a gravity take-up system. Results of simulation studies on the belt conveyor model have been compared to results of industrial tests carried out at the site of the conveyor operation using a mobile measurement system. The results of verifying the dynamic model have confirmed its utility for analysing dynamic phenomena occurring when the conveyor is operated, and demonstrated the complete suitability of simulation studies in the integrated process of designing belt conveyors.

KULINOWSKI P. **Badania symulacyjne jako element zintegrowanego procesu projektowania w aspekcie eksploatacji przenośników taśmowych**. Eksploatacja i Niezawodnosc – Maintenance and Reliability 2013; 15 (1): 83–88.

W niniejszym artykule przedstawiono badania symulacyjne nieustalonych stanów pracy przenośnika, jako nieodłączną i istotną część zintegrowanego procesu jego projektowania. Za pomocą uproszczonych schematów blokowych i równań, opisano budowę dynamicznego modelu przenośnika taśmowego oraz grawitacyjnego urządzenia napinającego taśmę. Wyniki testów symulacyjnych modelu przenośnika taśmowego porównano z wynikami badań przemysłowych, przeprowadzonych w miejscu eksploatacji przenośnika z wykorzystaniem mobilnego systemu pomiarowego. Wyniki weryfikacji modelu dynamicznego potwierdziły jego użyteczność w analizie zjawisk dynamicznych występujących podczas pracy przenośnika oraz wykazały pełną przydatność badań symulacyjnych w zintegrowanym procesie projektowania przenośników taśmowych.

Article citation info:
LOSKA A. Exploitation assessment of selected technical objects using taxonomic methods. Eksploatacja i Niezawodnosc – Maintenance and Reliability 2013; 15 (1): 1–8.

Andrzej LOSKA

# EXPLOITATION ASSESSMENT OF SELECTED TECHNICAL OBJECTS USING TAXONOMIC METHODS

# EKSPLOATACYJNA OCENA WYBRANYCH OBIEKTÓW TECHNICZNYCH Z ZASTOSOWANIEM METOD TAKSONOMICZNYCH*

*The article is an attempt to answer the formulated problems in industrial enterprises problems on practical aspects of use of specific measures to assess exploit of technical facilities. In this regard, bibliography study has been conducted, including an overview of opportunities to develop the values of selected exploitation characteristics, as well as industrial research as a need analysis of technical departments in the assessment of their performance. As a result of these studies and their conclusions method of preliminary mutual exploitation evaluation has been developed, based on the values of standardized and aggregated ranks of technical objects, in the context of exploitation measurements calculated. This method, as well as an example of its use, relating to a selected network technical system, are the subject of further sections of this article.*

***Keywords**: exploitation assessment, numerical taxonomy, rank.*

*Artykuł jest próbą odpowiedzi na formułowane w przedsiębiorstwach przemysłowych problemy dotyczące praktycznych aspektów wykorzystania określonych miar do oceny eksploatowania obiektów technicznych. W tym zakresie, przeprowadzono badania literaturowe obejmujące przegląd możliwości kształtowania wartości wybranych cech eksploatacyjnych, a także badania przemysłowe dotyczące analizy potrzeb służb technicznych przedsiębiorstw w zakresie oceny ich funkcjonowania. Wynikiem przeprowadzonych badań i sformułowanych w tym zakresie wniosków, została opracowana metoda wstępnej wzajemnej oceny eksploatacyjnej w oparciu o wartości normowanych i zagregowanych rang obiektów technicznych w świetle wyznaczanych miar eksploatacyjnych. Metoda ta, jak również przykład jej zastosowania, odnoszący się do wybranego sieciowego systemu technicznego są przedmiotem dalszej treści tego artykułu.*

***Słowa kluczowe**: ocena eksploatacyjna, taksonomia numeryczna, rangowanie.*

## Introduction

Reliable valuation of maintenance tasks is one of key criteria of the proper functioning of the maintenance departments in any industrial enterprise. It means the necessity of determining the values of selected features, and consequently the possibility of shaping the decision-making processes relating to implementation of maintenance work.

In industrial practice, it is used exploitation measures (indicators) in a wide variety. Their values refer to the individual technical objects, as well as to maintenance organization's activities. This variety can significantly influence the choice of particular set of features, in specific individual organizational and technical circumstances: in a positive way – by a clear reflection of assessment of exploitation policies, in a negative way – by too much emphasizing less important trends, and active "shaping" value of certain measures.

From a mathematical point of view, the exploitation problems of identified and formulated in industrial enterprises should be considered in the category of complex phenomena and processes, that require implementation of the works of technical, organizational and economic nature in time and spatial environment. This complexity is characterized by many features that translate into measures with different titers and scale rows, which means that they are mutually incomparable. Such comparability seems to be possible after reducing key measures to the so-called. "common denominator" based on standardization methods, and then their synthesis with the use of aggregation methods.

This article is an attempt to solve such the problem through the elaboration of rank method of technical objects in terms of the exploitation features. The resulting exploitation assessing method is one of the key elements of research, conducted by the author of this article, in the use of scenario techniques in modelling exploitation events and processes.

(*) Tekst artykułu w polskiej wersji językowej dostępny w elektronicznym wydaniu kwartalnika na stronie ***www.ein.org.pl***

## 2. Classification and characteristics of selected exploitation assessment models

There are several mathematical models underlying the quantitative assessment of exploit of technical objects and functioning of the maintenance organization. The individual sets of measurements are the subject of many publications, in the form:

- separate bibliography items, mostly in the form of sheet workbooks, containing an ordered list and description of specific measures, including in [26, 27, 32, 34, 36],
- parts of methods and techniques of maintenance management, as addition to the description of maintenance strategies and maintenance management systems, including in [2, 4, 9, 12, 14, 17, 22, 23, 33],
- parts of maintenance strategies and systems applications into certain industrial enterprises, including in [7, 11, 18],
- modes of interpretation (usually mathematical) and attempts to apply selected exploitation measures, including in [1, 3, 15, 31].

From a practical industrial point of view, developments and studies assigned to groups third and fourth are becoming especially importance. These include the concepts and practical solutions for the use of well-known mathematical models in practical applications. This is a direct and most important subject of the needs and expectations the majority of industrial centres.

Based on the diagnosis results presented in [20] review and analysis has led to the distinguish of these models which are most important, both in theoretical aspects – bibliography, and practical - the industrial. There are three general models in thisarea:

a) reliability model [5, 10, 12, 23, 28],
b) Overall Equipment Effectiveness (OEE) model [22, 33, 34],
c) Key Performance Indicators model (KPI) [27, 32].

### 2.1. The computable reliability model

The reliability model allows us to determine exploitation measures in statistical approach. In industrial practice, it is the result of these maintenance strategies, in which decisions concerning the possibility of use technical objects and the dates and scopes of maintenance tasks are directly related to the time analysis of the statistical sight of technical objects functioning, described by group models.Reliability model is reflected by the measures, that relate to:

a) exploitation objects in terms of technical – measures that are the result of identification of the technical condition (in the form of probability) referenced to particular classes (for example, the reliability function in terms of the exponential distribution [10, 28], failure intensity [5], or technical availability ratio [12]),
b) exploitation objects in terms of both – organizational and technical – measures which result from the identification of the technical condition, as well as organizational and economic activities of exploitation departments (eg. defined by [23] MTBF, MTTR or MFOT).

### 2.2. The computable Overall Equipment Effectiveness model (OEE)

The Overall Equipment Effectiveness model is the most important component of quantitative evaluation of TPM. Due to the high flexibility, this model is also used in these companies that have not implemented this strategy. It expresses the overall efficiency of maintenance by three main factors(Tab. 1).

It should be noted that due to the method of OEE calculating (product of the sub-indices), it is important not so much the absolute value of the OEE, but the conclusions resulting from the way of obtaining it.Mathematical interpretation of the OEE should have a geometric character. In particular, OEE can be presented in three dimensions, where the axes represent individual sub-indices. In this approach, presenting OEE as a vector, you can make conclusions and decisions arising from this model, which should relate to:

- absolute valueof OEE,
- influence of individual factors on the value of OEE,
- direction and value of changeof OEE.

### 2.3. The computable Key Performance Indicators model (KPI)

The Key Performance Indicators model includes a set of measures of productivity and efficiency. These measures allow for a comprehensive assessment of the implementation of the maintenance organization's objectives, meaning that in practice they must be closely related to the maintenance strategy of the company.From the examinations made, we can conclude that there are many varieties of KPI model, which are related to specific application. Therefore, for several years there has been a need to harmonize both the measures included in this model, as well as the interpretation of particular indicators and the general model of KPI. On this basis standard EN 15341:2007 (Maintenance – Maintenance Key Performance Indicators) has been developed, which contains a unified set of measures as part of the KPI model [27].

The standard contains 72 indicators, along with a detailed interpretation of the constituent components. These indicators may be subject to interpretation and comparison with the values obtained in other companies of the industry. Selected examples of indicators are:

E1 – total relative maintenance cost for technical object:

$$E1 = \frac{total\ maintenance\ cost}{asset\ replacement\ value} \tag{4}$$

T7 – availability of objects for preventive maintenance:

$$T7 = \frac{total\ operating\ time}{total\ operating\ time + downtime\ related\ to\ planned\ and\ scheduled\ maintenance} \tag{5}$$

*Table 1. Indicators of Overall Equipment Effectiveness OEE [22]*

| Availability | Performance efficiency | Rate of quality products |
|---|---|---|
| $D = \frac{t_d - t_p}{t_d}$ (1) | $E = \frac{t_c \cdot n}{t_o}$ (2) | $J = \frac{n-d}{n}$ (3) |
| $t_d$ - loading time<br>$t_p$ - downtime | $t_c$ - theoretical cycle time<br>n - processed amount<br>$t_o$ - operatingtime | n - processed amount<br>d - defect amount |
| $OEE = D \cdot E \cdot J$ | | |

## 3. The concept of exploitation assessment of technical objects

For complex organizational and technical conditions of exploitation systems and not very detailed explicit expectations of potential managers, variety of measures, can lead to:

- ambiguity of measures interpretation of the impact of individual factors on the exploitation efficiency of the objects understood in a broad sense,
- substantively unreasonable emphasize of selected aspects in contrast to other in the context of maintenance policy of the company.

In other words, for each maintenance indicator, there must be reasonably necessary to its determination, and also position and weight of each of the measures under consideration in terms of technical, organizational or economic are important.

Described factors generate the need to develop, verify and practical application of such assessment models, which include the necessary but also sufficient number and range of measures, in specific organizational and technical conditions Their importance shall be more appropriate for the purpose of company, and less to the particular interests of individual persons or organizational units.

The conclusions resulting from the bibliographic analysis and industrial studies are the starting point to develop a method of exploitation assessment based on recognized and defined theoretical (model) conditions and limitations as well as observations and practical experience (industrial).

Proposed by the author method uses elements of taxonomic methods that are known and applied in the field of socio-economic sciences [8, 16, 25]. In this case they are helpful in selecting, organizing, and grouping of the analyzed phenomena and events in the fields: space, essential and timing. Effect of these is transformation of diagnostic variables describing the various parts of the analyzed phenomena in a dispersed way in a synthetic variable (aggregated), which is kind of resultant considered events and exploitation processes. In this view, the construction of the exploitation assessment procedure consists of three key aspects:

- selection and hierarchization of diagnostic features (diagnostic feature is here assumed broader than the typical terms of exploitation and reliability, so by [25] it is the potential and the initial feature that allows to explain a particular phenomenon),
- standardization of dissimilar diagnostic variables, in order to achieve uniform titers,
- aggregation of standardized variables, to output a synthetic variable (aggregated) for the determining the values of rank of comparable technical objects.

Selection allows you to isolate those features describing the technical objects and exploitation processes that can have a significant role in the assessment process. The second criterion for features selection is the availability of measurement. In the aspect of practical use of measures to evaluate exploitation of technical object and exploitation processes, there can be distinguished a set of several key features, that would be the basis for the selection. Such features, that have been characterized in detail [12, 19] and systematized in [38], should include: condition, reliability, quality, functionality, efficiency, maintainability diagnosis. These features should be rather treated as a groups, than a single elements. Within each group, there can be localized measures (indicators) describing and evaluating some exploitation aspects of technical objects as well as maintenance departments functioning.

Hierarchization is a part of the arrangement of selected features in order to determine explicit diagnostic variables and to specify their nature. In the exploitation area, nature of the diagnostic variables allows you to organize the attributes into three groups (by [8]):

- stimulants, for which high values of characteristics are desired (eg. mean time between failures – MTBF),
- destimulants, for which low values of characteristics are desired (eg. cost of emergency work),
- nominants, for which "normal" values of characteristics are desired (eg. costs of corrective work as a result of preventive tasks).

Action in relation to the harmonization of the nature of the variables should be carried out according to the postulate of uniform preference, which is to extract and assign attributes to one of the above categories, choice of the trend and to make so called the inverse transformation of those features which have been classified into groups with opposing trends. In other words, destimulants can be converted to stimulants based on established limits (for example, the theoretical values or minimum and maximum values collected in the entire history of measurements made). In relation to nominant, we can assume that any deviation from the values of normal level is an unfavuorable phenomenon. Therefore, such a transformation is necessary to establish their level of "normal" and then involves two steps: transformations in destymulants, which are features of absolute deviation from the level of "normal" and then in the stimulants.

The next step, after the selection and ordering of diagnostic variables, is the normalization of features, that results from the dissimilar values of the variables. This process should proceed according to the additivity postulate [16], which means that it is necessary to transform the original diagnostic variables to get a value-free titers and standardized in term of magnitude order. According to [16] such a process can be carried by the following general relation:

$$x_i' = \left( \frac{x_i - A}{B} \right)^p \quad (i = 1, \ldots, n) \tag{6}$$

where: $x'_i$ – output normalized value of the i-th realization of the variable,
$x_i$ – unnormalized value of the i-th realization of the variable,
n – number of observations,
A, B, p – parameters with values depended on the method of normalization.

Adequate normalization methods, including standardization, unitarization or quotient transformation with a reference value, were discussed in detail in the, including [8, 16].

The last step is the aggregation. This is process, which leads directly to obtain a synthetic variable. In the approach considered here, it is rank describing the value of the individual technical objects, in terms of analyzed events and exploitation processes. Aggregation is usually carried out on the basis of the so-called additive formulas [16]. They represent different forms of sum of the products of standardized features and corresponding weights. Typical procedure of aggregation consist of looking for the numerical values of following vector of the aggregate:

$$[Q_i] = \begin{bmatrix} Q_1 \\ Q_2 \\ \vdots \\ Q_n \end{bmatrix} i = (1, 2, \ldots, n) \tag{7}$$

where: $Q_i$ – aggregate value of the function determined for the i-th object.

A typical form of aggregation is the correlation function [37]:

$$Q_i = \sum_{j=1}^{s} z_{ij}\omega_j i = (1,2,\ldots,n), \omega_j \epsilon R_+ \quad (8)$$

where: $z_{ij}$ – value of the i-th assessment of the j-th variant,
$\omega_j$ – weight value.

Another example of the aggregation function is its weighted value referenced to the arithmetic mean [24]:

$$Q_i = \frac{\sum_{j=1}^{s} z_{ij}\omega_j}{\sum_{j=1}^{s} \omega_j} i = (1,2,\ldots,n), \omega_j \epsilon R_+ \quad (9)$$

The equations (8) and (9) show, that important role in the aggregation process fulfills the weights system, which can be based on expert opinion – on the one hand, as well as statistical procedures with the use of collected information on the variables – on the other hand.

## 4. The rank method of technical objects in view of their exploitation characteristics

The methodological and conceptual assumptions about the possibilities and needs of the exploitation assessment became the basis for a rank process of selected technical objects. The purpose of rank process is exploitation ordering of equivalent technical objects based on the history of events and processes with all their circumstances. There have been specified following initial conditions:

- the basis of rank method includes broad set of measures,as a determinant of a comprehensive exploitation assessment of the technical objects and maintenance organization functioning,
- proposed rank method is based on general assumptions of taxonomic methods (described earlier),
- all weights assigned to each measurement and decision-making levels and the way of measures organizing in the assessment table, have been defined in a subjective manner, based on expertise and consultation,
- rank method subjects to peer evaluation (peer comparison), equivalent technical objects (in terms of maintenance management) for analysis therefore, itself rank value is not important but it is important its relation to the ranks of other objects.

The first step is selection of measures (indicators) representing a quantitative basis for assessing the exploitation technical objects. Based on recognition made, it should be noted clearly, that a certain set of measures is individual in each specific case, depending on the detailed technical and organizational conditions of the company and its maintenance department. Independently of selection of specific measures, classification is a key aspect of the method. At this point, the measures arrangement was made in three main categories:

- economic measures (indicators), which express the cost value of the selected exploitation aspects,
- technical measures (indicators), which express the time value of the selected exploitation aspects,
- organizational measures (indicators), which express the non-technical (around of exploitation) value of the selected exploitation aspects.

The collection of sample measures, that have been selected based on [27] and arranged according to the above system, is shown in Tab. 2.

The selected measures of performance describe in a quantitative manner the various aspects, and thus, they are expressed in different units, mutually not comparable. According to the basic assumptions of the method, it is equivalence of all the necessary measures, in other words, these measures must be reduced to the same rating scale. In addition, we are dealing here with both stimulants and destimulants. It is therefore proposed to perform a normalization process, including unification of values, taking into account:

- express the value of assessment in relative terms (related to the maximum and minimum measure values obtained in the entire history of measuring in the organizational and technical system),
- express the value of assessmentin the range <0 , 10>, which will allow to reduce individual measures from the appointed form (eg. zł/m$^3$) to the not appointed form in one range (od 0 do 10), thus possible to compare,
- establish a uniform trend of the indicators (according to the author, a better solution is a positive trend - stimulants - greater value is better).

Based on the above criteria, you can determine the value of assessment for exploitation measures:

1. For the measures of a positive trend – stimulants:

*Table 2. Sample exploitation measures (own ellaboratoin based on [27])*

| Economic measures | Technical measures | Organizational measures |
|---|---|---|
| The measure (indicator) of operation costs related to the production quantity<br>The measure (indicator) of operation costs and lack of service and production quantity<br>The measure (indicator) of personnel costs related to the total maintenance costs<br>The measure (indicator) of material resources use cost<br>The measure (indicator) of specialized tools and equipment use cost<br>The measure (indicator) of sharing corrective tasks costs in the total maintenance costs<br>The measure (indicator) of sharing preventive tasks costs in the total maintenance costs<br>The measure (indicator) of sharing diagnosis tasks costs in the total maintenance costs<br>The measure (indicator) of sharing breakdown tasks costs in the total maintenance costs | The measure (indicator) of the breakdown actions time<br>The measure (indicator) of the corrective actions time<br>The measure (indicator) of the preventive actions time<br>The measure (indicator) of the diagnosis actions time<br>The measure (indicator) of mean time between failures (MTBF)<br>The measure (indicator) of mean time to repear (MTTR)<br>The measure (indicator) of mean force outage time (MFOT)<br>The measure (indicator) of the technical object availability<br>The measure (indicator) of the maintenance tasks effectiveness<br>The measure (indicator) of the effectiveness of maintenance tasks planning | The measure (indicator) of maintenance employees participation rate in a total amount of company's own staff<br>The measure (indicator) of maintenance indirect employees participation rate in the total amount of maintenance employees<br>Potential ratio of staff in the planning process<br>The measure (indicator) of number of maintenance activities with accidents<br>The measure (indicator) of number of maintenance activities with maintenance hazards<br>The measure (indicator) of number of maintenance activities with environmental events<br>The measure (indicator) of number of maintenance activities with environmental hazards<br>Potential ratio of staff in the preventive tasks<br>Potential ratio of staff in the corrective tasks<br>Potential ratio of staff in the diagnosis tasks<br>Potential ratio of staff in the breakdown tasks<br>The measure (indicator) of maintenance employees overtime |

$$OC_{is} = \frac{10 \cdot M_i}{M_{i_{\max}} - M_{i_{\min}}} \tag{10}$$

where: $OC_i$ – selected (i-th) exploitation assessment,
$M_i$ – selected (i-th) exploitation measure,
$M_{imax}$ – maximum value of exploitation measure in the whole history measuring in the given organizational and technical system,
$M_{imin}$ – minimum value of exploitation measure in the whole history measuring in the given organizational and technical system.

It is assumed that for all measures considered here, the minimum value $M_{imin} = 0$, so:

$$OC_{is} = \frac{10 \cdot M_i}{M_{i_{\max}}} \tag{11}$$

2. For the measures of a negative trend - stimulants- destimulants:

$$OC_{id} = 10 - \frac{10 \cdot M_i}{M_{i_{\max}} - M_{i_{\min}}} \tag{12}$$

for $M_{imin} = 0$:

$$OC_{id} = 10 - \frac{10 \cdot M_i}{M_{i_{\max}}} \tag{13}$$

Determined values can be ordered in the table of exploitation measures (Tab. 3).

*Table 3. Exploitation assessment table*

| | Economic measures weight $k_1$ | Technical measures weight $k_2$ | Organizational measures weight $k_3$ |
|---|---|---|---|
| Level 1 weight $p_1$ | $a_{11}$ | $a_{12}$ | $a_{13}$ |
| | $OC_{E1},...,OC_{Em}$ (sum of the weights is 1) | $OC_{T1},...,OC_{Tm}$ (sum of the weights is 1) | $OC_{O1},...,OC_{Om}$ (sum of the weights is 1) |
| Level 2 weight $p_2$ | $a_{21}$ | $a_{22}$ | $a_{23}$ |
| | $OC_{Em+1},...,OC_{En}$ (sum of the weights is 1) | $OC_{Tm+1},...,OC_{Tn}$ (sum of the weights is 1) | $OC_{Om+1},...,OC_{On}$ (sum of the weights is 1) |
| Level 3 weight $p_3$ | $a_{31}$ | $a_{32}$ | $a_{33}$ |
| | $OC_{En+1},...,OC_{Ep}$ (sum of the weights is 1) | $OC_{Tn+1},...,OC_{Tp}$ (sum of the weights is 1) | $OC_{On+1},...,OC_{Op}$ (sum of the weights is 1) |

where:
$OC_{Ei}$ - exploitation assessment of an economic type,
$OC_{Ti}$ - exploitation assessment of an technicaltype,
$OC_{Oi}$ - exploitation assessment of an organizational type

This table includes:

- types of exploitation assessments (economic, technical, organizational), the sum of the weights must be equal to one($k_1 + k_2 + k_3 = 1$),
- decision-making levels, the weights have the following values: $p_1 = 4$, $p_2 = 2$, $p_3 = 1$.

From the data included in the assessment table (Tab. 3), it should be determined:

1. Exploitation assessment matrix:

$$W = \begin{bmatrix} a_{11} & a_{12} & a_{13} \\ a_{21} & a_{22} & a_{23} \\ a_{31} & a_{32} & a_{33} \end{bmatrix} \tag{14}$$

where:

$$a_{ij} = \sum_{i=1}^{N} OC_{ij} \cdot g_i \tag{15}$$

$$\sum_{i=1}^{N} g_i = 1 \tag{16}$$

$a_{ij}$ – standarized weighted sum of exploitation assessment calculated for the object,
$OC_{ij}$ – exploitation assessment,
$g_i$ – weight value referred to the single assessment.

2. Vector of tasks category:

$$K = \begin{bmatrix} k_1 \\ k_2 \\ k_3 \end{bmatrix} \tag{17}$$

where:
K – the set of weight related to the category (economic, technical, organizational),
$k_i$ – weight of the i-th category.

Vector of category enables you to define weights for certain types of assessments. This allows the proper definition of the importance of company maintenance. For example:

- high value of economic category weight at lower value of technical and organizational category weight may point to carry out maintenance activities with particular emphasis on the resulting cost,
- high value of technical category weight at lower value of economic and organizational category weight means the implementation of maintenance activities, reliability and efficiency improvement with less emphasis on cost and number of man hours.

The values of the category vector can be shaped in any way, with the assumption that:

$$\sum_{i=1}^{N} k_i = 1 \tag{18}$$

3. Vector of decision-making levels:

$$P = \begin{bmatrix} p_1 \\ p_2 \\ p_3 \end{bmatrix} \tag{19}$$

where:
$p_i$ – weight of the i-th level of the organizing company:
$p_1$ – weight of company level,
$p_2$ – weight of technical departmentlevel,
$p_3$ - weight of maintenance department level.

Vector of decision-making levels allows you to emphasize these assessments that in the decision making process have a specific meaning in relation to company maintenance policy This role results main-

ly from maintenance strategy as well as organizational and decision-making structures, that are built on the basis. In particular, the vector includes:

- weight of company level ($p_1$) - taking into account the strategic decisions and the associated assessment, taking into account the strategic decisions and the associated assessment directly related to operational policy and the functioning of the maintenance department as a whole,
- weight of technical department level - taking into accountdecisions and the related assessment of the planning and implementation of maintenance activities,
- weight of maintenance department level - taking into account operating decisions and the related assessment of the specific ways of implementing of maintenance tasks.

The hierarchical nature of the levels of decision-making and responsibility for specific maintenance tasks allow to determine the value of vector of decision-making levels, applying the principle that the weight of the higher level is a multiple of the weight directly to a lower level:

$p_3 = 1$,
$p_2 = 2$,
$p_1 = 4$.

The values of the vector of decision-making levels are contractual in nature and can be differently shaped in relation to another company.

Based on pre-defined and determined matrices and vectors, rank of the object is calculated, as a result of aggregation:

$$R = (W \cdot K) \cdot P^T \tag{20}$$

In particular:

$$R = \left( \begin{bmatrix} a_{11} & a_{12} & a_{13} \\ a_{21} & a_{22} & a_{23} \\ a_{31} & a_{32} & a_{33} \end{bmatrix} \cdot \begin{bmatrix} k_1 \\ k_2 \\ k_3 \end{bmatrix} \right) \cdot \begin{bmatrix} p_1 \\ p_2 \\ p_3 \end{bmatrix}^T \tag{21}$$

*Table 4. Table of exploitation assessment for an example network technical system*

| | Economic measures weight $k_1 = 0,5$ | | Technical measures weight $k_2 = 0,3$ | | Organizational measures weight $k_3 = 0,2$ | |
|---|---|---|---|---|---|---|
| Level 1 | $a_{11}$ | | $a_{12}$ | | $a_{13}$ | |
| weight $p_1 = 4$ | Assessment | Weight ($g_i$) | Assessment | Weight ($g_i$) | Assessment | Weight ($g_i$) |
| | $OC_{E1}$<br>$OC_{E2}$<br>$OC_{E3}$<br>$OC_{E14}$ | 0,35<br>0,25<br>0,2<br>0,2 | $OC_{T9}$<br>$OC_{T10}$<br>$OC_{T14}$<br>$OC_{T15}$<br>$OC_{T16}$<br>$OC_{T17}$ | 0,2<br>0,15<br>0,2<br>0,25<br>0,1<br>0,1 | $OC_{O1}$<br>$OC_{O2}$<br>$OC_{O3}$ | 0,4<br>0,35<br>0,25 |
| Level 2 | $a_{21}$ | | $a_{22}$ | | $a_{23}$ | |
| weight $p_2 = 2$ | Assessment | Weight ($g_i$) | Assessment | Weight ($g_i$) | Assessment | Weight ($g_i$) |
| | $OC_{E4}$<br>$OC_{E5}$<br>$OC_{E6}$<br>$OC_{E7}$<br>$OC_{E8}$ | 0,35<br>0,25<br>0,2<br>0,1<br>0,1 | $OC_{T11}$<br>$OC_{T12}$<br>$OC_{T13}$ | 0,45<br>0,25<br>0,3 | $OC_{O4}$<br>$OC_{O9}$ | 0,6<br>0,4 |
| Level 3 | $a_{31}$ | | $a_{32}$ | | $a_{33}$ | |
| weight $p_3 = 1$ | Assessment | Weight ($g_i$) | Assessment | Weight ($g_i$) | Assessment | Weight ($g_i$) |
| | $OC_{E9}$<br>$OC_{E10}$<br>$OC_{E11}$<br>$OC_{E12}$<br>$OC_{E13}$ | 0,3<br>0,25<br>0,2<br>0,15<br>0,1 | $OC_{T3}$<br>$OC_{T14}$<br>$OC_{T5}$<br>$OC_{T6}$<br>$OC_{T7}$<br>$OC_{T8}$ | 0,25<br>0,2<br>0,2<br>0,15<br>0,15<br>0,05 | $OC_{O5}$<br>$OC_{O6}$<br>$OC_{O7}$<br>$OC_{O8}$ | 0,35<br>0,25<br>0,15<br>0,25 |

$$R = \begin{bmatrix} a_{11} \cdot k_1 + a_{12} \cdot k_2 + a_{13} \cdot k_3 \\ a_{21} \cdot k_1 + a_{22} \cdot k_2 + a_{23} \cdot k_3 \\ a_{31} \cdot k_1 + a_{32} \cdot k_2 + a_{33} \cdot k_3 \end{bmatrix} \cdot \begin{bmatrix} p_1 \\ p_2 \\ p_3 \end{bmatrix}^T \tag{22}$$

$$R = \left[ (a_{11} \cdot k_1 + a_{12} \cdot k_2 + a_{13} \cdot k_3) \cdot p_1 + (a_{21} \cdot k_1 + a_{22} \cdot k_2 + a_{23} \cdot k_3) \cdot p_2 + (a_{31} \cdot k_1 + a_{32} \cdot k_2 + a_{33} \cdot k_3) \cdot p_3 \right] \tag{23}$$

Determined rank is the value of the object in relation to other ranked objects.

## 5. Example of ranks calculating for objects of the selected network technical system

Presented rank method can be applied in many cases of technical systems exploing under the following terms:

- it is necessary to extract the equivalent of comparable objects or parts of technical systems,
- it is necessary to prepare complete data resources on all exploitation events that occurred within the object.

Taking into account above guidelines, it is assumed that the subject of example is a water supply system - typical network technical system. The system functions as a collective water supply which consists of the recognition, treatment and water supply to its customers. The exploitation specificity of water supply system is determined by three aspects [13]:

- vast majority of the water supply system components operate in difficult to access location (such as underground), which makes it difficult or impossible to carry out such preventive work, which are typical for manufacturing companies (eg, review),
- proper functioning of the water supply system is required to ensure continuity and quality of facilities within an extensive technical infrastructure geographically dispersed over a large area,
- specificity of construction and location of the water supply system causes, that The largestsharehavethe works carried outwithin the breakdown maintenance strategy, and the lowest numberof objects issupportedunder the predictive maintenance strategy.

For this example it was assumed that objects, that are the basis for decision making and subject of analysis, are fragments of pipeline assigned to particular streets, assigned to particular streets, with all the technical components. An ordered set of weights and assessments are shown in Tab. 4.

$OC_{ij}$ values have been designated on the basis of:

- mathematical formulas of indicators presented in Tab. 2. and included in [27],
- formulas (10) – (13).

Part of a set measure values and the corresponding assessments for the selected of technical objects (streets) are shown Tab. 5. The table includes the results of the analysis of six of the nearly one hundred objects, which allows to show the idea and possibility of practical realization of the proposed method, as well as a practical way to restrict the presentation area.

As a result of the calculation, according to equations (15) – (16), matrix values have been designated for individual objects (Tab. 6).

Next, rank vector of objects (streets) was calculated, based on the (20) – (23).

| Object (street) | R |
|---|---|
| Object 1 | 152,8236 |
| Object 2 | 159,8538 |
| Object 3 | 162,3891 |
| Object 4 | 163,4277 |
| Object 5 | 171,5911 |
| Object 6 | 177,6439 |

*Table 5. Part of a set measure values and the corresponding assessments for the selected of technical objects (streets)*

| Object (street) | $E_1$ | $OC_{E1}$ | $T_{11}$ | $OC_{T11}$ | $O_6$ | $OC_{O6}$ |
|---|---|---|---|---|---|---|
| Object 1 | 0,3493 | 9,7049 | 0,0004 | 0,2278 | 0,0251 | 9,9094 |
| Object 2 | 3,7983 | 6,7916 | 0,0006 | 0,2941 | 0,0709 | 9,7439 |
| Object 3 | 5,1721 | 5,6312 | 0,0006 | 0,3448 | 0,1270 | 9,5411 |
| Object 4 | 0,0335 | 9,9716 | 0,0004 | 10,000 | 0,0098 | 9,9646 |
| Object 5 | 0,2591 | 9,7811 | 0,0004 | 5,0000 | 0,1807 | 9,3468 |
| Object 6 | 0,098 | 9,9171 | 0,0002 | 0,2564 | 0,0521 | 9,9812 |

*Table 6. The set of matrix elements of the exploitation assessments W for selected technical objects*

| Object (street) | a11 | a12 | a13 | a21 | a22 | a23 | a31 | a32 | a33 |
|---|---|---|---|---|---|---|---|---|---|
| Object 1 | 7,5390 | 7,0727 | 10 | 8,9896 | 5,2279 | 9,3259 | 9,1634 | 6,9476 | 9,9463 |
| Object 2 | 5,8716 | 7,0509 | 10 | 9,1802 | 4,9882 | 9,5678 | 9,1657 | 5,5745 | 10,000 |
| Object 3 | 5,3614 | 5,6458 | 10 | 8,6021 | 5,1581 | 9,7208 | 7,1919 | 5,0159 | 9,7836 |
| Object 4 | 7,4951 | 8,0000 | 10 | 6,0269 | 9,6029 | 8,3353 | 9,9798 | 6,1449 | 9,5250 |
| Object 5 | 7,9525 | 7,5000 | 10 | 7,3498 | 7,3529 | 9,7100 | 9,9798 | 7,4237 | 9,6677 |
| Object 6 | 7,3723 | 7,6213 | 10 | 9,1224 | 3,8801 | 8,6855 | 9,8824 | 7,4913 | 9,9073 |

## 6. Conclusions

According to the author, the article is part of the discussion on ways and effects of the operational assessment, on-going among employees of the maintenance departments of industrial companies. Presented here, rank method of technical objects can be an attempt to answer to the constantly present question in this area:

- which measures are most adequate in the considered organizational and technical system?
- what would be the importance (weight) of a particular measure in the considered organizational and technical system?
- which criteria (measures) should be the basis for comparing objects and/or maintenance departments?

It should be noted that the prepared method is a developmental. At the current stage industrial research is being conducted. They depend on verifying the correctness and effectiveness of the rank method based on data from the real working environment - the activities of maintenance departments – water and sewage, production companies. Verification will allow to make parameterization and positioning of the rank method, which relates to certain ambiguities of the method and its weak points, which concern:

- measures selection,
- ways of determining the weights,
- full use of the objects rank in company strategic planning.

In terms of optimizing of weights and measures selection, author is going to use the methods from the area of Analytic Network Process, whose precursor is T. Saaty [29, 30] and which are developed in different areas by many other authors, such as [6, 35].

The developed rank method is a part of research conducted by the author at the Institute of Production Engineering of the Silesian University of Technology. These studies concern the ways of modelling events and exploitation processes using the scenario methods.

## Bibliography


1. Adamkiewicz A, Burnos A. The maintenance of the ship turbines with the application of the key performance indicators. Journal of POLISH CIMAC "Diagnosis, Reliability and Safety" 2010; Vol. 5 No. 2: 7-16.
2. Brown M. Managing Shutdowns, Turnarounds & Outages. Hoboken: Wiley Publishing Inc., 2004.
3. Burnos A. Universal maintenance performance indicator for technical objects operated on floating units. Szczecin: Zeszyty Naukowe Akademii Morskiej 2011; 27 (99) z. 1: 34-39.
4. Campbell J, Jardine A, McGlynn J. Asset Management Excellence. Optimizing Equipment Life – Cycle Decisions. Boca Raton: CRC Press, 2011.
5. Chmurawa M, Bińkowski W. Podstawy niezawodności i eksploatacji maszyn roboczych. Gliwice: Wydawnictwo Politechniki Śląskiej, 1980.
6. Downarowicz O. Wybrane metody ergonomii i nauki o eksploatacji. Gdańsk: Politechnika Gdańska, 2000.
7. Drożyner P., Mikołajczak P. Assessment of the effectiveness of machine and device operation. Eksploatacja i Niezawodnosc – Maintenance and Reliability 2007; 3 (35): 72–75.
8. Grabiński T, Wydymus S, Zeliaś A. Metody taksonomii numerycznej w modelowaniu zjawisk społeczno-gospodarczych. Warszawa: PWN, 1989.
9. Grenčík J, Legát V. Maintenance audit and benchmarking – search for evaluation criteria on global scale. Eksploatacja i Niezawodnosc – Maintenance and Reliability 2007; 3 (35): 34-39.
10. Hebda M. Elementy teorii eksploatacji systemów technicznych. Radom: MCNEMT, 1990.
11. Jasiulewicz-Kaczmarek M. Participatory Ergonomics as a Method of Quality Improvement in Maintenance. Ergonomics and Health Aspects of Work with Computers 2009; Vol. 5624: 153–161.
12. Kaźmierczak J. Eksploatacja systemów technicznych. Gliwice: Wydawnictwo Politechniki Śląskiej, 2000.
13. Kaźmierczak J, Loska A, Dąbrowski M. Use of geospatial information for supporting maintenance management in a technical network

system. Belgrade: Proceedings of International Conference "Euromaintenance 2012", 2012.
14. Kelly A. Strategic Maintenance Planning. Oxford: Butterworth-Heinemann, 2006.
15. Kornacki A, Sokołowska E. The estimation of smooth operation time until failure with the application of the Akaike Information Criterion (AIC). Eksploatacja i Niezawodnosc – Maintenance and Reliability 2010; 1 (45): 69–76.
16. Kukuła K. Metoda unitaryzacji zerowanej. Warszawa: Wydawnictwo Naukowe PWN, 2000.
17. Levitt J. The Handbook of Maintenance Management (second edition). New York: Industrial Press Inc., 2009.
18. Loska A. (red.): Przeprowadzenie dla potrzeb Pionu TR oceny wydajności wykonawstwa własnego do identyfikacji przyczyn złej jakości prac i umożliwienia doskonalenia jakości usług wykonywanych przez pracowników pionu TR. Zabrze-Rybnik: Praca badawcza wykonana na zlecenie Elektrowni Rybnik S.A. Politechnika Śląska, 2009.
19. Loska A. Przegląd metod modelowania jako podstawa budowy scenariuszy eksploatacyjnych. Opole: Konferencja Komputerowo Zintegrowane Zarządzanie, Oficyna Wydawnicza Polskiego Towarzystwa Zarządzania Produkcją 2010; t. 2: 152–161.
20. Loska A. Przegląd modeli ocen eksploatacyjnych systemów technicznych. Opole: Konferencja Komputerowo Zintegrowane Zarządzanie, Oficyna Wydawnicza Polskiego Towarzystwa Zarządzania Produkcją 2011; t. 2: 37–46.
21. Loska A. Remarks about modelling of maintenance processess with the use of scenario techniques. Eksploatacja i Niezawodnosc – Maintenance and Reliability 2012; 14 (2): 92–98.
22. Nakajima S. Introduction to TPM. Total Productive Maintenance. Portland: Productivity Press, 1988.
23. Niebel W.B. Engineering Maintenance Management. Second edition. New York: Marcel Dekker Inc., 1994.
24. Pahl G., Beitz W. Nauka konstruowania. Warszawa: WNT, 1984.
25. Pawłowski Z. Ekonometria. Warszawa: PWN, 1980.
26. Peters R.W. Maintenance Benchmarking and Best Practices: A Profit - and Customer - Centered Approach. Ney York: McGraw-Hill, 2006.
27. Polska Norma PN-EN 15341:2007 – Maintenance – Maintenance Key Performance Indicators. Warszawa, Polski Komitet Normalizacyjny, 2007.
28. Radkowski S. Podstawy bezpiecznej techniki.Warszawa: Oficyna Wydawnicza Politechniki Warszawskiej, 2003.
29. Saaty T. How to make a decision. The Analytic Hierarchy Process. European Journal of Operational Research 1990; 48 (1): 9–26.
30. Saaty T. Theory and Applications of the Analytic Network Process. Decision making with benefits, opportunities, costs and risks. Pittsbourgh: RWS Publications, 2009.
31. Skotnicka-Zasadzień B, Biały W. An analysis of possibilities to use Pareto chart for evaluating minimgmachines'failure frequency. Eksploatacja i Niezawodnosc – Maintenance and Reliability 2011; 3 (51): 51–55.
32. Smith J. The KPI Book. Stoubridge: Insight Training & Development Limited, 2001.
33. Suzuki T. TPM in Process Industries. Portland: Productivity Press, 1994.
34. The Productivity Development Team. OEE for Operators. New York: Productivity Press Inc., 1999.
35. Triantaphyllou E. Using the analytic hierarchy process for decision making in engineering applications some challenges, International Journal of Industrial Engineering: Applications and Practice 1995; Vol. 2 No. 1: 35–44.
36. Wiremann T. Developing Performance Indicators for Managing Maintenance (second edition). New York: Industrial Press, 2005.
37. Zeliaś A. Przestrzenno-czasowe modelowanie i prognozowanie zjawisk gospodarczych. Kraków: Wydawnictwo Akademii Ekonomicznej w Krakowie, 1993.
38. Żółtowski B. Podstawy diagnostyki maszyn. Bydgoszcz: Wydawnictwo Akademii Techniczno-Rolniczej w Bydgoszczy, 1996.

**Andrzej LOSKA, Ph.D. (Eng.)**
Institute of Production Engineering
Silesian University of Technology
ul. Roosevelta nr 26, 41-800 Zabrze, Poland
E-mail: Andrzej.Loska@polsl.pl

Article citation info:
GUO C, WANG W, GUO B, PENG R. Maintenance Optimization for SystemsWith Dependent Competing Risks Using a Copula Function. Eksploatacja i Niezawodnosc – Maintenance and Reliability 2013; 15 (1): 9–17.

Chiming GUO
Wenbin WANG
Bo GUO
Rui PENG

# MAINTENANCE OPTIMIZATION FOR SYSTEMS WITH DEPENDENT COMPETING RISKS USING A COPULA FUNCTION

# OPTYMALIZACJA EKSPLOATACJI DLA SYSTEMÓW Z ZALEŻNYMI ZAGROŻENIAMI KONKURUJĄCYMI PRZY WYKORZYSTANIU FUNKCJI KOPUŁY

*This paper develops a joint copula reliability model for systems subjected to dependent competing risks caused by two degradation processes and random shocks. The two degradation processes follow gamma processes and the random shocks follow a non-homogeneous Poisson process (NHPP). Their interdependence relationship is modeled by a copula function, which is determined by a two-stage method based on simulated data. It is shown that the proposed model can provide more precise results than the model without considering the dependent relationship. Through the proposed reliability model, two maintenance models are studied and compared. It is found that the inspection cost has significant effects on the choosing of maintenance policy.*

***Keywords**: dependent competing risks, copula function, simulated data, degradation, random shocks, maintenance optimization.*

*W niniejszej pracy opracowano wspólny model niezawodności z użyciem kopuły dla systemów poddawanych zależnym zagrożeniom konkurującym powodowanym przez dwa procesy degradacji i zaburzenia losowe. Owe dwa procesy degradacji reprezentują typ procesu gamma, podczas gdy zaburzenia losowe są typem niejednorodnego procesu Poissona (non-homogeneous Poisson process - NHPP). Ich związek wzajemnej zależności modelowany jest przy użyciu funkcji kopuły, która jest wyznaczana na podstawie dwuetapowej metody opartej o dane symulowane. Wykazano, iż proponowany model może zapewnić bardziej precyzyjne wyniki niż model, w którym nie ujęto związku zależności. W oparciu o proponowany model niezawodności, badane i porównywane są dwa modele eksploatacji. Stwierdzono, iż koszt przeglądu ma duży wpływ na wybór polityki eksploatacyjnej.*

***Słowa kluczowe**: zależne ryzyka konkurujące, funkcja kopuły, dane symulowane, degradacja, zaburzenia losowe, optymalizacja eksploatacji.*

## 1. Introduction

Competing risks are quite common situations in industry for systems or components which can be subjected to more than one causes of failure at the same time and fail due to one of them [17,19]. Therefore, it is beneficial to consider the competing risks for the maintenance scheduling.

Many studies treat the competing risks as independent failure processes. Lehman [17] investigated a class of degradation-threshold-shock models in which the failure is caused by the competing risks of degradation and trauma. Bocchetti et al. [2] proposed a model to describe the competing risks caused by wear degradation and thermal cracking for the cylinder liners in marine diesel engine. Due to the complex features of lifetime data, Jiang [13] developed a competing risk model involving a geometric distribution and an exponential Poisson distribution to model bus-motor failure data. Li and Pham [18] presented an inspection-maintenance model for systems subjected to two degradation processes and random shocks. Zhu et al. [34] presented a maintenance model that maximizes the unit availability by determining the degradation threshold level and the time to perform preventive maintenance (PM). Kharoufeh et al. [14] derived the system lifetime distribution and the limiting average availability for a periodically inspected system, which is subjected to degradation and random shocks modulated by a homogeneous Poisson process. Wang et al. [30] studied the impact of shocks on the product and found that the shocks had a significant impact on the product reliability.

The assumption of s-independence between competing risks may cause underestimation or overestimation of the system reliability and has substantial impacts on maintenance optimization [3]. Therefore, it is essential to take account of the dependent relationship in order to model the reliability more accurately and make more appropriate maintenance strategy.

Some recent papers have incorporated the dependent relationship into the reliability modeling process. Su and Zhang [26] studied the reliability assessment for GaAs lasers based on competing risk model. The results show that the dependence between the traumatic failure and degradation has a great influence on the accuracy of reliability assessment. Considering the dependency between wear failure and shock failure, Jiang and Coit [12] developed reliability models with two classes of shock processes and a linear degradation process. The arrival of each shock impacts both the soft failure process and the hard failure process. Pan and Balakrishnan [21] proposed to use a bivariate Brinbaun-Saunders distribution to describe the dependent relationship between the two gamma degradation processes and developed an inferential method for the corresponding model parameters. Singpurwalla [25] proposed a general framework for an appreciation of competing risks and degradation involving interdependent stochastic processes under the notion of a hazard potential. Pan and Zhao [22] treated the

problem of accelerated failure with competing causes of a degradation failure mode and multiple traumatic failure modes. Abbring and van den Berg [1] studied the dependent competing risks models with a mixed proportional hazard for each risk. Wang and Coit [27] proposed a general modeling and analysis approach for reliability prediction based on multiple degradation measures and illustrated the approach with multivariate Normal distributions.

There has also been a growing interest in considering the maintenance optimization with dependent competing risks in recent years. Klutke and Yang [15] studied the average availability of maintained systems subject to shocks and graceful degradation with hidden failures. Huynh et al. [10] developed a dependent competing risk model by assuming the arrival rate of shocks as a function of the degradation level, and proved the value of condition monitoring to the maintenance decision-making. Later Huynh et al. [11] developed age-based maintenance strategies with minimal repairs for systems based on the same competing risk model. Wang and Pham [28] studied a multi-objective optimization problem of imperfect preventive maintenance policy for a single-unit system subjected to the dependent competing risks, by simultaneously maximizing the system asymptotic availability and minimizing the system cost rate. It is assumed that fatal shocks will cause the system to fail immediately, whereas nonfatal shocks will increase the system degradation level by a certain cumulative shock amount. In order to give a more explicit dependent relationship, Chen [7] used the degradation level as a variable of the arrival rate function of the fatal shock, and an inspection/replacement policy is discussed based on the proposed model. Castro [4] developed a dependent relationship for two competing failure modes in which the non-maintainable failure number affects the maintainable failure rate. The optimal number of PMs and the interval between successive PMs are determined with the objective of minimizing the expected cost rate. Zequeira and Bérenguer [32] studied the imperfect maintenance policies with the consideration of two competing failure modes, where the hazard rate of the maintainable failure mode depends on the hazard rate of the non-maintainable failure mode. Deloux et al. [9] considered a system with two failure mechanisms due to an excessive deterioration level and a shock. The optimal maintenance strategy is studied in an approach which combines statistical process control and condition-based maintenance. Peng et al. [23] presented a preventive maintenance policy for systems subjected to multiple competing failures where the external random shocks contribute to the internal degradation.

Previous researches have mainly investigated the dependence relationships among degradation processes by multivariate normal distribution, and modeled the failure rate with covariates etc. Though the system reliability functions can be deduced directly, these approaches are insufficient to cope with the complexity of the modern system in reality [29, 33].

Copula is a powerful tool to model the dependence of random variables, and the copula based models allow for flexible specification of the dependence structure between competing random variables [3, 24]. Zhou [33] proposed a bivariate degradation modeling framework based on gamma processes and copula function is used to describe the dependence between performance characteristics. Wang and Pham [29] developed a flexible s-dependent competing risk model to describe the dependence between random shocks and the degradation process by employing time-varying copulas. Lo and Wilke [20] extended the copula graphic estimator to model multiple dependent competing risks and applied the model to the unemployment duration data from Germany. However, copula function has seldom been applied to model the dependence structure in maintenance optimization.

In practice, systems are usually subjected to competing risks involving both degradation and shocks, as investigated by many researchers [6, 10, 12, 15 and 30]. In this paper, a system suffering dependent competing risks caused by two degradation processes and random shocks is studied. With the dependence structure modeled by copula function, a joint reliability function is developed based on the simulated data and the maintenance optimization is investigated.

The remaining paper is organized as follows. Section 2 investigates the system failure process and deduces the marginal reliability function for the system suffering two degradation failure processes and random shocks. Section 3 develops the system reliability model based on a copula function and provides a parameter estimation procedure based on simulated data. Section 4 presents two maintenance models based on the joint copula reliability function. In Section 5, a numerical example is presented to illustrate the procedure to determine the joint reliability function and investigate the maintenance optimization for the two maintenance policies.

## 2. Dependent competing risks

Consider a system subjected to competing risks due to two degradation processes and random shocks. The two degradation processes have a dependent relationship with each other as each shock causes a sudden increment jump to both degradation processes simultaneously. The system fails if the cumulative deterioration of any degradation process exceeds a certain critical failure threshold.

### 2.1. Degradation processes without random shocks

Gamma processes have been extensively adopted to describe the gradual degradation phenomena e.g. corrosion [16], crack growth [5]. Let $X_i(t)$, ($i=1,2$) denote the accumulated deterioration for the $i$ th degradation process at time $t$, where the initial state of the system is perfect with $X_i(0)=0$. Assume that $\{X_i(t), t\ge 0\}$, ($i=1,2$) is a stationary gamma process where $X_i(t)-X_i(s)$ is gamma distributed for all $0\le s<t$. Without considering the influences of the shock process, $X_i(t)-X_i(s)$, $0\le s<t$ has a gamma probability density function (pdf) with shape parameter $\alpha_i(t-s)>0$ and scale parameter $\beta_i>0$:

$$f_{\alpha_i(t-s),\beta_i}(x_i)=\frac{\beta_i^{\alpha_i(t-s)}x_i^{\alpha_i(t-s)-1}e^{-\beta_i x}}{\Gamma(\alpha_i(t-s))}I_{\{x_i\ge 0\}}, \tag{1}$$

where $\Gamma(\alpha)=\int_0^\infty u^{\alpha-1}e^{-u}du$ is the gamma function. $I_{\{x_i\ge 0\}}=1$ if $x_i\ge 0$ and $I_{\{x_i\ge 0\}}=0$ otherwise.

The average deterioration rate is $u_i=\alpha_i/\beta_i$, and its variance is $\sigma_i^2=\alpha_i/\beta_i^2$. Though the constant deterioration rate may be unsuitable for the realistic degradation process, a monotonic transformation of the time scale can make the real deterioration rate constant [31]. With the choice of $\alpha_i$ and $\beta_i$, such a process can be very flexible to model various deterioration behaviors of the system.

The stochastic process $\{X_i(t), t\ge 0\}$ is time continuous and monotonically increasing, and the system fails once $X_i(t)$ exceeds a predetermined failure threshold $L_i$. Though the system may be still functioning after crossing the failure threshold, it cannot perform its function as required and is regarded as "failed" for economical or security reasons. The time to failure (TTF) of the $i$ th degradation process can be expressed as $TL_i=\inf\{t \mid X_i(t)\ge L_i\}$, and its cumulative distribution function (cdf) can be obtained as:

$$F_{TL_i}(t) = P(TL_i \le t) = P(X_i(t) \ge L_i) = \int_{L_i}^{\infty} f_{\alpha_i t, \beta_i}(x)dx = \frac{\Gamma(\alpha_i t, \beta_i L_i)}{\Gamma(\alpha_i t)}, \quad (2)$$

where $\Gamma(a,x) = \int_x^{\infty} t^{a-1} e^{-t} dt$.

The pdf for TTF of the $i$ th degradation process is

$$f_{TL_i}(t) = \frac{\partial}{\partial t} F_{TL_i}(t) = \frac{\alpha_i}{\Gamma(\alpha_i t)} \int_{L_i \beta_i}^{\infty} (\ln(u) - \psi(\alpha_i t)) u^{\alpha_i t - 1} e^{-u} du, \quad (3)$$

where $\psi(a) = \frac{\Gamma'(a)}{\Gamma(a)} = \frac{\partial}{\partial a} \ln \Gamma(a)$ is called the digamma function.

The reliability function corresponding to the $i$ th degradation process is

$$R_{TL_i}(t) = 1 - F_{TL_i}(t) = 1 - \frac{\Gamma(\alpha_i t, \beta_i L_i)}{\Gamma(\alpha_i t)}. \quad (4)$$

### 2.2. Shock process

Shocks may be generated internally within components or introduced externally from the environment outside. Most shocks are harmful to the system operation, and can reduce the system residual useful life. In this paper, a cumulative shock model is employed to describe the shock process. The probabilities for the shock damages to occur in different time intervals are assumed to be independent.

The log-linear process (LLP) is very flexible and has been widely used to describe the occurrence of random events, such as the wear of cylinder liner [2]. Here the shock process is described by the LLP, and the random shocks are assumed to occur in a non-homogeneous Poisson process (NHPP) with intensity function

$$\lambda(t) = r\,\mathrm{e}^{ct}, \; r \in (0,\infty), \; c \in (-\infty, +\infty). \quad (5)$$

Let $N(t)$ denote the number of shocks until time $t$, then the expected number of shocks until time $t$, denoted by $W(t)$, is given by

$$W(t) = E[N(t)] = \int_0^t re^{cs} ds = \begin{cases} \frac{r}{c}(e^{ct} - 1), & c \ne 0 \\ rt, & c = 0 \end{cases}. \quad (6)$$

Further, the probability distribution of $N(t)$ is

$$P(N(t) = n) = \frac{(W(t))^n}{n!} e^{-W(t)}. \quad (7)$$

The amount of damage caused by the $k$ th shock to the $i$ th degradation process is denoted by $S_{ik}$ and $S_{ik} \sim N(\mu_i, \sigma_i^2)$. Furthermore, the accumulated shock damages to the $i$ th degradation process until time t is expressed as $Z_i(t) = \sum_{k=1}^{N(t)} S_{ik}$.

Consider $G(l) = P(S_{ik} \le l)$ as the cdf for all $S_{ik}$. The cdf for the accumulative shock damage to the $i$ th degradation process incurred by the shock process is

$$P(Z_i(t) \le z) = P(\sum_{k=1}^{N(t)} S_{ik} \le z)$$
$$= P(N(t) = 0) + \sum_{j=1}^{\infty} G^{(j)}(z) P(N(t) = j) = e^{-W(t)} + \sum_{j=1}^{\infty} \Phi(\frac{z - j\mu_i}{\sqrt{j\sigma_i^2}}) \frac{(W(t))^j}{j!} e^{-W(t)}, \quad (8)$$

where $G^{(j)}(z)$ is the j-fold convolution with itself.

### 2.3. Degradation processes with random shocks

Section 2.1 investigated the reliability of the system subjected to the degradation process, without considering the influences induced by the shock process. In practical applications, the random shocks may exist and have impacts on the degradation processes. [29]

In this paper, the random shocks will induce a sudden increment to the degradation process. Considering the dependent relationship of degradation processes and random shocks, the $i$ th degradation process state $Y_i(t)$ includes two parts: the wear caused by the system aging and the sudden increments induced by the random shocks. The $i$ th degradation at time $t$ can be expressed as $Y_i(t) = X_i(t) + Z_i(t)$. Denote the TTF for the $i$ th degradation by $T_i$. The reliability function for the $i$ th degradation process with random shock damages is given by

$$\begin{aligned} R_i(t) &= P(T_i > t) = P(Y_i(t) < L_i) = P(X_i(t) + Z_i(t) < L_i) \\ &= \sum_{k=0}^{\infty} P(X_i(t) + Z_i(t) < L_i \mid N(t) = k) P(N(t) = k) \\ &= P(N(t) = 0) P(X_i(t) < L_i) + \sum_{k=1}^{\infty} P(N(t) = k) \int_0^{L_i} P(X_i(t) + z < L_i) dG^{(k)}(z) \\ &= e^{-W(t)} (1 - \frac{\Gamma(\mathsf{a}_i t, \mathsf{b}_i L_i)}{\Gamma(\mathsf{a}_i t)}) + \sum_{k=1}^{\infty} \frac{(W(t))^k}{k!} e^{-W(t)} \int_0^{L_i} (1 - \frac{\Gamma(\mathsf{a}_i t, \mathsf{b}_i (L_i - z))}{\Gamma(\mathsf{a}_i t)}) dG^{(k)}(z). \end{aligned} \quad (9)$$

The pdf of TTF for the ith degradation process with random shocks can be expressed as

$$f_i(t) = -\frac{dR_i(t)}{dt}. \quad (10)$$

## 3. System reliability analysis

The system failure occurs if any of the degradation processes $Y_i(t)$ reaches the failure threshold $L_i$. Therefore, the system reliability at time $t$ is

$$R(t) = P(Y_1(t) < L_1, Y_2(t) < L_2) = P(X_1(t) + Z_1(t) < L_1, X_2(t) + Z_2(t) < L_2) \quad (11)$$

If the two degradation processes are independent, the system reliability function can be written as

$$R(t) = R_1(t) R_2(t). \quad (12)$$

However, Eq. (12) is unable to provide the accurate system reliability estimation for our case, as there is dependency between the two degradation processes due to the random shocks. It is difficult to calculate $R(t)$ by Eq. (11) directly, so we need to find another way to predict the reliability of the system subject to dependent competing failures.

### 3.1. A Copula approach

A Copula function is a powerful tool to model the dependence structure of the competing failure processes. One advantage of the copula function is that the joint reliability function can be modeled directly through the univariate marginal reliability functions of the individual failure processes, (i.e. $F_1(t)$, $F_2(t)$) and the copula has no constraints on the univariate marginal distribution.

The cdf of TTF for the two degradation processes can be expressed as $F_i(t) = 1 - R_i(t)$ ($i = 1, 2$), and the joint cdf of $T_1$ and $T_2$ is denoted by $H(t_1, t_2)$. According to Sklar's theorem, there exists a unique copula $C$ such that

$$P(T_1 \le t_1, T_2 \le t_2) = H(t_1, t_2) = C(F_1(t_1), F_2(t_2), \Theta), \tag{13}$$

where $\Theta$ is the parameter vector of the copula function.

Meanwhile, the joint reliability function of the system with $t_1$ and $t_2$ can be expressed as

$$\bar{H}(t_1, t_2) = P(T_1 > t_1, T_2 > t_2). \tag{14}$$

Because $R_1(t)$ and $R_2(t)$ are decreasing functions, the system reliability at time $t$ ($t_1 = t_2 = t$) can be expressed with the survival copula function as [8, 24]

$$\begin{aligned} R(t) &= \bar{H}(t_1, t_2)|_{t_1=t_2=t} \\ &= R_1(t_1) + R_2(t_2) - 1 + C(F_1(t_1), F_2(t_2), \Theta)|_{t_1=t_2=t} \\ &= R_1(t) + R_2(t) - 1 + C(F_1(t), F_2(t), \Theta). \end{aligned} \tag{15}$$

There is another approach to construct the system reliability with a copula function, as shown in [29]. The joint reliability function can be directly modeled by a copula function and can be written as

$$R(t) = \bar{H}(t_1, t_2)|_{t_1=t_2=t} = C(R_1(t_1), R_2(t_2), \Theta)|_{t_1=t_2=t} = C(R_1(t), R_2(t), \Theta). \tag{16}$$

The results of Eq. (15) and (16) may be different, and we will compare the two approaches in Section 5.

### 3.2. Parameter estimation

Assume that the parameters of the marginal reliability functions for the degradation processes are already given. In order to predict the system reliability, we need to estimate the copula parameters based on the known marginal distributions. The pdf of the joint distribution $\bar{H}(t_1, t_2)$ can be denoted as $f(t)$ as $t_1 = t_2 = t$. Further, we can obtain $f(t)$ from Eq. (15) as

$$\begin{aligned} f(t) &= f(t_1, t_2)|_{t_1=t_2=t} \\ &= -\frac{\partial^2}{\partial t_1 \partial t_2}(R_1(t_1) + R_2(t_2) - 1 + C(F_1(t_1), F_2(t_2), \Theta))|_{t_1=t_2=t} \\ &= f_1(t_1) + f_2(t_2) - c(F_1(t_1), F_2(t_2), \Theta) f_1(t_1) f_2(t_2)|_{t_1=t_2=t} \\ &= f_1(t) + f_2(t) - c(F_1(t), F_2(t), \Theta) f_1(t) f_2(t), \end{aligned} \tag{17}$$

where $c(F_1(t_1), F_2(t_2), \Theta) = \dfrac{\partial^2}{\partial F_1(t_1) \partial F_2(t_2)} C(F_1(t_1), F_2(t_2), \Theta)$ is the copula density function.

Similarly, $f(t)$ for Eq. (16) is given as

$$f(t) = f(t_1, t_2)|_{t_1=t_2=t} = -c(R_1(t_1), R_2(t_2), \Theta) f_1(t_1) f_2(t_2)|_{t_1=t_2=t}, \tag{18}$$

where $c(R_1(t_1), R_2(t_2), \Theta) = \dfrac{\partial^2}{\partial R_1(t_1) \partial R_2(t_2)} C(R_1(t_1), R_2(t_2), \Theta)$.

In this paper, the simulated data are used to estimate the parameters of the copula function and validate the effectiveness of the copula method. The proposed method can be divided into two stages.

In the first stage, we need to simulate the competing failure processes to obtain the system marginal reliability sample with the underlying dependent relationship between the degradation processes and the shock process at discrete times. The procedures are described as follows:

- Compute the degradation increment $X_i(t)$ $(i = 1, 2)$ of each degradation process at $t = m\Delta t$ ($m$=1,2,…), where $\Delta t$ is the time step for the degradation process simulation.
- Generate the shock arrival times following NHPP $\{t_1, t_2, ...., t_n\}$, ($t_n \le t$) and the corresponding shock damages to each degradation process $\{s_{i1}, s_{i2}, ..., s_{in}\}$.
- Compute the accumulated shock damage at time $t$ as $Z_i(t) = \sum_{k=1}^{n} s_{ik}$ for each degradation process.
- Compute the system reliability $\hat{R}(t) = \sum_{j=Num} I_{\{X_i(t_j)+Z_i(t_j) \le L_i\}} / Num$, where $I$ is an indicator function. $I = 1$, if $X_i(t) + Z_i(t) \ge L_i$ and $I = 0$ otherwise. $Num$ is the total number of simulations.

In the second stage, the Maximum likelihood estimator (MLE) is used to estimate the copula function parameters based on the simulated marginal reliability sample. Below are the procedures:

Consider $N_1$ simulated results for the degradation processes, which are denoted by $\{F_1(t_j), F_2(t_j)\}_{j=1,\cdots N_1}$. With Eq. (17) and (18), the log-likelihood function for the bivariate copula can be expressed respectively as

$$\ln L(\Theta) = \sum_{j=1}^{N_1} \ln c(F_1(t_j), F_2(t_j), \Theta), \tag{19}$$

$$\ln L(\Theta) = \sum_{j=1}^{N_1} \ln c(R_1(t_j), R_2(t_j), \Theta). \tag{20}$$

Using MLE, the copula parameters can be estimated as

$$\hat{\Theta} = ArgMax\{\ln L(\Theta)\}. \tag{21}$$

## 4. Maintenance models

This section presents two kinds of maintenance policies based on the joint copula reliability function for a non-repairable system. The first policy is a periodic inspection/replacement policy and the decision variable for maintenance decision maker is the inspection interval. The second policy is an age-based maintenance policy and the decision variable is the replacement age to be specified. For both maintenance policies, the objective is to minimize the average maintenance cost rate in long run.

### 4.1. Periodic inspection/replacement policy

Due to cost reasons and other practical issues, the system is inspected at a periodic interval τ. The inspection is perfect and instantaneous with a cost $C_I$ incurred. When any of the two degradation processes with the underlying shock damages exceeds the pre-set threshold, the system is deemed as failed though it still runs until the failure is identified at the next inspection. In case when a system failure is identified at an inspection, it is replaced instantly with a new one and the replacement time is negligible. The replacement can be seen as a renewal.

Denote the accumulative maintenance cost until time $t$ as $C(t)$. According to the renewal theory, we have

$$\lim_{t\to\infty}\frac{C(t)}{t}=\frac{E[CR]}{E[TR]}, \tag{22}$$

where $E[CR]$ is the expected total maintenance cost in a renewal cycle, $E[TR]$ is the expected length of a renewal cycle.

The maintenance costs in a renewal cycle are composed of inspection cost, replacement cost and the delay time cost during system failure period. The delay time cost is incurred by the loss of system performance during the system failure period. The expected total cost in a renewal cycle can be expressed as

$$E[CR]=C_I E[N_I]+C_D E[\xi]+C_R, \tag{23}$$

where $C_I$ is the cost associated with each inspection, $C_D$ is the delay time cost rate for the system failure duration, $C_R$ is the replacement cost after the system failure, $E[N_I]$ is the expected inspection number in a renewal cycle, $E[\xi]$ is the expected time that the system spends in failed state in a renewal cycle.

Denote the failure time of the system as $T=\min(T_1,T_2)$. If there are $i$ inspections in a renewal cycle, then we have $\{N_I=i\}=\{(i-1)\tau<T\le i\tau\}$. Therefore, the expected number of inspections in a renewal cycle is given as

$$E[N_I]=\sum_{i=1}^{\infty}iP(N_I=i)=\sum_{i=1}^{\infty}iP((i-1)\tau<T\le i\tau)=\sum_{i=1}^{\infty}i(F_T(i\tau)-F_T((i-1)\tau)), \tag{24}$$

where $F_T(t)$ is the cdf of the TTF of the system, which can be calculated by $1-R(t)$ based on Eq. (15) and (16).

If the system is identified as failed at the $i$ th inspection, then the delay time is $\xi=i\tau-T$. Therefore, the expected delay time of the system in a renewal cycle is

$$E[\xi]=\sum_{i=1}^{\infty}E[\xi\mid N_I=i]P(N_I=i)=\sum_{i=1}^{\infty}\left(\int_{(i-1)\tau}^{i\tau}(i\tau-t)dF_T(t)\right). \tag{25}$$

The expected length of a renewal cycle can be expressed as

$$E[TR]=\sum_{i=1}^{\infty}i\tau P(N_I=i)=\sum_{i=1}^{\infty}i\tau(F_T(i\tau)-F_T((i-1)\tau)). \tag{26}$$

Based on Eq. (22)-(26), the average maintenance cost rate in long run is given as a function of $\tau$ as

$$AVC(\tau)=\frac{C_I\sum_{i=1}^{\infty}i(F_T(i\tau)-F_T((i-1)\tau))+C_D\sum_{i=1}^{\infty}\left(\int_{(i-1)\tau}^{i\tau}(i\tau-t)dF_T(t)\right)+C_R}{\sum_{i=1}^{\infty}i\tau(F_T(i\tau)-F_T((i-1)\tau))}. \tag{27}$$

To minimize the average maintenance cost rate in long run, we can calculate the derivative of $AVC(\tau)$, as detailed in Appendix 1. By setting $AVC'(\tau)=0$, the optimal interval τ can be obtained for the periodic inspection policy.

### 4.2. Age-based replacement policy

Under this maintenance policy, the system is replaced at a specified age $\Psi$ without any inspection. When the system fails before $\Psi$, there will be a period of delay time for the system until $\Psi$ at a cost rate $C_D$, and the system will be correctively replaced with a cost $C_R$. Otherwise, the system will be preventively replaced with a cost $C_P$ at $\Psi$. Both the preventive replacement and the corrective replacement restore the system to as-good-as new state.

In this case, the expected cost rate in long run is given by

$$AVC(\Psi)=\frac{C_R F_T(\Psi)+C_P(1-F_T(\Psi))+C_D\int_0^{\Psi}F_T(t)dt}{\Psi},\ \Psi>0. \tag{28}$$

When $\Psi$ is very large, the cost rate will be large due to the high probability of failure and long delay time. On the other hand, when $\Psi$ is very small, the cost rate will also be large due to the high frequency of preventive replacement. Therefore there exists an optimal $\Psi$ to achieve the minimum expected cost rate. The derivation of Eq. (28) is given by

$$AVC'(\Psi)=\frac{(C_R f_T(\Psi)-C_P f_T(\Psi)+C_D F_T(\Psi))\Psi-(C_R F_T(\Psi)+C_P(1-F_T(\Psi))+C_D\int_0^{\Psi}F_T(t)dt)}{\Psi^2}. \tag{29}$$

By setting $AVC'(\Psi)=0$, the optimal $\Psi$ can be obtained for the age-based maintenance policy.

## 5. Numerical example

In this section, the joint copula reliability model is constructed and the two maintenance policies are studied for a system subjected to two degradation processes and random shocks. The two degradation processes are governed by gamma processes with parameters $\alpha_1=0.2$, $\beta_1=2$, $\alpha_2=0.3$, $\beta_2=2$. The failure thresholds for the two degradation processes are $L_1=6$, $L_2=8$. The random shocks follow a NHPP process with $r=0.1$, $c=0.01$. The random shock damages to the two degradation processes follow $S_{1,k}\sim N(0.2,0.1^2)$ and $S_{2,k}\sim N(0.5,0.2^2)$, respectively. The cost parameters are assumed as follows: $C_I$=1 per inspection, $C_P$=180 per PM, $C_R$=200 per replacement, $C_D$=100 per unit time.

### 5.1 Copula function selection

According to the copula function properties, we can use the marginal reliability function in Eq. (9) to construct the joint reliability function with the underlying dependent relationship. With the given

*Table 1. Simulated marginal reliability data with dependent relationship*

| Time | 75 | 80 | 85 | 90 | 95 | 100 | 105 | 110 | 115 |
|---|---|---|---|---|---|---|---|---|---|
| $R_1(t)$ | 0.9999 | 0.9999 | 0.9999 | 0.9970 | 0.9880 | 0.9590 | 0.9180 | 0.8700 | 0.8300 |
| $R_2(t)$ | 0.9999 | 0.9999 | 0.9980 | 0.9890 | 0.9390 | 0.8780 | 0.7450 | 0.6130 | 0.4630 |
| R(t) | 0.9999 | 0.9999 | 0.9980 | 0.9860 | 0.9270 | 0.8370 | 0.6630 | 0.4830 | 0.2930 |
| Time | 120 | 125 | 130 | 135 | 140 | 145 | 150 | 155 | 160 |
| $R_1(t)$ | 0.7680 | 0.7580 | 0.7410 | 0.7440 | 0.7650 | 0.7460 | 0.7500 | 0.7480 | 0.7350 |
| $R_2(t)$ | 0.3960 | 0.3050 | 0.2960 | 0.2750 | 0.2500 | 0.2670 | 0.2590 | 0.2570 | 0.2760 |
| R(t) | 0.1640 | 0.0063 | 0.0037 | 0.0019 | 0.0015 | 0.0130 | 0.0090 | 0.0050 | 0.0110 |

*Table. 2 Results of copula fitting for Type I reliability function*

| Copula type | Parameter (Θ) | LL | AIC | BIC | ARE |
|---|---|---|---|---|---|
| Gumbel | 1.9902 | 15.2297 | -28.4593 | -27.5689 | 0.4242 |
| Clayton | 0.6376 | **25.8857** | **-49.7713** | **-48.8809** | 0.4994 |
| Frank | 2.9086 | 3.0513 | -4.1027 | -3.2123 | 0.4823 |
| Gaussian | 0.9816 | 20.8389 | -39.6779 | -38.7875 | **0.4053** |
| Student's t | 0.6103 | 22.2799 | -42.5598 | -41.6694 | 0.4945 |

*Table 3. Results of copula fitting for Type II reliability function*

| Copula type | Parameter (Θ) | LL | AIC | BIC | ARE |
|---|---|---|---|---|---|
| Gumbel | 1.3195 | **25.6364** | **-49.2728** | **-48.3824** | 0.4912 |
| Clayton | 0.94423 | 2.1686 | -2.33719 | -1.44682 | 0.4433 |
| Frank | 2.9086 | 3.05135 | -4.1027 | -3.2123 | 0.4823 |
| Gaussian | 0.9832 | 20.8389 | -39.6779 | -38.7875 | **0.4053** |
| Student's t | 0.3226 | 22.2799 | -42.5598 | -41.6694 | 0.4816 |

parameters, we can simulate the competing failure processes for the system to obtain the marginal reliability functions and the joint reliability function with dependent competing risks (see table 1). In this paper, Gumbel copula, Clayton copula, Frank copula, Gaussian copula and t-copula are employed to fit the joint reliability distribution. Based on the simulated marginal reliability data in table 1, we can use MLE to estimate the parameters of the copula functions.

Denote the joint reliability function in Eq. (15) by Type I reliability function, and the joint reliability function in Eq. (16) by Type II reliability function.

The results for Type I reliability function are given in table 2. The criteria, Log-likelihood (LL), Akaike information criterion (AIC) and Bayesian information criterion (BIC) are used to show the goodness of fit. AIC and BIC are two criterion functions with the difference that the BIC also takes account of the sample size. Besides, the average relative error (ARE) criterion is used to judge the relative error between the fitted reliability data and the simulated reliability data, and determine which copula function has the highest precision to estimate the system reliability. The ARE is computed as

$$\text{ARE}=\frac{1}{N}\sum_{i=1}^{N}\left|\frac{R_{sim}(t_i)-R_{copula}(t_i)}{R_{sim}(t_i)}\right|$$

, where $R_{sim}$ is the simulated reliability result, $R_{copula}$ is the reliability computed with the copula function, $t_i$ corresponds to the time in table 1 and $N_1$ =18 in this case.

The results for Type II reliability function are given in table 3.

From the results in table 1 and 2, it can be seen that the Clayton Copula is the most suitable copula function for fitting Type I reliability function, the Gumbel Copula is the most suitable copula function for fitting Type II reliability function, but Gaussian copula has the highest precision for the system reliability estimation with Type I or Type II reliability function. The comparisons of the joint copula reliability functions are shown in Fig.1.

Through the comparison in Fig.1, we can see that the Gaussian copula is obviously better than other copula functions. Therefore, Gaussian copula is chosen to model the joint reliability of the sys-

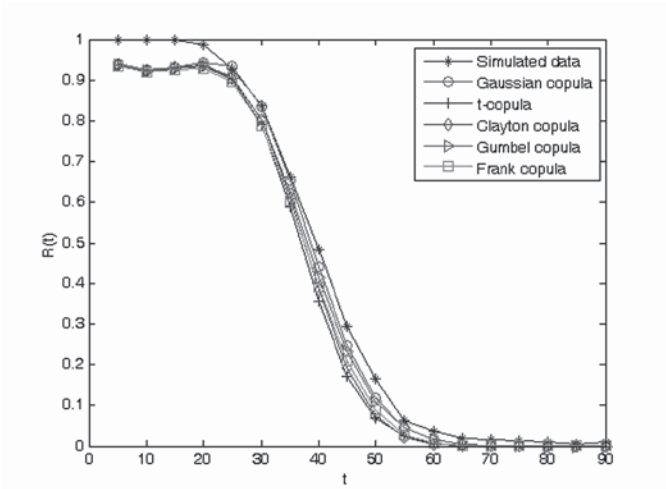


*(a) Type I reliability function*

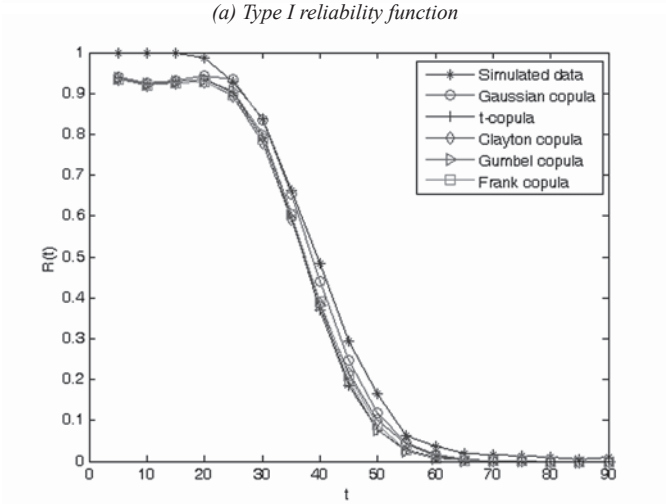


*(b) Type II reliability function*

*Fig.1. Comparison between the copula reliability with the simulated system reliability data*

tem with dependent competing risks and Type II reliability function is chosen as the system reliability function for simplicity.

Fig. 2 shows the comparison between the reliability computed by Gaussian copula reliability function in Eq. (16) and the independent reliability function in Eq. (12). It is shown that the proposed joint reliability function provides more precise results than the independent reliability function.

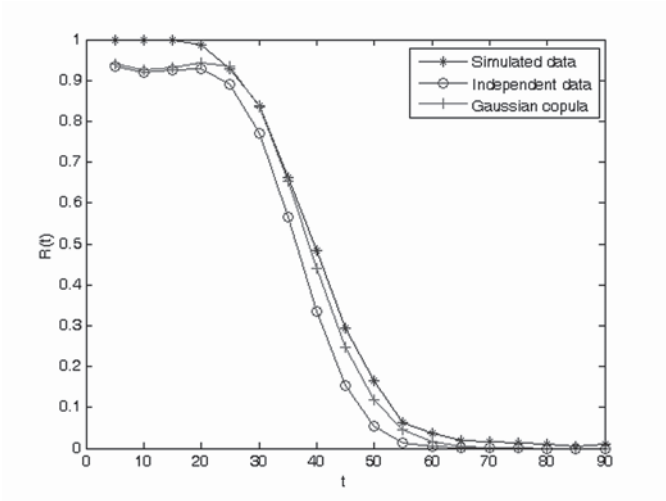


*Fig.2. Gaussian copula reliability versus independent reliability*

### 5.2. Maintenance optimization

Based on the Gaussian copula reliability function, we can use Eq. (27) to obtain the optimal inspection interval $\tau^*$=0.2 with minimum $AVC(\tau^*)$=15. Fig.3 illustrates the average maintenance cost rate in long run as a function of $\tau$.

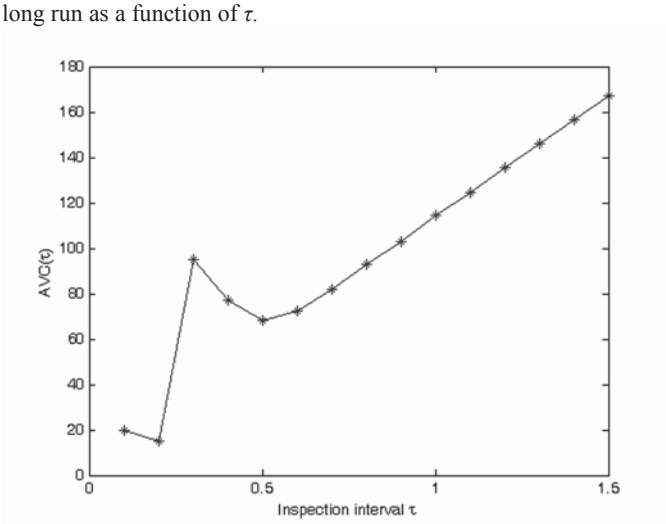


*Fig.3. Average long-run maintenance cost rate versus inspection interval $\tau$ with $C_I$=1*

For the age-based maintenance policy, we can use Eq. (29) to obtain the optimal replacement interval $\Psi^*$=28 with the minimum expected cost rate achieved as 16.17. Fig.4 depicts the expected cost rate in long run as a function of $\Psi$.

By comparing the optimal results of the two maintenance policies, it is found that the periodic inspection/replacement policy is more profitable than the age-based replacement policy (15<16.17). Actually, appropriate inspection plan can effectively reduce the maintenance cost when the inspection cost is not very high. However, when the inspection action costs too much, the periodic inspection/replacement policy will not show superiority over the age-based maintenance policy. Fig.5 shows the maintenance cost rate versus the inspection interval with $C_I$=20. The optimal cost rate $AVC(\tau^*)$=60>16.17 is achieved at $t^*$=0.2. This proves that the inspection cost is an important factor for choosing the maintenance policy.

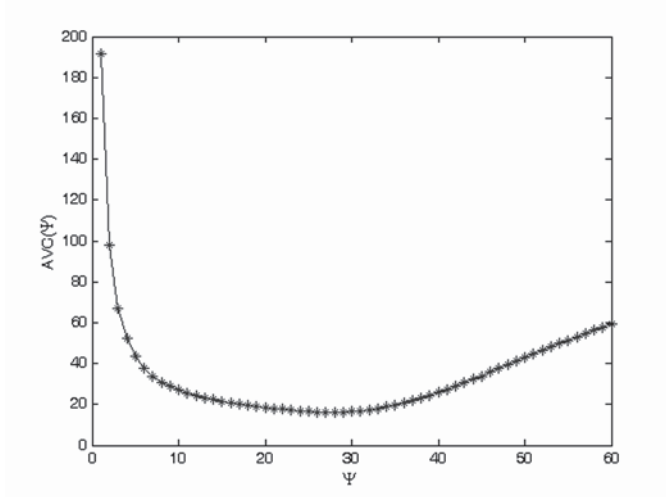


*Fig.4. Evolution of expected cost rate versus*

## 6. Conclusions

In this paper, we developed a joint copula reliability model for dependent competing risks with two degradation processes and random shocks. The random shocks can cause additional shock damages to the two degradation processes. A two-stage estimation method is proposed to estimate the parameters of the copula function based on

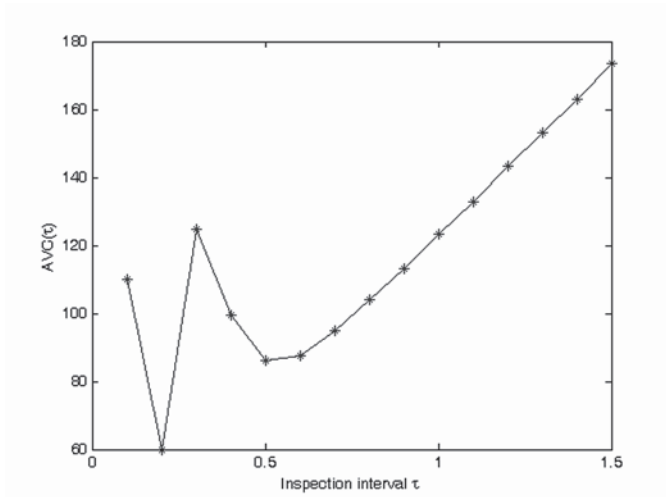


*Fig.5. Average long-run maintenance cost rate versus inspection interval $\tau$ with $C_I$=20*

simulated data. Gaussian copula function is chosen to model the system reliability with multiple dependent competing risks judging by the evaluation criteria. Based on the copula reliability model, we studied two maintenance policies for a non-repairable system. Through comparison, we find that the periodic inspection/replacement policy is superior over the age-based maintenance policy when the inspection cost is low. But when the inspection cost is high, the age-based maintenance policy will be more profitable than the periodic inspection/replacement policy.

*Acknowledgement: This work is partially supported by NSFC under grant numbers 60904002, 71231001, 71071097 and by the Fundamental Research Funds for the Central Universities of China, FRF-SD-12-020A.*

## Appendix 1

$$AVC'(\tau) = \frac{uv' - u'v}{u^2}$$

$$u = \sum_{i=1}^{\infty} i\tau (F_T(i\tau) - F_T((i-1)\tau)),$$

$$u' = \sum_{i=1}^{\infty} [i(F_T(i\tau) - F_T((i-1)\tau)) + i^2\tau f_T(i\tau) - i(i-1)\tau f_T((i-1)\tau)],$$

$$v = C_I \sum_{i=1}^{\infty} i(F_T(i\tau) - F_T((i-1)\tau)) + C_D \sum_{i=1}^{\infty} \left( \int_{(i-1)\tau}^{i\tau} (i\tau - t) dF_T(t) \right) + C_R,$$

$$v' = C_I \sum_{i=1}^{\infty} (i^2 f_T(i\tau) - i(i-1) f_T((i-1)\tau)) + C_D \sum_{i=1}^{\infty} \left( i \int_{(i-1)\tau}^{i\tau} f_T(t) dt + (1-i)\tau f_T((i-1)\tau) \right).$$

## Reference


1. Abbring H, van den Berg G. The identifiability of the mixed proportional hazards competing risks model. Journal of the Royal Statistical Society (B) 2003; 65(3): 701–710.
2. Bocchetti D, Giorgio M, Guida M, Pulcini G. A competing risk model for the reliability of cylinder liners in marine Diesel engines. Reliability Engineering and System Safety 2009; 94(8): 1299–1307.
3. Bunea C, Bedford T. The effect of model uncertainty on maintenance optimization. IEEE Transactions on Reliability 2002; 51(4): 486–493.
4. Castro I. A model of imperfect preventive maintenance with dependent failure modes. European Journal of Operational Research 2009; 196(1): 217–224.
5. Castro I, Barros A, Grall A. Age-based preventive maintenance for passive components submitted to stress corrosion cracking. Mathematical and Computer Modelling 2011; 54(1-2): 598–609.
6. Cha J, Finkelstein M. Burn-in for systems operating in a shock environment. IEEE Transactions on Reliability 2011; 60(4): 721–728.
7. Chen L, Ye Z, Huang B. Condition-based maintenance for systems under dependent competing failures. Proceedings of the 2011 IEEE IEEM, Singapore, 2011: 1586–1590.
8. Cherubini U, Luciano E, Vecchiato W. Copula method in finance. London: John Wiley & Sons.2004.
9. Deloux E, Castanier B, Bérenguer C. Predictive maintenance policy for gradually deteriorating system subject to stress. Reliability Engineering and System Safety 2009; 94(2): 418–431.
10. Huynh K, Barros A, Bérenguer C. A periodic inspection and replacement policy for systems subject to competing failure modes due to degradation and traumatic events. Reliability Engineering and System Safety 2011; 96(4): 497–508.
11. Huynh K, Castro I, Barros A, Bérenguer C. Modeling age-based maintenance strategies with minimal repairs for systems subject to competing failure modes due to degradation and shocks. European Journal of Operational Research 2012; 218(1): 140–151.
12. Jiang L, Feng Q, Coit D. Reliability analysis for dependent failure processes and dependent failure threshold. International Conference on Quality, Reliability, Risk, Maintenance, and Safety Engineering 2011. Houston TX USA: 30–34.
13. Jiang R. Discrete competing risk model with application to modeling bus-motor failure data. Reliability Engineering and System Safety 2010; 95(9): 981–988.
14. Kharoufeh J, Finkelstein D, Mixon D. Availability of periodically inspected systems with Markovian wear and shocks. Journal of Applied Probability 2006; 43(2): 303–317.
15. Klutke G, Yang Y. The availability of inspected systems subject to shocks and graceful degradation. IEEE Transactions on Reliability 2002; 51(3): 371–374.
16. Kuniewski S, van der Weide A, van Noortwijk J. Sampling inspection for the evaluation of time-dependent reliability of deteriorating systems under imperfect detection. Reliability Engineering and System Safety 2009; 94(9): 1480–1490.
17. Lehmann, A. Joint modeling of degradation and failure time data. Journal of Statistical Planning and Inference 2009; 139(5): 1693–1706.
18. Li W, Pham H. An inspection-maintenance model for systems with multiple competing processes. IEEE Transactions on Reliability 2005; 54(2): 318–327.
19. Li W, Pham H. Reliability modeling of multi-state degraded systems with multi-competing failures and random shocks. IEEE Transactions on Reliability 2005; 54(2): 297–303.
20. Lo S, Wike R. A copula model for dependent competing risks. Journal of the Royal Statistical Society, Series C: Applied Statistics 2010; 59(2): 359–376.
21. Pan Z, Balakrishnan N. Reliability modeling of degradation of products with multiple performance characteristics based on gamma processes. Reliability Engineering and System Safety 2011; 96(4): 949–957.
22. Pan, Z, Zhou J, Zhao P. Joint accelerated failure mode modeling of degradation and traumatic failure times. Proceedings of the World Congress on Engineering 2010, London, U.K.:1735–1738.

23. Peng H, Feng Q, Coit D. Reliability and maintenance modeling for systems subject to multiple dependent competing failure processes. IIE transactions 2011; 43(1): 12–22.
24. Sari J. Multivariate degradation modeling and its application to reliability testing. National University of Singapore. PhD thesis, 2007.
25. Singpurwalla N. On competing risk and degradation processes. IMS Lecture Notes-Monograph Series, 2nd Lehmann Symposium-Optimality 2006; 49: 229–240.
26. Su C, Zhang Y. System reliability assessment based on Wiener process and competing failure analysis. Jounal of Southeast University(English Edition)2010; 26(4): 554–557.
27. Wang P, Coit D. Reliability prediction based on degradation modeling for systems with multiple degradation measures. Annual Symposium RAMS 2004, South Windsor, CT. USA:302–307.
28. Wang Y, Pham H. A multi-objective optimization of imperfect preventive maintenance policy for dependent competing risk systems with hidden failure. IEEE Transactions on Reliability 2011; 60(4): 770–781.
29. Wang Y, Pham H. Modeling the dependent competing risks with multiple degradation processes and random shock using time-varying copulas. IEEE Transactions on Reliability 2012; 61(1): 13–22.
30. Wang Z, Huang H, Li Y, Xiao N. An approach to reliability assessment under degradation and shock process. IEEE Transactions on Reliability 2011; 60(4): 852–863.
31. Whitmore G, Schenkelberg F. Modelling accelerated degradation data using Wiener diffusion with a time scale transformation. Lifetime Data Analysis 1997; 3(1): 27–45.
32. Zequeira R, Bérenguer C. Periodic imperfect preventive maintenance with two categories of competing failure modes. Reliability Engineering and System Safety 2006; 91(4): 460–468.
33. Zhou J, Pan Z, Sun Q. Bivariate degradation modeling based on gamma process. Proceedings of the World Congress on Engineering 2010 Vol III, London, U.K.:17831788.
34. Zhu Y, Elsayed E, Liao H, Chan L. Availability optimization of systems subject to competing risk. European Journal of Operational Research 2010; 202(3): 781-788.

**Mr. Chiming GUO**
**Prof. Bo GUO**
Department of System Engineering
College of Information Systems and Management
National University of Defense Technology
Changsha, Hunan 410073, China
E-mail: guochiming@nudt.edu.cn

**Prof. Wenbin WANG**
**Dr. Rui PENG**
Dongling School of Economics and Management
University of Science and Technology Beijing
Beijing 100083, China
E-mail: wangwb@ustb.edu.cn

Article citation info:
PIENIAK D, OGRODNIK P, OSZUST M, NIEWCZAS A. Reliability of the thermal treated timber and wood-based materials in high temperatures. Eksploatacja i Niezawodnosc – Maintenance and Reliability 2013; 15 (1): 18–24.

Daniel PIENIAK
Paweł OGRODNIK
Marcin OSZUST
Andrzej NIEWCZAS

# RELIABILITY OF THE THERMAL TREATED TIMBER AND WOOD-BASED MATERIALS IN HIGH TEMPERATURES

# NIEZAWODNOŚĆ KONSTRUKCYJNA DREWNA MODYFIKOWANEGO TERMICZNIE I MATERIAŁÓW DREWNOPOCHODNYCH W PODWYŻSZONYCH TEMPERATURACH*

*Existing wood and wood-based materials have had several drawbacks limiting their use, which in consequence resulted in replacing them by other materials. The most significant problems were limitations regarding maximum dimensions of the components cross – section and capabilities of manufacturing of the large-scale components. Durability and flammability of surfaces were the limiting factors as well. Nowadays, thermally treated wood and wood composites are more and more commonly used in the engineering constructions, such as: glued laminated timber (GL), laminated veneer lumber (LVL) and thermally treated timber (TT). The timber undergoes a process of thermal degradation. In high temperatures timber structure is subject to simultaneous influence in the form of forces and thermal impacts. These factors influence stress distribution in the wood structure and limit its load capacity, reflecting structure decohesion. The aim of the presented studies was to determine impact of increased temperatures on strength of the wood materials and wood-based composites. Additionally, based on the results of the strength studies, analysis of the probability of survival in high temperatures was performed. Samples used in the static bending strength studies were made of the laminated veneer lumber – LVL, glued laminated pine timber – GL, and thermally treated – TT and non-treated spruce timber - NTT. The samples were in a cuboidal shape with dimensions of 20x20x300 mm. The evaluation of bending strength was performed by means of the universal strength device - FPZ 100/1 (VEB Thuringer Industriewerk Rauenstein, Germany). Fire temperatures conditions were simulated by blowing hot air (GHG 650 LCE). The studies were conducted in the following temperature ranges: 20, 50, 100, 150, 200 and 230ºC. Based on the obtained results a reliability analysis was performed. For the analysis a two-parameter Weibull distribution was applied. In case of materials with laminated structure – LVL and GL, an increase in standard deviation of the results of bending strength in the successive temperature ranges has been observed. Higher values of shape parameter c of Weibull distribution have been demonstrated for TT spruce timber (the highest c = 5.58) and NTT (the highest c = 3.31).*

***Keywords**: Fire temperatures, thermally treated timber (TT), glued laminated timber (GL), laminated veneer lumber (LVL), reliability, bending strength.*

*Dotychczasowe materiały drewniane i drewnopochodne miały wiele wad ograniczających ich zastosowanie, co prowadziło do zastępowania ich innymi. Największy problem stanowiły ograniczenia, co do maksymalnych wymiarów przekroju elementów oraz możliwości wykonywania elementów o znacznych rozpiętościach, również trwałość powierzchni a także łatwopalność ograniczały zastosowanie. Obecnie w konstrukcjach inżynierskich coraz częściej wykorzystuje się drewno modyfikowane termicznie oraz materiały drewnopochodne m.in. drewno klejone warstwowo (GL), drewno fornirowane warstwowe (LVL) oraz drewno modyfikowana termicznie (TT). Drewno jest materiałem ulegającym termicznej degradacji. W warunkach oddziaływania wysokich temperatur konstrukcja drewniana jest poddana jednoczesnym wymuszeniom w formie sił oraz oddziaływaniom termicznym. Oddziaływanie tych dwóch czynników wpływa na rozkład naprężeń w strukturze drewna oraz ogranicza nośność konstrukcji, powodując de kohezję struktury. Celem prezentowanych badań było określenie wpływu podwyższonych temperatur na wytrzymałość materiałów drewnianych i drewnopochodnych. Ponadto, na podstawie wyników badań wytrzymałości przeprowadzono analizę prawdopodobieństwa przetrwania w podwyższonych temperaturach. Próbki do badań wytrzymałości na zginanie statyczne zostały wykonane z drewna fornirowego warstwowego – LVL, drewna sosny pospolitej klejonego warstwowo – GL oraz drewna świerkowego poddanego – TT i niepoddanego modyfikacji termicznej – NTT, w formie prostopadłościanów o wymiarach 20x20x300mm. Oceny wytrzymałości na zginanie dokonano na uniwersalnej maszynie wytrzymałościowej FPZ 100/1 (VEB Thuringer Industriewerk Rauenstein, Germany). Temperatury środowiska pożaru symulowano za pomocą nawiewu gorącego powietrza (GHG 650 LCE). Oceny dokonywano w zakresach temperatur: 20, 50, 100, 150, 200, 230ºC. Uzyskane wyniki posłużyły ocenie niezawodności. W analizie wykorzystano dwuparametrowy rozkład Weibulla. W przypadku materiałów o strukturze laminowanej – LVL i GL zaobserwowano wzrost odchylenia standardowego wytrzymałości na zginanie w kolejnych zakresach temperatur. Wyższe wartości parametru kształtu c Rozkładu Weibulla zostały wykazane dla świerku TT (najwyższe c = 5.58) i NTT(najwyższe c = 3.31).*

***Słowa kluczowe**: Temperatury pożarowe, drewno klejone warstwowo (GL), drewno fornirowane warstwowe (LVL), drewno modyfikowane termicznie (TT), niezawodność, wytrzymałość na zginanie.*

(*) Tekst artykułu w polskiej wersji językowej dostępny w elektronicznym wydaniu kwartalnika na stronie ***www.ein.org.pl***

## 1 Introduction

Wood next to the stone and soil, is the oldest building material used by humans, and still one of the main raw materials applied in the engineering constructions. Increasing demands concerning the constructions result in necessity of improvement of mechanical – functional wood properties. Undoubtedly, new technologies of production of wood and wood- based structural components, as well as new types of bolts, contribute to the development of the constructions made of these materials. The wood is a flammable material undergoing thermal degradation. In the fire conditions a wooden structure is subject to the simultaneous influence in the form of forces and thermal impacts. Simultaneous interactions of these two factors influence stress distribution in the timber structure and cause a reduction of the load capacity of the construction. High temperatures occurring during the fire cause decohesion of the structure. The observable strength reduction of the timber, takes place already at temperatures above 65ºC [40]. At a micro-structural level the wood is a non-homogeneous cell composite, composed of cellulose, hemicellulose, lignin and other minor constituents [44].Cellulose is the largest part of volume of the timber. It consists of the long carbon chains, which are crucial for its strength. The hemicellulose consisting of branched amorphous polymers fills in the gap between the cellulose and lignin in the timber structure. The lignin is an amorphous polymer responsible for cohesion of timber structure, and it is a "bonding" factor [20]. Degradation of the dried cellulose occurs at temperature of about 300ºC, while degradation of hemicellulose occurs in the temperature range of 150 to 200ºC. Additionally, decomposition of the lignin, determining the cohesiveness of timber structure, takes place in the range between 220 and 250ºC [3, 17], while dehydration of lignin occurs at 200ºC. Construction timber has advantageous physical and technological properties, such as high strength and low deadweight. Till now, there have been some drawbacks due to limitations connected with maximum dimensions of the components cross-sections and manufacturing abilities of the large scale components. Nowadays, a woodworking technology, development of the treatment methods, shaping of such type of materials as well as their aesthetic properties, favor production of this kind of constructions. Possibilities of application of the special agents protecting wooden structures against a negative impact of the environmental conditions are being continuously developed, resulting in larger applications range of timber materials [8]. An application of water-resistant adhesives based on the synthetic resins together with a simple method of longitudinal joining by means of wedge joints, turned out to be especially important. It enabled much faster building method with the use of glued structural components with dimensions larger than the natural input product [25]. Joining of the wooden components by means of steel rod connectors gives more possibilities in the wood construction design and enables their local renovation with preservation of the overall structure [11]. Due to necessity to obtain high aesthetics of the interiors, in the public utility buildings wood and wood-based structures of large span are applied. In the buildings with compartments with high humidity (swimming halls), the timber proves to be a very advantageous constructional material. One of the most interesting large – scale constructions based on the timber materials is a sports hall in Hamar – "The Viking Ship" – 260 m long, 96 m wide, and 35 m high [38], or footbridge in Sromowce Niżne, which length and width together with ground ramps are 149.95 m and 3.5 m, respectively [5].

New types of timber are getting more and more popular, due to both strength as well as fire parameters, which have not been used in Europe till now. The timber from tropical countries is an alternative for the domestic brands and certainly its further investigations are to be continued [26]. In order to fulfill requirements of the modern architecture, where the most important is a freedom in the implementation of the architectural concepts, high fire resistance, necessity to obtain large structural spans, low maintenance, costs reduction and chemical resistance, the most commonly used materials are wood and wood-based composites, such as: glued timber (GL), laminated veneer lumber (LVL) and thermally modified timber (TT). However, it should be noticed that the above materials perform different functions in the constructions. The glued laminated timber composites (GL) are used in single family houses and apartment houses, as well as large-scale buildings such as production halls, market halls, sports halls, swimming pools or footbridges and bridges. The most commonly used type of timber for the production of glued components in Poland is pine or spruce, and rarely larch. A main adhesive used to produce this type of timber is a melamine adhesive, which is resistant to water and fire impact. The alternative solution is resorcinol adhesive, which is especially resistant to humidity. Both types of adhesives do not release any harmful substances, even during the fire [30]. The results of investigations have revealed that behaviour of GL in the conditions of higher temperatures strongly depends on the adhesive behaviour that bonds individual layers of the component [13]. The comparative studies of different types of timber, conducted with the use of conical calorimeter measuring heat release rate, have indicated that the charring rate of the glued timber samples decreases with the increase of timber density [42]. On the basis of specific bending strength a glued timber was divided into 5 classes: from GL24 to GL40. Grading of the sawn wood was carried out according to the standard requirements, based on the visual evaluation (for GL24 and GL28) and mechanically for the higher classes (GL32 and GL36). Due to such method of grading the classes GL24 and GL28 are the most available. The laminated glued timber after providing appropriate conditions such as chamfered edges and planed surface is resistant to fire. According to the guidelines of the Institute of Building, this type of components with a width below 12cm, are classified as low flame spread materials. The components with the width above 12cm or below 12cm with additional fire-proofing agent are classified as fire retardants. Fire resistance of the glued timber in a range of R15 to R60 can be achieved at the design stage by the proper statistical analysis and proper selection of the cross-sections.

Nowadays, laminated veneer lumber is used in many ways, starting from the ceiling beams, and bridge engineering, ending with window and door components [28]. Thanks to a laminar structure of the composite, constructional components based on LVL are very rigid, have a high resistance to fire and aesthetic appearance. Such components due to their homogeneity have an excellent dimensional stability, and nowadays they are available in a wide range of dimensions [29]. The adhesive resins bonding wood layers have a significant influence on the composite properties by decreasing adsorption of humidity, reducing impact of the acidic environment, and reducing curb weight [15]. Most often for the production of glued veneers phenol-formaldehyde adhesives are applied, while for bonding the external veneers melamine adhesives can be used as well [39]. In LVL composites the layers of the cut veneers of about 3–4 mm (most often 3.2mm) are applied [8]. The physical-mechanical parameters of LVL composite are mostly dependent on the type of the trees, from which the material originates, the type of adhesive, as well as a thickness of particular layers [1, 16]. Veneer layers in one structural component can be made of different species of wood. It has been studied and found that the sequence of the particular veneer layers made of different wood species influences the bending strength and modulus of elasticity [7]. A quality of timber used for the composite production and veneer species plays a significant role as well [37]. During a fairly long LVL composites strength studies [36], slightly higher LVL composite strength (a few percents) made of I class quality veneer comparing to II and III class veneers has been demonstrated. Number of knots and their location in the material structure [41], as well as consistency of the fibers direction with the direction of the force vector, have been proved to have an impact on the strength [33].

Thermal treatment of the timber is one of the new technologies aiming at improvement of its properties. A thermally treated timber (TT) is widely used also in Poland. Most of the thermally treated timbers available on the market are the exotic types. Thermally treated domestic timber such as spruce timber can become an alternative for the exotic timber in the longer time horizon. Modification of the timber structure improves some of its physical – mechanical properties, mostly hardness and wear resistance [21], it also improves dimensional stability of the timber components and its biological resistance, as well as reduces the amount of moisture absorbed by the wood [18, 27]. The improvement of this property occurs as a result of chemical composition, mainly due to degradation of hemicellulose [14]. This process also improves resistance to the aggressive environment and wood decay, and what is important from the aesthetic point of view – enables obtaining dark decorative colour [19]. Timber thermal treatment is usually performed in a range of temperatures between 160 and 280ºC [12], while exposure time depends on the size of the treated timber components as well as their humidity, and ranges between 15 and 24 hours. It is known that thermal treatment of timber in some cases, conducted at the specific temperatures and exposure times can lead to the reduction of the ultimate wood strength.

On the basis of the obtained results from the conducted strength studies, a reliability analysis of the above mentioned wood-based composites and thermally treated timber in high temperatures was performed. In case of static structures a reliability evaluation is possible based on the probability of not exceeding of the limit state of the load capacity or failure of the construction [24]. Probability of failure or in other words probability of not survival can be determined based on the distribution of the random variable of material strength and distribution of this variable as a function of temperature in which the object is present. The above assumption brings reliability of the construction to the strength reliability and its components. The strength reliability specifies in both a synthetic and correct way, the essence of all studies and strength investigations as well as their final purpose [2]. In this case failure is equal to probability of not survival of the engineering object or its component, while reliability is a probability of survival. The crucial issue in the construction reliability analysis is a level of reliability analysis. The analysis can be conducted in a scope of deterministic static-strength evaluations and probabilistic safety evaluation of the constructions. Three levels of the analysis can be distinguished: point level – more strictly, level of the construction material particle, section level – cross-section of the construction component, object level – structural building layout. This paper presents the analysis performed on the first level, based on the results of the ultimate strength studies conducted in high temperatures conditions.

## 2. Materials and methods

### 2.1. Studied material

Samples for static bending strength investigations were in a shape of cuboids with dimensions of 20x20x300 mm, according to PN-72-/C-04907 standard [45]. In the studies four types of samples were used: glued timber composite (GL), composite of laminated veneer lumber (LVL), treated spruce sawn (TT) and non-treated spruce sawn (NTT). In order to obtain GL samples a melamine adhesive and pine sawn were used. The samples were made by combining two components of identical dimensions to obtain a standard sample as described above. The ultimate strength of the studied material was at the level of GL28 class. Material used for LVL sample originated from the manufacturers of such materials. The standard samples were made of seven layers of spruce veneer of the equal thickness and the same direction of fibres. The fibres direction in all studied samples was consistent with the long axis of the sample. Before starting investigations the samples had been stored at 20°C for a period of 6 months, after this time humidity of the samples was about 8%.

Thermal treatment of the pine samples (TT) was performed in three stages, as shown in the first figure (Fig.1). First stage consisted in a placement of the samples in the drier and heating to 100°C for 30 minutes. Next, temperature was raised successively to 120°C for 60 minutes. During that time a process of drying of the timber took place, humidity decreased to around zero.

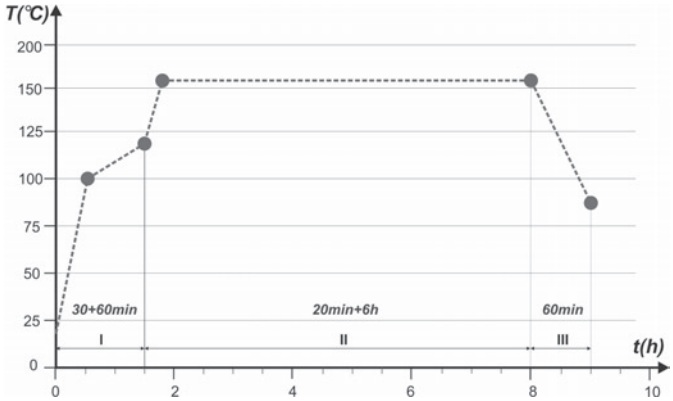


*Fig. 1. Process of thermal timber treatment [authors' work]*

The second stage consisted in the extensive heating. This phase had a significant impact on the final effect of the treatment. At this stage the temperature was raised to 160°C in 20 minutes and samples were stored in such temperature for 6 hours. The third stage included cooling and conditioning. At this stage temperature in the drier was reduced to 80-90°C, which lasted for 60 minutes. The samples were gradually cooled down. Afterwards they were wrapped in aluminium foil.

The same spruce sawn was used for both thermally treated (TT) and non-treated samples (NTT).

Investigations were performed on the group of 204 samples (66 - LVL, 54 – GL, 42 – NTT and 42 – TT), in equal quantities in each group, specified by the temperature level.

### 2.2. Strength investigations

Strength tests have been carried out by the three-point bending method. Strength investigations were conducted with the use of universal resistance device FPZ 100/1 (VEB Thuringer Industriewerk Rauenstein, Germany), which enabled static loading and maintaining it in a vertical position at the specified level. The maximum static force produced by the device was 100 kN. The device had four velocity ranges of traverse. During the studies I/III traverse velocity range was used, corresponding to velocities range of 0.021÷0.84 mm/min. The traverse velocity range was established by a potentiometer placed in a centre of velocities range.

In order to determine the bending strength a following equation was applied:

$$R_{bw} = \frac{3P_{\max} \cdot l}{2b \cdot h^2} \tag{1}$$

where:

*$P_{max}$ – force breaking the sample [N]*
*l – sample length [mm]*
*b – sample width [mm]*
*h – sample height [mm]*

Strength investigations were carried out in high temperatures until sample failure.

### 2.3. Simulation of fire temperatures

Before the main strength studies, some preliminary studies were conducted in order to determine temperature ranges for the experiment and exposure times up to the temperature equalization in the whole sample volume. During the preliminary studies some openings were made in the samples, in which thermocouples, type K, were placed to measure temperature in the geometric centre of each sample. A heating time was determined as the time after which the temperature foreseen in the schedule was measured with the thermocouple.

As the initial the ambient temperature of 20°C was assumed. The limit temperature was 230°C, which is close to ignition temperature of the wood surface. Additionally, the studies were conducted for the following temperature ranges: 50°C, 100°C, 150°C and 200°C.

During the main studies temperature was measured at the surface of the sample by means of two thermocouples being in contact with a side surface of the sample. Loading of the sample was performed after reaching a specified temperature value and maintaining it for a period of time established during the preliminary studies. Value of the breaking force and temperature were recorded in a real time. Temperature increase in a chamber was obtained by blowing with hot air (GHG 650 LCE, Bosch, Germany). Temperature range at the outlet of the nozzle was 50-560°C, and a hot air flux was adjustable in a range between 250 and 500 l/min.

### 2.4. Reliability analysis

Reliability analysis was performed based on the results obtained during a three-point bending strength test. In highest temperature the reliability was analysed on the basis of Weibull model.

For the analysis a two-parameter Weibull distribution was applied. Weibull cumulative distribution function (with positive $\sigma_0$, $c$, and $\sigma_u$ parameters), is described by the following relationship [22]:

$$P_f = 1 - \exp\left[-V\left(\frac{\sigma - \sigma_u}{\sigma_0}\right)^c\right] \tag{2}$$

where:

*σ – breaking load,*
*$\sigma_0$ – scale parameter,*
*c – shape parameter,*
*$\sigma_u$ –location parameter,*
*e – constant (e = 2.71828...),*
*V – sample volume.*

In the analyzed case $P_f$ is a probability of failure of the sample made of wood or wood-based composite. Value of the probability contains in a set between 0 and 1. In case when the load at which probability of failure equals 0 is known (in the presented analysis it is the highest known breaking load at 20ºC), the probability can be calculated from the following relationship:

$$P_f = \left(\frac{n}{N^* + 1}\right) \tag{3}$$

where:

*N* - total number of samples,*
*n – set of the ranked samples.*

In case a sample size – sample volume $V$ is constant in all subgroups of population determined by the successive temperature ranges, it can be omitted in the calculations [10, 35].

Assumption of the location parameter $\sigma_u = 0$ reduces Weibull distribution to the two-parameter distribution. The above assumption brings failure probability range to the beginning, to the known highest breaking load value. Under these assumptions the equation takes the following form:

$$1 - P_f = 1 - \left(1 - \exp\left[-\left(\frac{\sigma}{\sigma_0}\right)^c\right]\right) \tag{4}$$

The above equation can be simplified by using the logarithm to the form of $y = ax + b$ by:

$$\ln\left[\ln\left(\frac{1}{P_s}\right)\right] = c\ln(\sigma) - c\ln(\sigma_0) \tag{5}$$

where:

*$P_s$ – survival probability (equals 1 – Pf).*

An intersection of $Y$ axis depends on $-c\ln(\sigma_0)$, a slope of the curve is a shape parameter of Weibull distribution - $c$. Sample size has an influence on the determination coefficient $R^2$, which decides on the quality of prediction of the Weibull distribution parameters [31]. Thus, the higher it is the better selection quality of the shape parameter ($R^2$ values are shown in Figure 2).

## 3. Results of the studies

Descriptive statistics of the bending strength results are shown in table 1.

Logarithmic distribution of non-failure wood samples probability in high temperatures is shown in Figure 2.

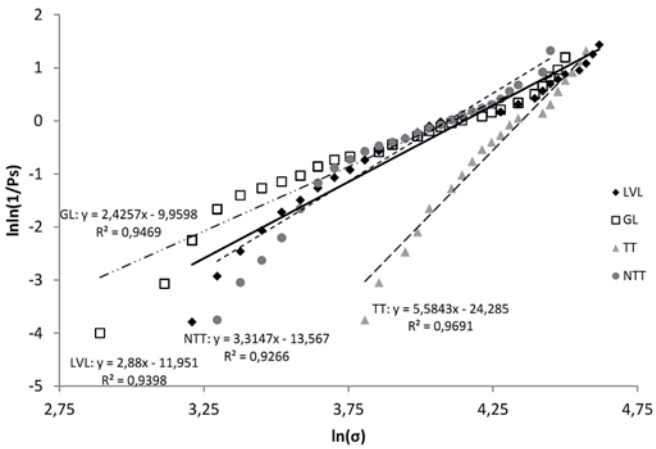


*Fig. 2. Logarithmic distribution of failure probability as a function of bending strength of the sample in high temperatures*

## 4. Results and discussion

Studies on the bending strength of wood indicate that humidity and temperature of timber applications significantly influence on mechanical strength of wood [23,43]. The decrease of wood humidity improves mechanical properties, while the temperature increase aggravates these properties. The presented results show that high temperatures influence on the strength decrease. In case of thermally treated spruce timber (TT), reduction of the bending strength at 230ºC was 42.21%, while in case of non-treated timber (NTT) it was 58.19%, in relation to the one obtained at 20 ºC. Wood-based composites LVL and GL at 230 ºC maintained 33.32% and 28.57% of the strength obtained at 20ºC, respectively. A similar level of a residual value at 230 ºC was obtained in studies presented in an article [20]. In the article, the results were determined from compression forces parallel to grain, what may indicate on s similar process of these properties degradation.

Regarding natural material, the observed strength of NTT was lower in all temperature ranges, however value of bending strengths

*Table 1. Descriptive statistics of the bending strength results*

| Temp. [°C] | Bendig strength $R_{bw}$ [MPa] | | | | | | | | |
|---|---|---|---|---|---|---|---|---|---|
| | N | Average | Min | Max | Std. dev. | Coaf. of var.. % | Residual strength % | Strength degradation intensity [MPa/ °C] | $\sigma_0$ [MPa] |
| LVL | | | | | | | | | |
| 20 | 11 | 90,82 | 81,00 | 101,25 | 7,13 | 7,86 | 100,00 | - | 58 |
| 50 | 11 | 77,52 | 72,00 | 87,75 | 5,54 | 7,15 | 85,36 | 0,44 | |
| 100 | 11 | 55,02 | 45,00 | 63,00 | 5,07 | 9,21 | 60,58 | 0,45 | |
| 150 | 11 | 47,05 | 38,25 | 54,00 | 4,32 | 9,19 | 51,81 | 0,16 | |
| 200 | 11 | 38,45 | 31,50 | 45,00 | 4,55 | 11,83 | 42,34 | 0,17 | |
| 230 | 11 | 30,27 | 24,75 | 36,00 | 4,19 | 13,85 | 33,33 | 0,27 | |
| GL | | | | | | | | | |
| 20 | 9 | 85,75 | 81,00 | 90,00 | 3,81 | 4,44 | 100,00 | - | 62 |
| 50 | 9 | 75,75 | 67,50 | 85,50 | 6,16 | 8,13 | 88,34 | 0,33 | |
| 100 | 9 | 56,75 | 49,50 | 69,75 | 7,01 | 12,34 | 66,18 | 0,38 | |
| 150 | 9 | 46,50 | 36,00 | 58,50 | 7,79 | 16,76 | 54,23 | 0,21 | |
| 200 | 9 | 32,00 | 24,75 | 38,25 | 5,00 | 15,63 | 37,32 | 0,29 | |
| 230 | 9 | 24,50 | 18,00 | 29,25 | 3,27 | 13,34 | 28,57 | 0,25 | |
| NTT | | | | | | | | | |
| 20 | 7 | 79,71 | 72,00 | 85,50 | 5,33 | 6,69 | 100,00 | - | 60 |
| 50 | 7 | 67,50 | 60,75 | 74,25 | 4,86 | 7,20 | 84,68 | 0,41 | |
| 100 | 7 | 53,68 | 45,00 | 60,75 | 5,42 | 10,10 | 67,34 | 0,28 | |
| 150 | 7 | 49,50 | 38,25 | 83,25 | 15,91 | 32,14 | 62,10 | 0,08 | |
| 200 | 7 | 38,57 | 33,75 | 42,75 | 3,54 | 9,18 | 48,39 | 0,22 | |
| 230 | 7 | 33,11 | 27,00 | 38,25 | 4,05 | 12,23 | 41,54 | 0,18 | |
| TT | | | | | | | | | |
| 20 | 7 | 89,68 | 83,25 | 96,75 | 4,93 | 5,50 | 100,00 | - | 76 |
| 50 | 7 | 87,43 | 83,25 | 92,25 | 3,03 | 3,46 | 97,49 | 0,08 | |
| 100 | 7 | 72,64 | 67,50 | 76,50 | 3,11 | 4,27 | 81,00 | 0,30 | |
| 150 | 7 | 67,18 | 63,00 | 72,00 | 3,54 | 5,27 | 74,91 | 0,11 | |
| 200 | 7 | 61,07 | 56,25 | 67,50 | 3,99 | 6,53 | 68,10 | 0,12 | |
| 230 | 7 | 51,75 | 45,00 | 56,25 | 4,31 | 8,33 | 57,71 | 0,31 | |

of TT and NTT at normal temperature (20ºC) were similar. It seems possible that thermal wood modification improves strength reliability. The decrease of humidity, in a technological process of thermal wood modification, results in polymers (cellulose) degradation [20]. This polymers significantly influence on mechanical strength of wood [4, 34]. According to Schaffer [32], lignin, located at the exterior of wood fibers, also influences on wood strength. The lignin structure may start to change at 55°C.

Together with temperature increase an increase of the coefficient of variability of the bending strength results have been observed, while in case of LVL and GL the increase was larger. This is not unfavourable since it significantly reduces abilities of precise evaluation of the construction condition and prediction of the hazard level at the point, where the temperatures of construction components are lower than their ignition temperature.

The strength degradation intensity of studied materials was higher in a first two temperature ranges (tab.1). Different connection has been shown only in case of TT materials, for which the decrease of strength was slight in a first range. It may be the result of thermal wood modification, which influences on transition of cellulose and hemicellulose vitrification. Additionally, it is indicated that transition of cellulose structure during thermal modification, under proper conditions, influences on rigidity improvement and other physical and mechanical wood properties [4].

A presented method of reliability analysis of the material is insufficient to evaluate reliability of the construction. The method does not include different functions performed by components made of the studied materials in the construction. It enables only a comparative reliability analysis of the materials. This method can be in a way referred to the first level of the construction reliability analysis, concerning one component of the construction. It means that the presented analysis, based on the simple three-point bending strength test, does not take into account a redistribution of forces to the other construction components as well as other methods of loading performance. In the reliability analysis, in case of the whole construction sections, which usually are serial sets of components, the analysis is performed for a so called "the weakest element". The reliability of the whole section being a serial arrangement, in the simplest concept is a product of reliability of its components [24]. A serial model can be applied also to the evaluation of the safety and reliability of the construction components statistically indeterminable, if redistribution of the internal forces is not allowed and statistical calculation methods are applied – stresses in all critical cross-sections of the construction are calculated and compared with the material strength [24].

A limiting factor of the presented analysis is concluding only based on the ultimate strength of the samples without the loading history. Moreover, as well known, a long-term strength of timber is much lower than the ultimate one. According to [6] after 10 years of operating it represents only about 60% of the ultimate strength, and after 50 years – about 50%.

In the presented publication survival probability (no failure) was analysed in two different ways. First the analysis as a function of strength (Fig. 2) was performed, without dividing into successive temperature ranges and using all available strength results from the successive temperature ranges. It enabled application of two-parameter Weibull distribution and obtaining shape and scale distribution parameters. Next, the analysis as a function of temperature of simulated fire conditions (Fig. 3) was performed. The aim of such procedure

was to obtain a single reliability distribution, continuous in the successive temperature ranges, for each of the materials instead of having many distributions for the successive temperature ranges. Applicability of the latter ones is much lower.

Based on the logarithmic distribution of failure probability in the temperature field, the higher values of shape parameter *c* of Weibull distribution have been obtained in case of spruce timber TT (the highest value c = 5.58) and NTT (the highest value c = 3.31). The lower

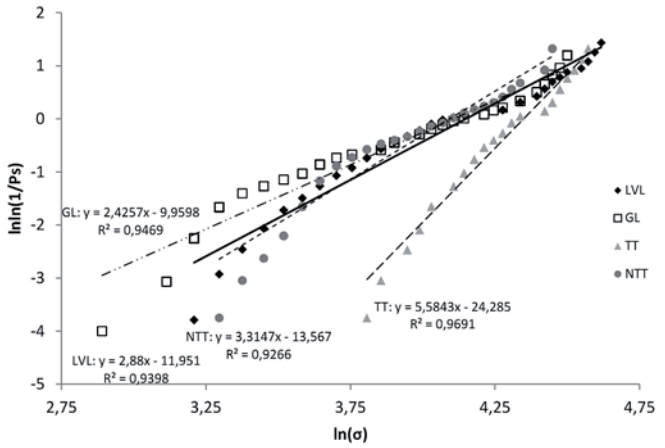


*Fig. 3.*

value of scale parameter of Weibull distribution indicates a larger scatter of the obtained results. The reason for the lower values of shape parameters for LVL (c = 2,88) and GL (c = 2,43) is most probably a laminar structure of composites.

## 5. Conclusion

The aim of this work is to determined the influence of high temperatures on the wood and wood-base materials strength. Additionally, based on experimental strength results, the analysis of survival probability in high temperatures ( 20–230 °C) has been carried out. Investigations were performed on the group of 204 samples (66 – LVL, 54 – GL, 42 – NTT and 42 – TT), in equal quantities in each group, specified by the temperature level. The test obtained static load and thermal treatment. The results lead to following conclusions:

High temperatures influence on the decrease of studied materials residual strength. The highest residual strength has been obtained for thermally modified wood (TT). It seems possible that the preliminary thermal treatment favor strength maintaining in high temperatures.

In case of non-treated spruce timber NTT and thermally treated TT the residual strength has been higher than in case of two wood-based composites (LVL and GL). Glued-laminated structure as a negative factor on behavior of these kind of materials under fire conditions should be considered.

The standard deviation increase of bending strength results of LVL and GL materials has been observed in following temperature ranges. There is probability that the highest unpredictability strength increase of these materials occurs in temperatures which are similar to wood ignition temperatures. It was different in case of non-treated spruce timber. The highest increase of the standard deviation of strength has been observed in 150°C - in this temperature the process of hemicellulose degradation is intensive.

Based on the logarithmic distribution of failure probability in the temperature field, the higher values of shape parameter *c* of Weibull distribution have been obtained in case of spruce timber TT (the highest value c = 5.58) and NTT (the highest value c = 3.31). The lower value of scale parameter of Weibull distribution indicates a larger scatter of the obtained results. The reason for the lower values of shape parameters for LVL (c = 2,88) and GL (c = 2,43) is most probably a glued-laminated structure, which does not improve material behaviour under fire conditions.

The presented studies show that in case of non-thermal test group materials determination quotient has low values ( below 0,95). It may be result of non-linear decrease of materials properties in high temperatures and increase behavior unpredictability.

## References


1. Baldwin RF. Plywood and veneer-based products, manufacturing practices (Wood technology books ser). Miller Freeman. San Francisco 1995.
2. Bąk R, Burczyński T. Wytrzymałość materiałów z elementami ujęcia komputerowego. Wyd. WNT. Warszawa 2001.
3. Beall F.C, Eickner H.W. Thermal degradation of wood components. Forest Products Research Paper 1970: 130.
4. Bhuiyan RT, Hirai N, Sobue N. Changes of crystallinity in wood cellulose by heat treatment under dried and moist conditions. Wood Sci Technol 2000; 46: 431–6.
5. Biliszczuk J, Hawryszków P, Maury A, Sułkowski M, Węgrzyniak M. Kładka dla pieszych w Sromowcach Niżnych. Rekordowa konstrukcja mostowa z drewna klejonego. Nowoczesne Budownictwo Inżynieryjne 2007; 11: 36-39.
6. Bliszczuk J, Bień J, Maliszewski P. Mosty z drewna klejonego. WKŁ Warszawa 1988.
7. Burdurlu E, Kilic M, Ilce A, Uzunkavak O. The effects of ply organization and loading direction on bending strength and modulus of elasticity in laminated veneer lumber (LVL) obtained from beech (Fagus orientalis L.) and lombardy poplar (Populus nigra L.). Construction and Building Materials 2007; 21: 1720–1725.
8. Caggins C.R. Timber preservation in building and construction. Construction and Building Materials 1989: 114–117.
9. Chui Y, Schneider M, Hang H. Effects of resin impregnation and process parametre on some proporties of poplar LVL. Forest products Journal 1994; 44: 74–78.
10. Davies D.G.S. The statistical approach to engineering design in ceramics. Proceedings of the British Ceramic Society 1973; 22: 429–452.
11. D Otero Chans, Estevez Cimadevila J, Martin Gutierrez E. Glued joints in hardwood timber. International Journal of Adhesion & Adhesives 2008; 28: 457–463.
12. Fengel D, Wegener G. Wood chemistry, ultrastructure, reactions. Berlin, Walter de Gruyter 1989.
13. Frangi A, Fontana M, Hugi E, Jobstl R. Experimental analysis of cross-laminated timber panels in fire. Fire Safety Journal 2009; 44: 1078–1087.
14. Gunduz G, Aydemir D, Karakas G. The effects of thermal treatment on the mechanical properties of wild Pear (Pyrus elaeagnifolia Pall.) wood and changes in physical properties. Materials and Design 2009; 30: 4391–4395.
15. Johansson C.J. Glued-in bolts. Timber engineering. STEP 1: lecture C14. Centrum Hout. Almere 1995.
16. Kamala B.S, Kumar P, Rao R.V, Sharma S.N. Performance test of laminated veneer lumber (LVL) from rubber wood for different physical and mechanical properties. Holz Roh Werkst 1999: 114–116.

17. Kamdem D.P, Pizzi A, Jermannaud A. Durability of heat-treated wood. Holz als Roh- und Werkstoff 2002; 60: 1–6.
18. Kartal S.N, Hwang W.J, Imamura Y. Combined effect of boron compounds and heat treatments on wood properties: Chemical and strength properties of wood. Journal of Materials Processing Technology 2008; 198: 234–240.
19. Korkut S, Akgul M, Dundar T. The effcts of heat treatment on some technological properties of Scots pine (Pinus sylvestris L.) wood. Bioresource Technology 2008; 99: 1861–1868.
20. Manríquez M.J, Moraes P.D. Influence of the temperature on the compression strength parallel to grain of paricá. Construction and Building Materials 2010; 24: 99–104.
21. Mazela B, Zakrzewski R, Grześkowiak W, Cofta G, Bartkowiak M. Resistance of thermally modified wood to basidiomycetes. Wood Technology 2004; 7: 253–262
22. Migdalski J. Inżynieria niezawodności. Poradnik. Wyd. ATR ZETOM. Warszawa 1992.
23. Moraes PD et al. Influence of temperature on the embedding strength. Holz Roh-Werkst 2005;63:297–302.
24. Murzewski J. Niezawodność konstrukcji inżynierskich. Wyd. Arkady. Warszawa 1989.
25. Neuhaus H.: Budownictwo drewniane, podręcznik inżyniera. Polskie Wydawnictwo Techniczne. Rzeszów 2006.
26. Njankouo J, Dotreppe J, Franssen J. Fire resistance of timbers from tropical countries and comparison of experimental charring rates with various models. Construction and Building Materials 2005; 19: 376–386.
27. Obataya E, Tanaka F, Norimoto M, Tomita B. Hygroscopicity of heat-treated wood 1. Effects of after-treatments on the hygroscopicity of heat-treated wood. Journal of Wood Science 2000; 46: 77–87.
28. Ozcifci A. Effects of scarf joints on bending strength and modulus of elasticity to laminated veneer lumber (LVL). Building and Environment 2007; 42: 1510–1514.
29. Ozcifci A, Okcu O. Impacts of some chemicals on combustion properties of impregnated laminated veneer lumber (LVL). Journal of materials processing technology 2008; 199: 1–9.
30. Przepiórka J, Żurowski P. Konstrukcyjne drewno klejone. Inżynier Budownictwa 2008; 10: 60–64.
31. Ritter JE, Bandyopadhyay N, Jakus N. Statistical reproducibility of the dynamic and static fatigue experiments. Ceramic Bulletin 1981; 60: 798–806.
32. Schaffer EL. Effect of pyrolytic temperatures on the longitudinal strength of dry douglas fir. J Test Eval 1973;1(4):319–29
33. Sei-Chang O. Applying failure criteria to the strength evaluation of 3-ply laminated veneer lumber according to grain direction by uniaxial tension test. Construction and Building Materials, 2010.
34. Sivonen H et al. Magnetic resonance studies of thermally modified wood. Holzforschung 2002;56(6):648–53.
35. Stanley P, Fessler H, Sivil AD. An engineer's approach to the prediction of failure probability in brittle components. Proceedings of the British Ceramic Society 1973; 22: 453–487
36. Strickler M.D, Pellerin RF. Tension proof loading laminated beams. Forest Prod J 1971; 21: 10–15.
37. Tichy RJ, Bodig GJ. Flexural properties of glued la pine dimension lumber. Forest Prod J 1978; 29.
38. Tomusiak A. Drewno klejone warstwowo. Materiały Budowlane 2001; 8: 92–93.
39. Uysal B. Bonding strength and dimentional stability of laminated veneer lumbers manufactured by using different adhesives after the steam test. International Journal of Adhesion & Adhesives 2005; 25: 395–403.
40. White RH, Dietenberger MA. Wood Products: Thermal Degradation and Fire. Encyclopedia of Materials: Science and Technology. Elsevier Science Ltd 2001: 9712–9716
41. Wolf R, Moddy R.C. Bending strength of vertically glued laminated beams. Forest Prod J. 1979; 30: 32–40.
42. Yang T, Wang S, Tsai M, Lin C. The charring depth and charring rate of glued laminated timber after a standard fire exposure test. Building and Environment 2009; 44: 231–236.
43. Young SA, Clancy P. Compression mechanical properties of wood at temperatures simulating simulating fire conditions. Fire Mater 2001;25: 83–93.
44. Younsi R, Kocaefe D, Poncsak S, Kocaefe Y. Computational and experimental analysis of high temperature thermal treatment of wood based on ThermoWood technology. International Communications in Heat and Mass Transfer 2010; 37: 21–28.
45. PN-72/C-04907: Środki ochrony drewna. Oznaczanie wpływu na wytrzymałość drewna.

**Daniel PIENIAK, Ph.D. (Eng.)**
**Paweł OGRODNIK, Ph.D. (Eng.)**
**Marcin OSZUST, M.Sc. (Eng.)**
Thr Main School of Fire Services
Department of Fire Safety Engineering
ul. Slowackiego 52-54, 01-629 Warsaw, Poland
E-mail: mechanika@sgsp.edu.pl

**Prof. Andrzej NIEWCZAS, Ph.D. (Eng.)**
High School of Economy and Innovations
Department of Transportation and Computer Sciences
ul. Melgiewska 7-9, 20-209 Lublin, Poland
E-mail: andrzej.niewczas@wsei.lublin.pl

Article citation info:
JAMROZIAK K, KOSOBUDZKI M, PTAK J. Assessment of the comfort of passenger transport in special purpose vehicles. Eksploatacja i Niezawodnosc – Maintenance and Reliability 2013; 15 (1): 25–30

Krzysztof JAMROZIAK
Mariusz KOSOBUDZKI
Jerzy PTAK

# ASSESSMENT OF THE COMFORT OF PASSENGER TRANSPORT IN SPECIAL PURPOSE VEHICLES

# OCENA WARUNKÓW KOMFORTU TRANSPORTU OSÓB W POJAZDACH SPECJALNEGO PRZEZNACZENIA*

*The article discusses the issue of comfort, that should characterize a vehicle which has been designed to work under special conditions. If the criteria of ensuring the proper comfort of the passengers of special purpose vehicles are not met, it might lead to a serious disturbances in perception and in other factors that affect the logical behavior. Performance characteristics generated by the body of the vehicle during tests on the range can be assessed only through research and then related to the characteristics of the human body-vehicle system. The presented results concern the assessment of the ride comfort in the selected vehicles under special conditions and capacity of the crew to effectively perform tasks after long-lasting ride.*

***Keywords**: special purpose vehicles, passenger transport, vibrations, comfort of a crew.*

*W artykule omówiono zagadnienia dotyczące komfortu, jakim powinien charakteryzować się pojazd do pracy w warunkach szczególnych. Nie spełnienie kryteriów właściwego komfortu u przewożonych osób pojazdami specjalnego przeznaczenia prowadzi do powstawania poważnych zaburzeń na tle percepcji i innych czynników niezbędnych w logicznym postępowaniu. Jedynie na drodze badań możemy ocenić charakterystyki generowane przez nadwozie w testach poligonowych i odnieść to do charakterystyk organizm ludzki-pojazd. Prezentowane wyniki dotyczą oceny charakterystyk komfortu poruszania się wybranymi pojazdami w warunkach szczególnych i możliwości wykonania zadań przez przewożony personel po długotrwałej jeździe.*

***Słowa kluczowe**: pojazdy specjalne, transport osobowy, drgania, komfort załogi.*

## 1. Introduction

The soldiers who perform their duties while on patrol could be exposed to various stimuli that can cause a fatigue, which can be divided into four categories [2]: muscular, sensory, intellectual and emotional. Unfortunately, it is almost impossible to modify the external treats which are typical for patrol duties – their influence is relatively stable in nature. On the other hand, we can reduce the internal threats, such as muscle fatigue and fatigue on emotional level. It should be mentioned that the need for security, together with some physiological needs, must be satisfied to enable human to undertake further activities [14]. Possibility for changes could be therefore sought in the proper construction of the vehicles that ensure the highest possible level of comfort of the crew. This kind of construction should raise the crew's sense of security by meeting the adequate standards of bulletproofing and shrapnel proofing [1, 25].

One of the areas that have been mentioned above, that significantly affects the quality of work performed by the crew of the patrol vehicle, is ride comfort. Assessment of this variable is usually performed using the ISO 3126 standard [7]. An alternative approach has been codified in british standard [3]. These standards evaluate riding comfort on the basis of the set of physical sensations associated with the dynamics of vehicle's motion, which include: accelerations and its changes in the transverse, longitudinal and vertical direction as well as the angular motion around $x$, $y$, $z$ axle – that is the transverse tilt motion, longitudinal slope and tilt movement. Information about the risks associated with the exposure of the human body to the vibrations that could cause a health problems can be found in [5] and limits of a permissible dose of the vibrations are determined in the regulation [21].

The literature concerning this subject is quite extensive and focused mainly on the studies regarding the improvement of performance of the civilian vehicles, with particular emphasis put on the driver's place of work [4, 8, 10, 22, 26, 27]. Especially the work of Griffin [6] extensively presents the requirements and correlations between the standards [3, 7] and the requirements of the European Union's in the scope of health and safety of people exposed to the vibrations generated by the vehicles.

Results of the assessment of ride comfort of military special purpose vehicles are very limited. Partial assessment has been presented in the papers [11, 15, 16, 20]. One of the papers [18] summarizes the results of evaluation of ride comfort of different vehicles, including military vehicles, but provides no details about the type of vehicle. Additionally, the paper [15] summarizes the results in the form of accelerations transmitted to the human body in defined one third octave bands, but only for the selected track-laying vehicles. More detailed information have been presented in the paper [20], where the groups of track-laying vehicles and wheeled vehicles have been compared in the scope of specific doses of maximal permissible concentrations and intensities (NDN). Data on military vehicles concerns most frequently the level of ballistic protection – basing on the asumption that this paramether of the vehicle is the most important and the ride comfort is rather considered to be an issue of secondary importance [12, 13].

(*) Tekst artykułu w polskiej wersji językowej dostępny w elektronicznym wydaniu kwartalnika na stronie ***www.ein.org.pl***

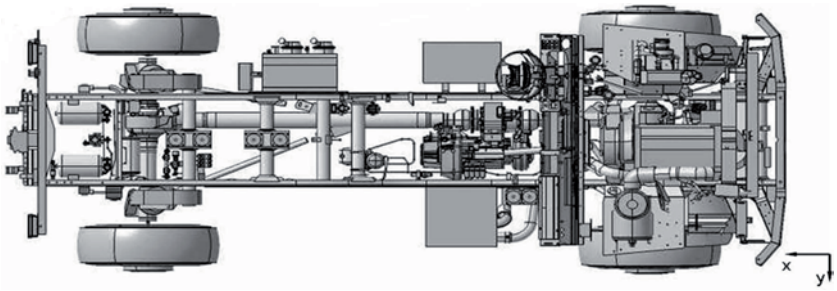


*Fig. 1. The chassis of UNIMOG 437.465 with an engine OM924LA Euro3 163kW – view from the top [19]*


*Fig. 2. The chassis of UNIMOG 437.465 with an engine OM924LA Euro3 163kW – view from the top [19]*

*Table 1. Technical parameters of military chassis [19]*

| Dimensions | | Masses | |
|---|---|---|---|
| Axle base | 3860 mm | The share of mass – front axle | 3,1 t |
| Length | 5994 mm | The share of mass – rear axle | 1,9 t |
| Front overhang | 1043 mm | Complete vehicle kerb weight | 5,0 t |
| Rear overhang | 1091 mm | Permissible load of front axle | 12,5 t decreased by the load of the rear axle, but no more than 6,0 t |
| Width | 2440 mm | Permissible load of rear axle | 7,1 t` |
| Wheel track | 1556 mm | Permissible total weight | 12,5 t |
| Clearance | 553 mm | | |
| Approach angle | 40° | | |
| Departure angle | 38° | | |
| Tyres | 365/80 R20 with run-flat segment | | |

*Table 2. Recorded speeds of the tested vehicle for different road pavements*

| Test section | Asphalt road | Gravel road | Driving on railway sleepers | Mountain road | Road made of symmetrically arranged concrete slabs | Road made of asymmetrically arranged concrete slabs |
|---|---|---|---|---|---|---|
| Driving speed [km/h] | 50 | 30 | 10 | 10 | 50 | 50 |

Previous publications [22, 23] focused also on the analysis of the selected parts of the vehicles, mainly in terms of quality and safety of their construction. Meanwhile, the analysis of the usage of patrol vehicles shows, that they usually cover very long distances. Because of that, besides of safety guaranteed by proper ballistic protection, minimalization of the negative influence of vibrations on the human body is an important factor that afects the capacity of the crew to undertake specific actions after the long-lasting ride. Lack of information in this area encouraged authors to make an attempt to assesse the riding comfort of the vehicle of the class M-ATV (MRAP All Terrain Vehicle).

## 2. The object of the research

The research has been conducted on the prototype of the Armored Multi Role Vehicle (AMRV G10) on the chassis of the Mercedes UNIMOG U5000 series, in the military version, model 437.465 (Fig. 1) [8].

Technology demonstrator made in the ballistic development for 10 people (Fig. 2) has been subjected to the road tests with taking into account data compiled in the Table 1.

The measurements have been conducted in one of the european centers for road tests of special and off-road vehicles. Out of the many test sections that are in the disposition of the center, studies have been conducted on the pavements: asphalt, gravel and one made of concrete slabs of symmetrically and asymmetrically arranged vertical faults. Additionally, tests were also carried out on the special road section that simulates the mountain road, driving on railway sleepers and that forces significant torsion of load-carrying structure and thus a large tilts of the vehicle's body. Figure 3 presents the reconnaissance map of the test track. Different driving speeds have been determined for the selected road sections – its combination is shown in Table 2. Time of ride through the whole test track was 1680±120 seconds.

## 3. Formulation of the problem

Description of the quantitative measurements of vibrations that affect the human body has been specified in regulation [21] concerning the maximal permissible concentrations and intensities (NDN) of health hazards in the workplace. This regulation distinguishes short-term vibrations (up to 0.5 hours) and full day vibrations (8 hours) and defines the influence of vibrations on human body while distinguishing between vibrations of general and local influence. This paper presents the values of NDN resulting from the actual time of driving through the entire measured section as well as its convertion to 8 hours of driving. Permissible values of NDN have been shown in Table 3.

The concept of dominant weighted acceleration of vibration has been introduced for the vibrations of general influence. This is the largest value of the weighted acceleration of vibrations, selected from the three directional components of acceleration (in point of fact

*Table 3. Permissible values of NDN for the protection of health [21]*

| Type of vibration | Permissible values (NDN) for daily exposure to mechanical vibrations | Permissible values (NDN) for short-term exposure to mechanical vibrations |
|---|---|---|
| Vibrations of general influence | $A(8)_{dop} = 0,8\frac{m}{s^2}$ | $a_{w0,5dop} = 3,2\frac{m}{s^2}$ |

*Table 4. Accelerations acting on the human body in typical situations*

| Type of motion | $a_x$ [m/s²] | $a_y$ [m/s²] | $a_z$ [m/s²] |
|---|---|---|---|
| walk | 0,6 | 0,6 | 1,0 |
| march | 1,0 | 0,7 | 2,5 |
| run | 2,0 | 1,0 | 4,0 |

*Table 5. The values of effective weighted accelerations of vibrations*

| | Driver | Passenger no. 1 | Passenger no. 2 |
|---|---|---|---|
| $a_{wx}$ | 0,062 | 0,102 | 0,102 |
| $a_{wy}$ | 0,102 | 0,062 | 0,062 |
| $a_{wz}$ | 0,016 | 0,018 | 0,024 |

*Table 6. The doses of vibrations absorber during a single ride*

| | Driver | Passenger no. 1 | Passenger no. 2 |
|---|---|---|---|
| $A(8)_{2s\min x}$ | 0,021 | 0,034 | 0,034 |
| $A(8)_{2s\min y}$ | 0,034 | 0,021 | 0,021 |
| $A(8)_{2s\min z}$ | 0,004 | 0,004 | 0,006 |

*Table 7. The daily doses of vibrations*

| | Driver | Passenger no. 1 | Passenger no. 2 |
|---|---|---|---|
| $A(8)_x$ | 0,087 | 0,143 | 0,143 |
| $A(8)_y$ | 0,143 | 0,087 | 0,087 |
| $A(8)_z$ | 0,016 | 0,018 | 0,024 |

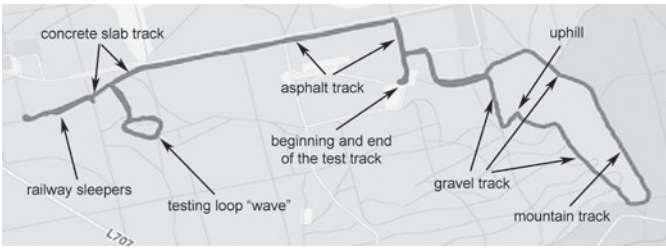


*Fig. 3. Map of the test track of the length of 10 km*

one directional component). On that basis, depending on the time of influence of the vibrations, calculations are carried out:

a) if the total time of influence of the vibrations during the day is $t \le 1,8e10^3$ seconds, the dominant value $a_{w\max}$ is selected of all the defined effective weighted accelerations of vibration $a_{wli}$ with taking into account relevant coefficients:

$$1,4a_{wx};\quad 1,4a_{wy};\quad a_{wz} \tag{1}$$

The largest value which is equal to the daily exposure to mechanical vibration (NDN) is selected among three defined values.

b) if the total time of influence of the vibrations is $t > 1,8e10^3$ seconds, the eight-hour exposure A (8) is determined for each direction l = x, y or z, according to the formula:

$$A_x(8) = 1,4a_{wx}\sqrt{\frac{t}{T}};\quad A_y(8) = 1,4a_{wy}\sqrt{\frac{t}{T}};\quad A_z(8) = a_{wz}\sqrt{\frac{t}{T}} \tag{2}$$

where: $a_{wx}$; $a_{wy}$; $a_{wz}$ – maximal effective weighted values of acceleration for the directions *x, y* or *z*; *t* – time of the route; $T=2,88e10^4$ s.

Obtained value of the dose of vibrations for the daily exposure is compared with the permissible value presented in the Table 3. This relation helps to reduce the duration of the measurements under the assumption that considered route, where measurements are carried out, is representative of the 8-hour working time of the driver (operator of the machine). Presented relations are the basis for quantitative analysis of vibrations.

Qualitative analysis has been also conducted to show the distribution of amplitudes of accelerations for the selected directions and frequencies. The most adverse vibrations are considered to be those

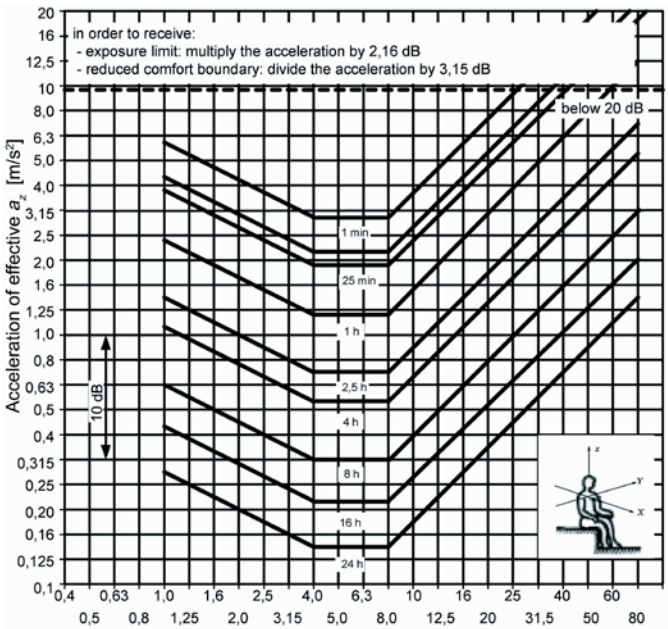


*Fig. 4. The course of changes in sensitivity of the human body to the vertical vibrations [7]*

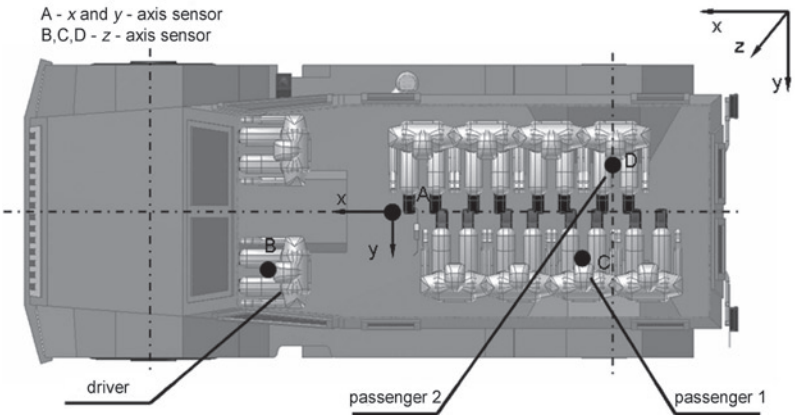


*Fig. 5. Schematic location of PCB acceleration sensors of T352 series*

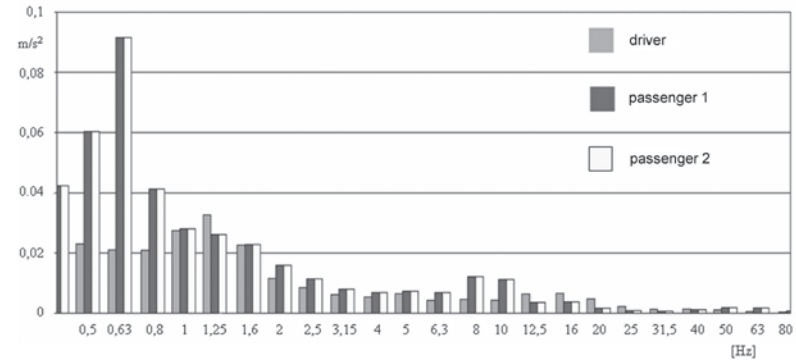


*Fig. 6. The chart of the frequency of accelerations in one third octave bands in the x axis*

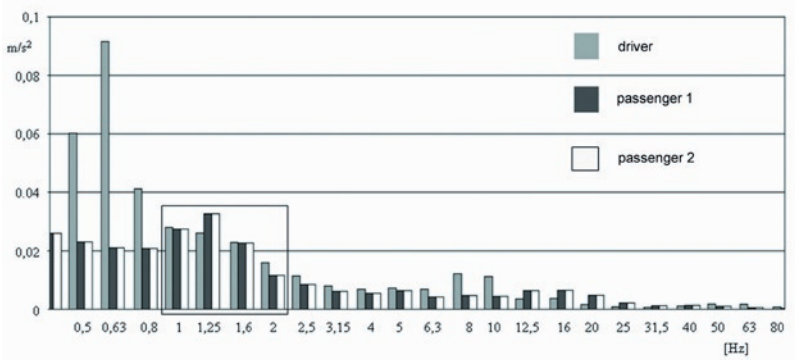


*Fig. 7. The chart of the frequency of accelerations in one third octave bands in the y axis*

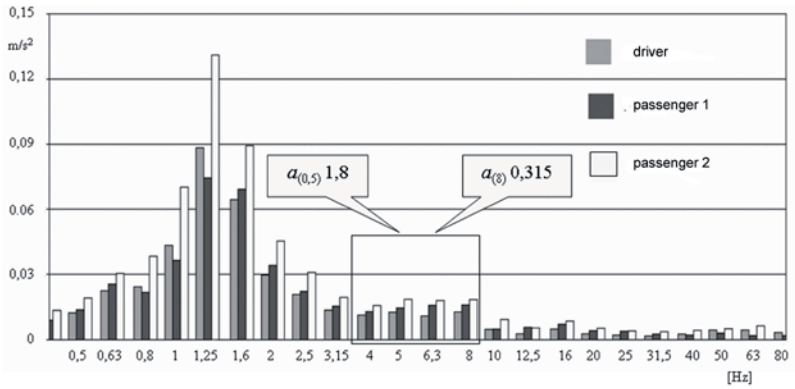


*Fig. 8. The chart of the frequency of accelerations in one third octave bands in the z axis*

in the range of 4÷8 [Hz] for the vibrations along the axis of the body (*z*) and in the range of 1÷2 [Hz] for the horizontal transverse and longitudinal axle (*x* and *y*) [7]. The course of changes in sensitivity of the human body to the vertical vibrations is presented in the Figure 4 and accelerations acting on the human body in typical situations in Table 4.

## 4. The course of research

The values of acceleration have been measured with PCB sensors of T352 series and were recorded on a storage device using a 24-channel recorder LMS SCADAS Recorder with sampling rate *v=400 [Hz]* and 24-bit resolution, which together gave a bandwidth of *200 [Hz]*. Sensors have been located in the horizontal, longitudinal and transverse axle of the vehicle and in vertical axis on driver's seat as well as in the transport compartment, which allowed to measure the acceleration of the general influence. Passengers seats were located along the walls of the vehicle in such way that people were sitting side-facing and face to face to each other. Passenger no. 1 have been sitting before the rear axle of the vehicle and passenger no. 2 directly behind it. It was assumed that the horizontal accelerations experienced by the driver and passengers will be measured by the common sensor, which has been located in the middle of the vehicle at the height of the passengers seats (Fig. 5). The frequency range 0,5÷80 [Hz] that was important due to the comfort of riding, have been determined based on the appropriate standards [7]. GPS system coupled with the recorder has been used to record the speed of the vehicle and its route.

## 5. Results and analysis

On the basis of conducted measurments, the values of effective weighted accelerations of vibrations have been determined: $a_{wx}$; $a_{wy}$; $a_{wz}$ . The results are presented in Table 5.

Given that the time of a single ride took an average of $1{,}8e10^3$ seconds, it allowed to determine the doses of vibrations that have been absorbed by the driver and passengers bodies during a single ride. The results are shown in Table 6.

Assuming that the time of driving in the vehicle equals 8 hours, the daily doses of vibrations were determined and are presented in the Table 7.

The qualitative assessment of the vibrations transmitted to the body of driver and passengers has been conducted based on the charts of the frequency of accelerations in one third octave bands in the directions *x*, *y* and *z*. The results are shown in Figures 6 to 8.

## 6. Summary

Assessments of the comfort of the passengers during transportation in special purpose vehicles (off-road vehicles of high mobility) were narrowed down into two areas. In the area of quantitative studies, the doses of vibrations that affect the human body have been defined on the scale of permissible parameters for short-term exposure and the daily exposure. Special focus has been given to the most disadvantageous case, that is the verti-

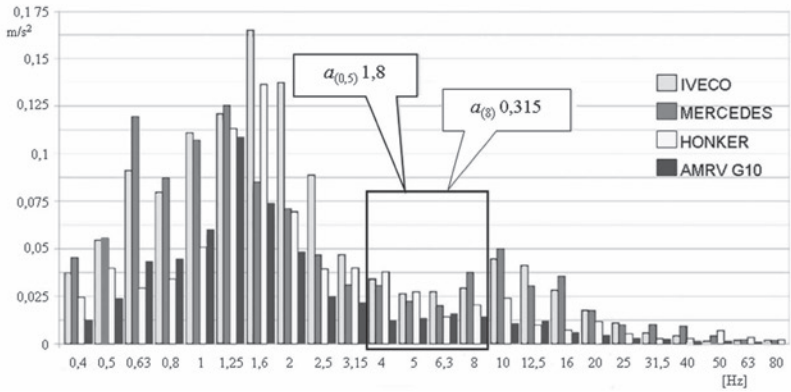


*Fig. 9. The partial diagram of accelerations in one third octave band in z axis for the selected special purpose vehicles*

cal acceleration (of *z* axis, Fig. 8). In the area of qualitative studies, an analysis concerned illustrating (Fig. 6 to 8) the distribution of the amplitudes of accelerations for the determined directions with taking into account the particular frequencies. Special focus has been given to the values determined by the regulations [7] such as the adverse vibrations in the range of 4÷8 [Hz] for vertical accelerations and in the range of 1÷2 [Hz] for the transverse and longitudinal accelerations.

The presented results of the analysis of spectrum of accelerations in the selected points of the vehicle, lead to the following conclusions:

- available ride comfort for driver and passengers does not exceed the limits for the vibration dose established in the regulations [21]. This leads to the conclusion that this dimention, although affects the overall ride comfort, is not dominant. So, if we want to provide better driving conditions, we should reduce the negative impact of other factors mentioned in the introduction. Furthermore, when comparing the values of the dose of vibrations to the similar results obtained by other special purpose vehicles (Fig. 9), we may conclude that the tested vehicle provides the lowest values of accelerations and the smallest doses of vibration, which means that it is the most comfortable vehicle [12],
- partial decomposition of the accelerations determined on the basis of conducted tests and related to the regulations [7] gives a qualitative picture of vibrations that occur in the analyzed points of measurement. This distribution is advantageous and there is an evidence of significant decline in the value of accelerations in the range of 4÷8 [Hz].

The presented results of assessment of ride comfort for the selected group of vehicles operated by the user (Fig. 9) aimed at showing that the vehicles of Honker 2000 type that have been critically reviewed by its users in terms of durability, provide the similar ride comfort of passengers to the Mercedes 290G and are much better than Iveco 4012 if concerning the values of accelerations in the range of 0,5÷80 [Hz]. The parameters presented in the graphical form (Fig. 9) show that driving Iveco 4012 can be associated with accelerations that may exceed passengers tolerance. Characteristics of the ride comfort of the vehicle is similar to characteristics of the trucks. Comparison of the spectrum of accelerations prepared for three vehicles (Honker, Mercedes, Iveco) was a base while designing new vehicle. In this case, the detailed analysis of the passengers ride comfort have been conducted on the early stage of the project to check if the characteristics of accelerations are in the range that is established in the regulations. The results of comparison of the most adverse accelerations (in the *z*-axis) presented below confirm the right selection of characteristics of the chassis and also the technical parameters or the seats.

## References


1. AEP-55, Volume 1 (Edition 1). Procedures for evaluating the protection level of logistic and light armoured vehicles" is a NATO/PfP Unclassified publication 2005.
2. Bąk J. Zmęczenie kierowcy: przyczyny, skutki, zapobieganie. Bezpieczeństwo Ruchu Drogowego, 2003: 1; 4–7.
3. British Standards Institution BS 6841. Measurement and evaluation of human exposure to whole-body mechanical vibration. London 1987.
4. Duarte MLM, Oliveira EA, Donadon LV. Whole-body vibration exposure values for car passengers on rough roads. A focus on health. Proceedings of the Second American Conference on Human Vibration, June 4-6 Chicago, IL 2008. Department of Health and Human Services Centers for Disease Control and Prevention, National Institute for Occupational Safety and Health. Pittsburgh Research Laboratory. DHHS (NIOSH) Publication No. 2009–145: 132–133.
5. Griffin M.J. Healt effects of vibration – the known and unknown. Proceeding of the First American Conference on Human Vibration, June 5-7 Morgantown, West Virginia, USA, 2006. Department of Health and Human Services/Center of Disease Control and Prevention, National Institute of Occupational Safety and Health, DHHS (NIOSH) Publication No. 2006–140: 3–4.
6. Griffin M.J. Minimum health and safety requirements for workers exposed to hand-transmitted vibration and whole-body vibration in the European Union; a review. Occup Environ Med., 2004: 61; 387–397.
7. International Standard ISO 2631. Mechanical vibration and shock-evaluation of human exposure to whole body vibration. Part 1, General requirements. Geneva, Switzerland: International Organization for Standardization. ISO 2631-1:1997.
8. James P. Dickey JP, Eger TR, Geenier S, Oliver ML, Boileau PE. The nature of multiaxis six-degree-of-freedom vehicle vibrations in forestry, mining, and construction heavy equipment. Proceedings of the Second American Conference on Human Vibration, June 4-6 Chicago, IL 2008. Department of Health and Human Services Centers for Disease Control and Prevention, National Institute for Occupational Safety and Health. Pittsburgh Research Laboratory. DHHS (NIOSH) Publication No. 2009–145: 119–120.
9. Jamroziak K, Kosobudzki M, Ptak J. Construction phases of selected components of M-ATV class vehicle prototype. Journal of Science of the Gen. Tadeusz Kosciuszko Military Academy of Land Forces, Wroclaw 2011: 1; 98–109.
10. Jurecki RS, Stańczyk TL. The test methods and the reaction time of drivers, Ekspolatacja i Niezawodnosc – Maintenance and Reliability, 2011: 3(51); 84–91.
11. Kosobudzki M, Smolnicki T, Jamroziak K, Bocian M. Ocena warunków transportu żołnierzy samochodami ciężarowo – osobowymi wysokiej mobilności na podstawie danych akcelerometrycznych. Raport z pracy badawczej, WSOWL, Wrocław 2010, Materiały niepublikowane.
12. Kosobudzki M, Stańco M. Kowalczyk M. Rozkład przyspieszeń w charakterystycznych punktach pojazdu dla wybranych warunków ruchu samochodów terenowych. Górnictwo Odkrywkowe, 2008: 4-5; 253–256.

13. Kosobudzki M, Stańco M. Widmo obciążeń dynamicznych człowieka jadącego kołowym transporterem opancerzonym. Górnictwo Odkrywkowe, 2010: 4;137–139.
14. Maslov A. Motywacja i osobowość. PWN, Warszawa 2006.
15. Nakashima AM. The effect of vibration on human performance and health. A review of recent literature. Defence R&D Canada, Technical Report, DRDC Toronto TR 2004–089.
16. Nakashima AM, Borland MJ, Abel SM. Measurement of Noise and Vibration in Canadian Forces Armoured Vehicles. Industrial Health 2007: 45; 318–327.
17. Nilson T, Nelson TM, Carlson D. Development of fatigue symptoms during simulated driving. Accident Analysis and Prevention, 1997: 29(4); 479–488.
18. Paddan G, Griffin MJ. Evalation of whole-body vibration in vehicles. Journal of Sound and Vibration, 2002: 1(253); 195–213.
19. Raport merytoryczny z realizacji projektu celowego Nr 381/BO/B. Dom Samochodowy Germaz Sp. z o.o., Wrocław 2010, Materiały niepublikowane.
20. Rozali A, Rampal KG, Shamsul Bari MT, Sherina MS, Shamsul Azhar S, Khairuddin H, Sulaiman A. Low Back Pain and Association with Whole Body Vibration Among Military Armoured Vehicle Drivers in Malaysia. Med J Malaysia, 2009: 3(64); 197–204.
21. Rozporządzenie Ministra Pracy i Polityki Społecznej z dnia 29.11.2002r. w sprawie najwyższych dopuszczalnych stężeń i natężeń czynników szkodliwych dla zdrowia w środowisku pracy, Dz.U. nr 217 poz.1833 (zmiany w Dz.U 2005 nr 212 poz. 1769).
22. Rusiński E, Koziołek S, Jamroziak K. Quality assurance metod for desing and manufacturing process of armoured vehicles, Ekspolatacja i Niezawodnosc – Maintenance and Reliability, 2009: 3(43); 70–77.
23. Rusiński E, Koziołek S, Jamroziak K. Critical to Quality Factors of Engineering Design Process of Armoured Vehicles. Solid State Phenomena. Trans Tech Publications Inc. Switzerland, 2010: 165; 280–284.
24. Saroj KL, Ashley C. A critical review of the psychophysiology of driver fatigue. Biological Psychology, 2001: 55; 173–194.
25. STANAG 4569. Protection levels for logistic and light armoured vehicle occupants. NATO/PfP Unclassified 1998.
26. Wasserman J, Mullinix L, Neal K, Khanal S, Wasserman D. Environmental Effects on Truck Driver ISO 2631 Acceleration Exposure. Proceeding of the First American Conference on Human Vibration, June 5-7 Morgantown, West Virginia, USA, 2006. Department of Health and Human Services/Center of Disease Control and Prevention, National Institute of Occupational Safety and Health, DHHS (NIOSH) Publication No. 2006-140: 123–124.
27. Wasserman J, Mullinix L, Khanal S, Hinton G, Wasserman D. Training Simulators Extend Laboratory Testing Techniques for WBV Analysis. Proceeding of the First American Conference on Human Vibration, June 5-7 Morgantown, West Virginia, USA, 2006. Department of Health and Human Services/Center of Disease Control and Prevention, National Institute of Occupational Safety and Health. DHHS (NIOSH) Publication No. 2006-140: 138–139.

**Krzysztof JAMROZIAK, Ph.D. (Eng.)**
**Mariusz KOSOBUDZKI, MA (Eng.)**
The General Tadeusz Kosciuszko
Military Academy of Land Forces
ul. Czajkowskiego109, 51-150 Wrocław, Poland
e-mail: krzysztof.jamroziak@wso.wroc.pl, m.kosobudzki@wso.wroc.pl

**Jerzy PTAK, MA (Eng.)**
Car House Germaz Ltd.
ul. Strzegomska 139, 54-428 Wrocław, Poland
e-mail: jptak@germaz.pl

Article citation info:
KRAWCZYK M. Conditions for Unmanned Aircraft Reliability Determination. Eksploatacja i Niezawodnosc – Maintenance and Reliability 2013; 15 (1): 31–36

Mariusz KRAWCZYK

# CONDITIONS FOR UNMANNED AIRCRAFT RELIABILITY DETERMINATION

# PRZESŁANKI DETERMINUJĄCE NIEZAWODNOŚĆ SAMOLOTÓW BEZPILOTOWYCH*

*In the paper the required level of reliability is determined for several Unmanned Aerial Vehicles developed in Poland in order to get an achievement enabling these vehicles to operate within the Single European Sky. Calculations were made on the basis of an air crash model as well as the model capable to estimate the number of casualties resulting from an aircraft catastrophe. The provided examples allow us to specify Tactical and Technical Conditions pertaining in particular to the area of the operation of the aforementioned aircraft.*

*Keywords: Unmanned Aerial Vehicle, ground impact model, mid-air collisions model, hazard analysis.*

*W pracy wyznaczono niezbędną niezawodności kilku opracowanych w Polsce samolotów bezpilotowych, której osiągnięcie umożliwia ich eksploatacje w połączonej przestrzeni powietrznej. Obliczenia prowadzone były wg modelu katastrofy powietrznej oraz modelu pozwalającego na oszacowanie liczby ofiar na skutek rozbicia się samolotu. Podane przykłady pozwalają na sprecyzowanie Warunków Taktyczno – Technicznych, w szczególności dotyczących obszaru eksploatacji tychże samolotów.*

*Słowa kluczowe: samolot bezpilotowy, model zderzenia z ziemią, model kolizji powietrznej, analiza zagrożenia.*

## 1. Introduction

The concept of an unmanned aerial vehicle (UAV) is not new as the first structures of this type were manufactured as early as in the First World War. In order to evaluate the current "scale of the phenomenon", the easiest way to do it is a collective specification following the Jane's Unmanned Aerial Vehicles and Targets catalogues that demonstrates that at the moment there are more than 400 UAVs and 120 flying targets that have been formally classified.

What makes their use in the public sector so rare if they show conspicuously identified advantages in terms of their use? One of the reasons is undoubtedly an insufficient level of reliability of current solutions that leads to a potentially unacceptably high probability of an accident or a catastrophe.

The basis for implementation of any UAV system for use in a civil and definitely in the Single European Sky (SES) in the future is a positive completion of a proper certification process. In the case of Europe, an entity that supervises actions of this type is EASA (the European Aviation Safety Agency) whose objective is to develop guidelines for a certification program referred to as CS (Certification Specifications). In the US market, a relevant certifying agency is the FAA (Federal Aviation Administration).

Pursuant to the assumptions adopted by the FAA and EASA [4] and [14], the UAV certification process, as assumed, is based on vast expertise and regulations that have been developed for civil aircraft, in particular, the guidelines for ensuring flying safety of civil aircraft in the following documents:

- AMC 25-1309 for transportation aircrafts,
- FAA AC 23 –1309-1C – for GA aircrafts.

Allocation of a specific UAV to one of the classes (Tab. 1) as anticipated in the legislation. In involves a comparison of its kinetic energy with the average kinetic energy of aircraft of a given class. It is simultaneously assumed that the maximum kinetic energy of a UAV is calculated for two following scenarios:

a) A UAV lands in an unfamiliar area for unintended reasons, then its calculation speed is assumed to be 130% of the speed of attraction in the configuration of landing;
b) The control over a UAV is lost which results in its crashing, then its calculation speed is assumed to be 140% of the maximum operating speed.

## 2. Catastrophic Events Involving UAVs

Apart from the economic issues related to a failure, downtime and finally with the destruction of an aircraft, the problem of a UAV catastrophe may be considered from the perspective of ensuring the level of reliability of UAVs, in order:

a) to not exceed a critical probability of a catastrophe in the air $\kappa_{UAVkr}$, calculated for one hour of flight;
b) in the event of its catastrophe featuring the probability equal $\sigma_{UAV}$, the ratio of third parties (on the surface) has not exceeded a critical value of $\gamma_{UAVkr}$, calculated into one hour of flight;

The values of $\kappa$ and $\gamma$ ratios have been adopted pursuant to a theory of controlling the risk [14], [6] stating that "*Catastrophic conditions of damage must be extremely unlikely"*. The critical value of $\kappa_{UAV}$ is assumed to be (according to Table 1) a constant $\kappa_{UAVkr} = 10^{-9}$, regardless of the type of UAV – a perpetrator of a crash which is equivalent to the FAA and EASA recommendations of the maximum level of hazard of a civil aerial vehicle flying in SES. In order to determine the value of $\sigma_{UAVkr}$, Table 1 may be found useful because it specifies the figures of probability of an event subject to the class of a civil aerial vehicle [14]. A method that allows transformation of the contents of Table 1 to make it useful for a UAV, will be presented in a description of a model of catastrophe involving a crash of a UAV.

Exemplary calculations have been made for thirteen UAVs, including seven UAVs that are currently manufactured or designed in Poland and five manufactured abroad. The smallest MAV Black Widow has a MTOW (Maximum Take-off Weight) of $m = 60g$, but for the largest Global Hawk $m = 11\ 622kg$. All UAV parameters required for

(*) Tekst artykułu w polskiej wersji językowej dostępny w elektronicznym wydaniu kwartalnika na stronie ***www.ein.org.pl***

*Table 1. Probability of an event (according to EASA)*

<table>
<tr><th colspan="2" rowspan="2">Document</th><th colspan="7">Probability of an event</th></tr>
<tr><th>$10^{-3}$</th><th>$10^{-4}$</th><th>$10^{-5}$</th><th>$10^{-6}$</th><th>$10^{-7}$</th><th>$10^{-8}$</th><th>$10^{-9}$ below</th></tr>
<tr><td colspan="2">FAA SSH</td><td colspan="2">P</td><td colspan="2">O</td><td colspan="2">E.O</td><td>E.N</td></tr>
<tr><td colspan="2">CS 25</td><td colspan="2">P</td><td colspan="4">N</td><td>E.N</td></tr>
<tr><td rowspan="4">CS 23</td><td>IV</td><td colspan="2">P</td><td colspan="2">O</td><td colspan="2">E.O</td><td>E.N</td></tr>
<tr><td>III</td><td colspan="2">P</td><td colspan="2">O</td><td>E.O</td><td colspan="2">E.N</td></tr>
<tr><td>II</td><td colspan="2">P</td><td>O</td><td>E.O</td><td colspan="3">E.N</td></tr>
<tr><td>I</td><td>P</td><td>O</td><td>E.O</td><td colspan="4">E.N</td></tr>
</table>

Class

***P – Likely ; O – Remote; E.O – Extremely remote; N – Unlikely; E.N – Extremely unlikely.***
***Class I Typical with a piston engine below 6000lbs,***
***Class II – Piston multi-engines or turbine engines below 6000lbs,***
***Class III Typical with piston engine, piston multi-engines or turbine multi-engine above 6000lbs,***
***Class IV – Commuter category.***

*Table 2. Calculation parameters of exemplary UAVs*

| Ref. | UAV | MTOW [*kg*] | S [$m^2$] | $S_R$ [$m^2$] | $\varepsilon_G$ | $\varepsilon_A$ |
|---|---|---|---|---|---|---|
| 1 | Global Hawk | 11622 | 50.00 | 546.00 | 0.93 | 1 |
| 2 | Predator | 1 021 | 13.50 | 51.00 | 0.58 | 1 |
| 3 | Czajka | 473 | 10.20 | 21.94 | 0.21 | 1 |
| 4 | Pheonix | 270 | 56.80 | 3.31 | 0.09 | 1 |
| 5 | Shadow 200 | 159 | 2.99 | 12.00 | 0.24 | 1 |
| 6 | Samonit 2 | 50 | 2.05 | 3.20 | 0.13 | 0.5 |
| 7 | OCP Jet | 40 | 1.10 | 3.59 | 0.18 | 0.4 |
| 8 | SMCP Szerszeń | 39 | 1.82 | 2.48 | 0.12 | 0.39 |
| 9 | MJ-7 Szogun | 29 | 1.11 | 2.33 | 0.13 | 0.29 |
| 10 | SMCP Komar | 25 | 1.10 | 1.92 | 0.12 | 0.25 |
| 11 | FlyEye | 11 | 0.95 | 0.71 | 0.10 | 0.11 |
| 12 | Mini | 4.36 | 0.60 | 0.28 | 0.09 | 0.043 |
| 13 | Black Widow | 0.06 | 0.03 | 0.01 | 0.06 | 0.0006 |

calculations included in Table 2 where: $S$ – is a surface of reference, $S_R$ – striking zone, $\varepsilon_G$ – penetration ratio, a $\varepsilon_A$ – a ratio used in a model of air crash.

## 3. Reliability of UAVs and a number of casualties among third parties

Assuming that the level of safety of use of UAVs in SES may not be lower than a value assumed for civil and military aircrafts, based on the regulations of FAR/CS 25 and 35 maximum ratio of casualties caused by the UAV crash, EASA suggests that one should assume $\gamma_{UAVkr} = 10^{-6}$ which is a maximum of one casualty per million UAV flying hours.

Alternatively, in studies [8] and [14], authors assume the equivalence of the relation below, which seems to be more universal,

$$\gamma_{UAV_{kr}} = \sigma_{A/C_{kr}} \tag{1}$$

i.e. the equality of a ratio of the number of casualties for a UAV and the probability of a loss of a civil aircraft as a result of an event of a catastrophic nature, according to the FAA, resulting in:

a) casualties among the crew and passengers;
b) casualties among third parties;
c) usually the loss of an aircraft.

Both approaches (assumptions) for UAV of a weight of $m < 6\ 000 lbs$ propelled by piston engine, lead to the following assumption $\gamma_{UAVkr} = 10^{-6}$. For a bigger UAV or the ones with a turbine drive, in turn, these values will be smaller, according to the contents of Table 1.

The equation (1) may be transformed to the following,

$$\sigma_{UAV_{kr}} \cdot \Pi = \sigma_{A/C_{kr}} \tag{2}$$

where: $\sigma_{UAVkr}$ – probability of a catastrophe of a UAV, a $\Pi$ – probability of casualties in case of a UAV crashing to the ground. Thus, having known (from Table 1) the value of $\sigma_{A/Ckr}$, determine the required critical reliability of UAV, equal to

$$\mathrm{Re}_{UAV_{kr}} = 1 - \sigma_{UAV_{kr}} \tag{3}$$

there is a necessity to calculate the probability of having casualties upon crashing with a UAV, according to the following model,

$$\Pi = S_R \cdot D \cdot \varepsilon_G \tag{4}$$

where: $S_R$ – is a striking zone characteristic of each of the UAVs in questions, $D$ – population density in the area of a catastrophe, and $\varepsilon_G$ is a so-called penetration ratio taking into account the mitigation of

the effects of a catastrophe if potential victims are, e.g. in buildings that provide some shelter to them. The size of the striking zone is determined by means of an empirical relation below

$$S_R = 0.028 \cdot \left(\frac{m}{S}\right)^{2/3} \tag{5}$$

where: $m$ – is a weight of UAV determined [4] on the assumption that it is proportional to the energy of an aircraft at the moment of crash, made up mainly of its kinetic energy and the fuel explosion energy. The $S_R$ figures for the analysed UAVs are presented in Table 2 and Figure 1 presents them for the GA (General Aviation and Transportation) aircraft subject to a ballistic ratio $\beta$ determined pursuant to the following relation where $c_x$ is a resistance force ratio.

$$\beta = \frac{m}{c_x \cdot S} \tag{6}$$

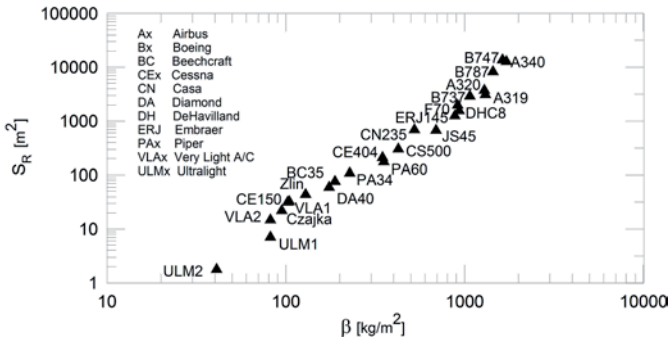


*Fig.1. A size of a striking zone for the selected UAVs, Gas and Transpiration*

A precise determination of a striking zone is of the utmost importance (linear dependency) for the precision of a model of the UAV catastrophe, for obvious reasons. Thus, an attempt was made to verify relation (5) involving a comparison of the real spot of the Tu 154M's catastrophe of 10 April 2010 in the vicinity of the Severny airport near Smolensk shown in Figure 2 with a value calculated according to relation (5). Assuming the data from Jane's catalogue, the calculation value $S_R$ for Tu 154M aircraft is $S_R = 3\,788m^2$. By calculation using a satellite image of the crash spot, we arrive at the following: $S_R \approx 150 \times 25 = 3\,750m^2$ which verifies relation (5) in a positive manner.

For the analysis of UAV system design, it is also useful to determine its reliability defined by the following relation,

$$\mathrm{Re}_{UAV_{kr}} = e^{\frac{-t}{MTBCF}} \tag{7}$$

*Fig. 2. Crash spot of the Tu 154M aircraft (Severny)*

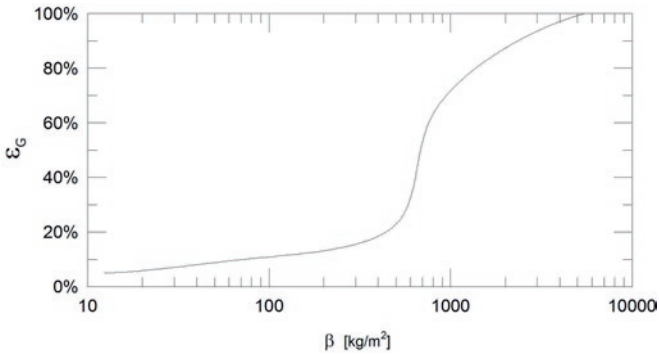


*Fig. 3. A penetration ratio subject to a ballistic ratio*

where, MTBCF is the Mean Time Between Critical Failure. A reverse of MTBCF is a number of defects (or a set of defects) of an UAV expected within an hour that would lead to a catastrophe.

A presented model of an assessment of the risk level imposed potentially by UAV for the third parties was subject to a model experiment that produced the following results specified in collective Table 3. Three various mission scenarios were taken into account:

a) flight between the EPMO airport located near Modlin, and EPSO located in the vicinity of Sochaczew. The flight route presented in Figure 2 of the total approximate length of $L$ = 38$km$ crosses three administrative districts: Nowy Dwór ($L_1$ = 24,5$km$), Warsaw West ($L_2$ = 5,5$km$) and Sochaczew ($L_3$ = 8$km$) which feature a population density of 61 – 103 60 persons per 1$km^2$ respectively;

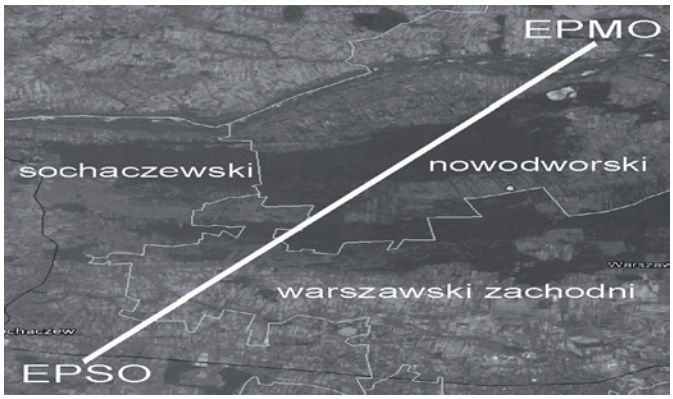


*Fig. 4. Flight route between EPMO and EPSO*

b) patrol mission in equal shares (25% each) over four suburbs of the Capital City of Warsaw featuring the highest population density defined as the number of inhabitants per 1km2, Ochota ($D_1$ = 9 215), Śródmieście ($D_2$ = 8 120), Wola ($D_3$ = 7 149) and Mokotów ($D_4$ = 6 372);
c) patrol mission in equal shares (25% each) over four suburbs of the Capital City of Warsaw featuring the lowest population density defined as the number of inhabitants per 1$km^2$ Białołęka ($D_1$ = 1 222), Bielany ($D_2$ = 4 142), Bemowo ($D_3$ = 4 532) and Żoliborz ($D_4$ = 5 654).

An order of UAVs in Table 3 is determined by their weight. The heaviest aircraft are at the beginning of the specification, and the lightest are at the end. It is clear that, as expected, the requirements pertaining to the reliability of UAVs usually reduce in proportion to their weight. Two UAVs are exceptions to the rule: no. 4 being stratospheric Phoenix and No. 7 an aerial target featuring a jet engine OCP – Jet. Through analysis of the contents of Table 3 we find that for a large Phoenix aircraft featuring a wing span of 38.2$m$ the requirements pertaining to its minimum reliability are significantly lower than the ones determined for an obviously smaller Czajka air-

*Table 3. A collective specification of the a, b and c model experiment results*

| Ref. | Aircraft | Mission „a" | | Mission „b" | | Mission „c" | |
|---|---|---|---|---|---|---|---|
| | | $Re_{UAVmin}$ | $MTBCF_{min}$ | $Re_{UAVmin}$ | $MTBCF_{min}$ | $Re_{UAVmin}$ | $MTBCF_{min}$ |
| 1 | Global Hawk | 0.99997 | 34 014 | 0.999999 | 999 999 | 0.999999 | 999 999 |
| 2 | Predator | 0.99950 | 1 981 | 0.999996 | 228 044 | 0.999991 | 114 986 |
| 3 | Czajka | 0.996759 | 308 | 0.999972 | 35 520 | 0.999944 | 17 910 |
| 4 | **Phoenix** | **0.949840** | **19** | **0.999564** | **2 294** | **0.999139** | **1 156** |
| 5 | Shadow 200 | 0.994817 | 192 | 0.999955 | 22 202 | 0.999911 | 11 195 |
| 6 | Samonit 2 | 0.964074 | 27 | 0.999688 | 3 203 | 0.999380 | 1 614 |
| 7 | **OCP-Jet** | **0.976927** | **43** | **0.999800** | **4 988** | **0.999602** | **2 515** |
| 8 | SMCP Szerszeń | 0.949923 | 19 | 0.999565 | 2 298 | 0.999137 | 1 158 |
| 9 | MJ-7 Szogun | 0.950772 | 20 | 0.999572 | 2 331 | 0.999152 | 1 178 |
| 10 | SMCP Komar | 0.935233 | 15 | 0.999437 | 1 777 | 0.998884 | 896 |
| 11 | FlyEye | 0.789390 | 4 | 0.998170 | 546 | 0.996371 | 275 |
| 12 | Mini | 0.466845 | ~1 | 0.995367 | 215 | 0.990813 | 108 |
| 13 | Black Widow | ~1 | ~0 | 0.729767 | 3 | 0.464069 | 1 |

craft. A reason for these facts is the relative small ballistic ratio of the Phoenix aircraft that gives, in turn, a small penetration ratio and a minimum relation of weight to the reference surface resulting in an exceptionally low (compared to the size of an aircraft) striking zone. Similar substantive reasons (mainly a relatively high penetration ratio) make the requirements pertaining to the minimum reliability of a smaller OCP-Jet aircraft featuring a relatively contained design higher than those of the larger and heavier Samonit – 2 UAV.

## 4. Reliability of the UAV and the risk of a collision in the air

It is useful to analyse the probability of a mid-air collision between a UAV and other SES users using the "gas model [5], [14] the idea of which has already been presented in Figure 5. In this model the UAV is treated as a particle - a material point moving inside the space of a controlled volume of **V**. Other civil users 1, 2..*n* however are treated as particles of a characteristic size $S_{expi}$ being a field of exposure (a front surface) *i* of this civil aircraft. At the same time it is assumed that for the entire time of observation **T**, a UAV is inside the controlled space and other users do not have any equipment and systems to prevent a collision (e.g. TCAS Traffic Collision Alert System). A probability of a catastrophe is calculated from the following relation:

$$_{UAV} = \frac{\sum_{i=1}^{n} L_i \cdot S_{\exp_i} \cdot \varepsilon_{A_i}}{V \cdot T} \tag{8}$$

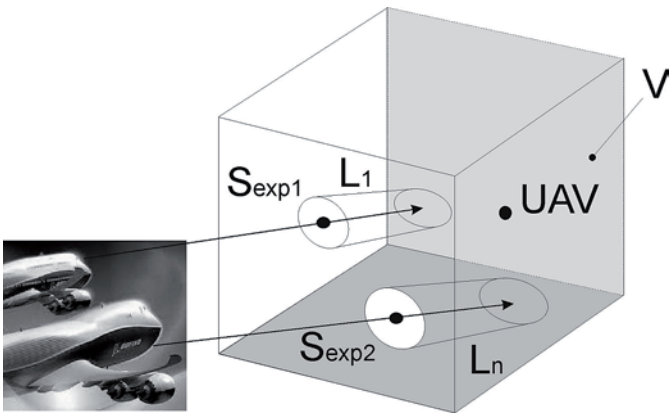


*Fig. 5. A concept of a "gas model" of a mid-air collision (according to [5])*

where: $L_i$ a road covered inside the space, and $\varepsilon_{Ai} \leq 1$ – is a ratio taking the inevitability of a catastrophe as a result of a collision of *i* of this aircraft with UAV. For the sake of calculation, it may be assumed that

$$\varepsilon_A = \begin{cases} m/100, m < 100kg \\ 1, m \geq 100kg \end{cases} \tag{9}$$

which means that each collision of an aircraft with a UAV the weight of which is $m > 100kg$ leads inevitably to a catastrophe. For UAVs of a weight of $m \leq 100kg$, however, the value of its ratio $\varepsilon_A$ decreases in a linear proportion assuming the ultimate value of $\varepsilon_A \approx 0$ for the smallest MAVs.

The presented model calculating the probability of an air collision was reviewed involving the required calculations based on observation of the real movement of aircraft traffic in the air space surrounding the Warszawa Okęcie (EPWK) Airport as shown in Figure 6. The dimension of a cuboid control zone was assumed to be $10^5 \times 10^5 \times 1{,}2 \cdot 10^4 m$. As shown in Figure 4, EPWK was located cen-

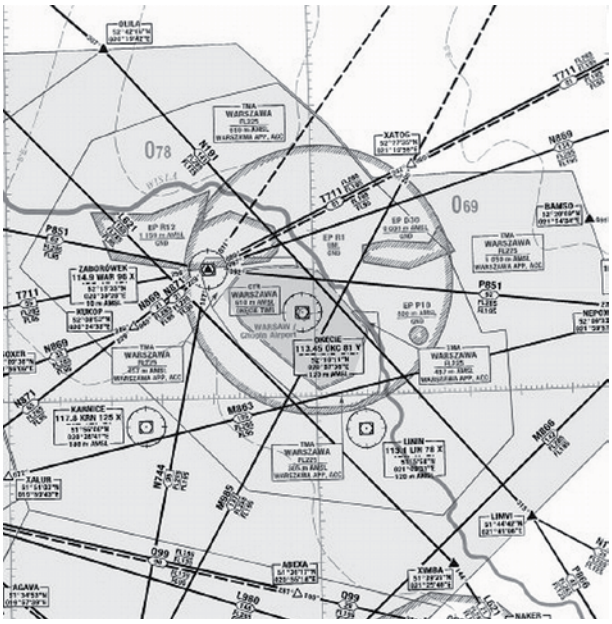

*Fig. 6. A "map" of a measuring zone with marked air routes for FL ≤ 285*

*Table 4. A collective specification of results of the a, b, c and d model experiment*

| Ref. | Aircraft | Mission „a" $\kappa_{UAVV}$ | Mission „b" $\kappa_{UAVFL<160}$ | Mission „c" $\kappa_{UAVFL=340}$ | Mission „d" $\kappa_{UAVLANDING}$ |
|---|---|---|---|---|---|
| 1 | Global Hawk | 3.99E-7 | 3.83E-7 | 2.14E-5 | 0.943 |
| 2 | Predator | 3.99E-7 | 3.83E-7 | 2.14E-5 | 0.943 |
| 3 | Czajka | 3.99E-7 | 3.83E-7 | 2.14E-5 | 0.943 |
| 4 | Phoenix | 3.99E-7 | 3.83E-7 | 2.14E-5 | 0.943 |
| 5 | Shadow 200 | 3.99E-7 | 3.83E-7 | 2.14E-5 | 0.943 |
| 6 | Samonit – 2 | 2.00E-7 | 1.91E-7 | 1.05E-5 | 0.472 |
| 7 | OCP – Jet | 1.60E-7 | 1.53E-7 | 0.88E-5 | 0.377 |
| 8 | SMCP – Szerszeń | 1.56E-7 | 1.49E-7 | 0.82E-5 | 0.368 |
| 9 | MJ-7 Szogun | 1.16E-7 | 1.11E-7 | 0.61E-5 | 0.274 |
| 10 | SMCP – Komar | 0.98E-7 | 0.95E-7 | 0.53E-5 | 0.236 |
| 11 | FlyEye | 0.44E-7 | 0.42E-7 | 0.23E-5 | 0.104 |
| 12 | Mini | 0.17E-7 | 0.17E-7 | 0.09E-5 | 0.041 |
| 13 | Black Widow | **0.002E-7** | **0.002E-7** | 0.01E-5 | 0.0004 |

trally relative to the base of the zone. The air traffic observations were performed for two morning peak hours between $7^{00} \div 9^{00}$ on 29th February 2012. At that time, there were 30 aircraft in the zone altogether. 10 of them took off from EPWK, 7 landed there and 15 crossed the zone at various *FL* (Flight Level) out of which 6 were performing a transit flight at *FL* 340. The altitude and speed of the flight as well as the length of the route covered by a given aircraft inside the measuring zone were recorded. Each of the observed aircraft was identified, which made it possible to determine its exposure zone of $S_{exp}$ based on the catalogue data.

The completed calculations and registrations made it possible to determine the probability of an air collision according to relation (8) with one of the UAVs that are present there (calculations were made for each of the UAVs from Table 3). In particular, four scenarios were assumed for the calculations presented in Table 4 in which a UAV hypothetically moved regardless of their operating parameters over the entire time of observation of the UAV:

a) inside the entire measurement zone;
b) below *FL* 160 (aircrafts taking off and landing);
c) on the top flying route at *FL* 340;
d) on the descending route starting from 10*NM*.

While analysing the calculation results presented in Table 4, it is obvious, that apart from a very small Black Widow the remaining UAVs pose a real, unacceptably high risk to current air traffic; this assumption is made pursuant to the model that they move in an uncontrolled manner in SES. The value of probability of occurrence of an air catastrophe involving a UAV strongly depends on the space in which a flight is performed. The probability of collision is definitely higher in the area of an approach to airports on pre-determined air routes. In the remaining areas, this likelihood is much lower but remains at the level recommended by FAA/EASA of $10^{-9}$ of catastrophes per one hour of flight.

Integration of UAV systems with SES requires development of new methods to protect the air traffic safety in terms of air collision, prevention and minimising the number of potential victims among third parties arising from a crash of an UAV.

The aforementioned models (of collision and crash of UAV) provide an effective tool for establishing the specified tasks.

In particular, *The UAV Crash Model* makes it possible to determine the required level of reliability of the entire UAV system in respect of ensuring the required level of safety related to the risk posed by a UAV in the event of its catastrophe, for third parties. While analysing the model, it is easy to notice that UAVs that are bigger and that move faster must be more reliable than MAVs, the potential risk of which is relatively low. The expected operating area also plays a major role. UAVs designed for operation in major urban agglomerations must definitely be more reliable compared to the ones used e.g. for patrolling of borders along which the population density is usually low.

## 5. Conclusions

Presented model indicates severe challenges for designers of major UAVs for which the total required MTBCF is comparable to the time of defects of a simple electronic (!) e.g. a simple fuse used in military aircrafts. Simple measures improving the reliability of these aircraft e.g.: application of the selected, top quality elements or redundancy of critical systems appears to be insufficient. Thus, it is probably a reason why decision-making entities (EASA, FAA) consider an option to implement a principle of permanent monitoring of UAV by a surface operator with an option of overtake of control as a matter of emergency in critical situations. On the one hand such solution imposes more stringent requirements pertaining to communication e.g. high reliability, short transmission delay or resistance to disturbance and on the other hand, it redefines a checklist of critical events that used to be classified as catastrophic for UAVs (i.e. shortens it).

*A mid-air collision model* is a sufficient premise for the development of special ATM (Air Traffic Management) procedures dedicated for UAVs and to integrate them with avionic systems of the equipment preventing air collisions e.g. TCAS (Traffic Collision Avoidance System). This model also shows that the reliability of systems preventing air collisions of these UAVs that according to assumptions are expected to move only in the areas of an approach to airports or on air routes must be higher than the ones designated to be used above an area designated for civil flights (HALE aircrafts) or operating locally at very low altitudes where there is practically no air traffic.

**Acknowledgement**: *The research work was financed from the funds of the Ministry of Science and Higher Education OR00011611 project.*

## References


1. Boeing. Statistical Summary of Commercial Jet Airplane Accidents Worldwide Operations 1959 – 2008. 2009.
2. Columbia Accident Investigation Board. Determination of Debris Risk to the Public, Due to the Columbia Breakup During Reentry. Report Volume II 2003.
3. DeGarmo M.T. Issues Concerning Integration of Unmanned Aerial Vehicles in Civil Airspace.Center for Advanced Aviation System Development 2004.
4. EASA. Advance -notice of proposed amendment (NPA) No 16/2005.
5. Endoh S. Aircraft Collision Models, M.S Thesis. Department of Aeronautics and Astronautics, Massachusetts Institute of Technology, Cambridge 1982.
6. FAA. System safety analysis and assessment for part 23 airplanes. AC No: 23.1309-1D, 2009.
7. Goraj Z,Frydrychewicz A,Świtkiewicz R, Hernik B, J. Gadomsk J, Goetzendorf-Grabowski T, Figat M,Suchodolski S, Chajec W. High altitude long endurance unmanned aerial vehicle of a new generation – a design challenge for a low cost, reliable and high performance aircraft. Bulletin of the Polish Academy of Sciences 2004; Technical sciences, vol. 52, no. 3.
8. King D.W, Bertapelle A, Moses C. UAV failure rate criteria for equivalent level of safety, International Helicopter Safety Symposium, Montréal 2005.
9. MurrayD.P. A Tiered Approach to Flight Safety Analysis. Keystone 2006.
10. Office of the Secretary of Defence. Airspace Integration Plan for Unmanned Aviation, 2004.
11. Pettit D, Turnbull A. General Aviation Aircraft Reliability Study, Hampton 2002; NASA/CR-2001-210647.
12. Prażewska M.Niezawodnośćurządzeńelektronicznych. WKiŁ Warszawa 1987.
13. Tsach S, Penn D, Levy A. Advanced technologies and approaches for next generation UAVS. 23rd Congress of International Council of the Aeronautical Sciences Toronto 2002.
14. Weibel R.E, Hansman R.J. Safety considerations for operation of UAVs in the NAS; Report No. ICAT-2005-1March 2005.



**Mariusz KRAWCZYK, Ph. D.**
Centre of New Technologies
Institute of Aviation
Al. Krakowska 110/114, 02-256 Warszawa, Poland
E-mail: mariusz.krawczyk@ilot.edu.pl

Article citation info:
BAIER A, ZOLKIEWSKI S. Initial research of epoxy and polyester warp laminates testing on abrasive wear used in car sheathing. Eksploatacja i Niezawodnosc – Maintenance and Reliability 2013; 15 (1): 37–43

Andrzej BAIER
Slawomir ZOLKIEWSKI

# INITIAL RESEARCH OF EPOXY AND POLYESTER WARP LAMINATES TESTING ON ABRASIVE WEAR USED IN CAR SHEATHING

# BADANIA WSTĘPNE ŚCIERALNOŚCI LAMINATÓW O OSNOWIE EPOKSYDOWEJ I POLIESTROWEJ DO ZASTOSOWANIA W BUDOWIE POSZYCIA WAGONU TOWAROWEGO*

*The subject of the work is to present the preliminary investigations over epoxy and polyester warp laminates and its abrasion. The exploitation of various types of containers used in industry is often connected with its usage of composite materials. The composite materials are exposed to tribological wear. Basing on reality and the common tribology wear hazard testing on abrasive wear of composite materials is well-founded and significant in technical and technological point of view. The results of the experimental part of the work are only the substitute of the widely presented researches over composite materials used in the structure of the side of the freight wagons. There are presented the results of the laminates, performed in the laboratory conditions depicting the real work conditions of freight wagons. There were compared the exemplified parameters of the geometrical profile of the structure mass losses of the investigated samples, both the epoxy and polyester and other used hardeners.*

***Keywords**: abrasive, friction, composite materials, laminates, tribology wear.*

*Praca dotyczy badań wstępnych ścieralności laminatów o osnowie epoksydowej i poliestrowej. Eksploatacja różnego rodzaju zbiorników do zastosowań przemysłowych często wiąże się z użyciem materiałów kompozytowych narażonych na zużycie tribologiczne. Zasadne jest więc podjęcie istotnych z technicznego i technologicznego punktu widzenia badań ścieralności tych materiałów. Prezentowane w pracy wyniki badań eksperymentalnych są jedynie częścią szeroko zakrojonych badań materiałów kompozytowych mających zastosowanie w budowie burt wagonów towarowych. Przedstawiono wyniki badań laminatów, przeprowadzonych na autorskim stanowisku laboratoryjnym do porównawczego badania zużycia ściernego odzwierciedlającego warunki pracy wagonu towarowego. Zestawiono przykładowe parametry struktury geometrycznej profilu oraz ubytki masowe badanych próbek zarówno w przypadku próbek epoksydowych jak i poliestrowych oraz różnych, zastosowanych utwardzaczy.*

***Słowa kluczowe**: ścieranie, tarcie, kompozyty, laminaty, zużycie trybologiczne.*

## 1. Introduction

The friction phenomenon occurs in all technical and technological processes and the fact that it is so common causes that friction is extremely vital from the engineering and scientific point of view. The simplified definition of friction determines its occurrence while different elements made from various or the same materials are in contact with each other. Testing of negative impact on the structure of materials, parts of machines and mechanisms is widely discussed. Friction phenomenon is the main reason why there are damages of machine parts, for instance in the case of abrasive wear which significantly worsens performance and very frequently makes it impossible to continue further exploitation, considerably decreasing reliability of the whole system. Taking into consideration the tribology wear is extremely important criterion on the stage of designing and selection of materials with determined resistance to abrasive action, which certainly may contribute to proper and failproof work produced technical items during designing and selecting materials with determined resistance to abrasion [1, 3, 7, 11, 23–27]. Crushing and cracking of materials and abrasive wear, fatigue and chemical consumption can be observed during such a tribology wear process. The tribologic wear appears due to the fact of friction force and states as one of the most crucial aspect of the durability and reliability of the construction. The abrasive wear is recognised to be the most common symptom of the tribologic consumption. It appears due to the mutual interaction of the materials moving towards each other. The most noticeable symptoms of such interactions are detachments of pieces of the inner layer of the material, gradual loss of the material volume and deterioration of the surface conditions. [3, 7, 8, 16, 17, 24].

Experimental testing of composite materials is still necessary and it is connected with determination of many material parameters and properties. Fibre reinforced composites are used in numerous applications. In these applications abrasive wear very often initiate the damage of the whole system. Conveyor aids, vanes, gears, bushes, seals, bearings, pumps handling industrial fluids/slurries containing abrasives, sewage; chute liners used in machineries in agriculture, earth moving, mining, etc. are some of such examples [2, 5, 6, 9, 18, 21, 22]. In the paper [19] the authors present that the wear rate increased with increasing applied load, abrasive size and decreased with sliding distance. Also, abrasive size was found to be effective for the composite. The interaction of load and abrasive size was found to be effective than those of other variables. Authors of the paper [4] present the experimental results of multi-pass two-body abrasive wear of fibreglass reinforced polyester composite. The authors indicated micro-cutting, micro-cracking, micro-fatigue, micro-fracture in matrix and in the fibres ends as dominating wear mechanisms. The tests were carried out under different experimental conditions, different loads, given rotational speeds, and different grit sizes of abrasive. Over the

(*) Tekst artykułu w polskiej wersji językowej dostępny w elektronicznym wydaniu kwartalnika na stronie ***www.ein.org.pl***

last years the methodology of designing and analyzing of composite materials in aspect of multiple desirable performance criteria have been evolved. In the work [20] an attempt has been made to analyze the impact of several selected parameters and their interactions on the percussive wear of the red mud filled epoxyglass fibre composites (using statistical method of Taguchi). This method has been also successfully applied for parametric evaluation in the percussive behaviour of polymer composites [10, 12].

The main aim of the work was to investigate preliminary the abrasive wear process of the chosen composite samples, namely epoxy and polyester ones, comparing the mass loss of the probes and analysis of the geometrical profile parameters before and after the experiments. There were compared the wear parameters of chosen laminates made of fibreglass and carbon fibres, with various weave and weight, as well as using variable hardening agents.

## 2. Idea of the laboratory stand and the research methodology

Materials used in the construction of car sheathing should be resistant enough so that the pouring cargo does not cause the destruction of its surface that could possibly unable further exploitation. Requirements towards engineering and exploitation of rail-vehicles are determined by subjective standards applied by International Union of Railways (UIC), the Organization for Cooperation of Railways (OSJD) and National Normalizing Committees. There have been no specific regulatory guides concerning the resistance to abrasion wear found yet applied to the construction of the freight wagon containers. These materials are verified due to their strength requirements (disruptive strength, exploitation and fatigue strength and vibration strength and buffer impact strength).

The purpose of this work was to choose a proper conception and methodology of initial researches concerning abrasability and testing of selected composite samples. During the investigation the author's conception of the laboratory stand was chosen. In the author's laboratory stand the working conditions of car sheathing were considered after multiple loading and reloading. The basic idea of the proposed laboratory stand (fig. 1) is based on the rotational cylinder driven into rotary motion by means of an electric engine. The simplicity of that concept makes it possible to build a laboratory stand with low costs and to provide easy operation and maintenance of the stand. Further information concerning the control system, parameters of drive, parameters of abrasive material and degree of filling the cylinder in the laboratory work and particular parameters can be found in the article [1].

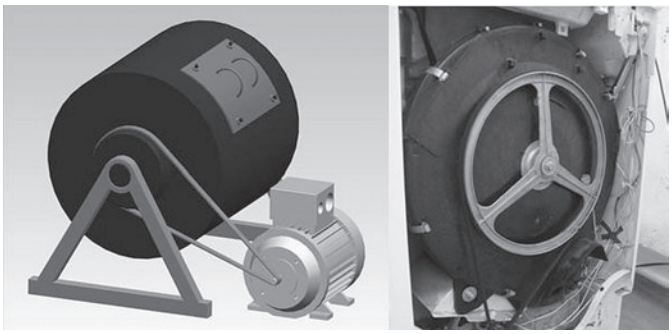

*Fig. 1. The concept and implementation of laboratory stand for testing of resistance to abrasion*

Dimensions of samples were limited in such a way that the sample could be situated inside the rotational cylinder. Dimensions of the tested element were determined as: length from 170 to 190 mm and width from 30 to 100 mm. Dimensions of the tested samples are also limited by the doors of cylinder where the sample is fixed. Thickness of

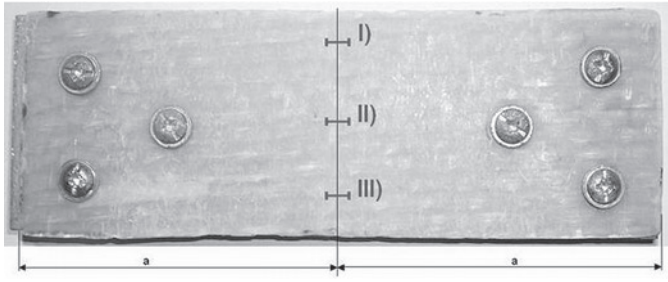


*Fig. 2. The three ways of measurement by means of the profilometer*

the sample should be less than 10 mm. The choice of actual dimensions meeting the requirements depends on concrete users specifications.

Carrying out the research relies on setting the number of cylinder rotations (there is the abrasive material in it) between consecutive measurements of the sample. It is extremely important to set the proper rate of rotation of cylinder for stable work of laboratory device. The rotary velocity is an especially important parameter in the case of described laboratory stand. It enables stable work of the device in a set of tests provided. In the considered case the rotary velocity equals 60 rpm in a steady state.

The laboratory stand gives an opportunity to close the abrasive process to real conditions. However, to carry out the research helping to evaluate if the selected composite materials are good for practical application it is necessary to define material parameters describing the degree of abrasive wear during the tests. This led to observation on what the impact of abrasion (mineral abrasive) on the tested sample was.

The first parameter which was used to check abrasive wear of the sample is the visual evaluation of the tested element. Before and after the research the surface quality of the sample was estimated visually. Determination of the impact of abrasive material on the sample became possible. Evaluation carried out in this way is, however, subjective and inaccurate and because of this it cannot be the only feature considered in comparison of tested materials.

Another parameter defining the changes following the measurement of the tested material is the mass decrement. The sample was weighed before and after the tests, which helped to define what kind of material loss is caused by abrasive material during the tests. The material loss is the comparative parameter among different laminates which were tested. The precision of weighing is approximately 0,01 g.

Additionally, the samples were tested by means of the profilometer to notify in what way abrasive material is acting on the surface of the sample. This led to define roughness (which shows the damages brought about by abrasive material) and the assessment of maximal depth of damage. The measurement was conducted using the Tylor – Hobson SURTRONIC 3+ profilometer (fig. 2).

The profilometer enables conducting the research of geometrical surface structure of material and defining parameters connected with it and also graphical representation of the results in the form of charts. For performing the research of abrasibility of composite materials the chart of roughness were generated. They allow assessing the surface quality of the tested elements. The measurements were provided on three measuring lengths in the middle of the sample (fig. 2). Each of the measuring lengths is composed of five elementary segments. The elementary segments of 0,8 mm and measuring length of 4 mm length were selected according to the ISO 4288 norm.

## 3. Composites grinding tests

In this paper the chosen results of experimental tests on the laboratory stand are presented. The selected laminate samples were tested determining comparative resistance to abrasive wear (table 1).

*Table 1. Juxtaposition of the tested laminates*

| No. | Warp | Reinforcement | Liczba i ułożenie warstw | Mass of resin per one square metre G.S.M. recommended /used | Reinforcement part | Thickness of the sample / mass of the sample | Hardening agent |
|---|---|---|---|---|---|---|---|
| *1* | *Epoxy resin Epidian 6* | *Fibreglass with twill weave, 450g/m²* | *5 (0/90/0/90/0)* | *330g/300g* | *60%* | 2,59mm/31,74g | Hardening agent PAC 80g per 100g of resin |
| 2 | Polyester resin Polimal 1094 AWTP-1 | Roving, 400g/m² | 3 (0/90/0) | 350g/365g | 50% | 1,46mm/20,47g | Hardening agent Luperox K-1 con. 1,5% |
| 3 | Polyester resin Polimal 1094 AWTP-1 | Fibreglass with twill weave, 450g/m² | 3 (0/90/0) | 350g/355g | 56% | 1,61mm/20,52g | Hardening agent Luperox K-1 con. 1,5% |
| 4 | Epoxy resin Epidian 6 | Roving, 400g/m² | 4 (0/90/90/0) | 350g/355g | 54% | 2,13mm/25,14g | Hardening agent Luperox K-1 con. 1,5% |
| 5 | Polyester resin Polimal 1094 AWTP-1 | Roving, 400g/m² | 3 (0/90/0) | 350g/350g | 53% | 1,69mm/19,12g | Hardening agent PAC 80g per 100g of resin |
| 6 | Polyester resin Polimal 1094 AWTP-1 | Fibreglass with twill weave, 450g/m² | 4 (0/90/90/0) | 350g/385g | 54% | 2,55mm/28,43g | Hardening agent PAC 80g per 100g of resin |
| 7 | Epoxy resin Epidian 6 | Fibreglass with twill weave, 450g/m² | 3 (0/90/0) | 330g/335g | 57% | 1,33mm/20,02g | Hardening agent Luperox K-1 con. 1,5% |
| 8 | Epoxy resin Epidian 6 | Fibreglass coated by aluminum with twill weave, 290g/m² | 7 (0/90/0/90/0/90/0) | 225g/240g | 55% | 2,43mm/31,63g | Hardening agent PAC 80g per 100g of resin |
| 9 | Epoxy resin Epidian 6 | Carbon fibre with twill weave, 280g/m² | 3 (0/90/0) | 330g/265g | 51% | 1,19mm/13,97g | Hardening agent Luperox K-1 con. 1,5% |

### 3.1. Abrasive material

The choice of the abrasive material for the tests was done in the experimental random way. Relatively fast wearing of the applied charge was the biggest problem during the experiment. Granite was applied as the abrasive material, which enabled verification of grindability in critical conditions. The stones caused abrasion and devastation of the surface that also resulted in mutual abrasion and rounding of sharp edges. It required frequent (after each cycle of the test) exchange of the abrasive material.

### 3.2. Tested samples

The most common group of composite materials used in different industries are laminates. Laminates are produced by saturating a chosen fabric (fibreglass, carbon fibre, amide fibre) with epoxy resin or polyester resin and further they are moulded in the layer form. The surface of the material is consisted of resin which determines resistance to abrasion of material. The tests were done on the samples consisted of epoxy resin (fig. 3) and polyester together with various types of fabric, the collection of samples was presented in table 1.

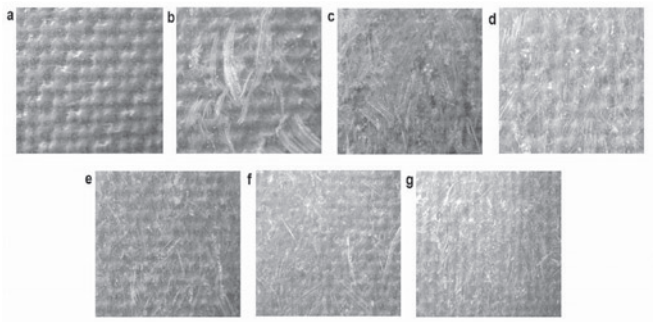


*Fig. 3. Visual assessment of the surface quality of exemplary laminate made of epoxy resin and fibreglass with twill weave (the sample 1): a – before the tests; b – after 1000 rotations; c - after 2000 rotations; d- after 3000 rotations*

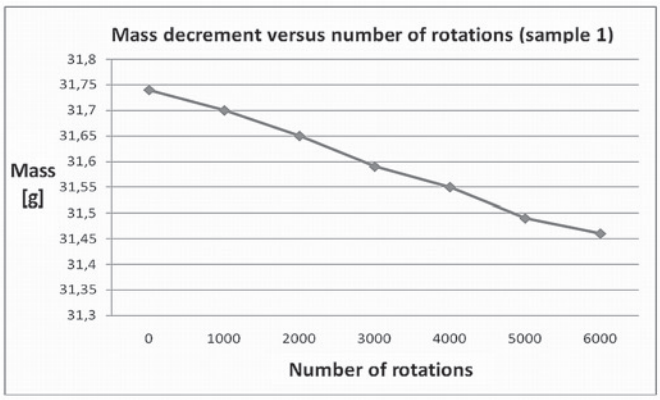


*Fig. 4. Chart presenting the dependence of mass of woven fibreglass with twill weave laminate made of epoxy resin on the number of cylinder rotations (in the laboratory stand)*

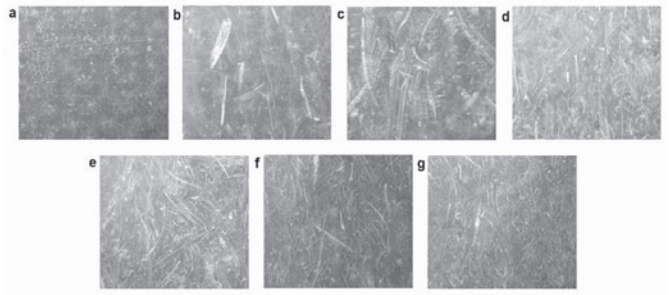


*Fig. 5. Picture presenting the surface quality of the woven glass roving laminate (the sample 2 in table 1): a – before the test, b – after 1000 rotations, c – after 2000 rotations, d – after 3000 rotations, e – after 4000 rotations, f – after 5000 rotations, g – after 6000 rotations*

The sample measurements were conducted evaluating influence of the dimensions of the tested element on the abrasion process. A number of tests were carried out changing the size of the analyzed material and observing the results of tests.

After the initial research, the dimensions of the samples (length, width and thickness) did not change results of the experiment. The surface of the samples was tested in the same way in each case. It was assumed that the dimensions of the tested samples were 50mm of width and 170 mm of length and various thicknesses (depending directly on the used fabrics, resins, hardening agents and fabrication technology).

### 3.3. Exemplary results

The epoxy resin samples tests (fig. 3) and the polyester resin sample tests (fig. 5) were carried out. Different fabrics were used by comparison. The parameters of selected samples are presented in table 1.

The measurement of mass decrement evoked by abrasion was taken before each stage of the research and mass dependence on the number of cylinder rotations is presented in figure 4. The values of mass decrement after each stage of the research are close to each other, however, the mass decrement is not exactly proportional.

In figure 5 the woven glass roving laminate made of polyester resin is presented. In the same way (fig. 3) the six stages of the research were done every one thousand rotations till six thousand ones. In figure 5 the change of surface quality of the sample is presented. During the following tests the increase in number of scratches and general worsening of the laminate surface can be observed. The observed scratches, grooves, spallings are distributed randomly on the surface of the laminate, what is a result of the non-oriented abrasion character and simultaneously it is a true representation of the real wear and tear of material used in the freight wagons construction.

*Table 2. Parameters of geometrical structure of the fibreglass (g.s.m. 450g/m²) sample surface in the epoxy resin (sample 1) warp before the test*

| Fibreglass epoxy laminate – measurements values | | | | | |
|---|---|---|---|---|---|
| | I | II | III | Avg. | |
| $R_p$ | 2,21 | 2,29 | 2,24 | 2,25 | Maximum peak height |
| $R_v$ | 1,17 | 1,22 | 1,15 | 1,18 | Maximum valley depth |
| $R_z$ | 3,38 | 3,51 | 3,39 | 3,43 | Average distance between the highest peak and lowest valley in each sampling length |
| $R_c$ | 2,07 | 1,71 | 1,70 | 1,83 | Average height of profile elements |
| $R_t$ | 9,16 | 5,96 | 6,05 | 7,06 | Maximum height of the profile |
| $R_a$ | 0,52 | 0,48 | 0,43 | 0,48 | Arithmetic average of the roughness profile |
| $R_q$ | 0,68 | 0,65 | 0,64 | 0,66 | Root mean-square-average |

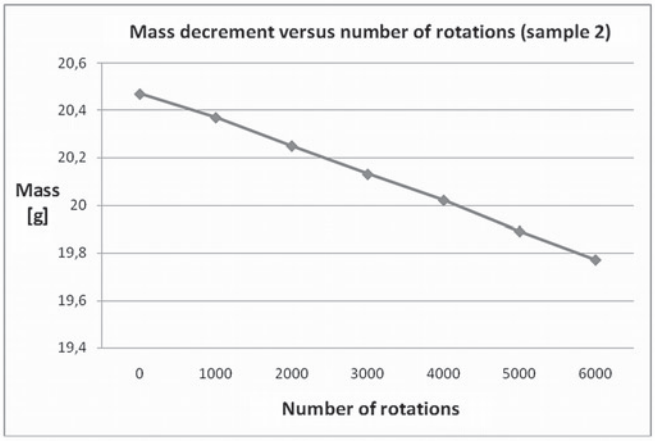


*Fig. 6. Chart presenting the dependence of mass of woven glass roving laminate made of polyester resin (the sample 2 in table 1) on the number of cylinder rotations (in the laboratory stand)*

*Table 3. Parameters of geometrical structure of the fibreglass (g.s.m. 450g/m²) sample surface in the polyester resin warp (sample 3) before the test*

| Fibreglass polyester laminate – measurement values | | | | |
|---|---|---|---|---|
| | I | II | III | Avg. |
| $R_p$ | 1,46 | 1,62 | 1,56 | 1,55 |
| $R_v$ | 1,08 | 1,09 | 1,13 | 1,10 |
| $R_z$ | 2,54 | 2,71 | 2,68 | 2,65 |
| $R_c$ | 1,16 | 1,18 | 1,07 | 1,14 |
| $R_t$ | 3,70 | 3,50 | 3,35 | 3,52 |
| $R_a$ | 0,35 | 0,34 | 0,33 | 0,34 |
| $R_q$ | 0,46 | 0,47 | 0,46 | 0,46 |

The dependence of mass on the number of the cylinder rotations during the test for the sample 2 (table 1) is presented in figure 6. In this case the mass decrement preserves its linear character.

In the table 2 there are presented the parameters of the geometric structures of the investigated sample made of fibreglass in the matrix of epoxy resin (sample 1).

The most common parameter of the surface roughness is an arithmetic average of the roughness profile ($R_a$). The parameter enables to find precise information about the geometrical structure of the profile with ordinate layout of the profile. Therefore the measures were filled in with the following parameters of geometric structures: the maximum height of the profile ($R_z$), average height of profile elements ($R_c$), maximum height of the profile ($R_t$) and root mean-square-average ($R_q$), on which the most influential are the single highest and deepest ones. The highest value of the surface roughness is a sum of the maximum peak height ($R_p$) and maximum valley depth ($R_v$). In majority of cases very important for exploitation is also kurtosis ($R_{ku}$) and skewness of the profile ($R_{sk}$), which not only characterise the height and depth of the profile but also their shape.

In the table 3 there are presented the parameters of the geometric structure of the sample made of fibreglass of basis weights 450g/m² in the matrix of polyester resin (sample 3).

*Table 4. Juxtaposition of averaged parameters of geometrical structure of the epoxy fibreglass (sample 1) sample surface and the polyester fibreglass sample (sample 3) before and after the first stage of the test*

| Designation of the parameter | Fibreglass epoxy laminate – measurements values | | | | Fibreglass laminate in the polyester resin warp – measurements values | | | | Results comparison | | | |
|---|---|---|---|---|---|---|---|---|---|---|---|---|
| | A | B | C | D | E | F | G | H | I | J | K | L |
| | Before the tests | After the tests | Absolute difference **\|B-A\|** | Difference in percentage terms **A/C** | Before the tests | After the tests | Absolute difference **\|F-E\|** | Difference in percentage terms **E/G** | Absolute difference **\|A-E\|** | Difference in percentage **(I/A)/(I/E)** | Absolute difference **\|B-F\|** | Difference in percentage **(K/B)/(K/F)** |
| $R_p$ | 1,68 | 4,92 | 3,24 | 193 | 1,67 | 5,37 | 3,7 | 222 | 0,01 | 1/1 | 0,45 | 9/8 |
| $R_v$ | 0,9 | 8,42 | 7,52 | 836 | 1,16 | 7,55 | 6,39 | 551 | 0,26 | 29/22 | 0,87 | 10/12 |
| $R_z$ | 2,57 | 13,33 | 10,76 | 419 | 2,83 | 12,92 | 10,09 | 357 | 0,26 | 10/9 | 0,41 | 3/3 |
| $R_c$ | 1,3 | 6,43 | 5,13 | 395 | 1,25 | 6,8 | 5,55 | 444 | 0,05 | 4/4 | 0,37 | 6/5 |
| $R_t$ | 4,27 | 20,67 | 16,4 | 384 | 3,71 | 25,96 | 22,25 | 600 | 0,56 | 13/15 | 5,29 | 26/20 |
| $R_a$ | 0,34 | 1,93 | 1,59 | 468 | 0,42 | 1,99 | 1,57 | 374 | 0,08 | 24/19 | 0,06 | 3/3 |
| $R_q$ | 0,47 | 2,62 | 2,15 | 457 | 0,54 | 2,61 | 2,07 | 383 | 0,07 | 15/13 | 0,01 | 0/0 |

In tables 2 and 3, there are parameters of geometrical structure from the selected measuring length on the surface of composite samples in the epoxy resin warp and in the polyester resin warp presented. The results juxtaposition result from three measures in every determined section on the surface of three tested samples (the same type samples). The arithmetic averages of the results are presented in table 4. The geometrical structure parameters before and after the abrasive tests are compared each other.

Before the research the samples were fabricated in the epoxy resin warp or in the polyester resin warp. The fabricated specimens had similar almost the same parameters of geometrical structure. Despite similar values of the maximum peak height ($R_p$) of each sample, the polyester ones had much deeper maximum valley depth. This situation is connected with the fabrication technology and characteristic of used resin. Comparing individual values of roughness parameters presented in table 4, higher roughness of polyester composite samples before and after the tests can be observed.

After carrying out the first stage of the research, deterioration of the surface quality both in the case of the sample in epoxy resin warp and the sample in polyester resin warp can be seen. Large deterioration of the surface quality of the epoxy sample can be observed. This conclusion is confirmed by over 400 percentage increase in the values of roughness parameters ($R_a$, $R_q$, $R_z$, $R_c$, $R_t$). Similar damages can be observed in the case of composite samples in the polyester resin warp, but the maximum valley depth ($R_v$) and maximum height of the profile ($R_t$) distinguish from the common pattern. One can pay attention to much deeper maximum valley depth ($R_v$) in the case of the epoxy sample than in the case of polyester one. This situation can be also connected with numerous scratches and chippings on the surface of the composite sample. Furthermore in the polyester sample the increase in maximum peak height ($R_p$) was a bit higher the in the case of the epoxy sample.

Despite the fact that the average values (arithmetic $R_a$ and the root mean-square-average $R_q$) became much worse in the case of the composite sample in the epoxy resin warp, the maximum height of the profile $R_t$ in the percentage terms increased more in the case of the polyester sample than in the case of the epoxy one. Moreover, in the case of the registered value of the parameter ($R_v$) of the epoxy sample much higher increase in depth of valley can be seen.

*Table 5. Mass of the samples weiged after following stages of the test*

| Stage of the test /number of cylinder's rotations | Number of the sample | | | | | | | | |
|---|---|---|---|---|---|---|---|---|---|
| | 1 | 2 | 3 | 4 | 5 | 6 | 7 | 8 | 9 |
| | Mass of the sample [g] | | | | | | | | |
| 0 | 31,74 | 20,47 | 20,52 | 25,14 | 19,12 | 28,43 | 20,02 | 31,63 | 13,97 |
| 1/2000 | 31,65 | 20,25 | 20,28 | 25,06 | 19 | 28,21 | 19,94 | 31,43 | 13,79 |
| 2/4000 | 31,55 | 20,02 | 20,02 | 24,97 | 18,87 | 27,99 | 19,82 | 31,19 | 13,59 |
| 3/6000 | 31,46 | 19,77 | 19,78 | 24,87 | 18,76 | 27,76 | 19,71 | 30,97 | 13,39 |
| 4/8000 | 31,37 | 19,55 | 19,58 | 24,79 | 18,66 | 27,56 | 19,62 | 30,78 | 13,21 |
| 5/10000 | 31,27 | 19,31 | 19,34 | 24,69 | 18,54 | 27,35 | 19,52 | 30,58 | 13,02 |
| 6/12000 | 31,19 | 19,11 | 19,14 | 24,61 | 18,44 | 27,15 | 19,44 | 30,39 | 12,85 |
| Mass decrements in percentage terms [%] | 1,73% | 6,64% | 6,73% | 2,11% | 3,56% | 4,50% | 2,90% | 3,92% | 8,02% |

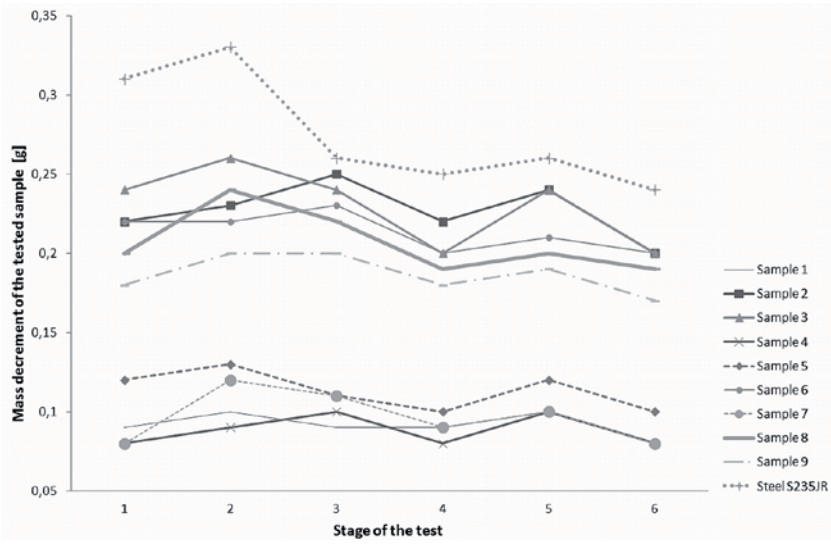


*Fig. 7. Juxtaposition of mass decrements of the tested samples*

In the table 5 there are shown the mass values of chosen samples, provided after six following stages of the experiment. Each and single time of the experiment the rotational cylinder on the laboratory stand was rotated 2000 times.

Figure 7 presents the graphs illustrating the mass losses of the chosen samples after six following stages of the experiment. Due to the specific wearing character suggested in the laboratory tests, the mass losses are not identical but show high similarities. Due to the fact it is easy to compare the individual values of the parameters and forecast the probable wear of the material in the conditions close to real.

While comparing the mass losses of the samples it was suddenly revealed that the composite in the matrix of epoxy resin shows less mass loss than the composite made in a matrix of polyester resin. The very same results were presented in the previous work [13], where the same materials samples were undergone the experiments. No matter what methods were used to provide the tests, considering the various loads, rotator velocity and the distance from the abrasive roll the results came out the same. On the other hand the composites made of the fibres with bigger weight shows relatively bigger mass loss in the proposed test than the composites of fibres with smaller weight. Such phenomenon appeared in both the examined materials with polyester and epoxy matrixes. Moreover, the hardener does not play any role in the experiment. The results of composites wear were presented in the work as well as in the others [4, 13–15]. Undoubtedly the lowest resistance was presented by the sample made of the carbon fibres with the smallest basis weight of all the chosen sample materials (sample 9). Additionally noticeable is the role of a hardener in the wear process. For the epoxy composites the better hardener is PAC from Organika Sarzyna, which shows better wear resistance. On the other hand, the hardener Luperox K1 produced by Arkema Inc suits better for the polyester composites, what actually does not influence positively the wear process.

Among the investigated samples the fibreglass composite 450 g.s.m. in the matrix of the epoxy resin shows the highest quality and resistance for wear, what is visible as the lowest mass loss and its value.

## 4. Final remarks

In the work the abrasive features of tested laminates were initially determined. The assessment of abrasive wear of composites materials and the determination of potential technical applications are possible thanks to the carried out research. In the research the method of periodical verification of the surface condition and mass decrement was used. Verifications follow after performing the specified number of rotations of the cylinder in the laboratory stand. The similar values resulting from tests were achieved on different stages of research, mass decrement of laminates oscillated around the close value preserving its linear character.

In this paper the most endurable laminate was determined. The research pointed out that the laminates made with the usage of epoxy resin have the greatest resistance to abrasive wear, much greater than the polyester ones. As the result of abrasion the surface of laminates consisting of epoxy resin had shallower scratches and the whole sample had lower mass decrement. Further measurements indicated that the resistance to abrasion of the considered composites was dependent on basis weight of fabric used to produce laminate. The research pointed out that the laminates made with the usage of epoxy resin have the greatest resistance to abrasive wear, much greater than the polyester ones. As the result of abrasion the surface of laminates consisting of epoxy resin had shallower scratches and the whole sample had lower mass decrement. Materials consisted of fabric with greater basis weight were characterized by smaller value of mass decrement of samples and also shallower scratches.

Damages of samples were observed thanks to the analysis of surface profile of the tested composites. The surface profile analysis of the investigated composites after applying loose abrasive material let us observe the damages coming out of the crushes on the laminates surfaces and better quality parameters of the profiles made of epoxy laminates.

In the first part of this measure process, when the material is smooth, there are scratches arising, which during the ongoing process of abrasion become wider, but after further damages of the surface their depth is becoming smaller. Testing of the steel sample made it possible to define the intensity of laminate surface abrasion. It turned out that such materials distinguish themselves with quite high resistance to abrasion. The steel sample had much deeper scratches and much bigger mass decrement [1].

If one analyses measurements results it can be stated that considered laminates are good for application in the construction of freight wagon taking into consideration the parameters of resistance to abrasion (mass decrements). When deciding which component to use to produce laminates one has to keep in mind that fabrics with high basis weight are the best for this purpose. Also, the epoxy resin is better than the others. The suitable selection of such elements will allow obtaining laminate which will be resistant to abrasion. There are the parameters that could exclude this group of materials from application for construction of freight wagon. That was crucial the technology of the composites to be chosen due to its general availability and economic point of view. Handmade laminates production technology caused occurrence of air bubbles inside the resin which attenuated the structure of the material. The proposed method of the experiment provides only the predictable and comparable results of the tested samples in the considered application. Percussive acting of abrasive material caused crushing of the laminate material in the places where the bubbles appeared. As a result if one would like to define the possible applications of the laminate materials in construction of freight wagon, the impact resistance tests should be carried out. Additionally it is worth considering the proper scale and energy of the device. To determine the usage of the investigated composites in structure of the sheathing coal cars it is absolutely necessary to provide numerous and complex experiments.

## References


1. Baier A, Zolkiewski S. Badanie zużycia ściernego materiałów kompozytowych. Wrocław: ZN Wyższej Szkoły Oficerskiej Wojsk Lądowych im. gen. T. Kościuszki, Rocznik XLIII, Styczeń – Marzec 2011, 1 (159): 21–36.
2. Bijwe J, Rekha Rattan, Fahim M. Abrasive wear performance of carbon fabric reinforced polyetherimide composites: Influence of content and orientation of fabric. Tribol. Int. 2007, 40: 844–854.
3. Capanidis D. Selected aspects of the methodology of tribological investigations of polymer materials. Archives of Civil and Mechanical Engineering 2007, VII, 4: 39–55.
4. El-Tayeb NSM, Yousif B. F. Evaluation of glass fiber reinforced polyester composite for multi-pass abrasive wear applications. Wear 2007, 262: 1140–1151.
5. Friedrich K. Friction and wear of polymer composites. Composite materials series 1. Amsterdam: Elsevier, 1986.
6. Gahr KHZ. Microstructure and wear of materials. Tribology series 10. Amsterdam: Elsevier, 1987.
7. Gierek A. Zużycie tribologiczne. Gliwice: Wydawnictwo Politechniki Śląskiej, 2005.
8. Hebda M, Wachal A. Trybologia. Warszawa: Wydawnictwo Naukowo-Techniczne, 1980.
9. Koziolek S, Rusinski E, Jamroziak K. Critical to Quality Factors of Engineering Design Process of Armoured Vehicles. Solid State Phenomena 2010, 165: 280–284.
10. Mahapatra SS, Patnaik A, Satapathy A. Taguchi method applied to parametric appraisal of erosion behavior of GF-reinforced polyester composites. Wear 2008, 265: 214–222.
11. Nawrocki J, Ryncarz A, Węglarczyk J. Teoria i praktyka rozdrabniania. Gliwice: Wydawnictwo Politechniki Śląskiej, 1989.
12. Patnaik A, Satapathy A, Mahapatra SS, Dash R. R. Erosive wear assessment of glass reinforced polyester–flyash composites using Taguchi method. Int. Polym. Process 2008, 23 (2): 1–8.
13. Pihtili H. An experimental investigation of wear of glass fibre–epoxy resin and glass fibre–polyester resin composite materials. European Polymer Journal 2009, 45: 149–154.
14. Pihtili H, Tosun N. Effect of load and speed on the wear behaviour of woven glass fabrics and aramid fibre-reinforced composites. Wear 2002, 252: 979–984.
15. Pihtili H, Tosun N. Investigation of the wear behaviour of a glassfibre-reinforced composite and polyester resin. Composites Science and Technology 2002, 62: 367–370.
16. Reis PNB, Ferreira JAM, Antunes FV. Effect of Interlayer Delamination on Mechanical Behavior of Carbon/Epoxy Laminates. Journal of Composite Materials 2009, 43, 22: 2609–2621.
17. Reis PNB, Ferreira JAM, Antunes F. Effect of adherend's rigidity on the shear strength of single lap adhesive joints. International Journal of Adhesion and Adhesives 2011, 31, 4: 193–201.
18. Rusinski E, Koziolek S, Jamroziak K. Quality Assurance Method for the Design and Manufacturing Process of Armoured Vehicles. Eksploatacja i Niezawodnosc – Maintenance and Reliability 2009, 3: 70–77.
19. Sahin Y, Ozdin, K. A model for the abrasive wear behaviour of aluminium based composites. Materials and Design 2008, 29: 728–733.
20. Sandhyarani B, Satapathy A. Tribo-performance analysis of red mud filled glass-epoxy composites using Taguchi experimental design. Materials and Design 2009, 30: 2841–2853.
21. Stachowiak GW, Batchelor AW. Engineering tribology. Amsterdam: Elsevier, 1993.
22. Thorp JM. Abrasive wear of some commercial polymers. Tribol. Int. 1982; 15: 89–135.
23. Wieleba W. The Mechanism of Tribological Wear of Thermoplastic Materials. Archives of Civil and Mechanical Engineering 2007, VII, 4: 185–199.
24. You-Bai X. On the tribology design. Tribol. Int. 1999, 32: 351–358.
25. Zolkiewski S. Selection and impact of parameters in designing of composite materials. 13th World Congress in Mechanism and Machine Science, Guanajuato, México, 19–25 June, 2011, A23_555: 1–10.
26. Zolkiewski S. Testing composite materials connected in bolt joints. Journal of Vibroengineering 2011, 13, 4: 817–822.
27. Zolkiewski S. Experimental and numerical testing of the epoxide resin based composite sandwich panel made from the woven glass roving laminate and the steel plate. XVIII международную научно - техническую конференцию “Машиностроение и техносфера XXI века”. XVIII International Conference of Machine-Building and Technosphere of the XXI Century. Doneck 2011, 4: 245–248.



**Prof. Andrzej BAIER, D.Sc. (Eng.)**
**Sławomir ŻÓŁKIEWSKI, Ph.D. (Eng.)**
Department of Mechanical Engineering
Silesian University of Technology
ul. Akademicka 2A, 44-100 Gliwice, Poland
E-mail: slawomir.zolkiewski@polsl.pl

Article citation info:
CHŁOPEK Z, LASOCKI J. Comprehensive environmental impact assessment of the process of preparation of bioethanol fuels of the first and second generation. Eksploatacja i Niezawodnosc – Maintenance and Reliability 2013; 15 (1): 44–50.

Zdzisław CHŁOPEK
Jakub LASOCKI

# COMPREHENSIVE ENVIRONMENTAL IMPACT ASSESSMENT OF THE PROCESS OF PREPARATION OF BIOETHANOL FUELS OF THE FIRST AND SECOND GENERATION

# KOMPLEKSOWA OCENA ODDZIAŁYWANIA NA ŚRODOWISKO PROCESU PRZYGOTOWANIA PALIW BIOETANOLOWYCH PIERWSZEJ I DRUGIEJ GENERACJI*

*The paper provides some information regarding comprehensive evaluation of the environmental hazard caused by the operation of automotive vehicles with internal combustion (IC) engines powered by bioethanol fuel. It presents the assumptions made for the life cycle assessment (LCA) of the environmental impact of fuel, carried out according to the Well-to-Wheel (WtW) method, where the fuel preparation stage, including the acquisition of raw materials as well as the production, transport, and distribution processes, and the vehicle operation stage are taken into account. The technologies and raw materials used to make bioethanol of the first and second generation have been presented and compared with each other. Results of research on greenhouse gas (GHG) emissions and non-renewable energy input in the process of preparation of bioethanol fuels of the first and second generation have been analysed. Nine versions of the production process, differing from each other in the process methods used and the types of the biomass processed, have been examined.*

***Keywords**: bioethanol, Well-to-Wheel analysis, pollutant emission, fuel production technology.*

*W pracy przedstawiono informacje na temat kompleksowej oceny zagrożenia środowiska przez eksploatację pojazdów samochodowych z silnikami spalinowymi zasilanymi paliwem bioetanolowym. Przedstawiono założenia analizy ekologicznej cyklu istnienia paliwa według metody Well–to–Wheel, uwzględniającej etap przygotowania paliwa, składający się z pozyskiwania surowców, wytwarzania, transportu i dystrybucji, oraz etap użytkowania pojazdów. Zaprezentowano i porównano technologie oraz surowce stosowane w wytwarzaniu bioetanolu pierwszej i drugiej generacji. Przeanalizowano wyniki badań emisji gazów cieplarnianych oraz zużycia energii ze źródeł nieodnawialnych w procesie przygotowania paliw bioetanolowych pierwszej i drugiej generacji. Rozważono dziewięć wariantów przebiegu procesu wytwarzania, różniących się zastosowaną technologią i rodzajem przetwarzanej biomasy.*

***Słowa kluczowe**: bioetanol, analiza Well–to–Wheel, emisja zanieczyszczeń, technologia wytwarzania paliw.*

## 1. Introduction

Ongoing growth in the production of fuels from renewable sources, where bioethanol is particularly important as a fuel made on the largest scale [15], has been observed for many years. This trend has chiefly resulted from the striving for energy security of individual countries and from environmental protection issues, as the powering of internal combustion (IC) engines with fuels of biological origin (biofuels) may not only improve the environmental performance of such engines but also reduce the environmental loading with pollutants at the fuel production stage.

The former of the above two reasons for increasing interest in biofuels is related to the need that the world economy should be made independent of crude oil supplies because of limited fossil fuel resources and a danger connected with the fact that the power raw materials needed by a large part of the world are concentrated in a small group of countries, which in many cases are politically unstable at that. As regards the energy security, the availability and prices of fuels are of particularly great importance because of the mass use of IC engines. The situation where these factors strongly depend on the moods prevailing in the world markets is highly unfavourable. Therefore, it seems reasonable to pursue a policy of diversification of energy sources based on fuels made from biomass, which, in the form of agricultural products and waste, is much more easily available for many countries than crude oil.

Environmental protection problems make another, equally important reason for increasingly common tackling of the issue of biofuels. Public interest in the problems of harmful environmental impact of IC engines, or of motorisation in general, is very often limited to the consideration of anthropogenic reasons for global climate changes, and sometimes to mere balancing of the emission of greenhouse gases (GHG), especially fossil carbon dioxide. Meanwhile, the most important and simultaneously the most painfully felt effect of the use of IC engines is the immediate danger arising from the emission of pollutants that are harmful to health of the local population. The areas of large urban agglomerations, where high intensity of vehicle traffic and unfavourable conditions of dissemination of exhaust gases result in high levels of pollutant immissions, make an extreme example.

The increasing interest in the use of renewable energy carriers creates the need to compare them with each other for the optimum solution to be chosen. Regardless of economic factors, a matter of overriding importance is the evaluation of environmental properties of specific biofuel types. Efforts are made at the same time to minimise the impact of such

(*) Tekst artykułu w polskiej wersji językowej dostępny w elektronicznym wydaniu kwartalnika na stronie ***www.ein.org.pl***

fuels on the environment and the local population, with this impact being understood in a complex way instead of being limited to its single aspect only. Such an approach means the gaining of qualitative and quantitative knowledge of the environmental risks related to the fuel at every stage of its life cycle. So far, the methods most frequently used are limited to pollutant emission measurements carried out in laboratory conditions, on chassis dynamometers (for complete vehicles) or on engine test beds (for engines only), with tests of various kinds, both static and dynamic, being run. Normally, the tests provided in type-approval procedures are used, but this, in principle, does not give grounds for the formulation of conclusions about the engine performance in actual service conditions. Tests of this kind make it possible to carry out only comparative analyses of fuel consumption and pollutant emission effects, but the formulation of judgments on the inventorying of pollutant emissions and energy inputs is inacceptable at all. Therefore, a tool is needed that would enable evaluation of the whole fuel preparation process, covering not only the final pollutant emissions from a vehicle being in service but also the acquisition of raw materials needed for the fuel production as well as the transport and distribution of the fuel as a finished product. Such a tool is the "Well-to-Wheel" method, the name of which (often abbreviated as WtW) might be interpreted as "from the source (of an energy carrier) to the wheel (of a vehicle)". It is a particular case of the application of the Life Cycle Assessment (LCA) method [12, 16] to motor fuels.

The topic of the discussion presented herein is comprehensive evaluation of the pollutant emissions and energy inputs connected with the process of preparation of bioethanol of the first and second generation. The vehicle operation stage has been excluded from the scope of the discussion; this is because the knowledge of environmental properties of fuels with respect to the pollutant emissions during vehicle operation is much better than that related to the fuel preparation stage. The environmental benefits resulting from the powering of IC engines with bioethanol fuels, such as very big reduction of particulate matter and carbon monoxide emissions, significant reduction of the emissions of nitrogen oxides and hydrocarbons (including polycyclic aromatic hydrocarbons), very good biodegradability and possibility to reduce the emission of fossil carbon dioxide because of renewability of raw materials (the use of pure bioethanol result in zero emission of fossil carbon dioxide) are generally known [1 – 4, 14, 19]. While the effects of any changes possible to be introduced at the vehicle operation stage are usually quite small, much more benefits may be expected from the optimisation of the processes of production and distribution of energy carriers. In the case of bioethanol production, the use of cellulose waste in place of the traditionally used sugarcane and maize may result in a significant reduction of the environmental loading.

## 2. Assumptions made for the Well-to-Wheel analysis of environmental hazard

The Well-to-Wheel method may be defined as a quantitative and qualitative analysis of the possible environmental impact of the processes connected with the whole conventional life cycle of a fuel. This cycle is divided into two stages. The first one is the fuel preparation stage, which covers the acquisition of raw materials for energy carriers, fuel production, transport of the fuel as a finished product, and fuel distribution. In English, this stage is referred to as "Well-to-Tank" (abbreviated as WtT), which has the meaning "from the source (of an energy carrier) to the tank (i.e. the fuel tank of a vehicle)". The second stage is related to the vehicle operation and its English name is "Tank-to-Wheel" (abbreviated as TtW); it should be interpreted as "from the tank (i.e. the fuel tank of a vehicle) to the wheel (of the vehicle)" [5 – 7, 19]. A schematic diagram of the Well-to-Wheel analysis has been graphically presented in Fig. 1, with the energy losses at specific parts of the process having been additionally shown.

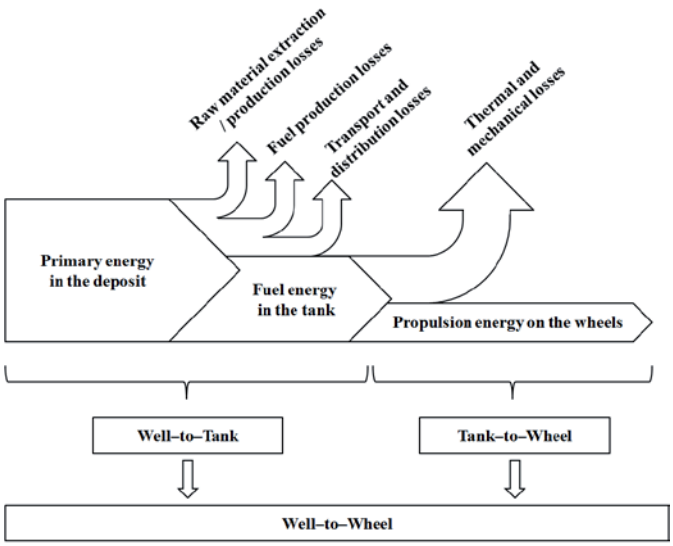


*Fig. 1. Schematic diagram of individual stages of the Well-to-Wheel analysis*

The Well-to-Wheel analysis is used to define and quantify the environmental loading resulting from the method of realisation of individual processes at every life cycle stage and then to evaluate this impact. These purposes are pursued by dividing successive stages into single processes (the whole scope of the analysis constitutes a "product system", i.e. a "fuel system" in this case), for which sets of input data (e.g. energy inputs, raw materials) and output data (e.g. products, intermediate products, waste, pollutant emissions) are determined. Thus, a material and energy balance is compiled, which is referred to as Life Cycle Inventory (LCI) [12, 16]. The necessary quantitative data are sourced in most cases from the economy sector and from the government administration bodies engaged in environmental protection. The analysis of this type produces highly valued results as it enables not only global assessment of the whole life cycle of a fuel but also separate evaluation of individual processes being parts of the life cycle.

The LCI analysis makes it possible to determine the values of cumulative pollutant emissions as obtained from the material balance, and cumulative energy inputs as obtained from the energy balance, in relation to a "functional unit" [12], e.g. 1 km of the distance covered by a vehicle or 1 MJ of energy contained in fuel.

The energy balance makes a basis for determining the amount of energy needed for the preparation of the fuel quantity consumed by the vehicle to travel a road section of unit length (expressed in [MJ/km] or [MJ/mi]) or the ratio of the fuel preparation energy to the energy contained in finished fuel (expressed in [MJ/MJ]) [6, 7, 19, 20].

The most popular environmental impact indicator is the total greenhouse gas (GHG) emission taken for the whole fuel life cycle. Specific gas emissions, with appropriate weights, are summed up to obtain the equivalent carbon dioxide emission (according to Directive 2009/28/EC of the European Parliament and of the Council of 23 April 2009 on the promotion of the use of energy from renewable sources):

$$m_{CO_2\,eq} = \sum m_x \cdot w_x \tag{1}$$

where: $m_x$ – emission of substance "x";
$w_x$ – potential share of substance "x" in the development of the greenhouse effect.

For selected substances, the "$w_x$" values are:
- Carbon dioxide – 1;
- Methane – 23;
- Dinitrogen monoxide – 296.

The emission of greenhouse gases is specified as mass emission of carbon dioxide equivalent, i.e. the mass of carbon dioxide equivalent in relation to the distance travelled by this vehicle (expressed in [g/km] or [g/mi]), or as an energy-related indicator of the emission of carbon dioxide equivalent, i.e. the mass of carbon dioxide equivalent corresponding to a fuel amount carrying 1 MJ of energy (expressed in [g/MJ]) [5 – 7, 19, 20].

The information obtained from the inventorying of pollutant emissions and energy inputs may be used for making comparisons between various fuel types; however, it cannot produce a full picture of the environmental impact of a specific fuel. Therefore, other indicators should additionally be taken into account where, based on results of the balance of inputs and outputs of individual processes, the said processes are considered accountable for specific environmental risks ("impact categories"), such as eutrophication, acidification, noise, vibrations, smog, electromagnetic radiation, dust, land-use change, depletion of the fossil fuel, mineral raw material, and water resources, climate changes, ozone layer depletion, etc. [12, 16]. Calculations of the impact of the fuel life cycle in the categories as mentioned above are made with the use of Life Cycle Impact Assessment (LCIA) methods, which include e.g. CML 2002, Eco-indicator 99, EDIP, EPS2000, Impact 2002+, LIME, LUCAS, MEEup, ReCiPe, Swiss Ecological Scarcity method, TRACI, or USEtox [9, 12, 16]. An unquestionable good point of these methods is a possibility to show a direct dependence between a process under consideration and the elements of the ecosystem affected by the process. On the other hand, much controversy is aroused by the subjectivity in the assessment proposed by individual methods, which leads to significant differences in the results obtained, even if identical input data are used.

In the European conditions, a popular Life Cycle Impact Assessment method is Eco-indicator 99 [5, 9, 12, 16]. It presents the environmental impact with the use of an "eco-indicator," in which environmental impact assessments in the following three damage categories are combined together:

- Damage to human health;
- Damage to ecosystem quality;
- Damage to resources.

The damage to human health is expressed in this method by the DALY indicator (Disability-Adjusted Life Year), which is a unit of measure of the impact of ill-health on the human being in terms of both the life time lost because of premature death (mortality) and the time lived in the state of disability (morbidity). This indicator is commonly used in health economy to define the state of health of a specific population, e.g. by the World Health Organization (WHO). In the Eco-indicator 99 method, models have been developed where respiratory diseases, tumours, climate change effects, ozone layer depletion (causing such diseases as cutaneous carcinoma or cataract), and harmful impact of ionising radiation have been taken into account and where the quantities measured include exposure to pollutants and pollutant immissions.

The damage to ecosystem quality is determined as the percentage of the species that vanish in a specific area due to the environmental impact of vehicles (i.e. the fuel production processes in the case under consideration). Here, such factors are taken into account as water and soil acidification and eutrophication, land-use change (e.g. deforestation), and "ecotoxicity", defined as the percentage of all the species present in the environment within a certain area and within a specific time interval and living under toxic stress (Potentially Affected Fraction or PAF).

In the third damage category, the resource depletion is assessed in terms of the quality of the remaining raw material resources, including petroleum-derivative fuels. It is determined as the increase in the energy to be spent for the extraction of 1 Mg of the raw material (expressed in [MJ/Mg]). In some cases, the scale of extraction of other chemical elements and compounds is considered.

In its final form, the eco-indicator is a figure that is the sum of the figures obtained for the three damage categories and weighted as appropriate.

A different approach has been adopted at the Swiss Ecological Scarcity method [5, 8], sometimes referred to as Ecoscarcity or UBP'06 (from German "*Umweltbelastungspunkte*") method. As it is in the case of the Eco-indicator 99 method, a few areas of the environmental impact of the product or process under investigation (e.g. the operation of an automotive vehicle) are taken into account. In this method, chiefly the pollutant emissions (with such factors as acidification and eutrophication, ozone layer depletion, etc.) and the use of natural raw materials are taken into account. The unique nature of this method lies in the determining of the difference between the current environmental loading in a specific area, i.e. "current flow," and the maximum acceptable loading defined by the existing legislative guidelines or political goals, referred to as "critical flow." The terms of "current flow" and "critical flow" have not been formalised yet; therefore, they should be understood as physical quantities that define the environmental impact of civilisation, e.g. pollutant immissions, mass emission, or specific brake emission of pollutants from internal combustion engines. According to the Swiss method, the result of the environmental impact assessment is presented in the form of an "eco-factor," the unit of which has been defined as the "eco-point" (EP) divided by the unit of measure of the polluting effect under consideration (for the GHG emissions, the eco-factor units would be [EP/g]). The eco-factor is calculated from the following formula [8]:

$$eco-factor = K \cdot \frac{1 \cdot EP}{F_n} \left( \frac{F}{F_k} \right)^2 \cdot c \qquad (2)$$

where: K – coefficient of relative harmfulness of the specific polluting effect;
F – current flow;
$F_n$ – normalised flow;
$F_k$ – critical flow;
c – constant.

Hence, the eco-factor may be defined as a measure of the potential environmental hazard imposed by a specific polluting effect. Its value rises with growing excess of the current emission or consumption of natural raw materials over the limits allowed. The coefficient of relative harmfulness of the polluting effect under consideration, present in the formula, is to adjust the calculation result by differentiating substances that exert more or less harmful environmental impact (as it is in the case of greenhouse gases). The current flow value is usually taken from the most recent statistical data available that concern the specific area.

The main good points of the Swiss Ecological Scarcity method are simplicity of calculations and direct relationship with the political targets and legislative limits that should be met in a specific area or country. This is the main difference between this method and the methods that are oriented at absolute evaluation of environmental damage (such as the Eco-indicator 99 method). On the other hand, however, the eco-factor values may only be determined for the substances for which any legislative limits or political targets actually exist.

In recapitulation of the discussion presented in this section and concerning the methods of comprehensive evaluation of motor fuels, two opposing trends can be identified. On the one hand, the scope of the Well-to-Wheel analysis should be as wide as possible, so that all the impact types are taken into account and their full environmental consequences are determined. On the other hand, however, the scope of the investigation should be unequivocally defined by introducing certain limitations and making specific assumptions for the comprehensive evaluation to be generally possible. In consequence, the obtaining of objective results is extremely difficult and the gen-

eralisation of conclusions may often lead to erroneous interpretation. Nevertheless, in the necessity of comprehensive evaluation of motor fuels and in consideration of the limitations presented, the use of the Well-to-Wheel method seems to be a reasonable solution.

## 3. Methods of production of bioethanol of the first and second generation

An unquestionable good point of bioethanol fuels is the possibility of obtaining such fuels from a wide range of raw materials. Based on the origin of the biomass used for the production, it has been agreed to divide biomethanol into the following "generations" [1, 14, 17, 18]:

- Biomethanol of the first generation, obtained from the raw materials that may be used in the food industry, e.g. maize, potato, rye, sugarcane, sugar beet, rice, and sweet sorghum; such materials contain monosaccharides (glucose, fructose), disaccharides (sucrose, lactose), or polysaccharides (starch);
- Biomethanol of the second generation, obtained from biomass rich in lignocellulose and from waste and by-products of the processing industry; the most important substrates include wood, grass, cane, straw, wood waste of the pulp and paper industry, cereal stover, maize cobs, waste of the milling and oil manufacture industries, used building timber, paper mill discards, municipal waste (dry part of the mass), molasses (by-product of sugar factories, rich in sucrose), and whey (lactose-containing waste of the milk processing industry).

At present, the world's most popular bioethanol production method is alcoholic fermentation with the use of microorganisms, chiefly yeast (*Saccharomyces cerevisiae*). In general, the biomethanol production process may be presented as consisting of three stages [11, 18]. The first one, referred to as saccharification, is the feedstock preparation process. It consists in preliminary hydrolysis to convert polysaccharides into monosaccharides. The second stage is the fermentation proper, which takes place in water environment under catalytic influence of the enzymes generated by the yeast. This process may be run periodically or continuously; the latter method is more efficient but requires a more complicated process system. The fermentation process is followed by the final stage, at which alcohol is separated by distillation. Thus, hydrated bioethanol is obtained, with about 5% water content. For the water content to be removed and, thus, anhydrous bioethanol (of more than 99% purity) to be obtained, a dewatering process should additionally be applied.

The most important differences between the processes of production of bioethanol of the first and second generation can be seen at the substrate preparation stage. The molasses and whey do not contain polysaccharides; therefore, they do not require any hydrolysis process to be carried out and they may be directly subjected to fermentation. The starch, which constitutes a reserve material in plants, is easily hydrolysed under the influence of enzymatic preparations. Lignocellulose as a structural material of plant cells is more resistant to the action of hydrolysing agents. It is a complex of three polymers, i.e. cellulose, hemicelluloses, and lignin of various chemical compositions bonded together with covalent and hydrogen bonds [10, 17, 18]. In this case, preliminary treatment of the feedstock is necessary to separate cellulose and hemicellulose from lignin, which is a macromolecular aromatic compound with no saccharide contents and, as such, does not undergo fermentation. In this process, acid hydrolysis, chiefly with the use of sulphuric acid, or enzymatic hydrolysis is employed. The latter method makes it possible to achieve high process efficiency and is now being developed, with the development work being aimed at a reduction in the high enzyme acquisition cost [10, 17, 18].

## 4. Environmental impact assessment of the process of preparation of bioethanol of the first and second generation

In this paper, selected results of evaluation of the environmental loading caused by the stage of preparation (Well-to-Tank stage) of bioethanol of the first and second generation have been presented and compared with each other. The numerical data have been taken from Swiss sources [11, 20] and they are predominantly related to the bioethanol production methods employed in that country, except for the bioethanol production from sugarcane (in Brazil), maize (in the USA), sweet sorghum (in China), and rye (in general European conditions). The scope of the analysis covers the activities related to plant growing, biomass conversion into alcohol in a production facility, transportation of bioethanol to filling stations, and distribution of the fuel to end-users. Nine versions of the production process, differing from each other in the types of the biomass processed and in the corresponding process methods used, which are now practically worldwide used and are reasonably cost-effective, have been examined. Three examples represent biofuels of the second generation, obtained from wood, grass, and whey. Additionally, corresponding results obtained for gasoline have been provided for comparison. The following symbols have been adopted:

- EtOH–Wo – bioethanol obtained from wood;
- EtOH–Gr – bioethanol obtained from grass;
- EtOH–Wh – bioethanol obtained from whey;
- EtOH–SB – bioethanol obtained from sugar beet;
- EtOH–SC – bioethanol obtained from sugarcane;
- EtOH–SS – bioethanol obtained from sweet sorghum;
- EtOH–MC – bioethanol obtained from maize;
- EtOH–Po – bioethanol obtained from potato;
- EtOH–Ry – bioethanol obtained from rice;
- G – gasoline.

The Well-to-Tank analysis has been based on inventorying the set of input and output data concerning the materials and energy that are involved in a specific process and exert an impact on the environment [20]. If a bioethanol production process results in the generation of by-products such as electricity, Dried Distillers Grains with Solubles (DDGS), or sugarcane bagasse then the allocation of emissions and energy inputs is based on estimated market prices of such products (it is proportional to the respective prices) [13]. However, other factors, of economic and social nature, have not been taken into account. Only the direct environmental impact (material and energy balance) has been calculated, with the side effects having been ignored (while e.g. the cultivation of plants for ethanol production on an area previously used for the growing of plants for food production purposes results sometimes in the necessity to import some food products from abroad, which entails additional transport activities). For the bioethanol made in Brazil, China, and the USA, the cost of transportation of finished fuel to Europe has been taken into account.

Results of calculations of the total amount of energy obtained from non-renewable sources and necessary to prepare bioethanol and gasoline carrying 1 MJ of energy (at the WtT stage) have been shown in Fig. 2.

The input of energy obtained from non-renewable sources and used for the bioethanol production in all the versions examined is significantly lower than the consumption of energy used for the production of gasoline. The highest figures, ranging from 0.9 to 1 MJ/MJ, have been recorded for the making of bioethanol from maize, potato, and rye. In the other cases, the level of 0.5 MJ/MJ has not been exceeded. The relatively high consumption of non-renewable energy at the production of bioethanol from maize in the American conditions results from significant quantities of fossil fuels used for the operation of agricultural machinery; for the bioethanol obtained from potato and rye, the high energy consumption is caused by low eco-

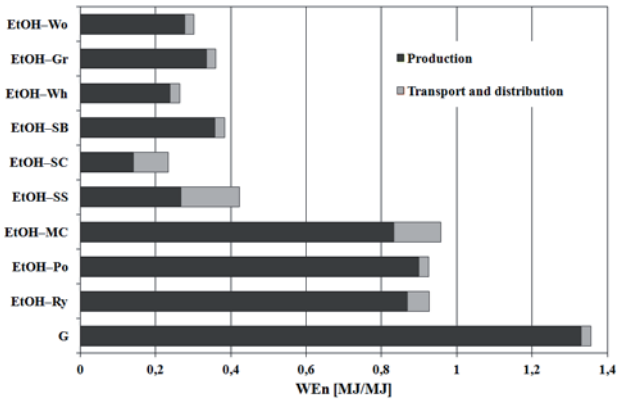


*Fig. 2. Total amount of non-renewable energy used to prepare fuel of 1 MJ energy content*

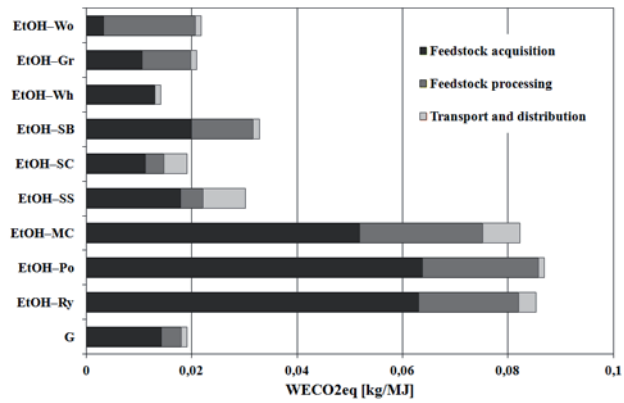


*Fig. 3. Energy-related GHG emission indicator determined for the stage of preparation of the fuels under consideration*

nomic value of the by-products and low rye yield per a unit area. The lowest consumption of energy obtained from non-renewable sources has been recorded for the preparation of bioethanol from sugarcane, which has resulted from high plant yield per a unit area thanks to good weather conditions in Brazil and, simultaneously, from the fact that a significant part of the energy needed for the production process has been sourced from the combustion of bagasse, which is a by-product of sugarcane processing. The low consumption of non-renewable energy at the production of sweet sorghum may be explained in a similar way; however, the amount of energy needed to transport finished fuel from China to Europe is higher than that in the case of Brazil. The very good result recorded for the production of bioethanol from whey (below 0.3 MJ/MJ) is explainable by the fact that, according to the allocation principles, bioethanol is accountable for as little as 20% of the energy input of the whole process while the predominating part is assigned to the by-products of high protein contents. The consumption of non-renewable energy for bioethanol production from wood and grass fell within the range of (0.3 ÷ 0.4) MJ/MJ and only slightly exceeded that recorded for bioethanol obtained from sugarcane, which is cultivated in the warm climate areas of Brazil with employing the well-developed mass production methods. In comparison with the European technologies (where potato, rye, and sugar beet are used) and with the Chinese and American solutions, bioethanol of the second generation offers a possibility of significant reduction in the consumption of energy obtained from non-renewable sources.

Results of the GHG emission balance in the form of an energy-related emission indicator determined for the bioethanol and gasoline preparation (WtT) stage have been presented in Fig. 3. The following three sub-stages have been singled out: feedstock acquisition (plant cultivation or crude oil extraction), fuel production, and fuel transport inclusive of distribution at filling stations. As it can be seen, a decisive role is played in most cases by the agricultural production. Local production of fuel in the country where the fuel is to be actually used will result in a significant reduction of the transportation emissions. As it happened in the case of the findings concerning the consumption of non-renewable energy at the fuel preparation stage, the highest indicator values have been obtained for the bioethanol production from maize, potato, and rye and the lowest figures are associated with whey and sugarcane. Only for the two latter materials, the results obtained are close to, or better than, those determined for gasoline. Slightly higher values of the energy-related GHG emission indicator have been found for the bioethanol preparation from wood and grass, although the biomass sources used at the fuel production technologies under consideration were mixed and significantly diversified, as they included energy plantations, forests, meadows of various types (natural and intensively fertilised) and, to a smaller extent, wastes. If exclusively the use of waste biomass were taken into account, the GHG emission at the feedstock acquisition stage could be fully eliminated.

Figs. 4 and 5 show a comparison between results of the environmental impact assessment of the process of preparation of bioethanol fuels and gasoline, determined with the use of two methods, i.e. the Swiss Ecological Scarcity method and the Eco-indicator 99 method, and presented in the form of eco-factor and eco-indicator values, respectively. Each of the methods, in accordance with its own scale, assigns a specific score corresponding to the environmental loading that results from the preparation of a fuel amount consumed by a vehicle to travel a distance of 1 km. Among the bioethanol fuels, the least harmful environmental impact at the WtT stage is exerted by biofuels of the second generation, obtained from whey, wood, and grass. For the bioethanol obtained from Brazilian sugarcane, a significant environmental risk is posed by the pre-harvest field burning, which translates into higher values of the impact assessment indicators. The biofuel preparation processes of the worst environmental performance are those where potato, maize, or rye is used as the feedstock. The outstandingly high eco-indicator value obtained from the Eco-indicator 99 method for rye is connected with the significant, for European conditions, land use degree; the high score given by the Swiss Ecological Scarcity method to the use of potato as the feedstock stems from soil contamination with fertilisers and pesticides.

The environmental impact assessment characteristics of the fuels under consideration in the eco-factor vs. energy-related GHG emis-

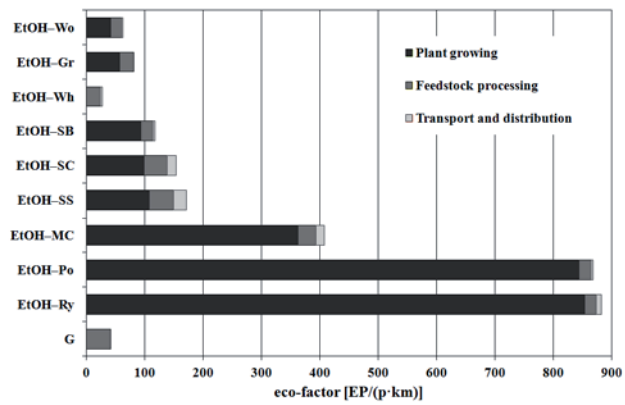


*Fig. 4. Environmental impact assessment of the fuel preparation processes as obtained from the Swiss Ecological Scarcity method*

sion indicator coordinate system have been presented in Fig. 6.

The points corresponding to specific fuels provide information about the emission of greenhouse gases and about the comprehensive environmental impact assessment of the whole fuel preparation (WtT) process carried out to the Swiss Ecological Scarcity method. Bioethanol fuels of the first and second generation and gasoline have

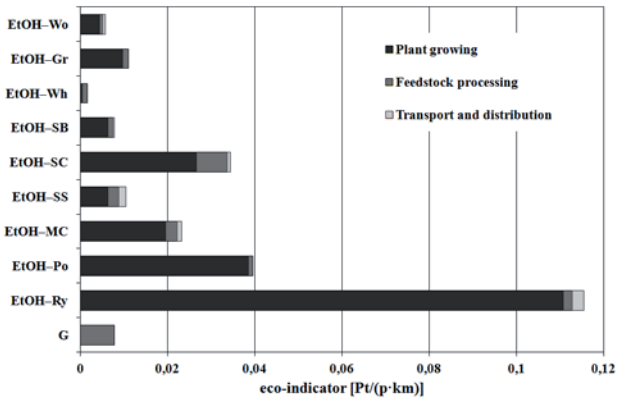


*Fig. 5. Environmental impact assessment of the fuel preparation processes as obtained from the Eco-indicator 99 method*

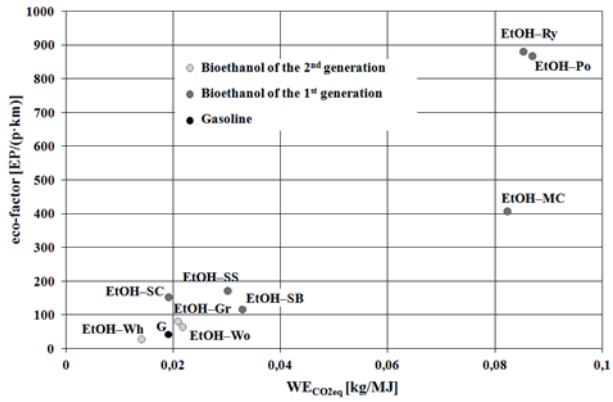


*Fig. 6. Comparison between the energy-related GHG emission indicator and eco-factor values determined for the processes of preparation of the fuels under consideration*

been indicated by green, red, and black colour, respectively. Based on an analysis of the research results, a statement may be made that for most of the bioethanol production options under consideration, the fuel preparation stage produces a higher environmental loading than that observed for gasoline. It should be stressed, however, that gasoline shows very unfavourable environmental properties at the fuel use (TtW) stage, especially a very high emission of fossil carbon dioxide [4 – 7, 19, 20]. As regards the bioethanol fuels, the technologies of making bioethanol of the second generation from whey, wood, and grass have been found to be the least harmful to the environment, in general terms.

## 5. Recapitulation

In connection with the fact that the use of fuels obtained from renewable energy sources becomes increasingly popular, a need arises to assess pollutant emissions and energy inputs in a comprehensive way, with taking into account not only the vehicle operation stage but also the whole fuel preparation process. Among the biofuels used now to power IC engines, bioethanol fuel takes the largest share in the world market [15]. This results from numerous ecological advantages of bioethanol, especially the possibility to reduce the emissions of pollutants harmful both to local populations and global ecosystem and the flexibility of bioethanol production technologies in respect of the raw materials used, such as edible plants with saccharide contents used for the production of biofuels of the first generation and lignocellulose and other wastes for the production of biofuels of the second generation.

Based on the discussion presented here, the following conclusions may be formulated on the comprehensive environmental impact assessment of the process of preparation of bioethanol fuels of the first and second generation:

1. For the assessment of pollutant emissions and energy inputs at the bioethanol preparation stage, the most important factor is the technology employed, especially the type of the biomass used as the feedstock.
2. The process of obtaining bioethanol of the second generation causes significantly lower environmental loading than it is in the case of bioethanol of the first generation. Additionally, zero pollutant emissions at the biomass acquisition stage may be achieved by exclusive use of waste raw materials sourced from e.g. the wood processing or paper industry rather than biomass acquired from the so-called energy plantations.
3. The technology of making biofuels of the second generation must be further developed and optimised towards the achieving of high process efficiency. A top priority task is the development of a method to reduce the costs of production of enzymatic preparations used at the lignocellulose hydrolysis process.
4. Thanks to the use of the Well-to-Wheel method, both qualitative and quantitative environmental impact assessment of the whole conventional life cycle of motor fuels is possible. Nevertheless, the assumptions and limitations imposed by the adopted scope of the analysis must be taken into account for the interpretation of the analysis results to be correct.
5. An important issue is the selection of comprehensive indicators of environmental loading, i.e. the selection of evaluation criteria. While the inventorying of pollutant emissions and energy inputs is based on simple principles of material and energy balancing, the existing life cycle impact assessment (LCIA) models show significant subjectivity.

The discussion presented supports the thesis that the use of bioethanol of the second generation makes it possible to gain clearly visible environmental benefits at the fuel production stage. Undoubtedly, the future of biofuels lies in the technologies of this kind, where waste raw materials and by-products are utilised.

## References

1. Baczewski K, Kałdoński T. Paliwa do silników o zapłonie samoczynnym. Warszawa: WKŁ, 2008.
2. Carlsson H, Fenton P. Bioethanol for sustainable transport: Results and recommendations from the European BEST project. Environment Health Administration, City of Stockholm. Stockholm, 2010.
3. Chłopek Z. Ecological aspects of using bioethanol fuel to power combustion engines. Eksploatacja i Niezawodnosc – Maintenance and Reliability 2007; 3: 65–69.
4. Chłopek Z. Ocena emisji zanieczyszczeń z silników o zapłonie iskrowym zasilanych paliwami: benzyną reformowaną i paliwem bioetanolowym E85. Transport Samochodowy 2009; 2: 61–78.
5. Chłopek Z, Lasocki J. Kompleksowa ocena zagrożenia środowiska przez eksploatację pojazdów samochodowych – Comprehensive evaluation of the environmental hazard caused by the operation of automotive vehicles. Archiwum Motoryzacji – The Archives of Automotive Engineering 2011; 4(54): 19–36, 109–126.

6. Edwards R, Mahieu V, Griesemann J, Larivé J, Rickeard D J. Well–to–Wheels Analysis of Future Automotive Fuels and Powertrains in the European Context. SAE Technical Paper 2004–01–1924.
7. EPA Lifecycle Analysis of greenhouse gas emissions from renewable fuels. U.S. Environmental Protection Agency. Washington DC, 2010.
8. Frischknecht R, Steiner R, Jungbluth N. The Ecological Scarcity Method – Eco–Factors 2006. A method for impact assessment in LCA. Environmental studies no. 0906. Federal Office for the Environment. Bern, 2009.
9. Goedkoop M, Spriensma R. The Eco–indicator 99: A damage oriented method for Life Cycle Impact Assessment. Methodology Report. Pre Consultants BV. Amersfoort, 2001.
10. Hamelinck C N, van Hooijdonk G, Faaij A. Ethanol from lignocellulosic biomass: techno–economic performance in short–, middle– and long–term. Biomass and Bioenergy 2005; 28: 384–410.
11. Jungbluth N, Chudacoff M, Dauriat A, Dinkel F, Doka G, Faist Emmenegger M, Gnansounou E, Kljun N, Schleiss K, Spielmann M, Stettler C, Sutter J. Life Cycle Inventories of Bioenergy. Ecoinvent report No. 17. Swiss Centre for Life Cycle Inventories. Dübendorf, 2007.
12. Kowalski Z, Kulczycka J, Góralczyk M. Ekologiczna ocena cyklu życia procesów wytwórczych (LCA). Warszawa: Wydawnictwo Naukowe PWN, 2007.
13. Luo L, van der Voet E, Huppes G, Udo de Haes H. Allocation issues in LCA methodology: a case study of corn stover–based fuel ethanol. The International Journal of Life Cycle Assessment 2009; 14: 529–539.
14. Marecka–Chłopek E, Chłopek Z. Eksploatacyjne aspekty zastosowania paliw pochodzenia biologicznego do zasilania silników spalinowych. Transport Samochodowy 2007; 4: 59–76.
15. Markevičius A, Katinas V, Perednis E, Tamašauskienė M. Trends and sustainability criteria of the production and use of liquid biofuels. Renewable and Sustainable Energy Reviews 2010; 14: 3226–3231.
16. Pieragostini C, Mussati M C, Aguirre P. On process optimization considering LCA methodology. Journal of Environmental Management 2012; 96: 43–54.
17. Sarkar N, Kumar Ghosh S, Bannerjee S, Aikat K. Bioethanol production from agricultural wastes: An overview. Renewable Energy 2012; 37: 19–27.
18. Szewczyk K W. Technologia biochemiczna. Warszawa: Oficyna Wydawnicza Politechniki Warszawskiej, 2005.
19. Unnasch S. Alcohol Fuels from Biomass: Well–to–Wheel Energy Balance. Proceedings of the 15th International Symposium on Alcohol Fuels (ISAF). San Diego, 2005.
20. Zah R et al. Ökobilanz von Energieprodukten: Ökologische Bewertung von Biotreibstoffen. EMPA. St. Gallen, 2007.

**Zdzisław CHŁOPEK, Ph.D. (Eng.), Assoc. Prof.**
Institute of Vehicles,
The Warsaw University of Technology
ul. Narbutta 84, 02-524 Warszawa, Poland
E-mail: zchlopek@simr.pw.edu.pl

**Jakub LASOCKI, M.Sc. (Eng.)**
Environmental Protection and Natural Energy Use Department,
Automotive Industry Institute
ul. Jagiellońska 55, 03-301 Warszawa, Poland
E-mail: j.lasocki@pimot.org.pl

Article citation info:
MARKOWSKI T, MUCHA J, WITKOWSKI W. FEM analysis of clinching joint machine's C-frame rigidity. Eksploatacja i Niezawodnosc – Maintenance and Reliability 2013; 15 (1): 51–57.

Tadeusz MARKOWSKI
Jacek MUCHA
Waldemar WITKOWSKI

# FEM ANALYSIS OF CLINCHING JOINT MACHINE'S C-FRAME RIGIDITY

# ANALIZA MES SZTYWNOŚCI C-RAMY URZĄDZENIA DO WYTWARZANIA POŁĄCZEŃ PRZETŁOCZENIOWYCH*

*This paper presents the results of FEM analysis for clinching joint machine's C-frame. Several versions of frame geometry were accounted for when analyzing the straining of material, including the mass reduction. The purpose of this FEM simulation was to determine the effect of mass reducing material recess on the structure rigidity. ABAQUS software was used to analyze the frame material straining from both the qualitative and quantitative point of view.*

***Keywords**: C-frame deflection, FEM modeling, clinching joints.*

*W artykule przedstawiono wyniki symulacji MES C-kształtnej ramy urządzenia do montażu połączeń konstrukcji blaszanych. Podczas analizy wytężenia materiału ramy wzięto pod uwagę kilka wariantów wykonania jej geometrii, uwzględniając zmniejszenie masy. Celem symulacji MES było wykazanie wpływu postaci wybrań materiału zmniejszających jej masę na sztywność takiej konstrukcji. Do tak postawionego zadania użyto programu ABAQUS umożliwiającego ilościową i jakościową ocenę wytężenia materiału ramy.*

***Słowa kluczowe**: ugięcie C-ramy, modelowanie MES, połączenia przetłoczeniowe.*

## 1. Introduction

Robot equipped assembly stations are extensively used in the industry branches. These stations are used especially in the automotive industry, where fully automated car body assembly lines equipped available (Fig. 1); these stations are equipped with industry robots and clinching joint machines with or without native material [8, 9, 12].

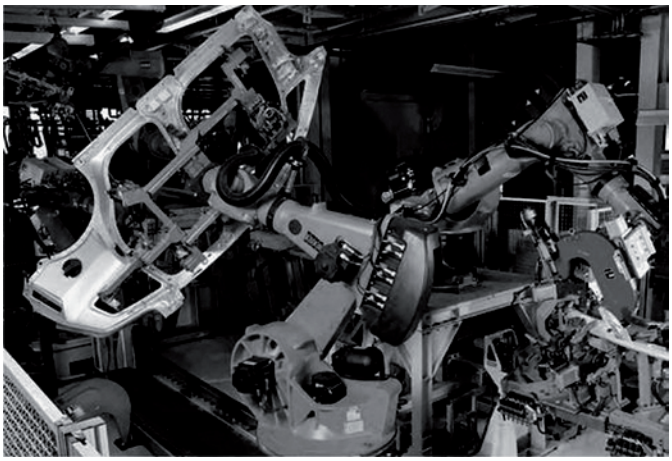

*Fig. 1. Automated lateral assembly station for car body element*

Joining car body elements is a fully automated process using the industry robot working with high speeds. This high speed work is related with high loads due to a robot path dynamics.

When designing the robot's manipulator movements, energy minimum and time loads are sometimes considered as a target functions to perform these movements at given design and dynamic limitations. The relation between forces affecting the system and the inertia forces is presented below in the matrix form:

$$H(q)\ddot{q} + h(q,\dot{q}) = P \tag{1}$$

where:

$H(q)$ – the inertia matrix of an industry robot's manipulator (IRM),

$h(q,\dot{q})$ – matrix of Coriolis centrifugal force and gravity of IRM,

$P$ – vector of generalized moments applied to IRM items [6].

It is reasonable to find a way to reduce unwanted IRM loads. One of possible solutions is to reduce the C-frame mass relatively while preserving its allowed deflection when joining sheet metal pieces.

The devices used both in mobile industry robots and fixed workstations can be equipped with C-frames (Fig. 2). When producing thick joints of sheet metals, the C-frames are replaced with heavy bodies, which due to their mass are used in fixed assembly stations.

Both mobile and fixed solutions can be driven by electric servomotors, pneumatic-hydraulic drives and controlled hydraulic cylinders. The electric servomotors offer the best capabilities of precise control. These drives are available as compact and modular devices of limited own mass. These constructions supplement existing and developing conventional press drives. They are used in highly demanding plastic working industry branches [14,15].

In the plastic working processes it is very important to achieve the adequate rigidity of a forming tool and the ma-

(*) Tekst artykułu w polskiej wersji językowej dostępny w elektronicznym wydaniu kwartalnika na stronie ***www.ein.org.pl***

chine body, e.g. the press frame. When these requirements are fulfilled, the produced item form repeatability os preserved [1, 2, 7].

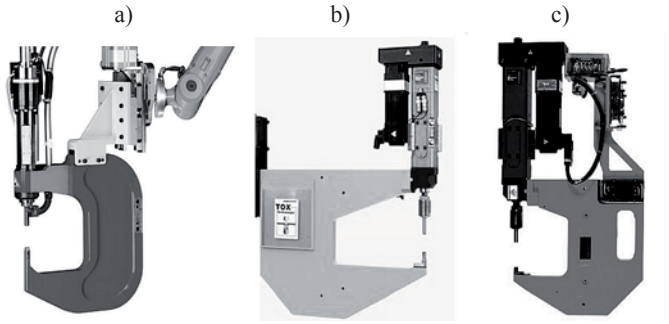


*Fig. 2. C-frames used in the industry robot manipulators: a), b) closed design, b) with opening*

The purpose of this paper is to present the strength analysis of effect of selected geometry versions of C-frame in the industry robot manipulator producing the thin-walled structures with clinching joints.

The calculations were performed for various frame geometry models at assumed identical maximum joining force and material type. The strength analysis was performed with the finite element method (FEM).

## 2. The frame deflection effect on tool positioning when forming the joint

The most developed sheet joining methods by local cold pressing include:

- local material restamping using round tools, and
- bonding the sheet metal layers by restamping with local notch [3,12].

For round clinching joints, the identical joint strength is achieved in each radial load direction. The rectangle clinching joints with notch have an irregular form and the joint behaves differently when changing the load direction [10].

From the point of view of the forming tools mating in the plastic working process, preserving the adequate machine body rigidity with its possibly low mass is critical [4].

Small rigidity of support C-frame results in an increased tool axis deviation and low repeatability, i.e. the joint round in its all radial directions.

The tool face deviation due to the force F by angle $\phi$ in relation to center c results in frame deflection by f (Fig. 3a). The axes of mating tools mounted in the frame are then deviated by angle $\gamma$. Due to the C-frame deflection, the base surface position to set the die is deviated, and this in turn changes parameter X value by $\Delta x$. The X displacement component affects achieving the clinching joint's bottom of a specified thickness X. The X value of a joint is a measured process parameter, which affects corresponding lock forming in materials being joined [11]. This is critical when joining thin sheet metals, as the joint walls may become drastically thin (Fig. 3b) [13].

For automated workstations, the diagnostic system monitors the machine status, and thus the joining process. Possible deviations from the starting values (standard ones determined in a specified test) in e.g. forming force are indicated on the operator panel (Fig. 4). Sudden change of its value may indicate the friction or fatigue wear of tool.

## 3. The assumptions of FEM analysis geometry models

When analyzing the rigidity of various frame geometry models we decided to use only fixed external dimensions and variables including mass reduction by implementing internal recesses. The full

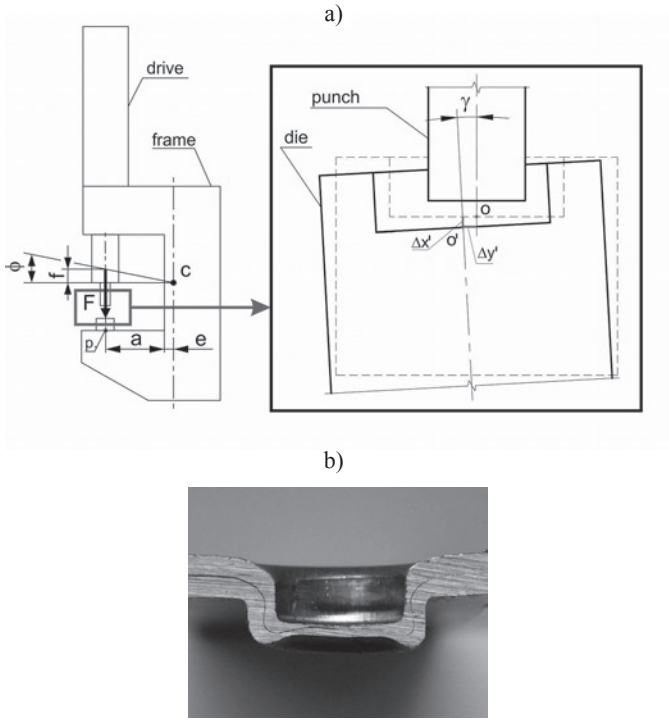


*Fig. 3. The effect of frame deflection on positioning and coaxiality of punch-die: a) graphical description, b) joint asymmetry*

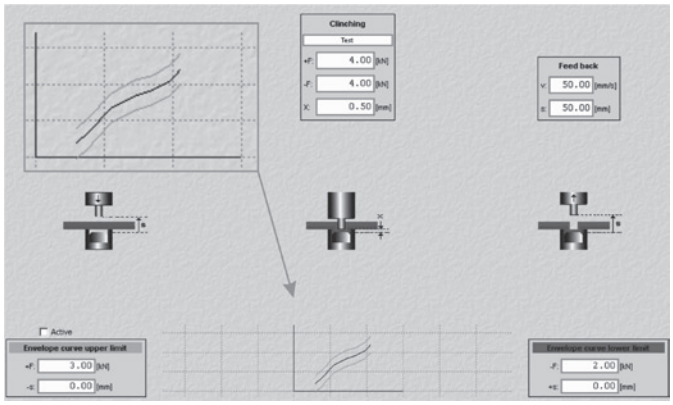


*Fig. 4. Example screenshot of servomotor control software's UI dialog box to set parameter X of joint forming*

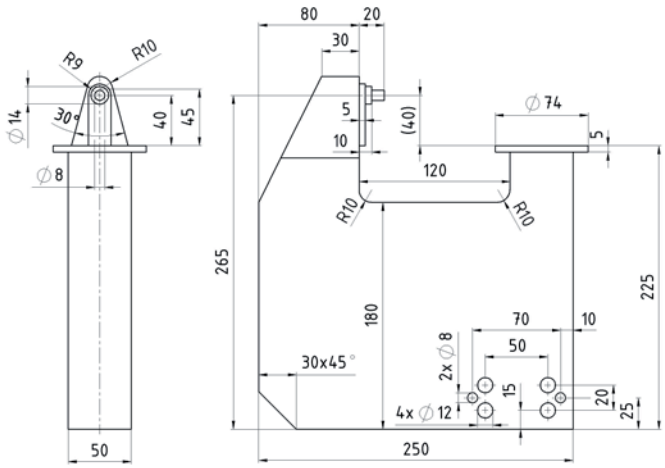


*Fig. 5. Geometry of an uniform frame — model I*

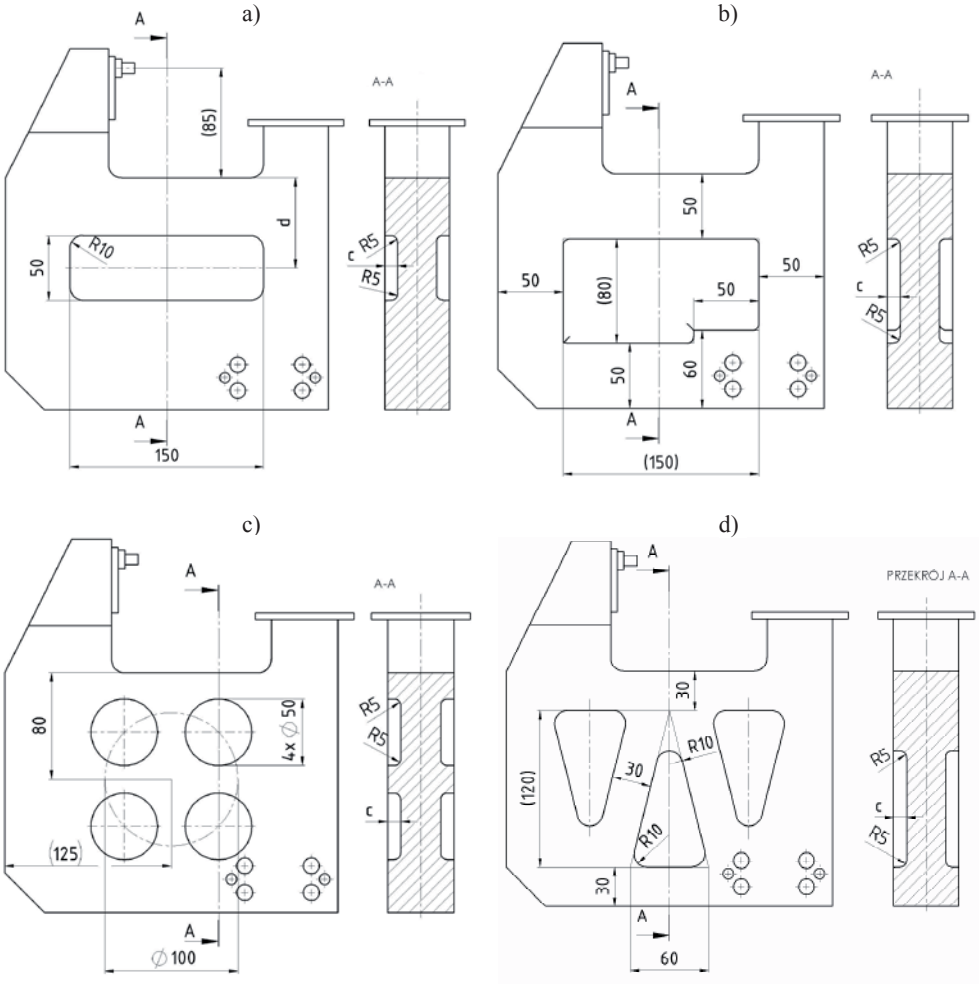


*Fig. 6. Geometry of modified frame — models II — VII*

*Table 1. Opening depth in a modified frame*

| Variable parameter | C-frame model version | | | | | | |
|---|---|---|---|---|---|---|---|
| | **M-I** | **M-II** | **M-III** | **M-IV** | **M-V** | **M-VI** | **M-VII** |
| | Fig. 5 | Fig. 6a | | Fig. 6b | | Fig. 6c | Fig. 6d |
| Recess depth **c** [mm] | 0 | 25 | 10* | 25 | 10 | 25 | 25 |
| * Base distance ***d*** for model **M-III** is 50, remaining values are 60, 70, 80, 90, 100 [mm] | | | | | | | |

*Table 2. Frame deflection values for various C-frame models*

| Axis deflection x $10^{-3}$ [μm] | C-frame model version | | | | | | |
|---|---|---|---|---|---|---|---|
| | **M-I** | **M-II** | **M-III** | **M-IV** | **M-V** | **M-VI** | **M-VII** |
| $\lvert\Delta \mathbf{x}\rvert$ | 435 | 662 | 449 | 604 | 447 | 486 | 515 |
| $\lvert\Delta \mathbf{y}\rvert$ | 193 | 214 | 186 | 227 | 185 | 192 | 232 |

frame was a base model (M-I; Fig. 5), for which remaining six were created (Fig. 6). The analysis of opening position effect was additionally performed for model M-III (Fig. 6a and Table 1).

When analyzing the opening position effect on frame deflection, its distance *d* was assumed in range 50 to 100 with 10 mm pitch (Fig. 6a and Table 1). In all models, the external dimensions and thickness were identical, and only the opening geometry in the frame was changed.

Performing the FEM analysis for C-frame loaded with force F allowed us to check how much the change of opening geometry increased the frame deflection. This will allow to perform the opening placement optimization task in the future. The geometry of full frame was taken from the product catalog of the C-frame manufacturer.

## 4. Modeling the frame load in ABAQUS software

Due to a simple structure, all geometrical models were created directly in MES Abaqus 6.10.1 software and digitized. The base model of full frame included the finite element mesh of 81,000 10-node tetragonal elements; the elements were designated in the program library as C3D10.

The boundary conditions and the external load (as a maximum joining force *F* on C-frame of these dimensions) were defined in the coordinate system of the model (*x y z*; Fig. 7a). The opening were skipped on the drive mounting flange, and the node displacement limitation on its surface in all directions and rotation limitation in relation to x, y, z axis of the system was assumed. The force *F* was 50 kN, modulus of elasticity for steel was $E = 2.1\text{x}10^5$ MPa, and the Poisson's coefficient was $\nu$=0.3. The solid model with force application points, the model anchorage points and the mesh generated for this model were presented on Fig. 7a and 7b.

The distribution of stress contour lines reduced based on H-M-H hypothesis and material displacement was observed for specified load force *F* of the C-frame. The analysis was performed as a static one.

The effect of material on the recess geometry on the distribution of stress contour lines reduced based on H-M-H hypothesis including stress concentrators was observed during the straining analysis of the C-frame. The deflection values and the mass change due to machine body material recess geometry was read. The deflection measurement was performed in the C-frame node, on the base surface for die positioning and mounting (Fig. 3a).

Different deflection values (Table 2) were achieved for individual model versions and such a selected measurement point. The example of frame deformation with rectangle through opening at the zoom in factor of 50 was presented on Fig. 8.

When forming the clinching joint, the C-frame absorbs the elastic strain energy $W_d$, thus achieving the potential energy of eclectically strained body:

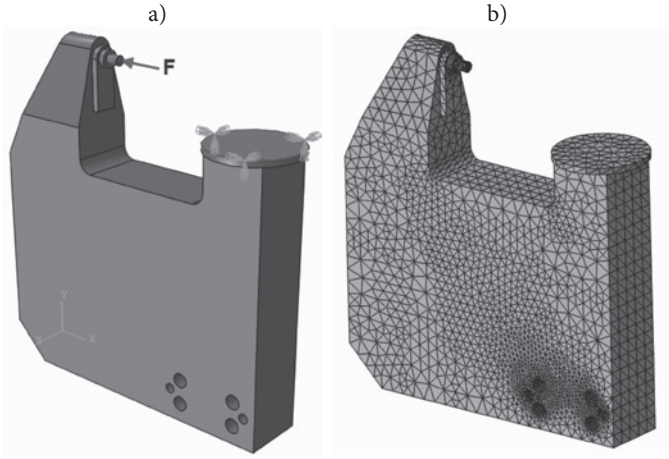


*Fig. 7. C-frame, base model view: a) solid model with boundary conditions and external load, and b) discreet model with finite element mesh*

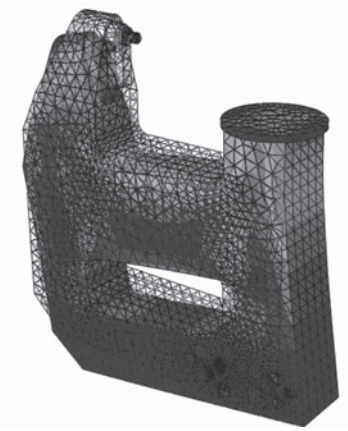

*Fig. 8. C-frame deformation after maximum forming force load (clinching joint) and its model under load condition (zoom in factor of 50).*

$$W_d = \frac{1}{2}\frac{F \cdot f}{10^3}[J] \tag{2}$$

Where:

$W_d$ – the potential energy of elastically strained frame [Nm],
$F$ – pressure force [N],
$f$ – frame deflection [mm].

The frame rigidity $C$ (the strain resistance) is a quotient of force $F$ and deflection $\Delta x = f$:

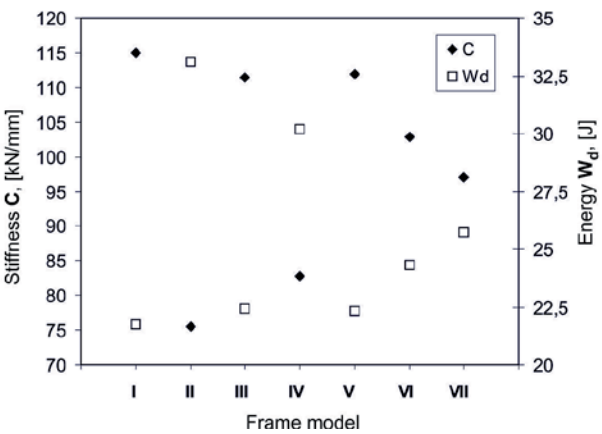


*Fig. 9. The relations between frame rigidity and elastic deflection energy*

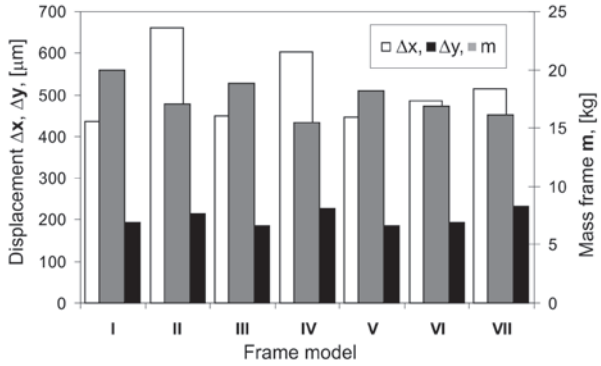


*Fig. 10. Mass and displacement changes in the measurement point of frame loaded with force 50 kN*

$$C = \frac{F}{\Delta x}, \left[\frac{kN}{mm}\right] \tag{3}$$

The relations between the rigidity and the frame elastic strain energy (for all models) were presented in Fig. 9. The lower the rigidity (value $C$), the more the frame absorbs the forming force energy $F$.

The frame had the highest mass, and thus the highest structure rigidity, and this in turn resulted in the smallest material displacement under load force of 50 kN (Fig. 10 and 11a). The highest mass reduction by 22.5% in relation to a solid frame was achieved for model M-IV. Such a form of frame material recesses (openings) resulted in increasing the frame deflection in $x$ and $y$ direction of the $xyz$ system.

As mentioned earlier, modern control systems enable frame deflection compensation in x axis direction with ±0.01mm accuracy, while it is almost impossible to compensate the deflection component in y direction. The smallest unwanted deflection in y direction was achieved for a frame with recess (model M-V), and the highest for

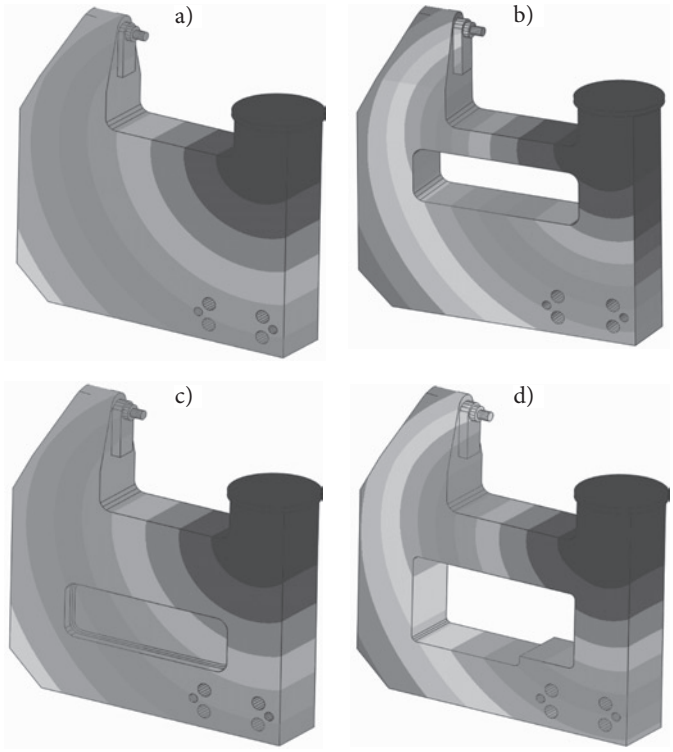


*Fig. 11a – d. The distribution of resulting displacement of C-frame for various material recess geometry (models M-I÷M-VII; $U_y$, mm)*

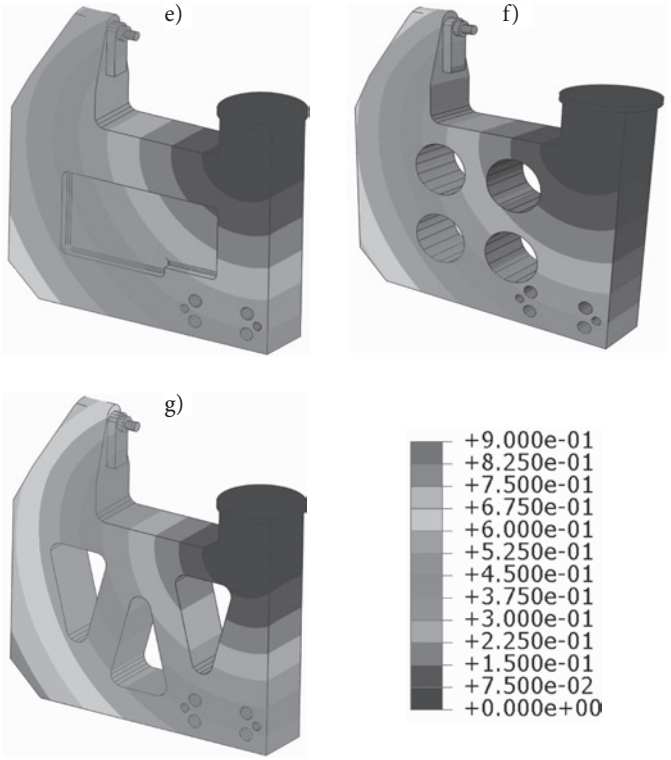


*Fig. 11e – g. The distribution of resulting displacement of C-frame for various material recess geometry (models M-I÷M-VII; $U_W$, mm)*

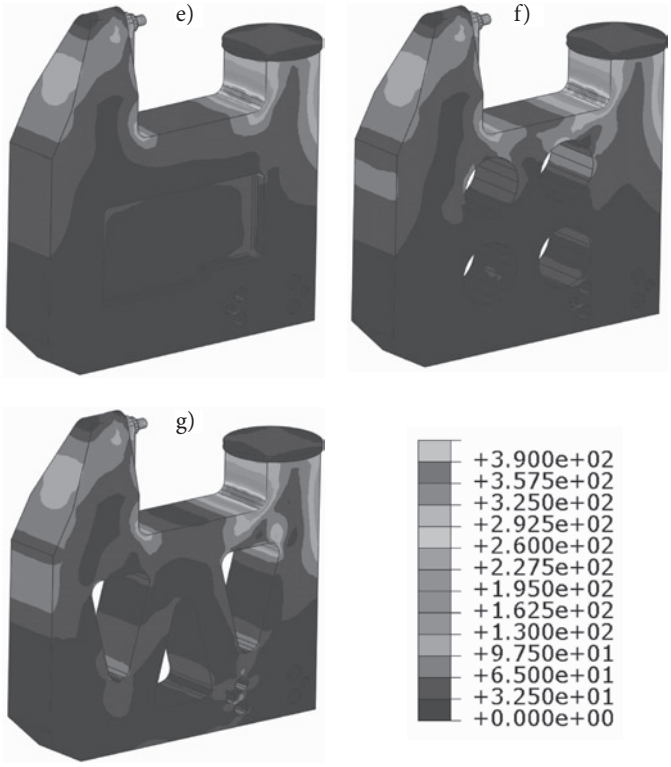


*Fig. 12e – g. The distribution of C-frame stress reduced based on H-H-H for various material recess geometry (models M-I÷M-VII; $\sigma_z$, MPa)*

model M-VII (Fig. 10), which included the discontinuity in form of triangle openings. The highest value of resulting displacements was observed for model M-II (Fig. 11b).

For all C-frame models, the highest material straining was located on the internal surface of wall arm radial transition into the remaining part of the body. The strain concentration was lower on internal surfaces of openings (Fig. 12b, d, f, g).

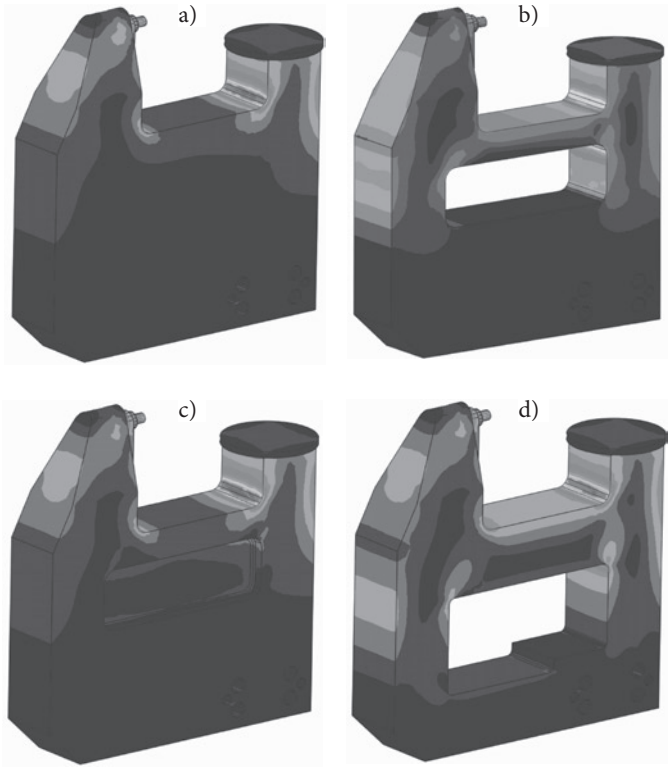


*Fig. 12a – d. The distribution of C-frame stress reduced based on H-H-H for various material recess geometry (models M-I÷M-VII; $\sigma_z$, MPa)*

The highest stress was observed in the location of the highest deflectioning load acting the geometrical stress concentrator area in model M-VII (Fig. 13). Therefore, in the future analyses we decided to examine the effect of transition surface radius value (2, Fig. 13) to the stress concentration and value in this area.

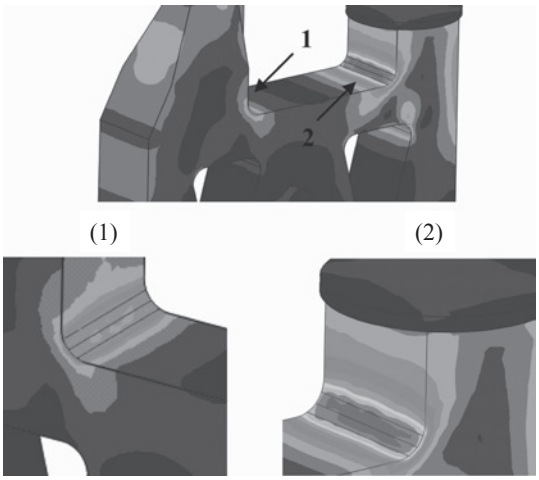


*Fig. 13. The stress concentration on the radial surface transition*

The change of rectangle opening placement distance (model M-II) significantly affects the behavior of loaded frame. The lowest displacement of the measurement point both in x and y axis of the FEM model coordinate system was achieved for d=100mm from the internal surface of the frame (Fig. 14). The lowest displacement in y axis direction was observed for distance d=60 mm (with d pitch of 10 mm).

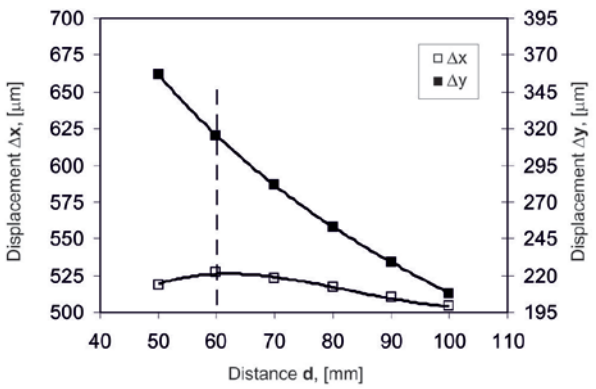


*Fig. 14. The displacement in the measurement point of model M-II with various placement of opening*

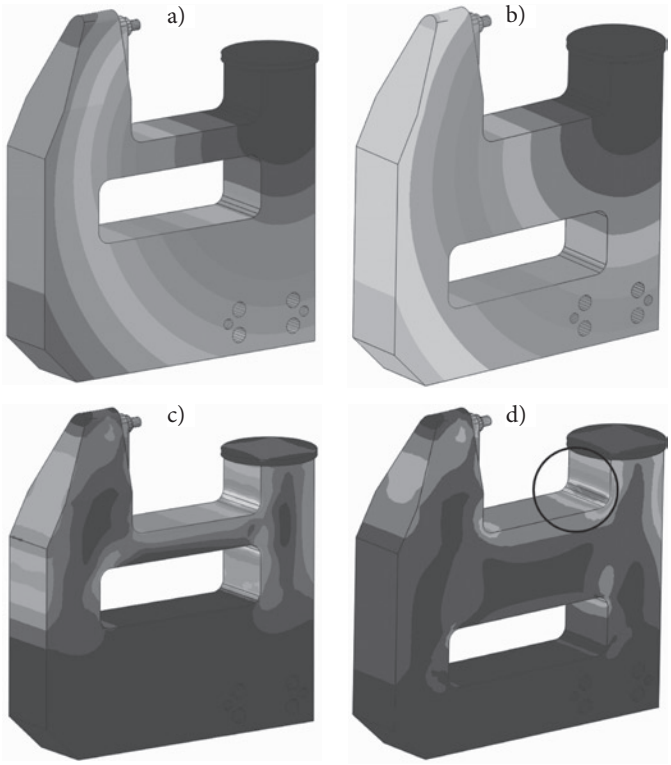


*Fig. 15. The effect of opening placement on resulting displacement of frame material (a) and (b) and the distribution of reduced stress contour lines (c) and (d)*

The displacement of opening from the C-frame arm base surface by 50mm increased its rigidity, thus increasing stress in the internal corner (the area indicated on Fig. 15d). At the lowest opening distance from this surface (d=50mm) such a created "beam" decreased the stress level in the corner, balancing the frame material stress in this area (Fig. 15c). Thus the base part of the die was deflectioned more (Fig. 15a).

The lowest deflection was observed in the version of C-frame with the opening distant the most from the loading force axis. When forming the joint, the machine body (C-frame) is loaded due to the joint forming. The machine body (including machine tools) state of stress is affected by several factors, and the most important are process forces and inertia forces [16]. Knowing these forces allows to estimate the strength of individual assemblies. The static rigidity of machine bodies is one the most important features affecting the dimension and form accuracy of work pieces [1, 2, 5, 17, 18].

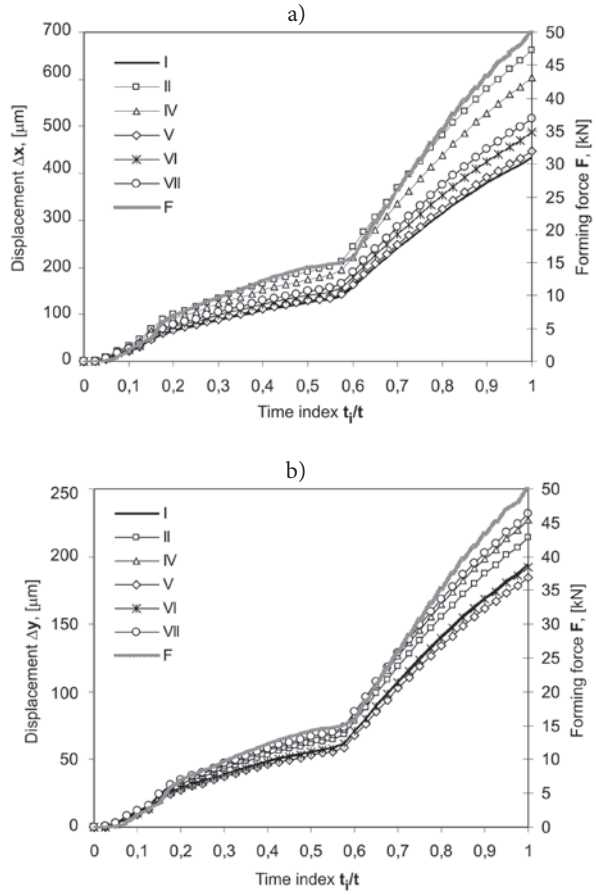


*Fig. 16. Material displacement values in the measurement point for variable straining force of C-frame (model M-I÷M-VII): a) Δx, b) Δy*

The effect of loading force history on deflection curve was also examined during the frame rigidity FEM analysis. For actual joining force curve (restamping steel sheets, thickness 1mm) the analysis of C-frame material displacement in the measurement point *p* was performed (Fig. 3a). The response characteristics for such a load was presented on Fig. 16a for Δx and Fi.g 16b for Δy respectively. The curves for model M-III were skipped due to very small slam differences in relation to results achieved for model M-V. For model M-V, the difference between resulting curves of x and y axis displacement for this model and for solid frame was the smallest.

In all frame models, the highest deflection was observed in the final clinching joint forming phase (Fig. 16). When accounting for identical joint forming conditions, the frame used for joint forming should be very rigid, i.e. its deflection characteristics should have the lowest displacement increase.

The final clinching joint forming phase conditions are close to the hydrostatic compression, resulting in a rapid force increase, which easily translates to the C-frame straining.

## 5. Summary

The "ready to use" C-frame of the clinching joint machine account for an applied load and features the arms of specific structure, enabling easy extension and retraction to and from the joint area. Preserving the adequate tool support rigidity while having relatively low frame mass is critical. The accuracy of tool positioning in the C-frame and frame deflection affect the tool's cutting edge or its coaxiality error. The designed frame can have opening to reduce its mass, but these openings must be of right dimensions, shale and placement.

The forming force curve presents the variable frame load during this process. When designing the body, the most important is to achieve possibly low mass while preserving the highest rigidity.

The conclusions of FEM analysis for displacement of measurement point loaded with force 50 kN are as follows:

– the placement of rectangle frame opening in relation to loading force direction affects the frame rigidity;
– preparing openings (recesses) on all material surface (model M-V) on two sides of frame results in the lowest displacement increase and relatively high mass reduction;
– the highest mass reduction while preserving the deflection change value in a direction lateral to force direction was achieved for model with four openings (model M-VI).

## References


1. Brecher C, Esser M, Witt S. Interaction of manufacturing process and machine tool. CIRP Annals - Manufacturing Technology 2009; 58: 588–607.
2. Chodnikiewicz K, Balendra R. The calibration of metal-forming presses. Journal of Materials Processing Technology 2000; 106: 28–33.
3. Di Lorenzo G, Landolfo R. Shear experimental response of new connecting systems for cold-formed structures. Journal of Constructional Steel Research 2004; 3–5: 561–579.
4. Dobrucki W. Podstawy konstrukcji i eksploatacji walcarki. Wydawnictwo Śląsk, 1981.
5. Kosmol J, Wilk P. Próba optymalizacji korpusu obrabiarki z zastosowaniem MES i algorytmu genetycznego. Modelowanie Inżynierskie 2008; 35: 59–66.
6. Kyrylovich V, Bogdanowski M. Zagadnienia zautomatyzowanego planowania ruchów robotów przemysłowych w elastycznych systemach montażowych. Technologia i Automatyzacja Montażu 2009; 1: 18–22.
7. Li YB, Wu DH, Huang MH, Lu XJ. Design of Parallel Bearing Structure for 800MN Forging Press with Consideration of Manufacturing Errors. Applied Mechanics and Materials 2011; 52–54: 2157–2163.
8. Mucha J. Rozwój technik wytwarzania złączy nitowych–nitowanie bezotworowe. Mechanik 2007; 5–6: 454–460.
9. Mucha J. Współczesne techniki łączenia cienkich blach-zaciskanie przez wytłaczanie (Clinching). Mechanik 2007; 11: 932–939.
10. Mucha J. The analysis of rectangular clinching joint in the shearing test. Eksploatacja i Niezawodnosc – Maintenance and Reliability 2011; 3: 45–50.
11. Mucha J, Bartczak B. Analiza procesu łączenia przetłoczeniowego blach. Archiwum Technologii Maszyn i Automatyzacji 2011; 3: 59–68.
12. Mucha J, Kaščák Ľ. Wybrane aspekty kształtowania okrągłych połączeń przetłoczeniowych. Problemy eksploatacji-Maintenance Problems 2010; 4: 29–38.
13. Mucha J, Witkowski W. Możliwości łączenia przetłaczaniem blachy stalowej o grubości poniżej 1 mm. Technologia i Automatyzacja Montażu 2012; 1: 46–49.
14. Plewiński A. Kierunki rozwoju maszyn do obróbki plastycznej. Obróbka Plastyczna Metali 2005; 4: 21–28.
15. Schenke C-C, Wiemer H, Großmann K. Analysis of servo-mechanic drive concepts for forming presses. Production Engineering. Research and Development DOI 10.1007/s11740-012-0391-9.
16. Staniek R, Zielnica J, Gessner A. Wpływ parametrów konstrukcyjnych na stan naprężeń i przemieszczeń w korpusie obrabiarki. Archiwum Technologii Maszyn i Automatyzacji 2010; 4: 159–168.
17. Wang ZX, Yu XL. Stiffness of the overall study for forging hydraulic press. Forging Technology 1990; 1: 1–2.
18. Zhou YD, Chu L, Bi DS. Structural optimization for hydraulic press frame. China Metalforming Equipment & Manufacturing Technology 2008; 2: 90–92.



**Prof. Tadeusz MARKOWSKI, Ph.D. (Eng.)**
**Jacek MUCHA, Ph.D. (Eng.)**
**Waldemar WITKOWSKI, M.Sc. (Eng.)**
Department of Mechanical Engineering
Rzeszow University of Technology
Al. Powstańców Warszawy 8, 35-959 Rzeszów, Poland
E-mails: tmarkow@prz.edu.pl, j_mucha@prz.edu.pl, wwitkowski@prz.edu.pl

Article citation info:
TOR-ŚWIĄTEK A, SAMUJŁO B. Use of thermo vision research to analyze the thermal stability of microcellular extrusion process of poly(vinyl chloride). Eksploatacja i Niezawodnosc – Maintenance and Reliability 2013; 15 (1): 58–61.

Aneta TOR-ŚWIĄTEK
Bronisław SAMUJŁO

# USE OF THERMO VISION RESEARCH TO ANALYZE THE THERMAL STABILITY OF MICROCELLULAR EXTRUSION PROCESS OF POLY(VINYL CHLORIDE)

# WYKORZYSTANIE BADAŃ TERMOWIZYJNYCH DO ANALIZY STABILNOŚCI PROCESU WYTŁACZANIA MIKROPORUJĄCEGO POLI(CHLORKU WINYLU)*

*Essential role in polymer processing takes processing conditions i.e. temperature, pressure, screw rotational speed and time. During the polymer modification in cellular and microcellular extrusion process significant changes in the process ensue. Influence of this two factors caused also another changes in properties and physical structure of obtained extruded products. Because of that, proper selection of processing conditions, specially temperature, machines and equipment parameters is necessary. Is such a case, process will be effective and stable.*

***Keywords**: Microcellular extrusion process, blowing agent, microspheres, polymer materials, thermovision.*

*Znaczącą rolę w procesach przetwórstwa tworzyw odgrywają warunki procesu takie jak temperatura, ciśnienie, szybkość obrotowa ślimaka, czas. Podczas modyfikacji tworzywa polimerowego w procesie wytłaczania porującego oraz mikroporującego na skutek działania podwyższonej temperatury oraz jednocześnie działania poroforu następują istotne zmiany w przebiegu procesu wytłaczania. Kolejną zmianą, jaką niesie za sobą wpływ obu czynników jest zmiana właściwości oraz struktury fizycznej otrzymanych wytworów. Z tego względu konieczny staje się taki dobór poszczególnych warunków przetwórstwa, w tym szczególnie temperatury oraz parametrów maszyn i urządzeń przetwórczych, aby proces mógł być prowadzony efektywnie i stabilnie.*

***Słowa kluczowe**: Wytłaczanie mikroporujące, środek mikroporujący, mikrosfery, tworzywo polimerowe, termowizja.*

## 1. Introduction

The course of each of the processes of polymer processing, both thermoplastic and thermosets depends on several factors, including selection of appropriate processing methods. Each method is characterized by significant conditions that must be satisfied that the process could not only exist, but above all to be effective, stable and efficient [6, 7, 13, 15]. Among the popular methods of processing such as injection molding, conventional extrusion or extrusion coating noteworthy is microcellular extrusion process [2, 12, 16]. It allows to receive the products of the altered physical mechanical and utility properties with different physical structure. Items that have been modified polymer material by means microcellular blowing agents characterized by a greatly reduced density, stiffness and hardness. Also exhibit less processing shrinkage and good damping properties. This creates new fields of applications of polymers, wherever it is important to weight, flexibility and hardness of the products [3].

Modification of the extrusion process, caused by microporosity of polymer material, takes place at the end of the extruder plasticizing system and must be carried out in order to use microcellular agent (blowing agent) spread in the right place [9]. The satisfactory operation of the process of microcellular extrusion processing ensure proper selection of polymeric material and blowing agent, processing conditions and the design of individual processing machines and tools placed at the production line [1].

Microcellular extrusion depends on inserting microcellular blowing agent into the material being processed under appropriate distributed processing conditions, changing the structure of materials into microporous. It is possible to obtain microporous products of the entire cross-section or having a solid outer layer and a microporous core of extrudate. This involves using a suitably embossed intensive cooling element, preventing the initiation process in the surface layer [2, 4].

The microporous structure of the extrudate obtained by the microcellular extrusion process primarily affected by such factors as the quantity dispensed and the temperature of the blowing agent in the subsequent processing zones of the extruder plasticizing and extrusion head. The values of these factors should be coordinated, and controlled the conduct of the process to obtain a uniform structure throughout the cross section of the profile generated. The most important is to establish and stabilize the selected temperature range, so it seems reasonable to thermal imaging of the process by thermal testing [15].

Currently, thermal tests are widely used in various fields of science and life, such as energy, construction, machinery diagnostics, electronics, environmental protection, medicine, marine salvage industry [10, 14]. Infrared, also known as thermography, deals with the detection, recording, processing and visualization of invisible infrared radiation emitted by objects. Obtained by measurements of infrared image (thermometer) is a mapping of temperature distribution on the surface of the observed object. The research intensity of the thermal phenomena are a rich source of information about the technical condition of machines, operation, and of the changes that occur during their operation [8, 9]. Allows to customize the functional characteristics of individual elements of technological line for a particular process and selection of processing conditions such that the process was carried out properly, and the resulting product was characterized by high quality [11, 16].

(*) Tekst artykułu w polskiej wersji językowej dostępny w elektronicznym wydaniu kwartalnika na stronie ***www.ein.org.pl***

## 2. The test stand and conduct of the study

Thermal studies of microcellular extrusion were carried out in extrusion technological line for profiles. The line included: extruder T-32-25, mandrel extruder head with a nozzle diameter of 5 mm, cooling and the receiving units. In the process, was changed the course of the rotational speed of the extruder screw using the 0,75; 1,02; 1,30; 1,57; 1,85 $s^{-1}$ and content of blowing agent in the input polymer material range of 0; 0,5; 1,0; 1,5; 2,0; 2,5 % mass with the reference to the mass of the plastic. Plasticized poly(vinyl chloride) Alfavinyl GFM-31-TR was modified by the means of microcellular blowing agent in the form of microspheres Expancel 930 MB 120 [5]. The temperature of particular plasticizing system zones of extruder was appropriately 100, 110, 120, 130 ºC, temperature of extruder head was 140 ºC and temperature of cooling factor was 17 ºC.

The thermal study of microcellular extrusion process uses infrared camera V-20, ER005-25 model. It allows to remote non-contact recording of the temperature distribution on the surface of the examined objects. The camera is equipped with a photovoltaic detector PDI-2TE-5 with high sensitivity. Image created by a mechanical scan system using mirrors and precision powertrain. Image was created point by point, line by line. With the help of the lens assembly, infrared radiation is focused onto a detector. Voltage generated by the detector is dependent on the radiation power. Through precise control of mirror motion is possible to measure the radiation point by point. Infrared detection system in the camera V-20 is based on a thermoelectrically cooled HgCdTe detector, which allows to perform temperature measurement from -10 to 500 ° C, the temperature resolution NEDT from 0.05 to 5°C, corresponding to the recorded temperature. Scanning angle is 30°, while creating thermogram consists of 57 600 points (240 points in 240 lines), with a line scan time of 7,2 ms. This camera allows the remote measurement, recording and visualization of infrared radiation emitted by machinery, tools, processing equipment and parts made of plastic, corresponding to the temperature of the surface [11, 13].

Stimulus objects during the ongoing process of microcellular extrusion were nozzle of extruder head and the microporous residue leaving the nozzle head. Recorded the infrared radiation emitted by the surface of the examined objects, which after processing has enabled the visualization in the form of thermal images. A detailed analysis of temperature measurement was carried out on the section of extrudate, which includes 29 points. We analyzed the change in temperature during the extrusion process of the selected point on the surface of the nozzle of extruder head and the surface of the extrudate at a distance of 40 mm from the nozzle.

## 3. Results

As a result of measurements of thermal infrared images were obtained (Fig. 1) together with the values of the examined surface temperature and its distribution facilities. Then the images were analyzed using specialized computer program Therm V20 ver. 2.2.2. On the basis of the results of micro-brewing temperature measurements directly after leaving the nozzle of extruder head in different measuring points drawn graphs of the measured temperature dependence of microporous extrudate, containing a microcellular blowing agent in

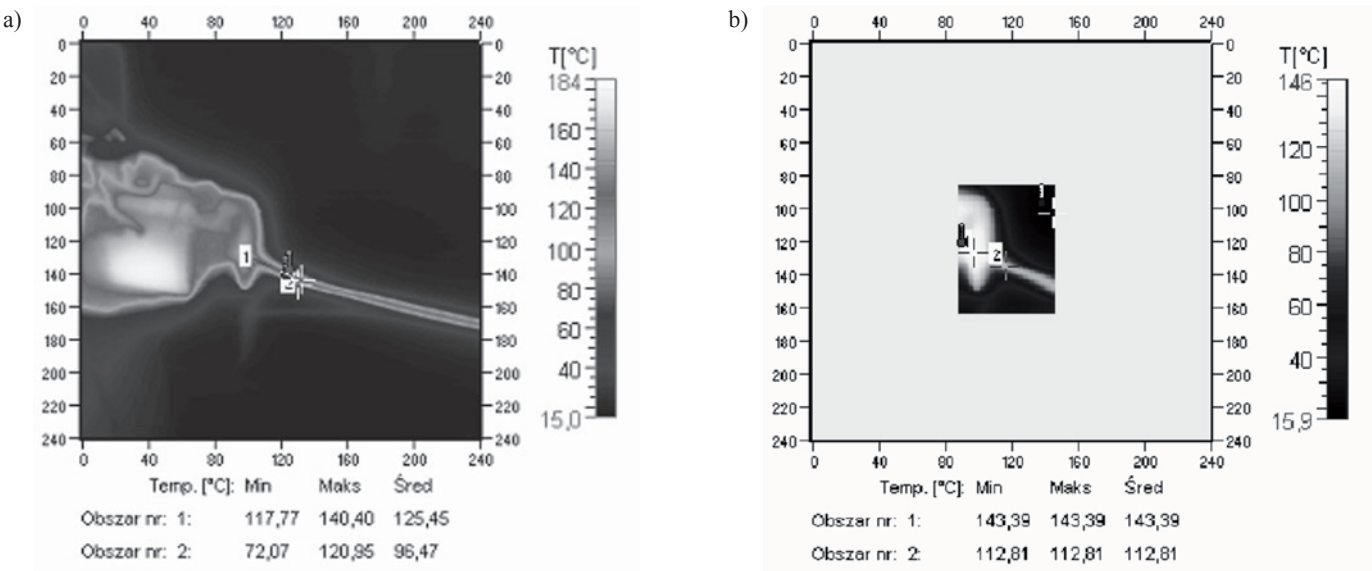


*Fig. 1. Examples of thermal images extrusion head and micro brewing: a) with the selected section of the extrudate surface measurement, b) with the selected measurement points on the surface of the nozzle head, and extrudate.*

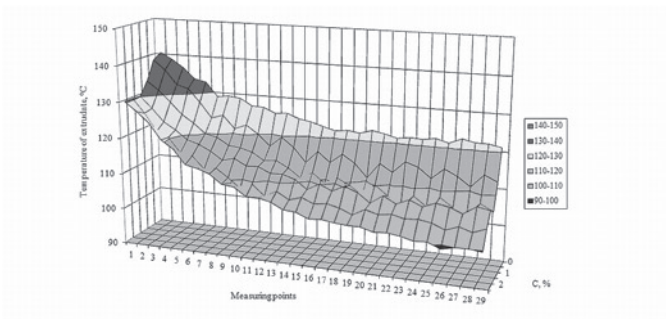


*Fig. 2. Dependence of the extrudate temperature in individual measuring points at a rate of screw rotation $v^1 = 0.75\ s^{-1}$ and the content of microspheres from 0 to 2.5% of the masses.*

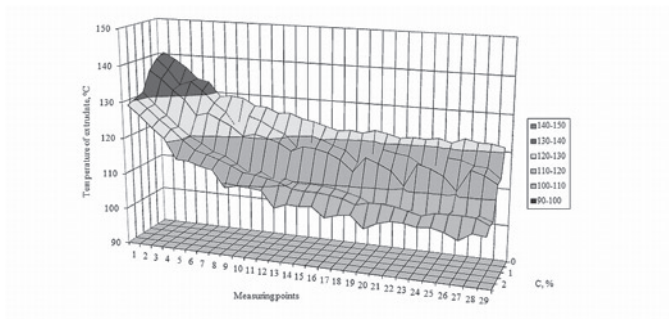


*Fig. 3. Dependence of the extrudate temperature in individual measuring points at a rate of screw rotation $v^2 = 1.02\ s^{-1}$ and the content of microspheres from 0 to 2.5% of the masses.*

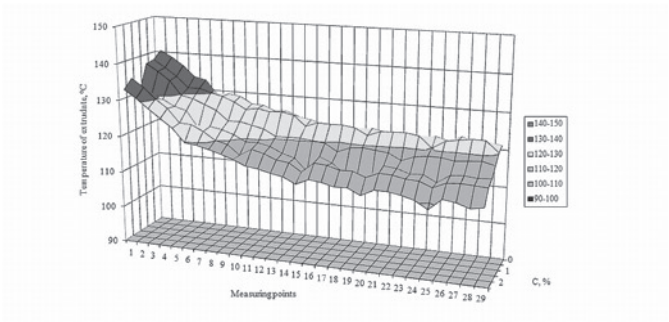


*Fig. 4. Dependence of the extrudate temperature in individual measuring points at a rate of screw rotation $v^3$ = 1.30 $s^{-1}$ and the content of microspheres from 0 to 2.5% of the masses.*

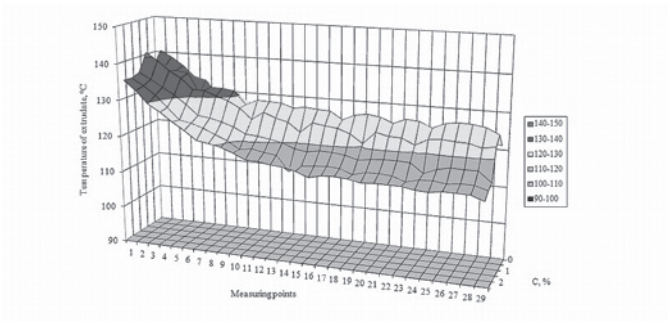


*Fig. 6. Dependence of the extrudate temperature in individual measuring points at a rate of screw rotation $v^5$ = 1.85 $s^{-1}$ and the content of microspheres from 0 to 2.5% of the masses.*

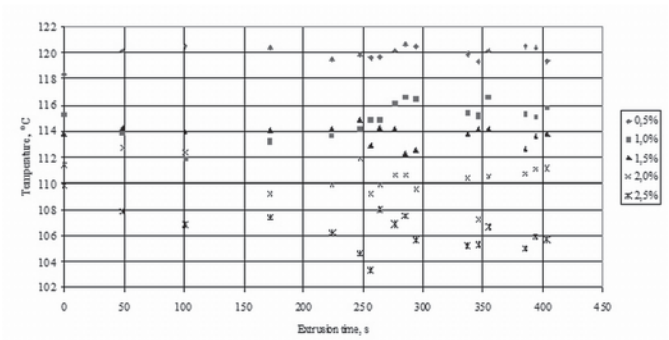


*Fig. 8. Dependence temperature of nozzle head on extrusion time with screw rotational speed $v^3$ = 1.30 $s^{-1}$ and content of microspheres range 0÷2,5% mass.*

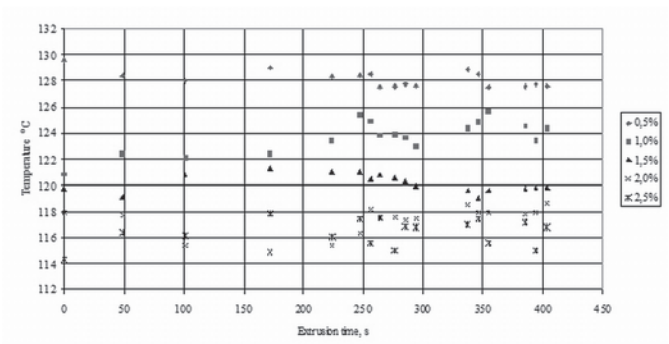


*Fig. 10. Dependence temperature of nozzle head on extrusion time with screw rotational speed $v^5$ = 1.85 $s^{-1}$ and content of microspheres range 0÷2,5% mass.*

the amount of 0 to 2.5% of the masses., changed at different rotational speeds of the screw in the 0.75 ÷ 1.85 $s^{-1}$. The relevant diagrams are shown in Figures 2 to 6.

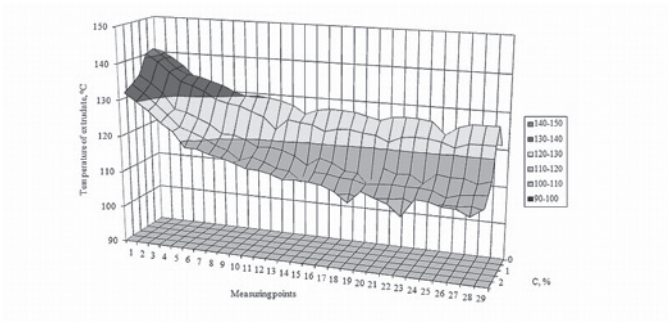


*Fig. 5. Dependence of the extrudate temperature in individual measuring points at a rate of screw rotation $v^4$ = 1.57 $s^{-1}$ and the content of microspheres from 0 to 2.5% of the masses.*

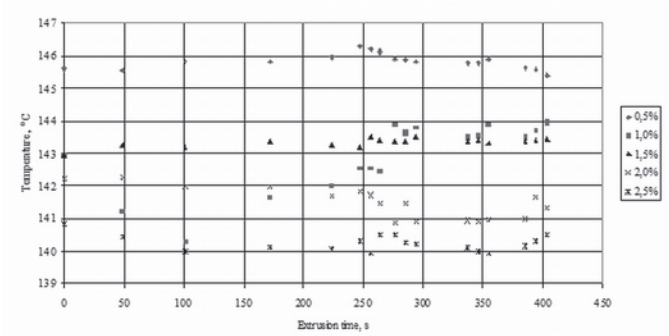


*Fig. 7. Dependence temperature of nozzle head on extrusion time with screw rotational speed $v^1$ = 0.75 $s^{-1}$ and content of microspheres range 0÷2,5% mass.*

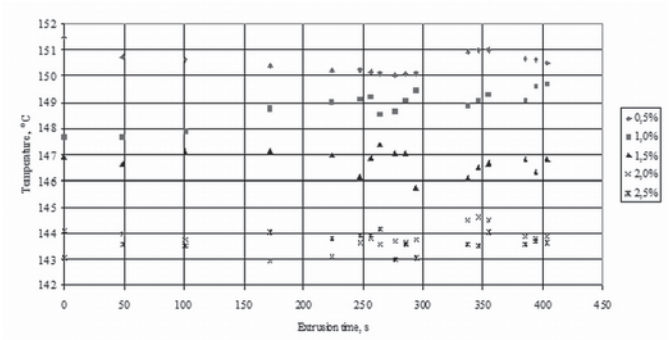


*Fig. 9. Dependence temperature of nozzle head on extrusion time with screw rotational speed $v^4$ = 1.57 $s^{-1}$ and content of microspheres range 0÷2,5% mass.*

Along with increasing the content of the microspheres measure temperature of poly(vinyl chloride) leaving the nozzle of extruder head has decreased, and in that changes the dosage was a decrease of 10.04°C. It can also assume that for the content of microcellular blowing agent of 1.5% masses. temperature of the extrudate was some stabilization at around 120°C, especially at the measuring points 13 ÷ 29$^{th}$. While increasing the screw rotation speed above the value of 1.30 $s^{-1}$ there was a rise in temperature for the microcellular extrudate in the range of content of microspheres with 0.5% and 1% of the mass and its decline for content of microsphere above 1.5%.

In Figures 7 ÷ 10 shows examples of the ranges of temperature changes during the extrusion of poly(vinyl chloride) with different contents of the microspheres on the surface of the nozzle head, and microcellular extrudate with minimum and maximum rotational speed of the extruder screw.

Analysis of temperature changes during the extrusion process the various materials can to some extent, the assessment of thermal stability of the process, and therefore also during the process of maintaining a homogeneous physical structure and properties of micro-extrudate. With the increase of screw rotation speed of 0.75 $s^{-1}$ to 1.30 $s^{-1}$ de-

creases the stability of the process, as evidenced by the increasing spread of the measured values of both the surface temperature of the nozzle extrusion head (from 1.49 to 2.08ºC) as and microporous extrudate (from 4.32 to 5.31ºC) and maximum deviations from the mean. Further increasing the screw rotation speed to 1.85 $s^{-1}$ stabilizes the process from the heat, since these reduce the size of its values corresponding to 1.61ºC and 3.27ºC.

In a similar way to change the maximum surface temperature deviations nozzle of extruder head and microporous extrudate than the average values. At least the screw rotation speed is equal to 0.96ºC for nozzle of extruder head and varies by 1.39ºC to a final value of 1.01ºC. Analogous changes in the surface microporous extrudate and reach higher values are respectively 2.58, 3.38 and 1.43ºC. Along with increasing the content of blowing agent in the plastic temperature stability of nozzle of extruder head increases, the microporous extrudate surface temperature decreases. Increasing the screw rotation speed increases the temperature stability of the microporous extrudate.

## 4. Summary

The research found that the inserting of blowing agent into poly(vinyl chloride) significantly affect the bottom-thermal phenomena in the microcellular extrusion process, especially during the flow in channels and extruder head for cooling the extrudate directly in the head. In the investigated range of content of microspheres measure the temperature drop extrudate leaving the extruder head is about 7%, which is likely to be attributed to endothermal effect accompanying widening of the microspheres during the microcellular process. Also increases the rate of cooling of the resulting extrudate with increasing microcellular blowing agent dosage. Decreasing the temperature difference between micro-extrudate, and the surrounding resort. This can have an impact on further steps in the process now taking place outside the extruder, especially in the calibration and the final cooling of the extrudate, thus in effect on the structure and properties of the resulting microporous creations.

The observed decrease in the microporous extrudate temperature increase the amount of blowing agent dosing may result from the characteristics of the microcellular agent used. Microspheres for the action of high temperature heat charge resulting in their expansion.

Stability of microcellular extrusion of poly(vinyl chloride) in the tested range of changes in the extruder screw rotation speed should be regarded as satisfactory, with the range of temperature-extrudate, forming element – nozzle of extruder head averaged only 1.7ºC with a maximum deviation from the value registered an average of at 3.6ºC. Micro brewing temperature variation during the process of the measured distance reached 4.3ºC.

The maximum difference in the microporous extrudate temperature during the process was just over 8ºC, which already may have a negative impact on the constitution of homogeneous structure and properties of the extrudate. Generally, obtaining a high thermal stability of the process favored the smallest and largest of the tested range, the extruder screw rotation speed, and low levels of blowing agents in the material to 1.5% by mass. In order to achieve high thermal stability of the process is preferred to use the minimum or maximum value of the extruder screw rotation speed and the content of microspheres in amounts up to 1.5% of the masses., the weight of material processed.

## Literature


1. Bieliński M. Techniki porowania tworzyw termoplastycznych. Wydawnictwo Uczelniane Akademii Techniczno-Rolniczej, Bydgoszcz 2004; 10–25.
2. Borkowski J. Spienianie. Praca zbiorowa „Przetwórstwo tworzyw sztucznych". Oficyna Wydawnicza Politechniki Warszawskiej, Warszawa 2000; 147–149.
3. Garbacz T, Tor A. Wpływ zawartości środka porującego na właściwości użytkowe zewnętrznych powłok kabli. Polimery 2007; 4: 286293.
4. Garbacz T, Samujło B. Wybrane właściwości geometrycznej struktury powierzchni wytworów porowatych otrzymanych z polietylenu. Polimery 2008; 6: 471–476.
5. Jonsson L, Rosskothen K.R. Mikrospharen – ein universelles Treibmittel. Kunststoffe – Plast Europe 2003; 7: 86–87.
6. Klepka T. Konstrukcje osiowo-symetrycznych wytworów o kształtach złożonych. Polimery 2008; 5: 48–54.
7. Krzyżak A, Sikora JW. Przetwarzalność tworzyw fenolowych wyznaczana metodą BIP. Polimery 2007; 1: 44–50.
8. Miękina W, Madura H. Podstawy teoretyczne pomiarów termowizyjnych. Praca zabiorowa pod red. H. Madury „Pomiary termowizyjne w praktyce". Agenda Wydawnicza Paku, Warszawa 2004; 10-26.
9. Qiong Zhou, Chuan-Bo Cong. Exo-endothermic blowing agent and its foaming behavior. Journal of Cellular Plastics 2005; 3: 225–234.
10. Różański L, Poloszyk S. Zastosowanie termowizji w diagnostyce maszyn. Praca zabiorowa pod red. H. Madury „Pomiary termowizyjne w praktyce". Agenda Wydawnicza Paku, Warszawa 2004; 75–83.
11. Samujło B.: Selected aspects of thermovision in extrusion process. ICPP-2007, International Conference on Polymer Processing, Beijing, Chiny 2007; 126–128.
12. Stewart R. Extrusion. Plastics Engineering 2005; 5: 18–27.
13. Tor A, Samujło B. Badania termowizyjne procesu wytłaczania mikroporującego poli(chlorku winylu). Przetwórstwo Tworzyw 2010; 4: 225–227.
14. Tor A. Charakterystyka procesu wytłaczania powlekającego. Eksploatacja i Niezawodnosc – Maintenance and Reliability 2005; 2: 18–22.
15. Tor-Świątek A, Sikora R. Modyfikacja poli(chlorku winylu) mikrosferami w procesie wytłaczania mikroporującego. Przetwórstwo Tworzyw 2011; 4: 248-251.
16. Wessel HC. Wytłaczanie profili ze spienionego PVC. Wytłaczanie Tworzyw Sztucznych. Wydawnictwo Plastech, Warszawa 1999; 34–38.



**Aneta Tor-ŚWIĄTEK, Ph.D. (Eng.)**
**Bronisław SAMUJŁO , Ph.D. (Eng.)**
Department of Mechanical Engineering
Lublin University of Technology
ul. Nadbystrzycka 36, 20-618 Lublin, Poland
E-mail: a.tor@pollub.pl; b.samujlo@pollub.pl

Article citation info:
KRÓLCZYK G, GAJEK M, LEGUTKO S. Predicting the tool life in the dry machining of duplex stainless steel. Eksploatacja i Niezawodnosc – Maintenance and Reliability 2013; 15 (1): 62–65.

Grzegorz KRÓLCZYK
Maksymilian GAJEK
Stanisław LEGUTKO

# PREDICTING THE TOOL LIFE IN THE DRY MACHINING OF DUPLEX STAINLESS STEEL

# PROGNOZOWANIE OKRESU TRWAŁOŚCI OSTRZA W OBRÓBCE NA SUCHO STALI NIERDZEWNEJ DUPLEX*

*This paper examines the influence of cutting parameters, namely cutting speed, feed and depth of cut onto tool life in DSS turning process. The study included developing a mathematical model to determine the tool life. Verification research has been carried out on CNC lathe, hence the test plan has been adjusted to the possibility of programmable machines controlling GE Fanuc series 0 - T. The comparison of results obtained by given experimental plan was performed in industrial company.*

***Keywords**: Duplex Stainless Steel, machining, turning, tool life, Responce Surface Method.*

*W artykule przedstawiono wpływ parametrów obróbki, a mianowicie prędkości skrawania, posuwu i głębokości skrawania na okres trwałości ostrza w procesie toczenia stali duplex. Badania obejmowały opracowanie modelu matematycznego dla określenia okresu trwałości ostrza skrawającego. Badania weryfikacyjne wykonywano na tokarce sterowanej numerycznie, stąd plan badań dostosowany został do możliwości programowych maszyny ze sterowaniem GE Fanuc seria 0 – T. Porównanie wyników przeprowadzono w warunkach produkcyjnych.*

***Słowa kluczowe**: stal nierdzewna, obróbka skrawaniem, toczenie, okres trwałości ostrza, metoda powierzchni odpowiedzi.*

### Nomenclature

| | |
|---|---|
| $a_p$ | depth of cut in mm |
| $f$ | feed rate in mm/rev |
| $v_c$ | cutting speed in m/min |
| $T$ | tool life in min |
| DSS | Duplex Stainless Steel |

## 1. Introduction

According to companies producing construction materials duplex stainless steel is gaining importance, which is reflected in the wide range of these products available in the market. One limitation of the efficiency of the turning of this steel is the consumption of cutting tool indexable tool inserts. According Olszak [10] DSS is classified as difficult-to-cut. In recent years, machinability of austenitic steels has been dealt by researchers such as Abou-El-Hossein K. A. et al., Akasawa T. et al., Charles J. et al., Ciftci I., Cunat P. J., Kosmač A., and Paro J. et al. [1, 2, 4, 5, 6, 7, 8, 11], while machining of DSS has been described by Bouzid Saï W. and Lebrun J. L. [3]. The wearing process of a tool point, which is largely dependent on cutting parameters, is an important factor. The wear of a tool point leads to deterioration in quality of machined surface. The basic requirement in the application of indexable tool inserts in industrial conditions is the total increase in production; not the precision performance of its particular machine parts. According to Smith [14], where the equipment stocks are consolidated and the materials used in cutting tools are more universal, we can, in industrial conditions, use a smaller number of types and geometry of the cutting tool. Smaller stocks of indexable tool inserts allow us to more effectively optimize the production process. The above-mentioned aspects, combined with the optimization of the cutting speed, feed and depth of cut, allow the desired production targets to be met. Due to an optimization of the cutting parameters, it is possible to take full advantage of the basic equipment; as a result you can expect a large increase in overall production efficiency. In order to know surface quality and dimensional properties is necessary to employ theoretical models making it feasible to do predictions in function of operation conditions. The response surface method (RSM) is practical, economical and relatively easy for use [13].

## 2. Experimental techniques

### 2.1. Workpiece and cutting tool materials

Machined material was 1.4462 (DIN EN 10088-1) steel with a ferritic-austenitic structure containing about 50% of austenite. The ultimate tensile strength UTS=700 MPa, Brinell hardness - 293 HB. The elemental composition of the machined material and technical details of the cutting tools are given in tables 1 and 2 respectively.

Cutting tool inserts of TNMG 160408 designation clamped in the tool shank of ISO-MTGNL 2020-16 type were employed. Based on the industry recommendations a range of cutting parameters T1: $v_c$ = 50 ÷ 150 m/min, $f$ = 0,2 ÷ 0,4 mm/rev, $a_p$ = 1 ÷ 3 mm was selected. The study was conducted within a production facility. The research program was carried out on a lathe CNC 400 Famot – Pleszew.

### 2.2. Research plan

As the method of optimization for DSS cutting parameters a static determined selective-multivariate uniform static - rotatable PS/

(*) Tekst artykułu w polskiej wersji językowej dostępny w elektronicznym wydaniu kwartalnika na stronie ***www.ein.org.pl***

*Table 1. Chemical composition of 1.4462 duplex stainless steel*

| Element | %C max | %Si max | %Mn max | %P max | %S max | %Cr | %Ni | %Mo | %N | Others |
|---|---|---|---|---|---|---|---|---|---|---|
| [%] at. | 0,03 | 1,00 | 2,00 | 0,030 | 0,020 | 21,0<br>23,0 | 4,50<br>6,50 | 2,50<br>3,50 | 0,10<br>0,22 | - |

*Table 2. Cutting tool specification*

| Tool | Substrate | Others |
|---|---|---|
| T1 | Hardness: 1350 HV3<br>Grade: M25, P35 | Coatings: Ti(C,N)-(2 μm) (Top layer)<br>$Al_2O_3$-(1.5 μm) (Middle layer)<br>TiN-(2 μm) (Bottom layer)<br>Coating technique: CVD |

*Table 3. Coded indication of the study plan*

| Test No. | Coded factors | | | Decoded real value | | |
|---|---|---|---|---|---|---|
| | $x_1$ | $x_2$ | $x_3$ | $v_c$ [m/min] | $f$ [mm/rev] | $a_p$ [mm] |
| 1 | -1 | -1 | -1 | 70 | 0,24 | 1,4 |
| 2 | -1 | -1 | +1 | 70 | 0,24 | 2,6 |
| 3 | -1 | +1 | -1 | 70 | 0,36 | 1,4 |
| 4 | -1 | +1 | +1 | 70 | 0,36 | 2,6 |
| 5 | +1 | -1 | -1 | 130 | 0,24 | 1,4 |
| 6 | +1 | -1 | +1 | 130 | 0,24 | 2,6 |
| 7 | +1 | +1 | -1 | 130 | 0,36 | 1,4 |
| 8 | +1 | +1 | +1 | 130 | 0,36 | 2,6 |
| 9 | -1,682 | 0 | 0 | 50 | 0,3 | 2 |
| 10 | 1,682 | 0 | 0 | 150 | 0,3 | 2 |
| 11 | 0 | -1,682 | 0 | 100 | 0,2 | 2 |
| 12 | 0 | 1,682 | 0 | 100 | 0,4 | 2 |
| 13 | 0 | 0 | -1,682 | 100 | 0,3 | 1 |
| 14 | 0 | 0 | 1,682 | 100 | 0,3 | 3 |
| 15 | 0 | 0 | 0 | 100 | 0,3 | 2 |
| 16 | 0 | 0 | 0 | 100 | 0,3 | 2 |
| 17 | 0 | 0 | 0 | 100 | 0,3 | 2 |
| 18 | 0 | 0 | 0 | 100 | 0,3 | 2 |
| 19 | 0 | 0 | 0 | 100 | 0,3 | 2 |
| 20 | 0 | 0 | 0 | 100 | 0,3 | 2 |

DS-P:λ program has been selected [12]. A choice of the PS/DS-P:λ program was dictated with the assumption that the second-degree polynomial function model will be a nonlinear model which can be reduced to a linear model. The second-degree polynomial function has been chosen because there are no restrictions in research related to the measurement technique. The required number of experimental points is $N = 2^3 + 6 + 6 = 20$ (Table 3).

There are eight factorial experiments (3 factors on two levels, $2^3$) with added 6 star points and centre point (average level) repeated 6 times to calculate the pure error [9].

## 3. Modeling tool life and its application

### 3.1. Tool life model

The aim of this study was an attempt to verify, in industrial conditions, the calculated value of the function describing tool life during turning DSS. Based on the PS/DS-P:λ program and the modeled experimental data of the polynomial function of tool life:

$$T = f(v_c;\ f;\ a_p) = 118{,}438 - 0{,}88687 \cdot v_c - 89{,}9855 \cdot f - 14{,}439 \cdot a_p + 0{,}0053856 \cdot v_c^2 + 400{,}4555 \cdot f^2 + 6{,}0762 \cdot a_p^2 - 1{,}3131 \cdot v_c \cdot f + 0{,}0029556 \cdot v_c \cdot a_p - 47{,}6564 \cdot f \cdot a_p, \quad (1)$$

Chosen results for maximum and minimum values of $v_c$ and $f$ and for average value of $a_p$ are presented in Table 4. It is evident that the results obtained on the basis of the model are consistent with the results obtained during the experiment.

*Table 4. Verified research parameters of the model of tool life*

| Cutting parameters | | | *T* - average value of research | *T* - calculation results |
|---|---|---|---|---|
| $v_c$ [m/min] | $f$ [mm/rev] | $a_p$ [mm] | | |
| 150 | 0,2 | 2 | 40 min 19,4 s | 42 min 27,9 s |
| 150 | 0,4 | 2 | 16 min 24,4 s | 14 min 04,0 s |
| 50 | 0,2 | 2 | 46 min 01,4 s | 49 min 06,5 s |
| 50 | 0,4 | 2 | 39 min 08,5 s | 46 min 58,4 s |

It is evident that the results obtained on the basis of the model are consistent with the results obtained during the experiment.

### 3.2. Verification study of the model

The evaluation of the mathematical model was performed using the Student's t test to compare two mean values of populations with normal distributions and homogeneous variances. Statistical calculations were performed with the Statistica 9.0 [15] program.

The assumptions of normality were examined using the Shapiro-Wilk test for the model of tool life (Table 5).

*Table 5. Tests of normality for the model of tool life*

| Variable | n | W | p |
|---|---|---|---|
| **Average value of research** | 4 | 0,8251 | 0,1555 |
| **Calculation results** | 4 | 0,7741 | 0,0633 |

As the level of significance of p is greater than 0,05 for the test case, there is no reason to reject the hypothesis of normal distribution.

Two general populations are examined with normal distributions $N(m_1, \sigma_1)$ and $N(m_2, \sigma_2)$, where the parameters of these distributions

are unknown. There are two sample sizes $n_1 = 4$ and $n_2 = 4$. On the basis of test results the hypothesis is tested $H_0$: $\sigma_1^2 = \sigma_2^2$, against the alternative hypothesis $H_1$: $\sigma_1^2 \neq \sigma_2^2$. The results of the calculations for the model of tool life are presented in Table 6.

*Table 6. The results of F-statistic model calculations for tool life*

| | |
|---|---|
| **F** | 1,5563 |
| **p** | 0,7251 |

Because p is greater than 0,05, there is no reason to reject the hypothesis of homogeneity of variance for each of the cases.

The two populations having normal distributions are being studied now $N(m_1, \sigma_1)$ and $N(m_2, \sigma_2)$, standard deviations are unknown, but equal, i.e. there is $\sigma_1 = \sigma_2$. Based on two sample sizes $n_1 = 4$ and $n_2 = 4$, the hypothesis is verified $H_0$: $m_1 = m_2$ against the alternative hypothesis $H_1$: $m_1 \neq m_2$. The average values from both samples are verified $\overline{x_1}$ and $\overline{x_2}$ and variances $s_1^2$ and $s_2^2$, then the value of t statistics according to the following formula:

$$t = \frac{\overline{x_1} - \overline{x_2}}{\sqrt{\frac{n_1 s_1^2 + n_2 s_2^2}{n_1 + n_2 - 2}\left(\frac{1}{n_1} + \frac{1}{n_2}\right)}} . \qquad (2)$$

The calculation results are presented in Table 7.

*Table 7. The results of t-statistic model calculations for tool life*

| | |
|---|---|
| **t** | -0,2566 |
| **p** | 0,8060 |

The significance level of p for the tested models is greater than 0,05 which means there is no reason to reject the hypothesis of equal averages. Therefore, it is shown on the significance level of 0,05, that the average value of research and the model are not significantly different. It can therefore be concluded that the designated model reflects changes in tool life represented by the empirical values.

## 4. Tool life as the function of cutting parameters

Table 8–10 shows results (values) of the tool life of *T*, depending on the particular technological cutting parameters in the turning process of duplex stainless steel. It was calculated on the basis of equation (1).

*Table 8. Values of tool life according to T for $T = f(a_p)$ for $v_c = 50 \div 150$ m/min and $f = 0{,}2 \div 0{,}4$ mm/rev obtained for the depths of cutting $a_p = 1$ mm, $a_p = 2$ mm, $a_p = 3$ mm*

| No | $v_c$ [m/min] | $f$ [mm/rev] | $T_{(ap=1)}$ [min] | $T_{(ap=2)}$ [min] | $T_{(ap=3)}$ [min] |
|---|---|---|---|---|---|
| 1 | 50 | 0,2 | 54,702 | 49,108 | 55,667 |
| 2 | | 0,3 | 54,395 | 44,036 | 45,829 |
| 3 | | 0,4 | 62,098 | 46,972 | 44,000 |
| 4 | 100 | 0,2 | 37,768 | 32,321 | 39,028 |
| 5 | | 0,3 | 30,895 | 20,683 | 22,624 |
| 6 | | 0,4 | 32,032 | 17,054 | 14,229 |
| 7 | 150 | 0,2 | 47,761 | 42,463 | 49,317 |
| 8 | | 0,3 | 34,323 | 24,259 | 26,347 |
| 9 | | 0,4 | 28,894 | 14,065 | 11,387 |

*Table 9. Values of tool life according to T for $T = f(v_c)$ for $f = 0{,}2 \div 0{,}4$ mm/rev and $a_p = 1 \div 3$ mm obtained for the cutting speed $v_c = 50$ m/min, $v_c = 100$ m/min, $v_c = 150$ m/min*

| No | $f$ [mm/rev] | $a_p$ [mm] | $T_{(vc=50)}$ [min] | $T_{(vc=100)}$ [min] | $T_{(vc=150)}$ [min] |
|---|---|---|---|---|---|
| 1 | 0,2 | 1 | 54,702 | 37,768 | 47,761 |
| 2 | 0,3 | | 54,395 | 30,895 | 34,323 |
| 3 | 0,4 | | 62,098 | 32,032 | 28,894 |
| 4 | 0,2 | 2 | 49,108 | 32,321 | 42,463 |
| 5 | 0,3 | | 44,036 | 20,683 | 24,259 |
| 6 | 0,4 | | 46,972 | 17,054 | 14,065 |
| 7 | 0,2 | 3 | 55,667 | 39,028 | 49,317 |
| 8 | 0,3 | | 45,829 | 22,624 | 26,347 |
| 9 | 0,4 | | 44,000 | 14,229 | 11,387 |

*Table 10. Values of tool life according to T for $T = f(f)$ for $v_c = 50 \div 150$ m/min and $a_p = 1 \div 3$ mm obtained for the feed $f = 0{,}2$ mm/rev, $f = 0{,}3$ mm/rev, $f = 0{,}4$ mm/rev*

| No | $v_c$ [m/min] | $a_p$ [mm] | $T_{(f=0,2)}$ [min] | $T_{(f=0,3)}$ [min] | $T_{(f=0,4)}$ [min] |
|---|---|---|---|---|---|
| 1 | 50 | 1 | 54,702 | 54,395 | 62,098 |
| 2 | | 2 | 49,108 | 44,036 | 46,972 |
| 3 | | 3 | 55,667 | 45,829 | 44,000 |
| 4 | 100 | 1 | 37,768 | 30,895 | 32,032 |
| 5 | | 2 | 32,321 | 20,683 | 17,054 |
| 6 | | 3 | 39,028 | 22,624 | 14,229 |
| 7 | 150 | 1 | 47,761 | 34,323 | 28,894 |
| 8 | | 2 | 42,463 | 24,259 | 14,065 |
| 9 | | 3 | 49,317 | 26,347 | 11,387 |

Those data can be useful for both technologist and the CNC machine tool operator.

## 5. Conclusions

The purpose of this article was to develop a methodology which can offer the possibility of predicting the tool life in the turning process of duplex stainless steel. Predicting the required parameter of tool life *T* in the process of dry machining is an important part of the process and impact of such conditions on the technological properties of the surface layer.

Factorial design of an experiment can be successfully employed using coated carbide cutting tools in turning DSS. The following conclusions have been drawn:

1. Second-order model predicting equations for tool life have been developed using response surface methodology for turning the DSS with coated tools.
2. The established equations clearly show that the cutting speed was main influencing factor on the tool life.
3. The predicted values and measured values are fairly close which indicates that the developed tool life prediction model can be effectively used to predict the tool life for the turning process. Using such models, a remarkable time and cost savings can be obtained.

## References


1. Abou-El-Hossein KA, Yahya Z. High-Speed End-Milling of AISI 304 Stainless Steels Using New Geometrically Developed Carbide Inserts. Journal of Materials Processing Technology, 2005, 162–163, 596–602.
2. Akasawa T. et al. Effects of Free-Cutting Additives on the Machinability of Austenitic Stainless Steels. Journal of Materials Processing Technology, 2003, 143–144, 66–71.
3. Bouzid Saï W, Lebrun JL. Influence of Finishing by Burnishing on Surface Characteristics. Journal of Materials Engineering and Performance, 2003, volume 12(1), 37.
4. Charles J. et al. Austenitis Chromium – Manganese Stainless Steel – A European Approach. Materials and Applications Series, 2010,volume 12, Euro Inox.
5. Ciftci I. Machining of Austenitic Stainless Steels using CVD Multi-Layer Coated Cemented Carbide Tools. Tribology International, 2006, 39, 565–569.
6. Cunat PJ. The Euro Inox Handbook of Stainless Steel. Materials and Applications Series, 2002,volume 1, Euro Inox.
7. Cunat PJ. Working with Stainless Steel. Materials and Applications Series, 2009,volume 2, EDP Sciences and Euro Inox.
8. Kosmač A. Electropolishing Stainless Steel. Materials and Applications Series, 2010, volume 11, Euro Inox.
9. Montgomery D. Design and Analysis of Experiments, 5th Edition, New York: John Wiley & Sons, Inc., 2003.
10. Olszak W. Obróbka skrawaniem. Warszawa: WNT, 2008.
11. Paro J. et al. Tool Wear and Machinability of X5 CrMnN 18 18 Stainless Steels. Journal of Materials Processing Technology, 2001, 119, 14-20.
12. Polański Z. Metody optymalizacji w technologii maszyn. Warszawa: PWN, 1977.
13. Sahin Y, Riza Motorcu A. Surface Roughness Model for Machining Mild Steel with Coated Carbide Tool. Materials & Design, 2005, 26, 321–326.
14. Smith GT. Cutting Tool Technology, Industrial Handbook. London: Springer-Verlag, 2008.
15. StatSoft, Inc. (2009). STATISTICA (data analysis software system), version 9.0. www.statsoft.com



**Grzegorz KRÓLCZYK, Ph.D. (Eng.)**
**Prof. Maksymilian GAJEK, D.Sc., Ph.D. (Eng.)**
Faculty of Production Engineering and Logistics
Opole University of Technology
ul. Prószkowska 76, 45-758 Opole, Poland
E-mails: g.krolczyk@po.opole.pl, m.gajek@po.opole.pl

**Prof. Stanisław LEGUTKO, D.Sc., Ph.D. (Eng.)**
Faculty of Mechanical Engineering and Management
Poznan University of Technology
ul. Piotrowo 3, 60-965 Poznań, Poland
E-mail: stanislaw.legutko@put.poznan.pl

Article citation info:
TANASIJEVIĆ M, IVEZIĆ D, JOVANČIĆ P, IGNJATOVIĆ D, BUGARIĆ U. Dependability assesment of open-pit mines equpment – study on the bases of fuzzy algebra rules. Eksploatacja i Niezawodnosc – Maintenance and Reliability 2013; 15 (1): 66–74.

Miloš TANASIJEVIĆ
Dejan IVEZIĆ
Predrag JOVANČIĆ
Dragan IGNJATOVIĆ
Uglješa BUGARIĆ

# DEPENDABILITY ASSESMENT OF OPEN-PIT MINES EQUPMENT – STUDY ON THE BASES OF FUZZY ALGEBRA RULES

# OCENA NIEZAWODNOŚCI SPRZĘTU WYKORZYSTYWANEGO W KOPALNIACH ODKRYWKOWYCH – BADANIA OPARTE NA REGUŁACH ROZMYTEJ ALGEBRY

*This article aims to present a new approach for assessing of maintenance support and model for its introduction into dependability concept. Process of expertise judgment is used directly for assessing the organization of maintenance support and it is shown in the form of linguistic variables as appropriate fuzzy sets. For the introduction of maintenance support into dependability, fuzzy composition is used. Since reliability and maintainability are also influential indicators of dependability, it was necessary to develop a methodology for fuzzification of corresponding reliability and maintainability probability functions. This methodology is developed by using empirical scaling. The proposed approach has been applied to different types of bulldozers, as a usual technical system that operates at open pit mine.*

***Keywords****: dependability, maintenance support, fuzzy sets, bulldozer.*

*Niniejszy artykuł ma na celu przedstawienie nowej metody oceny wspomagania obsługi oraz modelu opisującego jej zastosowanie w odniesieniu do pojęcia niezawodności. Proces wydawania opinii eksperckiej wykorzystano bezpośrednio do oceny organizacji wspomagania obsługi i przedstawiono go w postaci zmiennych lingwistycznych jako odpowiednie zbiory rozmyte. W celu odniesienia wspomagania obsługi do niezawodności, posłużono się kompozycją zbiorów rozmytych. Ponieważ nieuszkadzalność i obsługiwalność są również ważnymi wskaźnikami niezawodności, konieczne było opracowanie metodologii rozmywania odpowiednich funkcji prawdopodobieństwa działania i obsługi. Niniejsza metodologia została opracowana przy użyciu skalowania empirycznego. Proponowane podejście zastosowano w odniesieniu do różnych typów spychaczy, składających się na przeciętny układ techniczny funkcjonujący w obrębie kopalni odkrywkowej.*

***Słowa kluczowe****: stal duplex, obróbka skrawaniem, toczenie, okres trwałości ostrza, metoda powierzchni odpowiedzi.*

## 1. Introduction

Life cycle management of technical systems that are characterized by high investment value on the one hand, and by high specific work value, namely the high costs of unplanned shut downs on the other, is an especially complex and responsible task. Open pit mines and their equipment represent the genuine example of these technical systems. According to Study [16], an hour of unplanned break down at lignite open pit mines within Electric Power Industry of Serbia causes the expenses of around 10.000 € for coal and of around 3.000 € for overburden. Machines engaged on continual exploitation systems (bucket wheel excavator, stacker) today cost 10–12 € per kilo at average, and themselves can even weight several thousand tons. Machines belonging to auxiliary machinery can cost several thousand euros. Management of maintenance is very responsible duty, also as model for its determination and evaluation. In that sense, the science articles in the area of maintainability and reliability engineering, are very topical [2–4, 6–9, 11–18].

In order to simplify this management's task, it is needed to define indicators of quality of service for technical systems. Some authors Kuo[12] and Seo[14] assert that the life cycle of a technical systems must be seen from the point of costs, namely, the reduction of total life cycle costs for a certain product is considered as an essential part of technical system and serving. There are also the indicators that analyze technical system based to the ratio of the uptime and downtime. Among them, the best known are indicators of availability performance, namely dependability. Dependability concept was introduced through ISO-IEC standards [14]. Dependability includes availability performance, as its measure, with influencing factors – performances of reliability, maintainability and maintenance support. Implementation of dependability concept was developed in detail in IEC-300 standards where dependability objectives were defined and principles of dependability management systems were introduced. The special attention was devoted to degree of customers' satisfaction with appropriate product and consideration of entire product life-cycle phases concerning planning, design, production, operation and maintenance, and finally disuse. Some authors Avizienis [1] and Ebramhimipour [3] have defined dependability as an integrative concept which also includes safety. In any case, contemporary approaches to estimation of the quality of service level for technical systems are engineering that support system reliability and maintenance and consider them in the synthesis form. Dependability engineering [14], through various techniques and concepts of systems' sciences, considers the performance of technical system through its life cycle and estimates to what degree and for how long it can be relied on at any time. RAMS Engineering (Reliability Availability Maintainability Supportability) has the goal to reduce number of failures and minimize their consequences [13].

Analysis of these synthesized indicators can be carried out most easily through the mean time to restore equipment to its original working status or through the use of model for prediction on the basis of operational research [13] as well as through the use of fuzzy algebra rules [2], [6] and [10]. Secondly mentioned models are more complex for use, but they give mutual relation of influential parameters and enable finding the weak points of the technical system

Special place in grasping the availability and dependability of technical system, plays the choice of suitable conception of maintenance organization [4] and [11], and consequently of the level of maintenance support. In practice, various conceptions [9] are used - from the simplest ones such as breakdown maintenance, to the advanced ones such as predictive. Maintenance support hereby has the task to support the uninterrupted performance of suitable maintenance conception, namely to enable the required level of availability and dependability of technical system.

This paper presents procedure – model for estimation of maintenance support and dependability determination according to maintenance support and other influential indicators (reliability and maintainability). Furthermore, maintenance support is estimated on the basis of expert judgment, while reliability and maintainability monitoring period of up-time and down-time. In order to comprehend the impact of these various values to dependability, the rules of fuzzy algebra are used. In the article was also specifically developed procedure for reliability and maintainability probability functions fuzzification on the base of empirical scaling. Model is tested and implemented to dependability determination of different types of bulldozers operated at open pit mine Drmno.

It can be said that this article constitutes an improvement of the [6], when the dependability indicators were analyzed only on the base of expertise judgment, without of fuzzification of statistical data. Also, this paper presents a maintenance support evaluation model. Unlike performances of reliability and maintainability, maintenance support did not have a conventional system for evaluation,

## 2. Maintenance support analysis and dependability integration based to fuzzy sets theory

Maintenance support represents the ability of an organization in charge of maintenance to secure required maintenance of technical system under given condition, in accordance with maintenance policy. In other words, certain technical system has the appropriate maintenance support if the required maintenance activity is carried out at required place in the given time during a certain time period. Maintenance support is not directly influenced by construction characteristics of technical system which is the object of maintenance.

In analysis of logistic parameters as the maintenance support is, practically there is no other way for its estimation without utilization of experts' judgments given as linguistic descriptions. Fuzzy sets theory has arisen as appropriate tool that will work with linguistic form, apropos simultaneously with insufficiently accurate terms and expressions that hardly can be represented by models with numerical inputs, as well as with to some extent strongly determined facts. In this sense, fuzzy set theory will in this paper be used for the analysis of maintenance support through the procedure of identification of the fuzzy sets as well as for the integration on the dependability level using the procedure of composition of the fuzzy sets.

### 2.1. Identification of the fuzzy sets, maintenance support evaluation

By analysis of maintenance conditions that usually exist at complex industrial systems, for maintenance support systems [6] can be identified: maintenance through services by producers or licensed organizations, maintenance developed by consumer, maintenance by consumers' request and without organized maintenance.

Efficiencies of the first two cases are hard to be distinguished. Maintenance with services performed by producers or licensed organizations is characteristic for recent maintenance concepts. Here producers of equipments give guarantee for their correct operation. These types of maintenance support are provided by almost all producers of equipment which is produced in large series, such as auxiliary machinery of the open pit mines. Maintenance developed by consumers is somewhat obsolete maintenance concept but it is still present for complex and valuable systems which have been produced in small amounts and which can have significant modification in design during their lifetime. Huge bucket wheel excavators at open pit mines are good examples of such systems. Without consideration economic aspects of such maintenance policy, it can be estimated as quite successful, primary because close relationship of maintenance service with design development and modernization of such machines during their lifetime.

Maintenance by consumers' request can be characterized as very inertial concept, but it can satisfy demands with limited number of activities necessary for keeping system as available. However, the consequences of inertia, i.e. lacking of forehand and organized maintenance actions, can be very serious especially for systems implemented for expensive technological process. As the uncertainty and vagueness are inherent to this concept, its fuzzy set will have significantly wide range.

Inexistence of organized maintenance is connected to component and parts of systems which are rare, unique or reliable in the degree that any failure is unexpected (for example support construction, hollow shafts and planetary gears of large dimensions, etc.). Storage of such components would have high expenses but the failures of these components are frequently fatal for whole system.

According to four identified maintenance policy concepts, four linguistic variables for maintenance support can be introduced: excellently developed maintenance support, well developed maintenance support, limited maintenance support and inexistence of maintenance support. It is necessary to put these linguistic variables into appropriate coordinate system of membership function and measuring units. Maintenance support as well as the dependability is without conventional measuring units. In other words, maintenance support is inherently linguistic variable, i.e. without any measuring units. Therefore, in the case of analysis based on experts' estimations, as the measuring unit can be introduced class, as usually used concept for representing performances' quality [19] and [20]. Hence, the structure of maintenance support indicator with seven classes ($i$ =1 to 7) as measures of appropriate fuzzy sets will be as follows:

$$\boldsymbol{L} = \{1/\mu^1_L, 2/\mu^2_L, 3/\mu^3_L, 4/\mu^4_L, 5/\mu^5_L, 6/\mu^6_L, 7/\mu^7_L\};\ \mu^i_L \in [0,1] \quad (1)$$

Where is $\boldsymbol{L}$ mark for maintenance support (practically logistics) and $\mu^i_L$ membership function.

For two more efficiency concepts linguistic variables excellently developed and well developed are set up but without strict identification. In other words, maintenance through services by producers or licensed organizations can principally be identified as excellently developed maintenance support but without absolute certainty. The same is with maintenance developed by consumer and linguistic variable well developed. With strict identification of proposed linguistic variables and maintenance policies advantages of fuzzy sets utilization would also be neutralized. For example, obligation of producer to carry out maintenance actions doesn't necessary mean that the maintenance support is excellently developed. For remaining two less efficiently maintenance support options linguistic variables limited and inexistence are introduced. These two maintenance policies are quite easier for differentiation and strict identification with linguistic

variables is evident. Also, according to previous considerations outer linguistic variables excellently developed and inexistence are not mutually symmetrical. These settings are shown in Fig. 1.

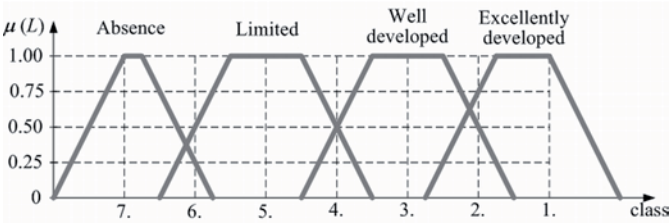


*Fig. 1. Maintenance support fuzzy sets*

### 2.2. Composition of the fuzzy sets, maintenance support and dependability

Composition of the fuzzy sets is a process of defining the relationship between fuzzy relations in order to obtain the score of synthesis of these relations. In our case, the score would represent dependability (*D*), while fuzzy relations are: reliability (*R*), maintainability (*M*) and maintenance support (*L*), namely all partial indicators of dependability. Synthesis was done based on appropriate max-min composition [10]:

$$D = R \circ (M \times L) \tag{2}$$

Conjunction "and", that is product with operator (°) is used in cases when fuzzy sets and/or relations simultaneously or there is no functional relationship between them. This product is here used for integration of performance that describes times in operation and failure time, i.e. reliability indicator with maintenance indicators. Functional relationship between maintainability and maintenance support certainly exists. These indicators can be even technologically dependent and the Cartesian product is used for their integration.

The Cartesian product [10] of maintenance related indicators, maintainability and maintenance support, i.e. appropriate membership function is defined as follows:

$$\mu_{M \times L} = (\mu^{ij}{}_{M \times L})_{n \times n} \tag{3}$$

with:

$$\mu^{ij}{}_{M \times L} = \min(\mu^{i}{}_{M}, \mu^{j}{}_{L}) \tag{4}$$

where the membership functions for maintainability and maintenance support are given as:

$$\mu_{M} = (\mu^{1}{}_{M}, \mu^{2}{}_{M}, \ldots, \mu^{n}{}_{M}) \tag{5}$$

$$\mu_{L} = (\mu^{1}{}_{L}, \mu^{2}{}_{L}, \ldots, \mu^{n}{}_{L}) \tag{6}$$

Composition of dependability membership function, for reliability membership functions:

$$\mu_{R} = (\mu^{1}{}_{R}, \mu^{2}{}_{R}, \ldots, \mu^{n}{}_{R}) \tag{7}$$

and the Cartesian product of maintainability and maintenance support membership function given in (3), can be determined as:

$$\mu_{D} = \mu_{R \circ M \times L} = (\mu^{j}{}_{D})_{1 \times n}, \tag{8}$$

here is:

$$\mu^{j}{}_{D} = \max(\min(\mu^{1}{}_{R}, \mu^{1j}{}_{M \times L}), \ldots, \min(\mu^{n}{}_{R}, \mu^{nj}{}_{M \times L})), j = 1, 2, \ldots, n. \tag{9}$$

Max-min composition defined in equation (9) set up maintenance support fuzzy sets as "critical" or more precise as fuzzy sets with the dominant influence to over all dependability. For example, if considered system is with excellent performances of reliability and maintainability but with relatively poor characteristic for maintenance support, overall performance of dependability will be also at low level and significantly lower than in some other combinations of these indicators. This is the essence of the integration of maintenance support in dependability. This feature characterized max-min composition as a "pessimistic" but it is often used in an analysis of technical systems.

Proposed fuzzy composition as an output has dependability performance in relation (by appropriate membership function) with classes (1 to 7):

$$\boldsymbol{D} = \{1/\mu^{1}{}_{D}, 2/\mu^{2}{}_{D}, 3/\mu^{3}{}_{D}, 4/\mu^{4}{}_{D}, 5/\mu^{5}{}_{D}, 6/\mu^{6}{}_{D}, 7/\mu^{7}{}_{D}\}; \mu^{i}{}_{D} \in [0,1] \tag{10}$$

Thereby, *L* is given in the form (1), while *R* and *M* are also given in relation to classes in the form:

$$\boldsymbol{R} = \{1/\mu^{1}{}_{R}, 2/\mu^{2}{}_{R}, 3/\mu^{3}{}_{R}, 4/\mu^{4}{}_{R}, 5/\mu^{5}{}_{R}, 6/\mu^{6}{}_{R}, 7/\mu^{7}{}_{R}\}; \mu^{i}{}_{R} \in [0,1] \tag{11}$$

$$\boldsymbol{M} = \{1/\mu^{1}{}_{M}, 2/\mu^{2}{}_{M}, 3/\mu^{3}{}_{M}, 4/\mu^{4}{}_{M}, 5/\mu^{5}{}_{M}, 6/\mu^{6}{}_{M}, 7/\mu^{7}{}_{M}\}; \mu^{i}{}_{M} \in [0,1] \tag{12}$$

Dependability, as the parameter of quality of service level, is a value without conventional evaluation system and measurement unit. Therefore, in this article it is given in the form of fuzzy sets depending from membership function $\mu_{(D)}$ and class (1 to 7). These settings are shown in Fig. 2.

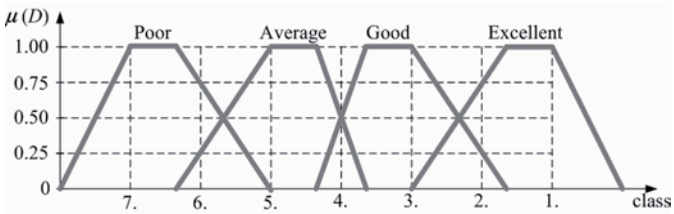


*Fig. 2. Dependability fuzzy sets*

The expression (10) of dependability performance is necessary to map back to the defined dependability fuzzy sets (Fig. 2). Best-fit method [19] is used for transformation of dependability description (10) to form that which defines grade of membership to fuzzy sets: poor, average, good, excellent (Fig. 2). This procedure is recognized as dependability identification. Best-fit method uses the distance (*d*) between dependability attained by "max-min" composition (10) and each of the dependability expressions to represent the degree to which *D* is confirmed to each of them (Fig. 2).

$$d_i(D, H_i) = \sqrt{\sum_{j=1}^{7} \left(\mu^{j}{}_{D} - \mu^{j}{}_{H_i}\right)^2}, i = 1, \ldots, 4; \; H_i = \{\text{excellent, good, average, poor}\} \tag{13}$$

The closer *D* is to the *i*-th linguistic variable, the smaller $d_i$ is. Distance $d_i$ is equal to zero, if *D* is just the same as the *i*-th expression in terms of the membership functions. In such a case, *D* should not be evaluated to other expressions at all due to the exclusiveness of these expressions.

Suppose $d_{i\,\min}$ (i = 1, 2, 3, 4) is the smallest among the obtained distances for *D* and let $\alpha_1$, $\alpha_2$, $\alpha_3$ and $\alpha_4$ represent the reciprocals of the relative distances between the identified fuzzy dependability description *D* and the each of the defined dependability expressions with reference to $d_i$. Then, $\alpha_i$ can be defined as follows:

$$\alpha_i = \frac{1}{d_i / di_{\min}}, \quad i = 1,2,3,4. \tag{14}$$

If $d_i = 0$ it follows that $\alpha_i = 1$ and the others are equal to zero. Then, $\alpha_i$ can be normalized by:

$$\beta_i = \frac{\alpha_i}{\sum_{i=1}^{4} \alpha_i}, \quad i = 1,2,3,4. \qquad \sum_{i=1}^{4} \beta_i = 1 \tag{15}$$

Each $\beta_i$ ($i$ = 1, 2, 3, 4) represents the extent to which $D$ belongs to the i-th defined dependability expressions. It can be noted that if $D$ completely belongs to the $i$-th expression then $\beta_i$ is equal to 1 and the others are equal to 0. Thus $\beta_i$ could be viewed as a degree of confidence that $D$ belongs to the $j$-th reliability expressions. Final expression for dependability performance is obtained in form (according to Fig.2):

$$D = \{(\beta_1, \text{“poor”}), (\beta_2, \text{“average”}), (\beta_3, \text{“good”}), (\beta_4, \text{“excellent”})\} \tag{16}$$

## 3. Reliability and maintainability integration

Maintenance support ($L$) is defined by expertise judgments and it is given directly in fuzzy form (1), as opposed to reliability and maintainability which are usually given in the form of function of time, $R(t)$ and $M(t)$. To calculate dependability (2), it is necessary to do the fuzzification of reliability function $R(t)$ and maintainability function $M(t)$ into the fuzzy numbers (11) and (12).

For determination of fuzzy numbers (11) and (12), it is necessary to:

- define relationship between classes (1 to 7) and registered periods of operation and periods of maintenance,
- define fuzzy numbers $R$ and $M$ to be the best approximations of functions $R(t)$ and $M(t)$, i.e. to define location and shape of fuzzy numbers according to classes as the measure of reliability and maintainability.

### 3.1. Relationship between classes and times

Recorded minimal and maximal periods in operation should be used as representatives of the seventh (the poorest) and the first (the best) classes of reliability, respectively. Theoretically it would be correct if the shortest and the longest expected time would be taken into consideration, i.e. times $t$ for $R(t) \to 0$, $R(t) \to 1$, $M(t) \to 0$ and $M(t) \to 1$. However, these times are usually excluded from consideration as unrealistic.

### 3.2. Location and shape of fuzzy numbers

The Weibull distribution is one of the most commonly used distributions in reliability engineering because of the many shapes it attains for various values of shape parameter. It can therefore model a great variety of data and life characteristics [7]. Periods until the unexpected failures - up times could be recorded and used for determination of reliability function as two parameters Weibull distribution:

$$R(t) = e^{-(\frac{t}{\eta})^{\beta}} \tag{17}$$

where β is shape and η is scale parameter.

Similarly, for maintainability function, periods necessary for repair of damages (i.e. for return in operation readiness) – down times could be measured. According to Ivkovic [7] if there is no unplanned delay in maintenance two parameters Weibull distribution could also be used for approximation of maintainability function, as:

$$M(t) = 1 - e^{-(\frac{t}{\eta})^{\beta}} \tag{18}$$

In both cases, the mean time and standard deviation could be calculated as

Mean time

$$\bar{T} = \eta \cdot \Gamma\left(1 + \frac{1}{\beta}\right) \tag{19}$$

Standard deviation $$\sigma = \sqrt{\eta^2 \cdot \left\{\Gamma\left(1+\frac{2}{\beta}\right) - \left[\Gamma\left(1+\frac{1}{\beta}\right)\right]^2\right\}} \tag{20}$$

where Γ is gamma function.

Approximation of reliability and maintainability function could be done by triangular or trapezoidal fuzzy number. In [2] triangular fuzzy numbers were used for probability density function approximation, as a practical model for approximation of Normal distribution, for example. In this paper, gives a different approach to approximation. Dependence between parameter $\beta$ in $R(t)$ and $M(t)$, and shape of fuzzy number is quite evident (Fig. 3). For the cases when Weibull distribution is inclined to Exponential distribution $(0,5 \le \beta \le 1,5)$ [7] triangular fuzzy number is optimal, while when Weibull distribution is inclined to Normal distribution $(2,5 \le \beta \le 4)$ [7] trapezoidal fuzzy number can be used for approximation. As the boundary value for shape parameter, $\beta = 2$ is adopted.

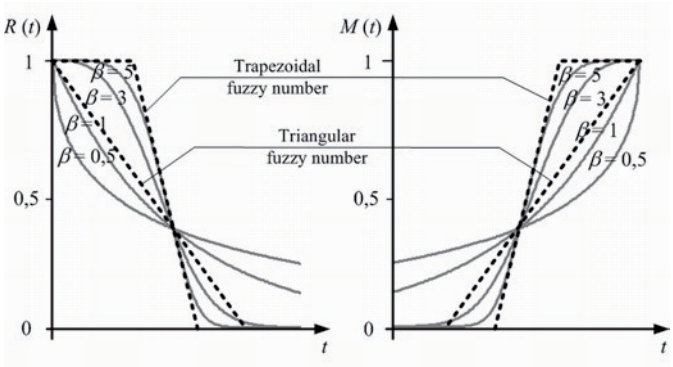


*Fig. 3. Selection of fuzzy number shape according to shape parameter β*

For approximation in the form of triangular fuzzy number, 3 break points have to be defined:

$$FN1 = (bp_1, bp_2, bp_3) \tag{21}$$

While the choice of mean time $\bar{T}$ for $bp_2$ break point is quite reasonable, selection of $bp_1$ and $bp_3$ is not so clear. The most logical choice is to connect these break points with standard deviation $\sigma$, as a dissipation measure, of recorded times around the mean time. For example, for Normal distribution, recorded time in the interval from $[\bar{T} - \sigma, \bar{T}, \bar{T} + \sigma]$ covering 68,26 per cent of all recorded time, while in the case of Exponential distributions rule covering rate is almost 100 per cent [7]. For Weibull distribution does not exist in principle, such rules, but depending on the parameter $\beta$, it can be determined individually. Hence, triangular fuzzy number can be defined as:

$$FN1 = (\bar{T} - x_1 \cdot \sigma, \bar{T}, \bar{T} + x_2 \cdot \sigma) \tag{22}$$

For the selection of scale factors $x_1$ and $x_2$ scaling method is used in this paper. This method is a sort of empirical scaling [5], it reaches scaling on the expected value level, which is itself obtained on the basis of empirical study [21] and expertise judgment [17]. Unit fuzzy number will be adopted to stand for the expected value and reliability and maintainability fuzzy set definitions [6], will be used as empirical data. On the basis of these definitions, which were used in a similar example [6], it can be asserted that symmetry is the common characteristic of majority reliability and maintainability fuzzy sets, and that the minimal width, regarding the center of fuzzy set, is 1.25·*c* (*c* is difference between two successive classes). Now, for the unit triangular fuzzy number (Fig. 4), scale parameters could be calculated as:

$$x_1 = x_2 = \frac{1.25 \cdot c}{\min\limits_i \sigma_i} \qquad (23)$$

where is $\min\limits_i \sigma_i$ the smallest registered value of standard deviation in the range of observed phenomena (different reliability/maintainability functions).

Trapezoidal fuzzy number *FN2*, as approximation of reliability/maintainability function is defined by 4 break points:

$$FN2 = (bp_1, bp_2, bp_3, bp_4) \qquad (24)$$

As in the case of triangular fuzzy set, mean time $\overline{T}$ and standard deviation $\sigma$ are used for definition of break points in trapezoidal fuzzy number:

$$FN2 = (\overline{T} - y_1 \cdot \sigma,\ \overline{T} - y_2 \cdot \sigma,\ \overline{T} + y_3 \cdot \sigma.\ \overline{T} + y_4 \cdot \sigma) \qquad (25)$$

Trapezoidal fuzzy numbers in reliability/maintainability fuzzy sets in Ivezic [6], are mostly symmetrical and minimal width of trapezoid fuzzy set was (2,5·*c*), so the unit trapezoidal fuzzy set can be defined in the form plotted in Fig. 5.

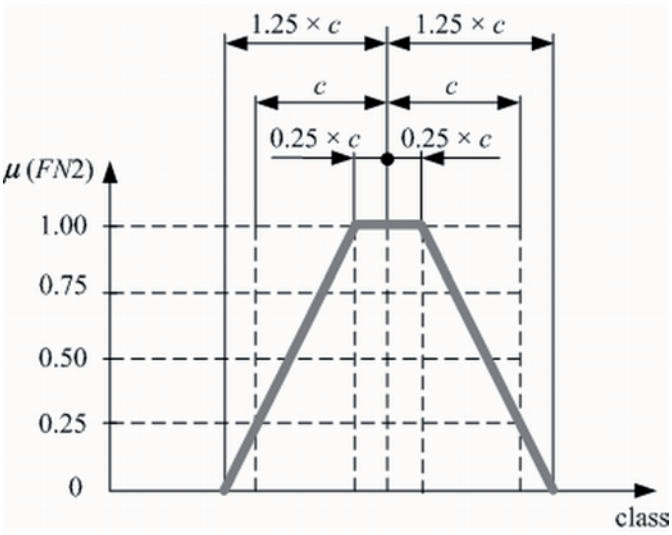


*Fig. 4. Unit triangular fuzzy set*

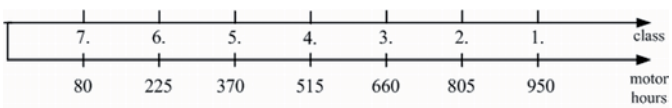


*Fig. 5. Unit trapezoid fuzzy set*

According to minimal standard deviation and adopted geometry of unit trapezoidal fuzzy number, scale parameters in expression (25) are calculated as:

$$y_1 = y_4 = \frac{1.25 \cdot c}{\min\limits_i \sigma_i}, \quad y_2 = y_3 = \frac{1.25 \cdot c}{\min\limits_i \sigma_i} \qquad (26)$$

For transformation of triangular/trapezoidal fuzzy numbers in the desirable form proposed by (11-12) intersections of obtained fuzzy numbers and ordinates of each class have to be calculated.

Proposed empirical scaling algorithm for determination of fuzzy membership function wideness can be considered as acceptable because in operations with fuzzy relations (fuzzy composition) the influence of fuzzy number with the highest degree of membership ($\mu(bp_2)$ = 1 for triangular and $\mu(bp_2) = \mu(bp_2) = 1$ for trapezoidal) is the most significant [10].

## 3. Case study: Dependability determination of bulldozers

At the lignite open pit mine Drmno (Serbia) [8] there are more than 120 machines within the auxiliary machinery. They are very important for the smooth realization of core operation, and any unplanned absence of machines can cause enormous costs. In the auxiliary machinery, bulldozers are certainly the most important and it is therefore necessary to observe the dependability of these machines. Three types of bulldozers (B1, B2, B3[1]) operated at open pit mine Drmno and they are considered in this article.

Technical and operational characteristics of considered machines are presented below:

**B1:** ***Engine:*** Liebherr D 9406 TI-E – 13000 ccm, Power 242 kW – 1800 r/min; Torque 1284 Nm;
***Transmission:*** Power shift – Hydrostatic; ***Speed:*** 11/11 km/h; ***Mass:*** 34800 kg;

**B2:** ***Engine:*** Cummins N14C – 15000 ccm, Power 238 kW – 1400 r/min; Torque 1647 Nm;
***Transmission:*** Power shift – Hydrodynamic; ***Speed:*** 10,6 /12,7 km/h; ***Mass:*** 36210 kg;

**B3:** ***Engine:*** CAT 3406E – 14600 ccm, Power 252 kW – 2386 r/min; Torque 1009 Nm;
***Transmission:*** Power shift – Hydrodynamic; ***Speed:*** 10,6 / 13,8 km/h; ***Mass:*** 37771 kg.

### 3.1. Maintenance support analyses

Maintenance support (*L*) is defined based to expertise judgment and is given directly in fuzzy form. For the selected bulldozers maintenance support is designed as maintenance through services by licensed organizations. Generally this type of maintenance support can be considered as excellent developed maintenance support. However, the quality of its implementation is not the same for all selected bulldozers and the evaluation of maintenance support was done through the questionnaires filled up by ten maintenance engineers. For machine B1, all of the 10 engineers responded that the maintenance support is "well developed"; for machine B2 all of the ten engineers responded that the maintenance support is "excellently developed", while for machine B3 seven engineers responded with "excellently" and three responded as "well developed."

Obtained fuzzy numbers for maintenance support are:

$\boldsymbol{L}_{\mathbf{B1}} = \boldsymbol{L}_{(well...)} = \{1/0, 2/0.5, 3/1.0, 4/0.5, 5/0, 6/0, 7/0\}$

$\boldsymbol{L}_{\mathbf{B2}} = \boldsymbol{L}_{(exc...)} = \{1/1.0, 2/0.75, 3/0, 4/0, 5/0, 6/0, 7/0\}$

$\boldsymbol{L}_{\mathbf{B3}} = \boldsymbol{L}_{(70\%\, exc.. + 30\%\, wel..)} = \{1/0.7, 2/0.675, 3/0.3, 4/0.15, 5/0, 6/0, 7/0\}$

1 Bulldozers: Liebher PR752 lit, DresstaTD25H, Caterpillar D8R, respectively

Calculation procedure for $L_{B3}$ is shown in Table I

*Table I. Calculating fuzzy number procedure for the case when expert estimation differs among the evaluated, as in the case of machine $L_{B3}$.*

| $L_{B3}$ | 1. class | 2. class | 3. class | 4. class | 5. class | 6. class | 7. class |
|---|---|---|---|---|---|---|---|
| Excellently developed 70 % | 1.0 × 70 % | 0.75 × 70 % | 0 × 70 % | 0 × 70 % | 0 × 70 % | 0 × 70 % | 0 × 70 % |
| Well developed 30 % | 0 × 30 % | 0.5 × 30 % | 1.0 × 30 % | 0.5 × 30 % | 0 × 30 % | 0 × 30 % | 0 × 30 % |
| Σ | **0.7** | **0.675** | **0.3** | **0.15** | **0** | **0** | **0** |

### 3.2. Reliability and maintainability analysis

Failures in undercarriage running wheels are characteristic for bulldozer B1, while gear-boxes and torque mechanisms failures are characteristic for B2 and B3, respectively. Algorithm for dependability function determination is well known, and in Table II only final reliability functions for different bulldozer types are presented. According to small number of available data median ranking and Bernard's approximation was used.

*Table II. Reliability functions for different bulldozers*

| Mach. | UP TIME [motor hours] | Reliability function | $\bar{T}$ [motor hours] | $\sigma$ [motor hours] |
|---|---|---|---|---|
| B1 | 187, 710, 822, 921 | $R(t)=e^{-(\frac{t}{828,43})^{1,24}}$ | 773,43 | 647,27 |
| B2 | 80, 100, 214, 386, 421, 622, 831 | $R(t)=e^{-(\frac{t}{434,83})^{1,18}}$ | 410, 97 | 363, 13 |
| B3 | 118, 480, 622, 710, 950 | $R(t)=e^{-(\frac{t}{712,54})^{1,20}}$ | 670,23 | 580,96 |

For maintainability function, periods necessary for return in operation readiness are measured for all three types of bulldozers. Maintainability function is determined in Table III.

*Table III. Maintainability functions for different bulldozers*

| Mach. | DOWN TIME [ hours] | Maintainability function | $\bar{T}$ [hours] | $\sigma$ [hours] |
|---|---|---|---|---|
| B1 | 6.8 ; 10; 10.5; 11; | $M(t)=1-e^{-(\frac{t}{10,54})^{4,23}}$ | 9,58 | 2,55 |
| B2 | 8,0; 10,2; 10,9; 11,4; 12,0; 13,7; 15,0; | $M(t)=1-e^{-(\frac{t}{12,57})^{5,20}}$ | 11,57 | 2,55 |
| B3 | 2,5; 3,5; 4,2; 5,1; 6,2; | $M(t)=1-e^{-(\frac{t}{4,84})^{2,97}}$ | 4,32 | 1,59 |

#### 3.2.1. Relationship between classes and times

For the analyzed bulldozers, 950 hours and 80 hours are the longest (machine B3) and the shortest (machine B2) recorded periods in operation. Relationship between classes and periods in operation is presented in Fig. 6.

Theoretical cases ($R(t) \to 0$ and $R(t) \to 1$) are excluded and justification for this approximation lies in the fact that, for example $R(t) = 0{,}0036$ means that some machine works about 3000 hours, i.e. about triple more than the largest recorded period in operation, or $R(t) = 1$ means that some machine is completely out of use.

The same logic is used for determination of relationship between periods in maintenance and classes of maintainability. For the first class i.e. the most quality is used period of 2.5 hours, while the seventh class corresponds to 15 hours in maintenance.

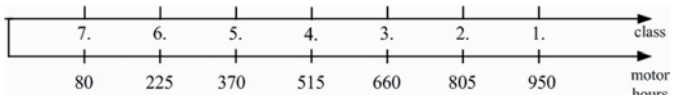


*Fig. 6. Dependence of periods in operation (motor hours) and classes of reliability*

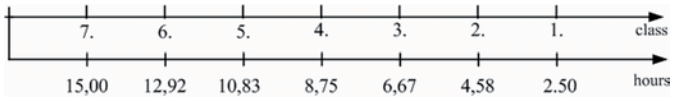


*Fig. 7. Dependence of periods in maintenance (hours) and classes of maintainability*

#### 3.2.2. Location and shape of fuzzy numbers

According to obtained reliability functions (Table II) shape parameters are: 1.18, 1.20 and 1.24, while in the case of maintainability functions (Table III), this parameter has the next values: 5.20, 2.97 and 4.23. Hence, triangular fuzzy numbers will be used for reliability functions, while maintainability functions will be approximated by trapezoidal fuzzy numbers.

Scale parameters are calculated as:

$$x_1 = x_2 = \frac{1.25 \cdot c}{\min\limits_i \sigma_{Bi}} = \frac{(1.25 \cdot 145)\ \text{motor hours}}{363.13\ \text{motor hours}} = 0.499$$

$$y_2 = y_3 = \frac{0.25\ \cdot c}{\min\limits_i \sigma_{Bi}} = \frac{(0.25 \cdot 2.08)\ \text{hours}}{1.59\ \text{hours}} = 0.328$$

$$y_1 = y_4 = \frac{1.25\ \cdot c}{\min\limits_i \sigma_{Bi}} = \frac{(1.25 \cdot 2.08)\ \text{hours}}{1.59\,\text{hours}} = 1.638$$

According to (21-23) and (24-26) scale parameter and fuzzy numbers, as the represents of reliability and maintainability of for selected machines, are calculated and plotted at Fig. 8–10.

$R_{B1}$ = (450.4, 773.4, 1096.5); $R_{B2}$ = (229.7, 411.0, 592.2); $R_{B3}$ = (380.2, 670.2, 960.2);

$M_{B1}$ = (5.4, 8.7, 10.4, 13.8); $M_{B2}$ = (7.4, 10.7, 12.4, 15,7); $M_{B3}$ = (1.7, 3.8, 4.8, 6.9);

From Figures 8-9 the values of intersection of fuzzy numbers B1, B2, B3, and ordinate for each class (from 1 to 7) could be taken, as it is explained at Fig. 10. These values determine reliability and maintainability fuzzy numbers in desirable form (11-12):

$\boldsymbol{R}_{B1}$ = {1/0.45, 2/0.90, 3/0.65, 4/0.20, 5/0, 6/0, 7/0};
$\boldsymbol{R}_{B2}$ = {1/0, 2/0, 3/0, 4/0.43, 5/0.77, 6/0, 7/0};
$\boldsymbol{R}_{B3}$ = {1/0.04, 2/0.54, 3/0.96, 4/0.46, 5/0, 6/0, 7/0};

$\boldsymbol{M}_{B1}$ = {1/0, 2/0, 3/0.38, 4/1.00, 5/0.88, 6/0.25, 7/0};
$\boldsymbol{M}_{B2}$ = {1/0, 2/0, 3/0, 4/0.41, 5/1.00, 6/0.85, 7/0.22};
$\boldsymbol{M}_{B3}$ = {1/0.38, 2/1.00, 3/0.12, 4/0, 5/0, 6/0, 7/0};

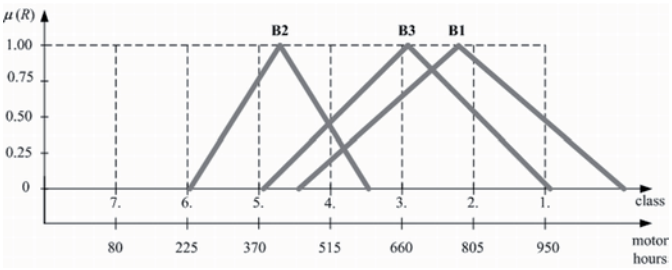


*Fig. 8. Reliability fuzzy numbers for selected bulldozers*

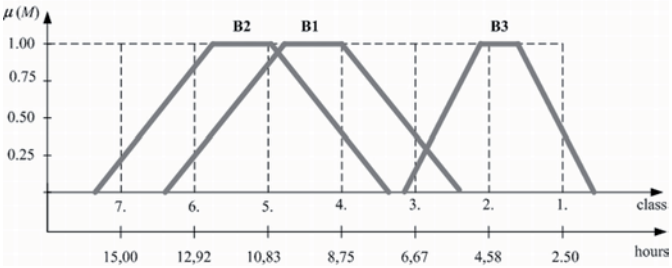


*Fig. 9. Maintainability fuzzy numbers for selected bulldozers*

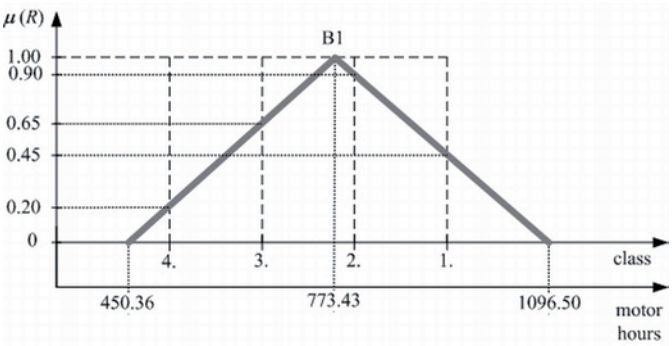


*Fig. 10. Reading the coordinates for reliability of bulldozer B1*

### 3.3. Bulldozers dependability determined by fuzzy model

For dependability determination, equation (2) is used. Calculation in detail is presented only for machine B1.

$\mu_{L(B1)} = (0, 0.5, 1, 0.5, 0, 0, 0);$

$\mu_{R(B1)} = (0.45, 0.9, 0.65, 0.2, 0, 0, 0);$

$\mu_{M(B1)} = (0, 0, 0.38, 1, 0.88, 0.25, 0);$

The first step of max-min composition (3-9) is used, as follows:

$\mu_{M \times L} = (\mu^{i\,j}{}_{M \times L})_{7 \times 7}$,

$$\mu^{i\,j}{}_{M \times L} = \min(\mu^{j}{}_{M}, \mu^{j}{}_{L}) = \begin{bmatrix} 0 & 0 & 0 & 0 & 0 & 0 & 0 \\ 0 & 0 & 0 & 0 & 0 & 0 & 0 \\ 0 & 0.38 & 0.38 & 0.38 & 0 & 0 & 0 \\ 0 & 0.5 & 1 & 0.5 & 0 & 0 & 0 \\ 0 & 0.5 & 0.88 & 0.5 & 0 & 0 & 0 \\ 0 & 0.25 & 0.25 & 0.25 & 0 & 0 & 0 \\ 0 & 0 & 0 & 0 & 0 & 0 & 0 \end{bmatrix}$$

For

$\mu^{j}{}_{D} = \max(\min(\mu^{1}{}_{R}, \mu^{1\,j}{}_{M \times L}), \ldots, \min(\mu^{7}{}_{R}, \mu^{7\,j}{}_{M \times L})), j = 1, \ldots, 7.$

Dependability of machine B1 is estimated as:

$\mu_{D(B1)} = \mu_{R \circ M \times L} = (\mu^{j}{}_{D})_{1 \times 7} = (0, 0.38, 0.38, 0.38, 0, 0, 0)$

Otherwise stated, in form (10): $D_{B1}$ = {1/0, 2/0.38, 3/0.38, 4/0,38, 5/0, 6/0, 7/0}

Dependability estimation (10) for other two types of bulldozers is obtained as:

$D_{B2}$ = {1/0.77, 2/0.75 3/0, 4/0, 5/0, 6/0, 7/0}
$D_{B3}$ = {1/0.54, 2/0.54, 3/0.3, 4/0.15, 5/0, 6/0, 7/0}

Transformation of obtained "classes related" fuzzy sets to linguistic dependability fuzzy sets by using best-fit method is straightforward and explained in detail in (13-16). Best-fit method and proposed dependability fuzzy set (Fig. 2) give the final dependability evaluation for the Machine B1 in the form (13):

$$d_1(D, excellent) = \sqrt{\sum_{j=1}^{7}\left(\mu^{j}{}_{D} - \mu^{j}{}_{iexcellent}\right)^2} = 1.19403$$

$$d_2(D, good) = \sqrt{\sum_{j=1}^{7}\left(\mu^{j}{}_{D} - \mu^{j}{}_{good}\right)^2} = 0.64475$$

$$d_3(D, average) = \sqrt{\sum_{j=1}^{7}\left(\mu^{j}{}_{D} - \mu^{j}{}_{average}\right)^2} = 1.16863$$

$$d_4(D, poor) = \sqrt{\sum_{j=1}^{7}\left(\mu^{j}{}_{D} - \mu^{j}{}_{poor}\right)^2} = 1.41269$$

Where is according to Fig.2.:

$\mu^{j=1\text{to}7}{}_{excellent} = (1, 0.75, 0, \ldots, 0);$ $\mu^{j=1\text{to}7}{}_{good} = (0, 0.25, 1, 0.5, 0, 0, 0);$

$\mu^{j=1\text{to}7}{}_{average} = (0, 0, 0, 0.5, 1, 0{,}25, 0);$ $\mu^{j=1\text{to}7}{}_{poor} = (0, \ldots, 0, 0.75, 1);$

For $d_{i\,min} = d_2$:

$$\alpha_1 = \frac{1}{d_4 / d_2} = 0.53998, \qquad \beta_1 = \frac{\alpha_4}{\sum_{i=1}^{4}\alpha_i} = 0.21192$$

$$\alpha_2 = \frac{1}{d_3 / d_2} = 1.00000, \qquad \beta_2 = \frac{\alpha_3}{\sum_{i=1}^{4}\alpha_i} = 0.39245$$

$$\alpha_3 = \frac{1}{d_2 / d_2} = 0.55171, \qquad \beta_3 = \frac{\alpha_2}{\sum_{i=1}^{4}\alpha_i} = 0.21652$$

$$\alpha_4 = \frac{1}{d_1 / d_2} = 0.45640, \qquad \beta_4 = \frac{\alpha_1}{\sum_{i=1}^{4}\alpha_i} = 0.17911$$

Finally, B1 dependability in linguistic fuzzy form:
$\boldsymbol{D}_{\mathbf{B1}}$ = {($\beta_4$, "poor"), ($\beta_3$, "average"), ($\beta_2$, "good"), ($\beta_1$, "excellent")} =
= {(0,17911, "poor"), (0,21652 "average"), (0,39245, "good"),(0,21192, "excellent")}

For machines B2 and B3, dependability is (Fig. 11) :

$\boldsymbol{D}_{B2}$ = {(0,09655, "poor"), (0,10133, "average"), (0,11003, "good"),(0,69209, "excellent")}
$\boldsymbol{D}_{B3}$ = {(0,16419, "poor"), (0,18100, "average"), (0,24820, good"), 0,40661, "excellent")}

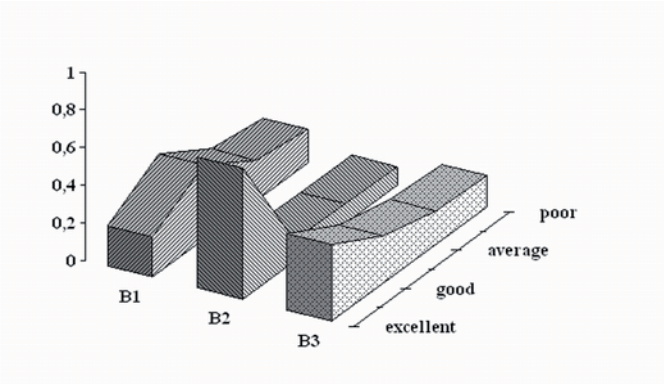


*Fig. 11. Dependability performances of different bulldozers types*

In this way, bulldozer with lowest dependability, i.e. availability, B1 has been identified. This bulldozer has mostly good dependability, while the two others are mostly excellent. Machine B1 also has the worst assessed maintenance support.

## 4. Conclusion

A new approach is proposed in this paper for maintenance support analyses in the framework of the dependability, based on rules of fuzzy algebra. In this approach, maintenance support is evaluated using expertise judgment and fuzzy sets. Thereby, it was necessary to differentiate between possible modes of organizing maintenance support, and to introduce measurement unit that represents quality level of maintenance support organization. The paper presents four possible organizing modes for maintenance support: maintenance through services by producers or licensed organizations, maintenance developed by consumer, maintenance by consumers' request and without organized maintenance. Each of them is conditionally defined, depending on classes as measurement unit. In order to get the necessary overview of the level of maintenance support organization, it is necessary to grasp it in the context of availability of the analyzed technical system, namely of dependability as a measure of availability.

Since dependability is influenced not only by maintenance support, but also by reliability and maintainability, which are usually represented as time functions, it is necessary to define fuzzification model, which will approximate in the best way these functions into a fuzzy form. That fuzzy form is complementary with fuzzy form of maintenance support. Fuzzification process is completed based on the principle of empirical scaling which as the assumption takes that Weibul distribution successfully covers all phenomena related to failures of realistic technical system, and introduces fuzzy set on the base of empirical study, apropos establish relation between measured times and their standard deviations and expected form of reliability/maintainability fuzzy sets. In this way all necessary conditions are accomplished to calculate dependability using rules of fuzzy algebra.

Dependability assessment itself is of great importance for the identification of weak points from the standpoint of quality of maintenance and reliability. In addition, it is very important to find their interdependence and the influence on dependability. This article shows a methodology that effectively considers primarily the level of maintenance support and provides the ability to integration on the level of dependability, on the basis of actual working conditions as a result of empirical studies. The proposed methodology was tested on the example of three bulldozers of different manufacturers, working in a lignite mine.

*Acknowledgement: The research work is supported by the Ministry of Education and Science of the Republic of Serbia.*

## References

1. Avizienis A, Laprie J, Randell B. Dependability and its threats - A taxonomy. IFIP 18th World Computer Congress, topical sessions. Proceedings, Toulouse, France. Kluwer 2004; 91–120.
2. Chen S.M. Fuzzy system reliability analysis using fuzzy number arithmetic operations. Fuzzy Sets and Systems 1994: 64: 31–38.
3. Ebramhimipour V, Suzuki K. A synergetic approach for assessing and improving equipment performance in offshore industry based on dependability. Reliability Engineering and System Safety 2006; 91(1): 10–19.
4. Emblemsvag J, Tonning L. Decision support in selecting maintenance organization. Journal of Quality in Maintenance Engineering 2003; 9(1): 11–24.
5. Hoos H.H, Stutzle T. On the Empirical Scaling of Run-time for Finding Optimal Solutions to the Traveling Salesman Problem. University of British Columbia, Department of Computer Science. Technical Report TR-2009-17, 2009.
6. Ivezic D, Tanasijevic M, Ignjatovic D. Fuzzy Approach to Dependability Performance Evaluation. Quality and Reliability Engineering International, 2008. Vol. 24(7), pp. 779–792.
7. Ivkovic S. Failures of mining machinery' elements. Faculty of Mining and Geology, Belgrade, Serbia, 1997. (In Serbian)
8. Jovancic P, Ignjatovic D. Designing of the maintenance system for mining equipment at Serbian lignite open pits – strategy definition. Conference Proceedings – X International Maintenance Conference EUROMAINTENACE 2010. Proceedings, Fiera di Verona, Italy 2010; 378–381.
9. Khanlari A, Mohammadi K, Sohrabi B. Prioritizing equipments for preventive maintenance (PM) activities using fuzzy rules. Computers and Industrial Engineering 2008; 54(2): 169–184.
10. Klir G.J, Yuan B. Fuzzy sets and fuzzy logic: theory and applications. Prentice Hall: New York, 1995.
11. Knapp G.M, Mahajan M. Optimization of maintenance organization and manpower in process industries. Journal of Quality in Maintenance Engineering 1998; 4(3): 168–183.
12. Kuo T.C, Huang S.H. Design for manufacture and design for 'X': Concepts, applications, and perspectives. Computers and Industrial Engineering 2001; 41(3): 241–260.
13. Saraswat S, Yadava G.S. An overview on reliability, availability, maintainability and supportability (RAMS) engineering. International Journal of Quality and Reliability Management 2008; 25(3): 330–344.
14. Strandberg K. IEC 300: the dependability counterpart of ISO 9000. Reliability and Maintainability Symposium. Proceedings, Orlando, FL, 1991; 463–467.

15. Seo K.K, Ahn B.J. A learning algorithm based estimation method for maintenance cost of product concepts. Computers and Industrial Engineering 2006; 50(1–2): 66–75.
16. Study: Selection of the optimal maintenance system at the Lignite Basin Kostolac, Public Enterprise" Electric Power Industry of Serbia" – University of Belgrade, Faculty of Mining and Geology, Faculty of Electrical Engineering, 2006.
17. Tanasijevic M, Ivezic D, Ignjatovic D, Polovina D. Dependability as criteria for bucket wheel excavator revitalization, Journal of Scientific & Industrial Research 2011; 70(1):13–19
18. Wang N, Kang R, Jia Z, Wang L. An algorithm for evaluation and analysis of stationary operational availability basing on mission requirements. Eksploatacja i Niezawodnosc – Maintenance and Reliability 2010; 46(2): 31–35.
19. Wang J, Yang J.B, Sen P. Safety analyses and synthesis using fuzzy sets and evidential reasoning. Reliability Engineering and System Safety 1995; 47(2): 103–118.
20. Wang J, Yang J.B, Sen P. Multy person and multy-atribute design evaluations using evidential reasoning based on subjective safety and coast analyses. Reliability Engineering and System Safety 1996; 52(2): 113–128.
21. Wu Y. Scale, Factor Intensity and Efficiency: An Empirical Study of the Chinese Coal Industry. Applied Economics, Taylor and Francis Journals 1993; 25(3): 325–334.

**Doc. Dr Miloš TANASIJEVIĆ**
**Prof. Dr Dejan IVEZIĆ**
**Doc. Dr Predrag JOVANČIĆ**
**Prof. Dr Dragan IGNJATOVIĆ**
University of Belgrade – Faculty of Mining and Geology,
Djusina 7, 11120 Belgrade, Serbia
E-mail: tan@rgf.bg.ac.rs; ivezic@rgf.bg.ac.rs; pjovancic@rgf.bg.ac.rs; gagi@rgf.bg.ac.rs

**Prof. Dr Uglješa BUGARIĆ**
University of Belgrade - Faculty of Mechanical Engineering,
Kraljice Marije 16, 11120 Belgrade, Serbia
E-mail: ubugaric@mas.bg.ac.rs

Article citation info:
CHŁOPEK Z. Research on energy consumption by an electrically driven automotive vehicle in simulated urban conditions. Eksploatacja i Niezawodnosc – Maintenance and Reliability 2013; 15 (1): 75–82.

Zdzisław CHŁOPEK

# RESEARCH ON ENERGY CONSUMPTION BY AN ELECTRICALLY DRIVEN AUTOMOTIVE VEHICLE IN SIMULATED URBAN CONDITIONS

# BADANIA ZUŻYCIA ENERGII PRZEZ SAMOCHÓD ELEKTRYCZNY W WARUNKACH SYMULUJĄCYCH JAZDĘ W MIEŚCIE*

*In recent years, dynamic development of electric drives in automotive applications has been taking place. Electrically driven vehicles are considered to offer a possibility of solving the most important ecological problems posed by motorisation. The paper presents results of testing the energy consumption by an electric car in conditions corresponding to actual operation of such vehicles, i.e. at drive tests where urban, extra–urban, and traffic jam conditions were simulated. The disitance energy consumption and total vehicle efficiency were determined at drive tests. An energy consumption characteristic was determined in pseudorandom conditions of urban operation of the car, with employing the Monte Carlo method for this purpose.*

***Keywords**: electric car, energy consumption, efficiency.*

*W ostatnich latach następuje dynamiczny rozwój napędów elektrycznych w motoryzacji. W samochodach elektrycznych upatruje się możliwości rozwiązania najważniejszych problemów ekologicznych motoryzacji. W pracy przedstawiono wyniki badań zużycia energii przez samochód elektryczny w warunkach odpowiadających rzeczywistej eksploatacji takich pojazdów, mianowicie w testach jezdnych symulujących ruch w miastach, poza miastami, a także w zatorach drogowych. Wyznaczono drogowe zużycie energii i sprawność ogólną pojazdu w testach jezdnych. Wyznaczono charakterystykę zużycia energii w warunkach pseudoprzypadkowych użytkowania samochodu w mieście. Wykorzystano do tego celu metodę Monte Carlo.*

***Słowa kluczowe**: samochód elektryczny, zużycie energii, sprawność.*

## 1. Introduction

Motorisation poses significant hazards to the environment. A considerable part of these hazards is connected with using combustion engines to power automotive vehicles. The most conspicuous hazards include exhaust and noise emissions and using–up of the natural resources necessary for the production of liquid and gaseous fuels. The use of electric motors for automotive applications makes it possible to eliminate exhaust emissions along transport routes and to reduce noise emission, because it is generally known that this has been made possible by the present–day technologies of electric drives [10, 14, 16, 26]. At the same time, however, we must be aware of the fact that the platitudinous term "zero–emission vehicles" is only a populist expression having merely a propaganda value and being of not very high standard at that. Firstly, there are a number of automotive pollutant sources other than the combustion engine, e.g. dust emission sources such as various tribological pairs in the vehicle, interaction between tyres and road surface, or stirring–up of road dust [4]. Secondly, a vehicle powered by an electric motor does not emit combustion gases, but the generation of the electric energy used to power the vehicle results in environmental pollution, too. The electricity generation is still based to a considerable extent on the combustion of fossil fuels, predominantly hard coal. Moreover, the technologies of electricity generation with the use of hard coal are not, in many cases, adequately clean; therefore, not only the greenhouse gas emissions but also the emissions of pollutants harmful to human heath cannot be thus avoided. Obviously, a solution of the future is the use of renewable energy, chiefly the energy directly obtained from solar radiation (photoelectric cells), and nuclear energy; particularly high hopes are placed on the use of nuclear fusion [20]. To assess the pollutant emissions from automotive vehicles during the whole cycle of production and use of energy carriers, the "Well-to-Wheel" analysis, i.e. the analysis from the source (of an energy carrier) to the wheel (of a vehicle), may be employed [25, 27]. This cycle is divided into two stages, namely "Well-to-Tank," i.e. from the source to the tank (of the energy carrier in the vehicle), and "Tank-to-Wheel," i.e. from the tank to the wheel [25].

Another issue is the evaluation of the environmental benefits gained from the application of electric drives to automotive vehicles, carried out with employing the Life Cycle Impact Assessment (LCIA) method[1] [12]. In this method, not only the information obtained by inventorying the energy and pollutant emissions but also specific environmental hazards such as eutrophication, acidification, noise, vibrations, smog, electromagnetic radiation, dust, land-use change, damage

1 In the English–to–Polish translation, it has become a common but incorrect and reprehensible practice to use the term "życie" (literally "life"), borrowed from English, in relation to objects other than organisms, and not only in official documents but also in scientific publications at that! According to the Dictionary of the Polish Language, "życie" is an organism's state consisting in an uninterrupted train of processes making it possible for the organism to react to stimuli and, usually, to move. According to the Encyclopaedia issued by Państwowe Wydawnictwo Naukowe (Polish Scientific Publishers PWN), "życie" is a biological phenomenon, complex and multidimensional, which cannot be described with the use of one simple definition. This phenomenon is exclusively known from the Earth; in this context, it is defined as having two basic meanings: it describes the state of a substance (referred to as an organism) that lasts from the coming up (birth) of the organism till the end of its individual existence, i.e. its death in most cases, or it describes the dynamic process that began on the Earth about 3.8 billion years ago and covered all the organisms that existed in the past and live now and derive from one initial form, including any mutual interrelationships and dependencies and their environmental impact.
The fact that the term "life" is used in English in the meaning of "existence" does not entitle the Poles to disregard the culture of the Polish language and to translate this term as "życie" (incorrect, literally "life") instead of "istnienie" (correct, literally "existence").

(*) Tekst artykułu w polskiej wersji językowej dostępny w elektronicznym wydaniu kwartalnika na stronie ***www.ein.org.pl***

to resources, e.g. water and raw materials used to produce fossil fuels, climate changes, ozone layer depletion, etc., are taken into account [12]. With respect to automotive vehicles, the LCIA method makes it possible to assess their environmental impact at all the vehicle existence stages, from production through operation right to the management of the vehicles when worn-out. Such an analysis may also cover the vehicle operation infrastructure. When the life cycle impact assessment method is applied to electrically driven automotive vehicles, many factors that are very harmful to the environment, especially the production and use of batteries and the management of the batteries that have been withdrawn from service, should be taken into consideration [1, 11, 13, 16, 18, 21, 27].

This cautious approach to the problem of electric vehicles is by no means inconsistent with the dynamic work on development of electric drives not only in small passenger cars but also in commercial vehicles [1, 8–11, 13–16, 18, 21–23, 26, 27] and in single–track vehicles [24].

An important problem is the evaluation of energy consumption by electric vehicles in conditions corresponding to the typical conditions in which such vehicles are actually used. At the current state of technical development, electric vehicles are thought of as being chiefly intended for urban traffic [1, 3, 8–11, 14–16, 18, 21–23, 26, 27]. In this connection, the conditions corresponding to the actual operation of electric vehicles represent urban traffic inclusive of special cases, i.e. the traffic in central urban areas and in suburbs. In this study, the traffic models to represent the actual electric vehicle operation conditions were adopted in accordance with the European UDC (Urban Driving Cycle) and American FTP-75 (Federal Transient Procedure) type approval tests, see Figs. 1 and 2, respectively [28]. The UDC test is a typical model of the driving of passenger cars and light–duty goods vehicles in towns, while the FTP-75 test covers both the urban and suburban traffic conditions. The test program described herein was

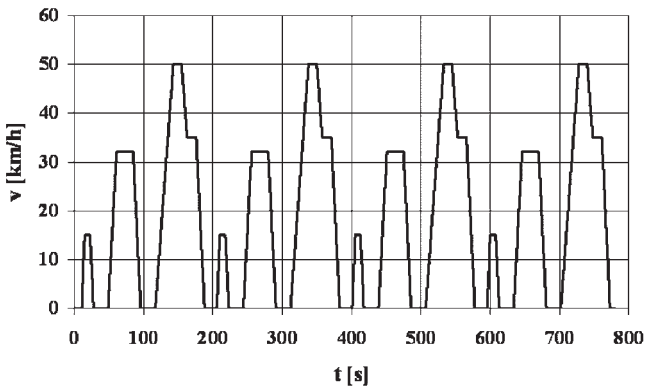


*Fig. 1. The UDC test*

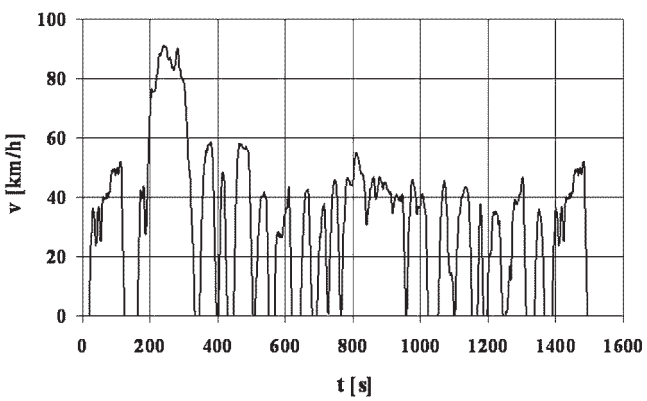


*Fig. 2. The FTP–75 test*

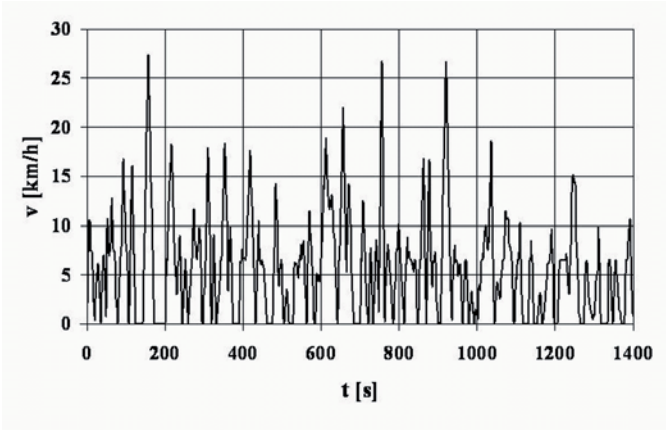


*Fig. 3. The Stop–and–Go test*

additionally extended by adding to it the Stop-and-Go test procedure, which represents the street jam traffic type, Fig. 3 [2, 6].

The traffic models adopted cover most of the passenger car traffic conditions occurring in urban areas.

## 2. The system of quantities adopted to describe the energy consumption by an electric vehicle

The system of quantities adopted to describe the energy consumption by an electric vehicle has been presented below.

For an electric vehicle without braking energy recuperation, the efficiency system is defined as follows:

– efficiency of the vehicle drive:

$$\eta_D = \frac{N_R}{N_T} \tag{1}$$

– efficiency of the battery charging:

$$\eta_{CH} = \frac{N_T}{N_{CH}} \tag{2}$$

– total efficiency:

$$\eta_G = \eta_{CH} \cdot \eta_D \tag{3}$$

where: $N_T$ – electric vehicle drive power;
$N_R$ – resistance–to–motion[2] power;
$N_{CH}$ – battery charging power.

For an electric vehicle with braking energy recuperation, the efficiency system is defined as follows.

– efficiency of the vehicle drive:

$$\eta_D = \frac{N_R}{N_T - N_U} \tag{4}$$

– efficietncy of the braking energy recuperation:

$$\eta_U = \frac{N_U}{N_B} \tag{5}$$

2 The term "resistance to motion" should be understood in this context as the phenomenon rather than the forces.

where: $N_B$ – electric machine braking power;
$N_U$ – braking energy recuperation power.

The distance energy consumption is defined as derivative of the energy consumed relative to the distance travelled. In particular:

– for an electric vehicle without braking energy recuperation, it is:

$$c = \frac{dL_T(s)}{ds} \tag{6}$$

where: $s$ – distance travelled by the vehicle;
$L_T(s)$ – work of the electric vehicle drive as a function of the distance travelled.

– for an electric vehicle with braking energy recuperation, the distance energy consumption is:

$$c = \frac{d\left(L_T(s) - L_U(s)\right)}{ds} \tag{7}$$

where: $L_U(s)$ – braking energy recuperated as a function of the distance travelled.

The average value of the distance energy consumption for the test is defined by the following formulas.

– for an electric vehicle without braking energy recuperation, it is:

$$c_{AV} = \frac{L_T}{s} = \frac{AV\left[N_T(t)\right]}{AV\left[v(t)\right]} \tag{8}$$

where: $t$ – time;
$L_T$ – work done by the electric drive of the vehicle during the test with test duration time $t_f$, see below:

$$L_T = \int_0^{t_f} N_T(t)\,dt \tag{9}$$

$s$ – distance travelled by the vehicle during the test, see below:

$$s = \int_0^{t_f} v(t)\,dt \tag{10}$$

AV – averaging operator.

– for an electric vehicle with braking energy recuperation, the distance energy consumption is:

$$c_{AV} = \frac{L_T - L_U}{s} = \frac{AV\left[N_T(t)\right] - AV\left[N_U(t)\right]}{AV\left[v(t)\right]} \tag{11}$$

where: $L_U$ – braking energy recuperated during the test, see below:

$$L_U = \int_0^{t_f} N_U(t)\,dt \tag{12}$$

A schematic diagram of the power flow in the powertrain[3] of an electric vehicle with electricity recuperation has been shown in Fig. 4.

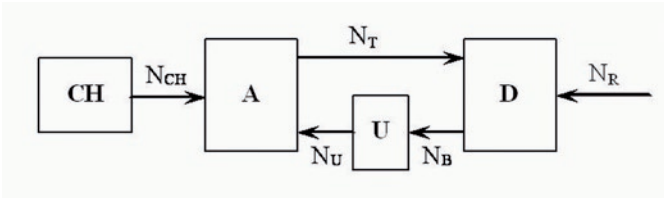


*Fig. 4. Schematic diagram of the power flow in the powertrain of an electric vehicle with electricity recuperation.*

*Legend: CH – battery charging system; A – battery; D – vehicle driving system; U – braking energy recuperation system; NCH – battery charging power; NT – electric vehicle drive power; NR – resistance–to–motion power; NB – electric machine braking power; NU – braking energy recuperation power*

Noteworthy is the fact that the energy balance in the driving system of a vehicle determines whether the vehicle state is static, i.e. the vehicle moves with a constant speed, or dynamic, i.e. the vehicle accelerates or decelerates. The electric machine braking power differs from the total vehicle braking power because the latter additionally includes the power dissipated in the braking system by friction brakes. A part of the electric machine braking power may be recuperated: the electric energy recovered during the braking process may be stored in the battery.

## 3. Results of empirical tests of an electric vehicle carried out on a chassis dynamometer

Empirical tests of the energy consumption by an electric vehicle were carried out on a chassis dynamometer at the Environmental Protection Centre of ITS (Motor Transport Institute) [3]. The test specimen was an electric passenger car Zilent Courant, made in the People's Republic of China. In the Zilent Courant car, the electric motors were exclusively powered from a battery of electric storage cells. The vehicle powertrain had no braking energy recuperation system. The vehicle running mass was 1 170 kg.

The power rating of the vehicle's electric motor was 8.5 kW. The car was provided with 10 maintenance–free lead–acid batteries, each of 12 V and 100 Ah rated voltage and capacity, respectively.

The maximum and economical speed of the car was 85 km/h and 40 km/h, respectively. The vehicle range when driven at the economical speed was claimed as not less than 150 km.

The car tested was classified in the category of vehicles of simple construction. It was provided with neither battery systems of new generation nor braking energy recuperation system. The utility indicators did not qualify the car tested to the category of modern electric vehicles, either. The vehicle range was short, the maximum speed was low, and the dynamic characteristics of the vehicle were all the more unsatisfactory. These features had an effect on the sceptical opinion about the passive safety and comfort of use of the vehicle.

The tests were carried out on a single-roller chassis dynamometer with controlled load characteristics, manufactured by AVL-Zöllner [3].

The parameters measured during the tests carried out on the chassis dynamometers included:

– vehicle speed measured on the chassis dynamometer roller;
– voltage of the battery set;

3 The term "driving system" is to be understood, consistently with the traditional meaning adopted in automotive sciences, as the system to transmit mechanical energy from the motor to the road wheels of a vehicle ("power transmission system"). The driving system taken together with the motor and the energy storage reservoir is referred to in this paper as "powertrain."

– current in the electric drive wiring of the vehicle.

The characteristic curve of the power absorbed by the chassis dynamometer was identified based on empirical vehicle coast–down tests [3].

The signals representing the quantities measured were recorded with 1 s sampling time. Each signal value recorded constituted an averaged result of a series of 10 measurements carried out with 0.1 s time intervals. The signals recorded were preliminarily processed to eliminate gross errors and to reduce the share of high–frequency noise. The gross errors were searched by analysing the current signal variance. To reduce the share of high-frequency noise in the signals recorded, the signals were subjected to low–pass filtration, with a Golay-Savitzky filter being used, where both-side approximation from 2 data points on each side to a polynomial of degree 2 was applied.

Results of the empirical vehicle tests carried out to the Stop-and-Go test procedure have been presented in Figs. 5 and 6. The former shows time histories of the current drawn from the battery set and of the voltage measured on the battery set terminals while time histories of the electric vehicle drive power and of the resistance–to–motion power can be seen in the latter.

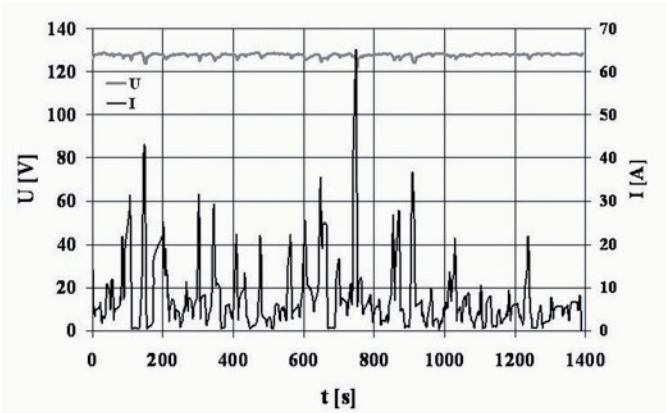


*Fig. 5. Current drawn from the battery set and voltage measured on the battery set terminals vs. time, at the Stop–and–Go test*

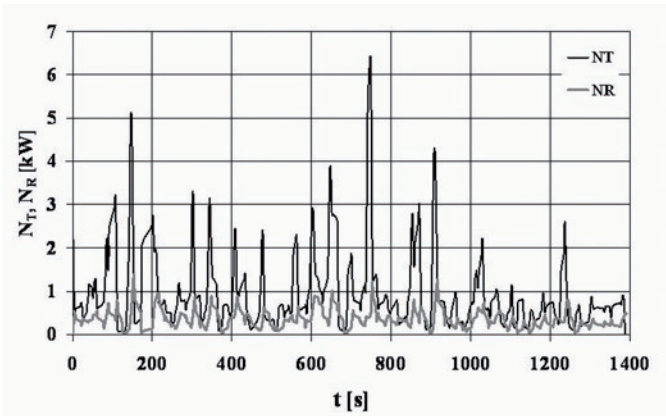


*Fig. 6. Electric vehicle drive power and resistance–to–motion power vs. time, at the Stop–and–Go test*

Results of the empirical vehicle tests carried out to the UDC test procedure have been presented in Figs. 7 and 8. Results of the empirical vehicle tests carried out to the FTP-75 test procedure have been presented in Figs. 9 and 10.

Based on the experimental tests, the total vehicle efficiency was determined. The total efficiency was calculated as the product of efficiency of the vehicle drive and efficiency of the battery charging. The efficiency of the vehicle drive was determined from empirical tests carried out. However, a problem was encountered with correct

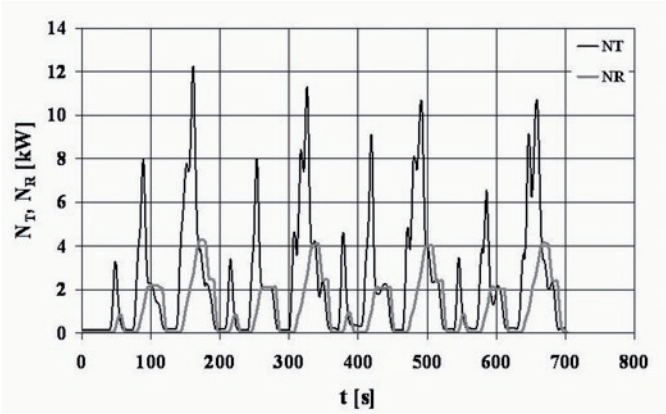


*Fig. 8. Electric vehicle drive power and resistance–to–motion power vs. time, at the UDC test*

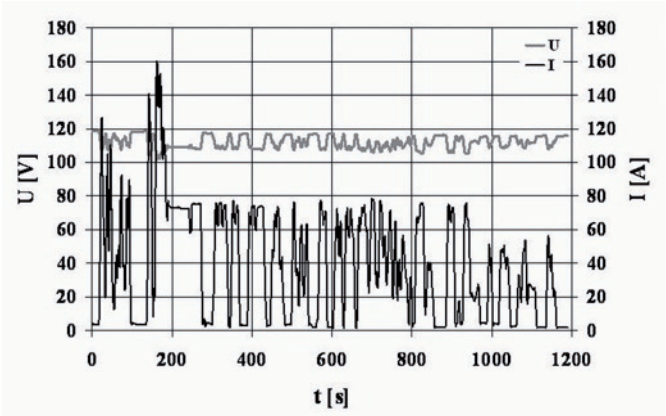


*Fig. 9. Current drawn from the battery set and voltage measured on the battery set terminals vs. time, at the FTP–75 test*

adopting of the battery charging efficiency. The vehicle drive and battery charging processes do not take place at the same time; therefore, the notion of total vehicle efficiency is rather symbolic and, in principle, the total efficiency may only be evaluated in the conditions of energy balance. The battery charging efficiency values that can be found the literature significantly differ from each other, depending on battery type. As an example, the battery charging efficiency has been specified in publication [10] as 0.86, while significantly lower values, even of the order of 0.6, were recorded for lead–acid batteries at the tests described in report [3]. Finally, the battery charging efficiency value was assumed as 0.65 for the purposes of the analyses presented herein.

The total vehicle efficiency values as recorded at specific tests have been shown together in Fig. 11.

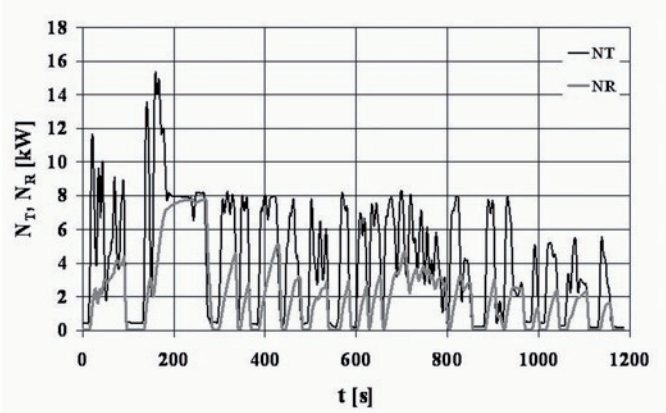


*Fig. 10. Electric vehicle drive power and resistance–to–motion power vs. time, at the FTP–75 test*

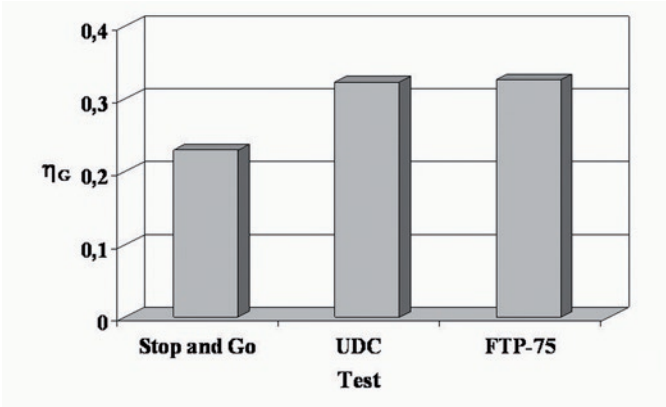


*Fig. 11. Total vehicle efficiency as determined from the Stop–and–Go, UDC, and FTP–75 tests*

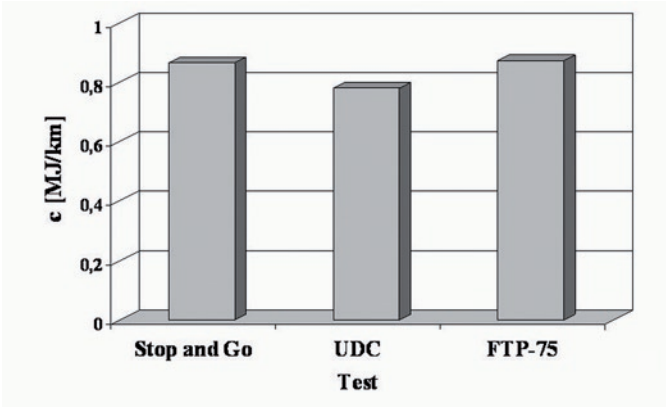


*Fig. 12. Average distance energy consumption as determined at the Stop–and–Go, UDC, and FTP–75 tests*

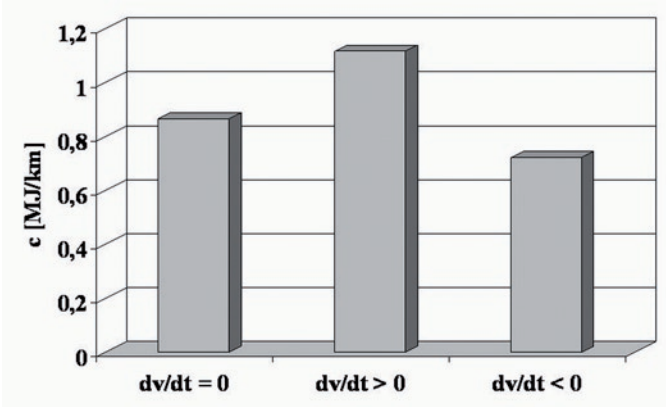


*Fig. 13. Average distance energy consumption as determined in the dynamic states of positive and negative acceleration at the Stop–and–Go test*

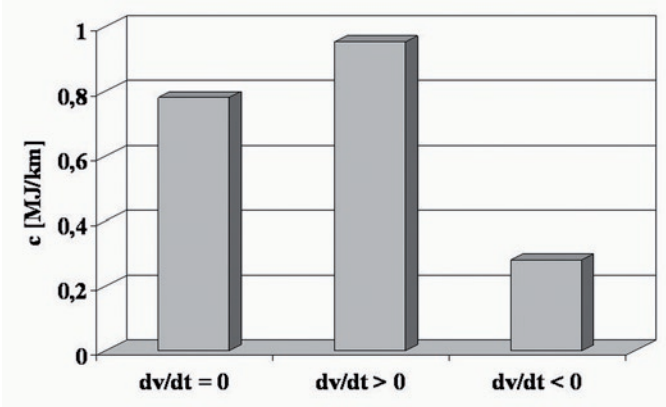


*Fig. 14. Average distance energy consumption as determined in the dynamic states of positive and negative acceleration at the UDC test*

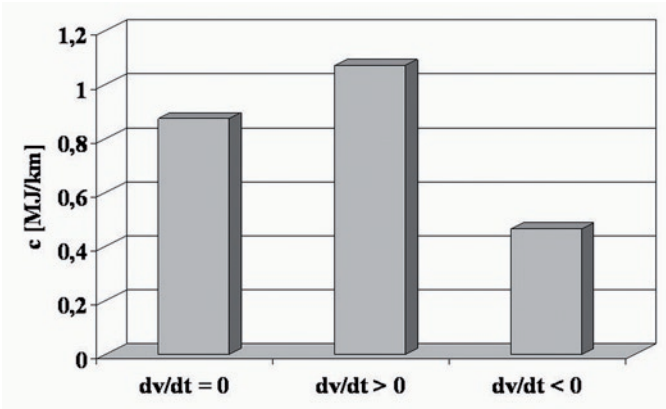


*Fig. 15. Average distance energy consumption as determined in the dynamic states of positive and negative acceleration at the FTP–75 test*

The total vehicle efficiency values recorded at the tests carried out for type approval purposes are similar to each other, although the tests significantly differed from each other in their dynamic parameters. However, these tests show much closer similarity to each other than to the Stop-and-Go test in respect of the average speed values. A considerably lower value of the total vehicle efficiency was recorded at the Stop-and-Go test, characterised by frequent acceleration and deceleration, with the average vehicle speed being about 5.8 km/h. The specific conditions of this test are likely to cause much higher energy losses. A similar situation can also be observed in the case of automotive vehicles powered with combustion engines [2, 6].

The average distance energy consumption has been presented in Fig. 12.

The average distance energy consumption values were similar to each other at the Stop-and-Go and FTP-75 tests, while this value recorded at the UDC test was visibly lower. This is probably related to the dynamic characteristics of the speed programs followed during the tests carried out. The FTP-75 and Stop-and-Go test programs are more dynamic in comparison with that of the UDC test, which can be seen e.g. in the frequency characteristics: the power spectral density of vehicle speed at the FTP-75 and Stop-and-Go tests exceeds that determined at the UDC test at high frequencies [6]. This is a consequence of the method of setting–up the test programs: the FTP-75 and Stop-and-Go test programs are built in conformity with the criterion of accurate time–domain simulation while the UDC program is synthesised in accordance with the criterion of similarity of point–type characteristics of test conditions and actual vehicle operation conditions.

Tests to determine the average distance energy consumption were also carried out in dynamic states, i.e. at positive and negative acceleration. Results of these analyses have been presented in Figs. 13, 14, and 15.

The analysis results are consistent with expectations: the distance energy consumption was higher during the vehicle acceleration phase. The biggest differences between the distance energy consumption values in the dynamic conditions under consideration occurred at the UDC test.

## 4. Determining of energy consumption characteristics in pseudorandom vehicle operation conditions

To determine energy consumption characteristics in pseudorandom vehicle operation conditions, the Monte Carlo method [5–7, 17] was used. The essence of the Monte Carlo method lies in using

generators of random or pseudorandom figures not only in numerical methods but also, and above all, in the creation of an intellectual random or pseudorandom reality the exploration of which would make it possible to get to know the causal and random properties of the reality being experienced [7].

The pseudorandom vehicle operation conditions are treated as a pseudorandom history of vehicle speeds, which is a realisation of the stochastic process of vehicle speeds [5, 6]. As a point-type characteristic of the vehicle speed process, the average vehicle speed is considered [5, 6]:

$$v_{AV} = \frac{s}{\tau} \tag{13}$$

where: $s$ – distance travelled by the vehicle;
$\tau$ – travel time.

The vehicle motion is modelled as a combination of the vehicle motions that take place during the Stop-and-Go, UDC, and FTP-75 tests.

The distance travelled by the vehicle is modelled as a linear combination:

$$s_{\Sigma} = \sum_{i=1}^{3} v_i \cdot t_i \tag{14}$$

where: $t$ – time treated as a random variable with uniform distribution;
$i$ = 1, 2, 3, representing the Stop-and-Go, UDC, and FTP-75 tests, respectively.

The time of duration of the pseudorandom test is:

$$t_{\Sigma} = \sum_{i=1}^{3} t_i \tag{15}$$

Hence, the average vehicle speed at the pseudorandom test is:

$$v_{AV\Sigma} = \frac{s_{\Sigma}}{t_{\Sigma}} \tag{16}$$

The energy consumed to drive the vehicle during the pseudorandom test is:

$$L_{D\Sigma} = \sum_{i=1}^{3} v_i \cdot t_i \cdot c_i \tag{17}$$

where: $c_i$ – average distance energy consumption at individual tests.

The total average distance energy consumption at the pseudorandom test is:

$$c_{\Sigma} = \frac{L_{D\Sigma}}{s_{\Sigma}} \tag{18}$$

A characteristic of the distance energy consumption in the pseudorandom vehicle operation conditions, taken as an example, has been shown in Fig. 16 in the form of a relation of the distance energy consumption vs. the average vehicle speed. Individual points represent successive experiments with pseudorandom generation of the duration times of the Stop-and-Go, UDC, and FTP-75 tests. A straight line to approximate the set of points in accordance with the least–squares criterion has also been plotted on the graph.

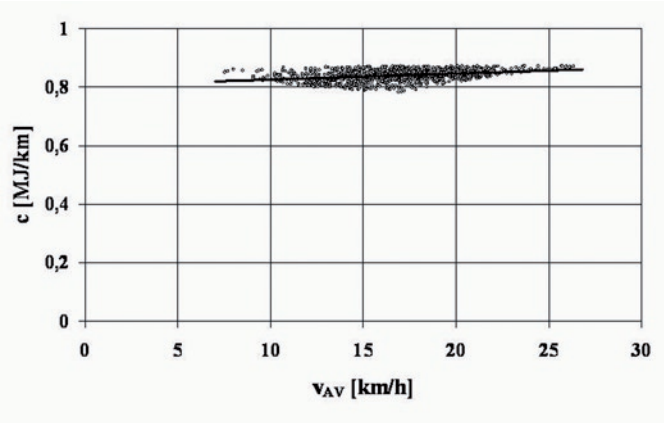


*Fig. 16. A characteristic of the distance energy consumption in the pseudorandom vehicle operation conditions*

As it can be seen from the characteristic map of points having been determined, the dependence of the distance energy consumption on the average vehicle speed in dynamic conditions fundamentally differs from the similar characteristic curve determined for combustion engines. The distance fuel consumption by automotive combustion engines considerably drops with rising average vehicle speeds providing that the speeds remain within the range of low speed values; in contrast to this, the characteristic curve determined for the electric vehicle showed low sensitivity to the average vehicle speed. Obviously, this conclusion should not be generalised because the characteristic map was determined for only one vehicle; however, this test result is interesting and worth attention.

Multiple pseudorandom experiments showed the characteristic maps obtained to be almost insensitive to the successive series of tests. This indicates very low sensitivity of energy consumption by an electric vehicle to pseudorandom vehicle operation conditions defined by the process of vehicle speeds.

## 5. Recapitulation

Electrically driven automotive vehicles are commonly believed to be the future of motorisation, chiefly for environmental protection reasons. Therefore, it is reasonable to investigate the properties of such vehicles in the aspect of energy consumption. The research work results presented herein have confirmed that the research method proposed is effective and makes it possible to obtain unbiased results. The proposed method of determining distance energy consumption characteristics in pseudorandom conditions with employing the Monte Carlo method is a remarkable procedure to investigate the energy consumption by electric vehicles.

At the current stage of technical progress, the major constraints on the proliferation of electric vehicles are imposed by the following:

- technical standard of electricity storage batteries, which are heavy, costly, insufficiently durable, and having low energy storage capacity, which makes it impossible to achieve adequate vehicle operation range;
- large–scale electricity generation technologies, where the methods commonly considered environment-friendly have not been adequately used until now.

The development in the field of electricity storage batteries is insufficiently dynamic for optimism to prevail as regards to the possibility of overcoming this barrier to development of electric vehicles in the nearest future.

The energy sources on the Earth may be classified as follows:

1. Energy of solar radiation, in particular:
   – internal energy of the atmosphere and earth crust;
   – biological fuels;
   – fossil fuels of biological origin;
   – kinetic energy of the movement of atmospheric air;
   – kinetic energy of water movements (gravitational and thermal currents).
2. Kinetic energy of the Earth and the Solar System (tidal energy, energy of internal friction).
3. Energy of chemical bonds in the substance of the Earth.
4. Nuclear energy of the substance of the Earth: decay energy (natural and artificial) and fusion energy (artificial).
5. Internal energy of the Earth.
6. Energy of cosmic radiation.

For ecological and economic reasons, the electricity generation technology should satisfy at least one of the following two requirements:

– renewability of energy sources or utilisation of the energy of the Earth;
– low pollutant emissions from the electricity generation process.

In this connection, the electricity generation technologies of the future are considered those where the following energy sources are to be utilised:

– renewable energy carriers, i.e. biofuels, air and water (kinetic energy), and solar radiation thanks to the use of photoelectric cells;
– energy of the Earth;
– nuclear fission;
– nuclear fusion.

In the future, the electricity generation problem may be expected to be no longer considered the most important barrier to the development of electric vehicles.

Another barrier to the popularisation of the use of electric vehicles is the infrastructure of battery recharging stations and the battery recharging technology (the battery recharging process takes much more time than the refuelling of vehicles with combustion engines powered with liquid or gaseous fuels).

Regardless of the limitations to the development of electric vehicles, one of the most important issues concerning the operation of such vehicles is the energy consumption problem, which determines to a considerable extent the economic effectiveness of electric road transport.

## References


1. Becker TA, Sidhu I., Tenderich B. Electric vehicles in the United States. A New model with forecasts to 2030. Center for Entrepreneurship & Technology, Technical Brief Number 2009.1.v.2.0. August 24, 2009.
2. BUWAL, INFRAS AG: Luftschadstoffemissionen des Strassenverkehrs 1950 – 2010. BUWAL–Bericht Nr. 255. 1995.
3. Chłopek Z. et al.: Badania empiryczne zużycia energii przez samochód elektryczny w warunkach symulujących rzeczywiste użytkowanie (Empirical tests of the energy consumption by an electric vehicle in conditions simulating actual operation of the vehicle). Report of ITS statutory work No. 6110/COŚ, Warszawa, 2012.
4. Chłopek Z, Jakubowski A. A study of the particulate matter emission from the braking systems of motor vehicles. Eksploatacja i Niezawodnosc – Maintenance and Reliability 2009; 4 (44): 45–52.
5. Chłopek Z, Laskowski P. Pollutant emission characteristics determined using the Monte Carlo Method. Eksploatacja i Niezawodnosc – Maintenance and Reliability 2009; 2 (42): 42–51.
6. Chłopek Z. Modelowanie procesów emisji spalin w warunkach eksploatacji trakcyjnej silników spalinowych (Modelling of exhaust emission processes in the conditions of operation of combustion engines in mobile applications). Prace Naukowe Politechniki Warszawskiej – Mechanika, Publishing House of the Warsaw University of Technology, 173/1999.
7. Chłopek Z. The cognitive interpretation of the Monte Carlo method for the techni¬cal applications. Eksploatacja i Niezawodnosc – Maintenance and Reliability 2009; 3 (43), 38–46.
8. Delucchi MA. Electric and gasoline vehicle lifecycle cost and energy-use model. Report for the California Air Resources Board. Final Report UCD-ITS-RR-99-04. Davis, California, Institute of Transportation Studies – University of California, 2000.
9. Delucchi MA. Emissions of greenhouse gases from the use of transportation fuels and electricity. Report ANL/ESD/TM-22, Argonne, Illinois, Argonne National Laboratory, 1991.
10. Eberhard M, Tarpenning M. The 21st century electric car. Tesla Motors Inc., 6 October 2006.
11. Gaines L, Singh M. Energy and environmental impacts of electric vehicle battery production and recycling. SAE Total Life Cycle Conference and Exposition, Vienna, 1995.
12. Goedkoop M, Spriensma R. The Eco-indicator 99. A damage oriented method for Life Cycle Impact Assessment. Methodology Report. Pre Consultants B. V. Amersfoort, 2001.
13. Hirabayashi T, Furuta S, Satou H. Cost estimation on advanced batteries for electric vehicle. 1992 ISATA Proceedings, SAE Paper 920238.
14. Hirota T. Nissan's electric and hybrid electric vehicle program. SAE Hybrid Vehicle Symposium, San Diego CA, 13–14 February 2008.
15. Kromer MA, Heywood JB. Electric powertrains: Opportunities and challenges in the US light-duty vehicle fleet. Publication No. LFEE 2007–03 RP.
16. Matthew-Wilson C. A critique of the economic and environmental value of electric cars. C. Matthew-Wilson, 2010.
17. Metropolis N, Ulam S. The Monte Carlo method. Journal of the American Statistical Association, Vol. 44, No. 247 (Sep., 1949), 335–341.
18. Núñez PJM et al. Electric vehicle. A cyclical story of death and resurrection. International Conference on Renewable Energies and Power Quality (ICREPQ'10), Granada (Spain), 23th–25th March, 2010.
19. Savitzky A, Golay MJE. Smoothing and differentiation of data by simplified least squares procedures. Analytical Chemistry, 36/1964, 1627–1639.
20. Surdacki P. Reaktor termojądrowy jako źródło energii wykorzystujące technologie plazmowe i nadprzewodnikowe (Thermonuclear reactor as an energy source where plasma and superconductivity technologies are used). A chapter in the monograph "Energia niekonwencjonalne i zagospodarowanie odpadów" („Unconventional energies and waste management"). Wydawnictwo Naukowe Gabriel Borowski, Lublin, 2010.

21. van Essen H, Kampman B. Impacts of electric vehicles – Summary report. Publication No. 11.4058.26, Delft, April 2011. www.cedelft.eu.
22. van Haaren R.: Assessment of electric cars' range requirements and usage patterns based on driving behavior recorded in the National Household Travel Survey of 2009. Study of the Solar Journey USA. Earth and Environmental Engineering Department, Columbia University, Fu Foundation School of Engineering and Applied Science, New York, December, 2011.
23. Wakefield EH. History of the electric automobile: Battery–only powered cars. Warrendale PA. SAE 1994.
24. Weinert J, MA C., Cherry C. The transition to electric bikes in China: history and key reasons for rapid growth. Transportation, 34/2007, 301–318.
25. Well-to-Wheels analysis of future automotive fuels and powertrains in the European context. WELL-to-WHEELS Report, Version 2c, EUCAR/CONCAWE/JRC, March 2007.
26. Westbrook MH. The electric car: Development and future of battery, hybrid and fuel-cell cars. IEE Power & Energy Series, 38. 2001.
27. Wheel to Well Analysis of EVs. MIT Electric Vehicle Team, MIT, April 2008. http://web.mit.edu/evt/summary_wtw.pdf.
28. Worldwide emission standards. Passenger cars and light duty vehicles. Innovation for the real world, Delphi, 2011/2012.

**Prof. Zdzisław CHŁOPEK, Ph.D. (Eng.)**
Motor Transport Institute
ul. Jagiellońska 80, 03–301 Warszawa, Poland
E–mail: zdzislaw.chlopek@its.waw.pl

Article citation info:
KULINOWSKI P. Simulation studies as the part of an integrated design process dealing with belt conveyor operation. Eksploatacja i Niezawodnosc – Maintenance and Reliability 2013; 15 (1): 83–88.

Piotr KULINOWSKI

# SIMULATION STUDIES AS THE PART OF AN INTEGRATED DESIGN PROCESS DEALING WITH BELT CONVEYOR OPERATION

# BADANIA SYMULACYJNE JAKO ELEMENT ZINTEGROWANEGO PROCESU PROJEKTOWANIA W ASPEKCIE EKSPLOATACJI PRZENOŚNIKÓW TAŚMOWYCH*

*This article presents simulation studies of transient working states of a conveyor as an indispensable, important part of the integrated process of its design. Simplified block diagrams and equations describe the structure of a dynamic model of a belt conveyor and a gravity take-up system. Results of simulation studies on the belt conveyor model have been compared to results of industrial tests carried out at the site of the conveyor operation using a mobile measurement system. The results of verifying the dynamic model have confirmed its utility for analysing dynamic phenomena occurring when the conveyor is operated, and demonstrated the complete suitability of simulation studies in the integrated process of designing belt conveyors.*

***Keywords**: conveyors, belt take-up systems, simulation studies, dynamic analysis, computer-aided design.*

*W niniejszym artykule przedstawiono badania symulacyjne nieustalonych stanów pracy przenośnika, jako nieodłączną i istotną część zintegrowanego procesu jego projektowania. Za pomocą uproszczonych schematów blokowych i równań, opisano budowę dynamicznego modelu przenośnika taśmowego oraz grawitacyjnego urządzenia napinającego taśmę. Wyniki testów symulacyjnych modelu przenośnika taśmowego porównano z wynikami badań przemysłowych, przeprowadzonych w miejscu eksploatacji przenośnika z wykorzystaniem mobilnego systemu pomiarowego. Wyniki weryfikacji modelu dynamicznego potwierdziły jego użyteczność w analizie zjawisk dynamicznych występujących podczas pracy przenośnika oraz wykazały pełną przydatność badań symulacyjnych w zintegrowanym procesie projektowania przenośników taśmowych.*

***Słowa kluczowe**: przenośniki taśmowe, urządzenia napinające taśmę, badania symulacyjne, analiza dynamiczna, komputerowe wspomaganie projektowania.*

## 1. Introduction

Due to their transport capacity and reliable operation, belt conveyors play a dominant role in systems for hauling useful minerals, both in open pit and underground mines. Belt conveyors transporting overburden can achieve capacities of 50,000 tons/h, the length of single installations can reach 20 km, and the power of their drives 12 MW. Belt conveyors with the greatest capacities, belt speeds and installed powers are used to transport overburden in open pit lignite mines, while designers face many interesting engineering challenges when designing overland conveyors more than ten kilometres long, designed for operating in difficult terrain and climate, as well as variable length belt conveyors used for drilling tunnels or working in underground hard coal mines [12].

Due to their operating environment and transport tasks, modern belt conveyors require the use of belts manufactured using state-of-the-art technologies, their drives are equipped with increasingly advanced and complex control systems, while belt support systems are optimised according to the criterion of cutting costs and increasing their durability. Many belt conveyors currently built are fitted with equipment tensioning the belt as a function of load on the driving system of the conveyor. New designs of conveyors must be drawn up using specialised software with constantly extended computational algorithms, making use of the latest results of industrial and operational research as well as laboratory experiments [12, 16]. State-of-the-art computer applications used globally to aid design activities exemplify the integrated design of belt conveyors with multi-option calculations, verifications and the selection of belt conveyor subassemblies, analyses of dynamic states and simulation studies conducted to select the best option according to assumed criteria [10, 12].

## 2. Integrated design of a belt conveyor

Belt conveyors are modular in structure and their designer's main job is to correctly select and combine ready subassemblies into a unique machine executing the planned transport task. The design of conveyors comprises a set of integrated processes executed by a design team, which encompasses analysing the transport task, the conditions and limitations of its execution, selecting operational parameters, making basic calculations, completing conveyor subassemblies taking into account economic conditions, as well as laboratory testing and simulation studies to adjust the operating parameters and set-points of control systems (Fig. 1). Machine examinations in industrial conditions to verify and calibrate computational models as well as accounting for the results of operational and diagnostic testing of selected belt conveyor components in the design process represents an important part of the integrated design of belt conveyors [5–7, 14–15, 18].

For belt conveyors, the transport task can be defined as a process whose purpose is to transport the set quantity of handled material within a defined time between the set loading and offloading locations. This determines the capacity of the conveyor as well as the route profile and layout, while the designer's job is to select the right belt speed and width and calculate basic operating parameters of the conveyor. This stage of the integrated computational design constitutes the initial calculation stage, mainly comprising calculations of the drive power and belt strength carried out using the basic method (Fig. 2).

(*) Tekst artykułu w polskiej wersji językowej dostępny w elektronicznym wydaniu kwartalnika na stronie ***www.ein.org.pl***

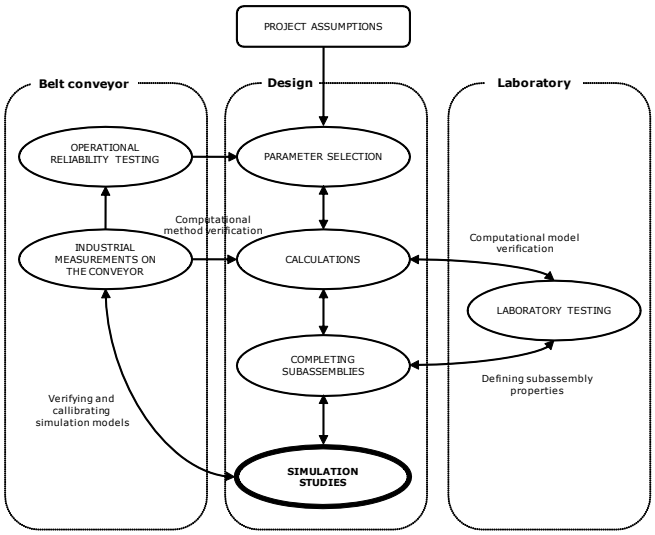


*Fig. 1. The diagram presenting the place of simulation studies in the integrated design process of a belt conveyor [12]*

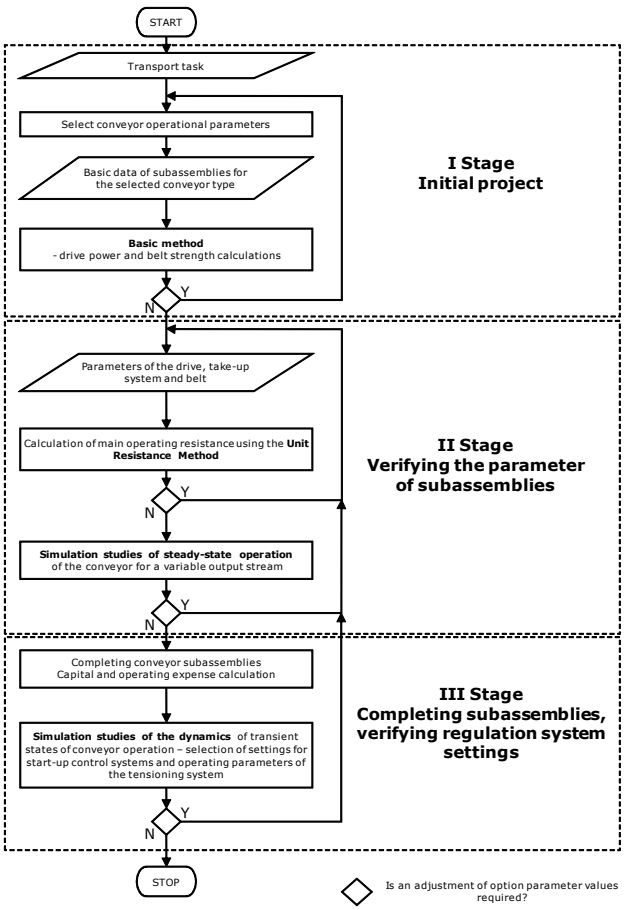


*Fig. 2. Algorithm of belt conveyor design [12]*

The next stage is to verify the selection of subassemblies: idlers, belt, driving and tensioning system. This stage should be supported by detailed calculations of main resistance of the belt using the Single Resistance Method [4]. This stage is concluded by simulation studies of the steady-state operation of the conveyor at variable capacities of loading points. The analyses cover the power consumption by the conveyor driving system, the belt loading state and its balance on curved sections of the conveyor route (Fig. 2).

The last, third stage of designing belt conveyors entails completing the subassemblies fitted to the conveyor and making an initial calculation of capital and operating expenses. At this stage the accuracy of the selection of subassemblies is finally verified by a process of simulation model studies of transient states of conveyor operation. The set-points of the start-up control system are adjusted and the operation of the tensioning device is analysed during conveyor start-up and breaking.

The diagram below shows the algorithm of the basic stages of the integrated process of designing belt conveyors (Fig. 2).

An important purpose of the simulation studies carried out at stages II and III of the integrated belt conveyor design is to analyse the belt tensioning system based on the results of calculations of the dynamics of transient operation states of the conveyor taking into account the rheological characteristics of the belt and the operating parameters of the drive control system.

The basic, widely used method for analysing the dynamics of transient states of conveyor belt operation is based on the assumption that all moving elements of the conveyor, i.e. those in translational motion like the transported material and the belt, and the rotating ones, i.e. the idlers and driving system subassemblies are concentrated in one point with a defined moving, moving with a constant acceleration or deceleration. In the case of a belt conveyor, this is too simplified, as due to the elastic properties of the belt not all moving elements of the conveyor are accelerated simultaneously. During the start-up, wave phenomena occur in the belt due to the profile of stress waves caused by the operation of drives and belt take-up systems. It does happen, particularly on very long conveyors, that the time delay between putting individual sections of the belt in motion ranges from several to tens of seconds. Thus calculation results produced using standard methods for assessing the dynamics of the start-up can be considered only approximate or preliminary for conducting more complex analytical procedures.

The problems associated with analysing the start-up of the conveyor and the operation of tensioning devices can be solved using a dynamic model of a belt conveyor with distributed parameters [8].

## 3. Dynamic belt conveyor model

In the conveyor model presented in Fig. 3, the reduced masses of drives, i.e. electric motors, couplings, gears and driving pulleys including the appropriate sections of the belt, the transported material and the reduced mass of the appropriate number of idlers were concentrated in the points where drives are installed. The reduced masses associated with the upper and lower belt were appropriately concentrated in centres of mass distributed along the conveyor route.

In the physical model devoted to analysing dynamic phenomena (Fig. 3), $\boldsymbol{x_i}$, represents the dislocations of individual points of the belt (i = 1, 2, ..., n). The resistance to belt motion along a given section of the conveyor is marked with $\boldsymbol{W_i}$ and it is assumed that the value and the sense of the resistance force depends on the belt speed $\boldsymbol{v_i}$. Depending on the formulated purpose of the model study, the value of resistances to motion is determined using standard methods [3, 17] or the single resistance method [4]. The components of the gravity force of the belt and the transported material placed on it, tangential to the direction of belt movement, are represented by $\boldsymbol{G_i}$, while $\boldsymbol{\delta_i}$ is the angle of slope relative to the modelled level of the $\boldsymbol{i}^{th}$ section of the belt. Active forces affecting the belt and coming from the drive are symbolised by $\boldsymbol{P_i}$ [8].

Due to rheological phenomena occurring in the belt during conveyor operation, belt models developed based on literature [13, 12, 19] were selected for analysing the uniaxial stress state. The selection of the belt rheology model depends on the purpose formulated for the simulation studies. If the analysis covers short-lasting, transient states of conveyor operation occurring during its start-up and breaking, the

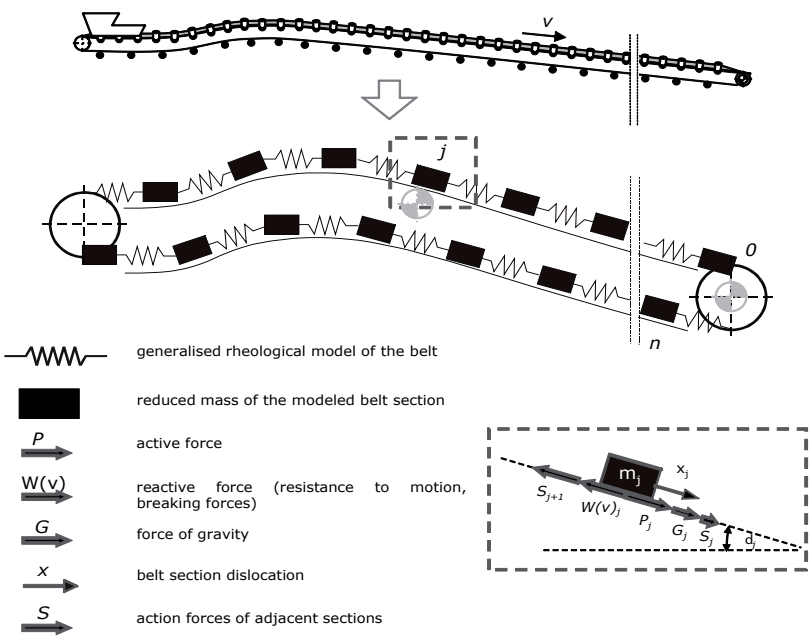


*Fig. 3 The model for analysing dynamic phenomena in a conveyor belt [8]*

two parameter Kelvin-Voigt model with a short stress relaxation time calibrated during simulation tests is sufficient. If the analysis concerns changes occurring during the steady-state operation of the conveyor with a variable load of handled material, it is necessary to use a standard model or a four-parameter one, which is a serial combination of two Kelvin-Voigt models [12].

The mathematical model of a belt conveyor is described by a system of second-order ordinary differential equations. Its matrix form is as follows [8]:

$$\mathbf{M}\cdot\ddot{x}(t)=\mathbf{N}\cdot\dot{x}(t)+\mathbf{K}\cdot x(t)+\mathbf{P}-\mathbf{W}+\mathbf{G} \tag{1}$$

where: **M** – reduced mass matrix;
**N** – damping coefficient matrix;
**K** – elasticity coefficient matrix;
**W** – resistance to motion matrix;
**P** – active force matrix;
***x(t)*** – dislocation matrix;
**G** – matrix of component gravity forces.

Fig. 4 below presents a fragment of a block model of a conveyor with a two-parameter rheological model of the belt. The equation of motion of the $j^{th}$ segment of this model is described by relationship (2), while its block diagram is shown in Fig. 5.

The method of modelling the driving force $\boldsymbol{P_i}$ depends on the type of the start-up system employed. For the purposes of the simulation studies conducted, a series of models were been developed of widely used drives described in the literature [12].

The equation of motion for the $j^{th}$ segment of a conveyor with a two-parameter rheological model of the belt has the following form:

$$m_{zrj}\ddot{x}_j = S_j - W_j - S_{j-1} + G_j + P_j \tag{2}$$

where: $S_j$ – sum total of elasticity and damping forces in the rheological model of the belt, [N];

$$S_j = k_j(x_{j+1}-x_j)+\eta_j(\dot{x}_{j+1}-\dot{x}_j) \tag{3}$$

where: $k_j$ – elasticity coefficient of the belt rheological model, [N/m];
$\eta_j$ – damping coefficient of the belt rheological model, [Ns/m];
$x$ – dislocation of the segment, [m];

The belt tensioning system which ensures the correct alignment of the belt and the correct operation of the driving system forms one of the most important subassemblies of a belt conveyor.

The belt tensioning devices used can be divided into two groups:
- with a constant position of the tensioning drum during conveyor operation: rigid tensioning systems;
- with a changing position of the tensioning drum during conveyor operation: gravitational, hydraulic and follow-up belt tensioning systems.

Fig. 6 below presents the physical model of a gravitational tensioning system widely used in above-ground conveyors. Fig. 7, in turn, shows a model, simplified compared to the block diagram in Fig. 5, of a belt tensioning segment in a dynamic model of a conveyor.

The calculated value of the speed and dislocation of an additional belt point $\boldsymbol{x_d}$ is substituted in the differential equation system describing the conveyor model.

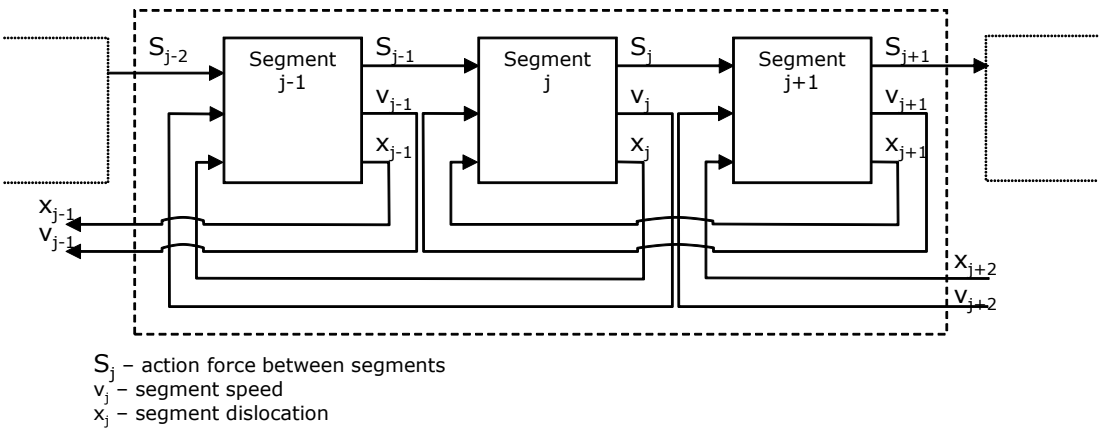


*Fig. 4. The fragment of a block model of a conveyor [12]*

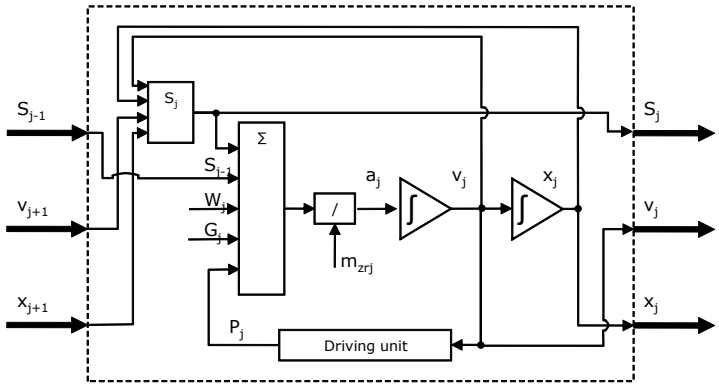


*Fig. 5. A block model of a driving segment in the dynamic conveyor model [12]*

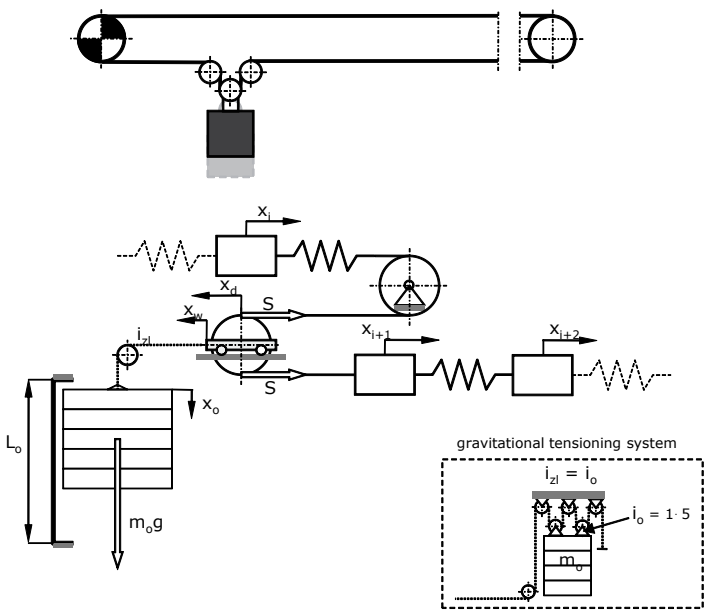


*Fig. 6. The diagram and a physical model of a gravitational tensioning device [12]*

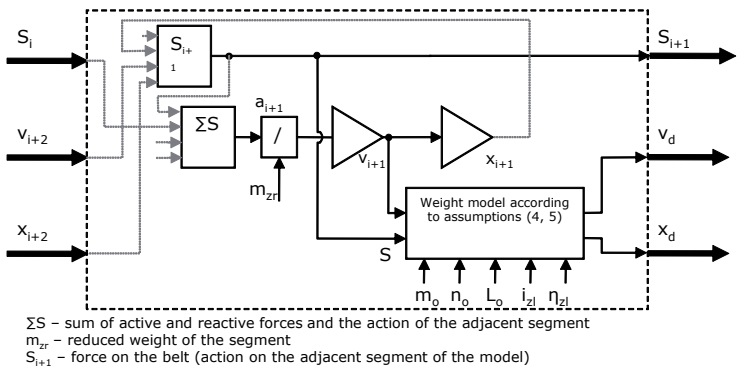


*Fig. 7. Simplified block model of a gravity tensioning segment in the dynamic conveyor model*

The acceleration of the weight is determined based on the following relationship:

$$a_o = \frac{2 \cdot S \cdot i_{zl} \cdot \eta_{zl}}{m_o \cdot n_o} - g \qquad [\mathrm{m/s^2}] \qquad (4)$$

where: $m_o$ – weight mass, [kg];
$n_o$ – number of weights; [-];
$S$ – force on the belt, [N];
$i_{zl}$ – ratio of the tackle system, [-];
$\eta_{zl}$ – tackle system efficiency $\eta_{zl} = f(v_o)$, [-];

After using an integration operation to determine the acceleration of the weight – $\boldsymbol{a_o}$, its dislocation – $\boldsymbol{x_o}$ and after accounting for the structural limitations of the length of the tensioning path $\boldsymbol{L_o}$, the value of the dislocation of the tensioning pulley is calculated. The calculation of this value accounts for the ratio of the tackle system and its efficiency, which varies depending on the speed of the weight $\boldsymbol{v_o}$. The value of the speed of the additional point $\boldsymbol{v_d}$ was determined from relationship (5).

$$v_d = v_{i+1} + 2v_w \qquad [\mathrm{m/s^2}] \qquad (5)$$

where: $v_d$ – additional point speed, [m/s];
$v_w$ – tensioning cart speed, [m/s];
$v_{i+1}$ – speed of the centre of gravity $i$+1, [m/s];

Operating parameters of a gravity-based tensioning system are adjusted using the number and the mass of weights and the tensioning path length.

Results of simulation studies of a conveyor with a winch and a gravity belt tensioning system verified against the results of industrial tests carried out at a copper ore mine [11] are presented below.

## 4. Verification of results from simulation studies of a discrete conveyor model with a gravity belt tensioning system

Simulation studies carried out using a discrete model of a conveyor made use of:

- the single resistance method (TT) to calculate the reactive forces of resistance to motion [4],
- a standard rheological model of the belt (3p) according to [13],
- a model of a gravity belt tensioning system;
- a model of the driving system with fluid start-up couplings;
- a variable sequence of motor start-up.

The list of selected parameters of processes and models of subassemblies adopted during simulation studies of the belt conveyor, simulation code: model3p-TT, is presented in publications [12, 13].

An analysis of results concerning changes of forces on the belt obtained by simulation studies of the discrete conveyor model (model3p-TT) and industrial tests (test) shows that the assumptions for building the model were formulated correctly. Values of the force ***S1*** obtained in model studies are greater than the measured value of the force ***STA***, which may be due to excluding the slippage of the belt on the drum actually occurring on the AB drum during all start-ups recorded (Fig. 8).

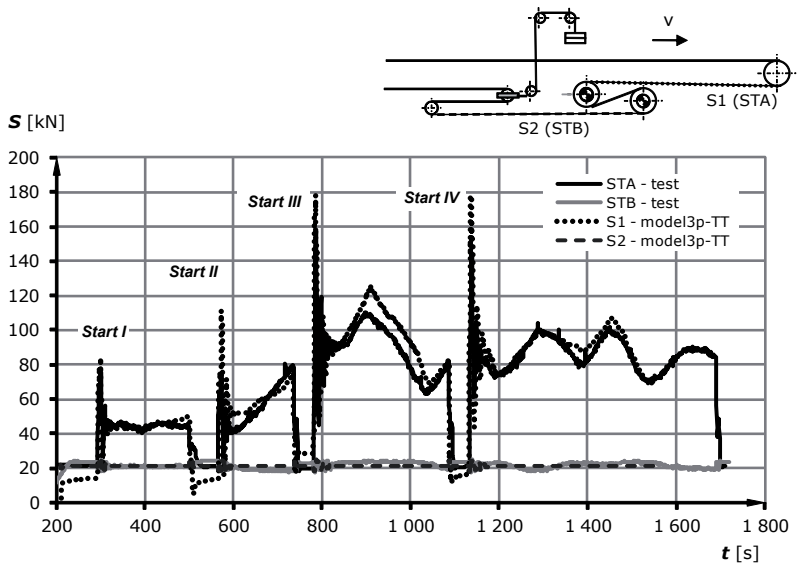


*Fig. 8. Changes of forces on the belt of a conveyor during steady-state operation, start-up and breaking – industrial test (test) and simulation studies of a discrete conveyor model (model3p-TT) [13]*

The verification of the discrete belt conveyor model mainly concerned transient states of operation, so Fig. 9 shows a comparison of results of industrial tests and simulation studies in the form of the dislocation of the tensioning pulley and the belt speed during conveyor start-ups I÷IV. During the recorded start-ups, the load of handled material on the conveyor varied [13], so the curves obtained by simulation studies can be considered satisfactory, and the adopted model of resistance to motion and the rheological model of the belt as correct. Apart from the possible errors in assessing the capacity of the conveyor, the inaccuracy of calculations of the drive power, the force on the belt and the length of the tensioning path may also be due to the approximate mapping of the conveyor route profile. Due to the lack of more precise survey information, the route of the conveyor was described using a single section with a constant slope, whereas the actual route of the conveyor consists of 2.5 m long segments founded on the floor of the mine pit. The variable slope angle of individual route sections in combination with a variable stream of handled material may significantly impact the momentary load on the drive.

The utility of results from simulation studies carried out using these models would be difficult to determine if

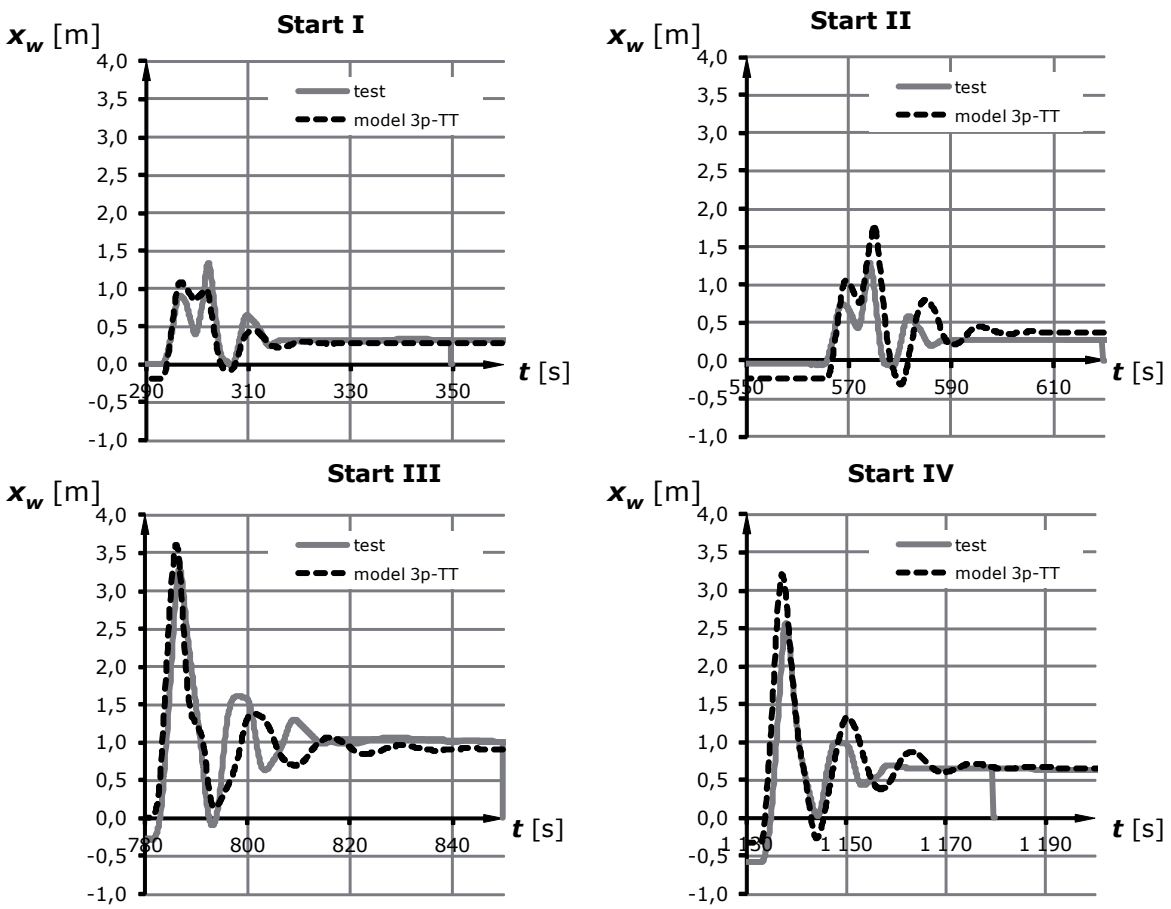


*Fig. 9. The time-profile of changes in the dislocation of the tensioning pulley – a comparison of industrial test results (test) and simulation studies using a standard belt model (model 3p-TT) [13]*

it were not for their verification at the operating site of the conveyor using a mobile measurement system. This system, constructed based on an original concept, together with the measurement apparatuses and the appropriate data processing procedures, has turned out to be completely suitable during measurements executed in industrial conditions, and the results obtained have painted a complete picture of the dynamics of transient operating conditions of the conveyor [11].

## 5. Summary

Designing a belt conveyor consists of executing a set of integrated processes to correctly select and combine its subassemblies into a unique machine meeting a defined transport requirement. This article presents simulation studies of conveyor operation as an indispensable, significant part of the integrated process of its design.

Simulation studies were executed using a dynamic model of a belt conveyor with distributed parameters, which includes models of belt tensioning devices as its integral parts. Their structure and place in the conveyor model was described using simplified block diagrams and equations [12]. The results of industrial tests of a belt conveyor conducted during its start-up, breaking and steady-state operation with a variable load of handled material were compared to the results of simulation studies on a belt conveyor model with a three-parameter rheological model of the belt [19] and a module for determining reaction forces based on unit resistances [4]. The driving system model used parameterized characteristics of fluid couplings determined on a VOITH test stand [9]. A comparison of the results obtained has shown that the discrete model of a belt conveyor with models of belt tensioning devices can be successfully used, with satisfactory accuracy, to simulate the start-up, breaking and continuous operation of a conveyor with a variable feed of transported material.

Simulation studies conducted during the design of a conveyor make it possible to select the appropriate subassemblies, optimum operating parameters and the correct set-points of regulation systems, thus significantly reducing future operational problems.

## 6. Literature


1. Advanced Conveyor Technologies Inc. Sidewinder. [online], 2011. http://www.actek.com/.
2. Conveyor Dynamic, Inc. Software: Beltstat, Beltflex, Beltcurv. [online], 2011. http://www.conveyor-dynamics.com/cdi_intro.htm.
3. Deutsches Instit. Normung. DIN 22101, Stetigfoerderer. Gurtfoerderer fur Schuttgutter, 2002.
4. Gładysiewicz L. Przenośniki taśmowe. Teoria i obliczenia. Oficyna Wydawnicza Politechniki Wrocławskiej, Wrocław, 2003.
5. Gładysiewicz L, Król R, Bukowski J. Eksperymentalne badania oporów ruchu przenośnika taśmowego. Eksploatacja i Niezawodnosc – Maintenance and Reliability 2011; 3: 17–25.
6. Hardygóra M, Komander H, Błażej R, Jurdziak L. Metoda prognozowania trwałości zmęczeniowej złączy wieloprzekładkowych taśm przenośnikowych. Eksploatacja i Niezawodnosc – Maintenance and Reliability 2012; 14(2):171–175.
7. Kacprzak M, Kulinowski P, Wędrychowicz D. Informatyczny system zarządzania procesem eksploatacji górniczych przenośników taśmowych. Eksploatacja i Niezawodnosc – Maintenance and Reliability 2011; 2: 81–93.
8. Kulinowski P. Badania modelowe nieustalonych stanów pracy przenośników taśmowych. Praca doktorska, Akademia Górniczo-Hutnicza, Kraków 1997.
9. Kulinowski P. Dynamic Start-up Calculations for Belt Conveyors with Measured Torque Curves of Fluid Couplings. Mine Planing and Equipment Selection 2004, A.A. Balkema Publishers, 2004; 443–448.
10. Kulinowski P. Informatyczne wspomaganie procesu projektowania przenośników taśmowych. Gospodarka Surowcami Mineralnymi, 2007; T.23, Z.4: 209–221.
11. Kulinowski P. Identyfikacja parametrów techniczno-ruchowych przenośników taśmowych z wykorzystaniem mobilnego systemu pomiarowego. Maszyny Górnicze, 2008; 3: 35–43.
12. Kulinowski P. Metodyka zintegrowanego projektowania górniczych przenośników taśmowych. Wydawnictwa AGH, 2012.
13. Kulinowski P, Zarzycki J, Furmanik K. Identyfikacja parametrów standardowego modelu reologicznego taśmy i jego wykorzystanie w symulacyjnych badaniach dynamiki przenośników taśmowych. Transport Przemysłowy i Maszyny Robocze 2012; 2: 3–8.
14. Kwaśniewski J. The use of monitoring to improve the raliability and endurance of continous coal handling systems. Archives of Mining Sciences, 2012 56(4): 651–664.
15. Mazurkiewicz D. Badania wydłużalności i wytrzymałości złączy klejonych w aspekcie opracowania komputerowego systemu monitorowania ich stanu w czasie pracy przenośnika taśmowego. Eksploatacja i Niezawodnosc – Maintenance and Reliability, 2010; 3(47): 34.
16. Overland Conveyor Company, Inc. Belt Analyst™. [online], 2011. http://www.overlandconveyor.com.
17. PN-M-46552:1993 Przenośniki taśmowe z krążnikami podpierającymi taśmę. Obliczanie mocy napędowej i sił napinających taśmę. Polski Komitet Normalizacji, Miar i Jakości. 1993.
18. Szybka J, Wędrychowicz D. Wyznaczanie strategii prewencyjnych odnów przenośników taśmowych. Materiały Szkoły Eksploatacji Podziemnej 2010, Kraków, 22–26 lutego 2010. Wydawnictwo IGSMiE PAN.
19. Zarzycki J. Wpływ własności reologicznych taśmy na parametry eksploatacyjne przenośnika. Praca doktorska, Akademia Górniczo-Hutnicza, 2011.



**Piotr KULINOWSKI, Ph.D. (Eng.)**
AGH University of Science and Technology, Krakow
al. Mickiewicza 30, 30-059 Kraków, Poland
Email: piotr.kulinowski@agh.edu.pl

## INFORMATION FOR AUTHORS

### Terms and Conditions of Publication:

- The quarterly „Maintenance and Reliability" publishes original papers written in Polish with an English translation.
- Translation into English is done by the Authors after they have received information from the Editorial Office about the outcome of the review process and have introduced the necessary modifications in accordance with the suggestions of the referees!
- Acceptance of papers for publication is based on two independent reviews commissioned by the Editor.

### Fees:

- Pursuant to a resolution of the Board of PNTTE, as of 2009 the publication fee for one text is 600 zloty + VAT.
- Coloured graphical elements in the submitted text require agreement from the Editor and are charged extra.

### Technical requirements:

- After receiving positive reviews and after acceptance of the paper for publication, the text must be submitted in a Microsoft Word document format.
- Drawings and photos should be additionally submitted in the form of graphical files in the *.tif, *.jpg or *.cdr (v. X3) formats.
- A manuscript should include (in accordance with the enclosed correct manuscript format: *.pdf, *.doc):
- names of authors, title, abstract, and key words that should complement the title and abstract (in Polish and in English)
- the text in Polish and in English with a clear division into sections (please, do not divide words in the text);
- tables, drawings, graphs, and photos included in the text should have descriptive two-language captions,
- if this can be avoided, no formulae and symbols should be inserted into text paragraphs by means of a formula editor
- references (written in accordance with the required reference format)
- author data – first names and surnames along with scientific titles, affiliation, address, phone number, fax, and e-mail address
- The Editor reserves the right to abridge and adjust the manuscripts.
- All submissions should be accompanied by a submission form.

**Editor contact info:** (Submissions should be sent to the Editor's address)

Editorial Office of „Eksploatacja i Niezawodność - Maintenance and Reliability"
Nadbystrzycka 36, 20-618 Lublin, Poland
e-mail: office@ein.org.pl

## INFORMATION FOR SUBSCRIBERS

### Fees

Yearly subscription fee (four issues) is 100 zloty and includes delivery costs.
Subscribers receive any additional special issues published during their year of subscription free of charge.

### Orders

Subscription orders along with authorization to issue a VAT invoice without receiver's signature should be sent to the Editor's address.

**Note**

In accordance with the requirements of citation databases, proper citation of publications appearing in our Quarterly should include the full name of the journal in Polish and English without Polish diacritical marks, i.e.,

**Eksploatacja i Niezawodnosc – Maintenance and Reliability**.